

Newcastle University

Manipulating flagellar gene regulation in
uropathogenic *Escherichia coli* to explore its
effect(s) on the urothelial proinflammatory response

Qusai Alsenani

Thesis submitted for the degree of Doctor of Philosophy

Biosciences Institute (Institute for Cell and Molecular Biosciences) Faculty of
Medical Sciences Newcastle University

February 2024

Covid 19 statement removed at the request of the author in the publication
version of this thesis

Abstract

Urinary tract infections (UTIs) are a global problem and the major pathogen associated with such infections is Uropathogenic *Escherichia coli* (UPEC). UTIs are classified according to the site of infection: cystitis describes a bladder infection and pyelonephritis a kidney infection. If not treated symptomatic UTIs can lead to bacteraemia, sepsis and death. An additional condition is asymptomatic bacteriuria (ASB), which mainly affects older and/or immunocompromised populations. ASB is associated with UPEC colonising the lower urinary tract (UT) without causing symptoms and often underlies symptomatic infections.

A panel of clinical uro-associated *E. coli* isolates recovered from cystitis, pyelonephritis, ASB and bacteraemia patients were characterised for motility and their ability to induce an innate response in urothelial cells, determined by the induction of NF- κ B and/or IL-8 synthesis. Data suggested a mix of motile and non-motile strains, but the motility patterns and abilities of the motile strains to induce an innate response were very variable. The aim of this thesis was to understand the factors underpinning this variation.

Lower UT tissues defend themselves from bacterial assaults via innate mechanisms involving urothelial receptors with the most important being Toll-like Receptor 5 (TLR5). TLR5 detects the bacterial flagellar subunit, flagellin and activation results in the synthesis of host defence agents and bacterial killing. Hence, flagellar appear key in inducing the urothelial host defences. Synthesising flagella is an energy-consuming process initiated only when motility is advantageous. This led to the hypothesis that growth fitness is important in the recognition of uro-associated *E. coli* by urothelial cells.

Chapter 3 describes experiments, measuring bacterial doubling times, and comparing the growth fitness of motile and non-motile clinical isolates. The motile (M) strain mean doubling time was 17.4 ± 3.0 min versus 19.7 ± 2.5 min for the non-motile (NM) strains ($P=0.011$). However, the range of doubling times was similar (M: 13.9-26.9 min; NM: 14.7-25.3min). These latter data argued against fitness being a primary driving factor in the variation of host recognition. To examine if variation linked to flagellar abundance strains were engineered, using *pSE_flhDC* to hyperexpress flagellar. The mutant strains showed increased motility and innate responses (2-fold) indicating that variability in the host responses linked to fluctuations in bacterial flagellar numbers and subsequent motility.

Chapter 4 confirmed these data by constructing and using Δ *flhDC* and Δ *clpP* mutants, which resulted in either a loss of flagellar or unregulated flagellar synthesis. Six strains were analysed NCTC10418, CFT073, 3408, MG1655, 5469 and 5489. To quantify flagellar numbers the *FlgE* of three strains NCTC10418, CFT073 and 3408 was replaced with *FlgEA240C* and the mutated cells stained with Alexa Fluor 488 maleimide. These cells were examined using fluorescence microscopy. Visualisation of the FlgEA240C foci of the Δ *clpP* mutants supported increases in flagellar numbers as well as an increase in the bacterial population carrying flagellar. These data further supported the concept that variability in the bladder host response is linked to population heterogeneity and flagellar abundance of the invading uropathogens.

Data presented in Chapters 3 and 4 related to bacteria cultured in enriched media, which physiologically does not reflect the UT environment. Experiments were therefore performed using three strains, 3408, 5469 and 5489 and their Δ *flhDC* and Δ *clpP* mutants grown in artificial urine media (AUM) at pH 5.5 (acid urine) and pH 6.5 (alkaline urine). Data showed growth in AUM was associated with a reduced motility and bladder innate response, and that pH did not impact these data.

In summary results have shown that uro-associated *E. coli* isolates, generally, regulate flagellar synthesis to allow colonisation or infection, but appear to exploit population heterogeneity to prevent recognition by urothelial cell TLR5 receptors and bacterial killing.

Acknowledgements

During My PhD journey, I faced many challenges, and without support I wouldn't have been able to overcome these. First of all, I would like to thank Allah for his blessing, mercy, and for giving me the strength to complete this work. I would like to express my gratitude to my supervisors Drs. Judith Hall and Phillip Aldridge, who have taught, inspired, supported and challenged me throughout my PhD studies, and whose profound wisdom, substantive support, professional guidance, and expertise helped making this thesis possible. Moreover, I would like to thank both of them for making this PhD a wonderful fruitful journey that I will cherish forever. I wish to also show my appreciation to my colleagues who have assisted me in my research endeavours especially Dr. Catherine Mowbray Dr. James Grimshaw and Dr. Maria Zakhour.

I would like to extend my thanks to the Government of Saudi Arabia for granting me a scholarship to study for a PhD in the UK, and I owe special thanks to the University of Hail for nominating me for the PhD scholarship programme. Finally, I cannot forget that during the PhD journey, I was accompanied by my lovely wife who has supported me selflessly and constantly. She was always there whenever needed. My thanks go to her and to my charming boys, Ahmad, and Abdullah for their patience and emotional support, which helped me through the PhD journey at Newcastle University. This time will never go to waste or be forgotten.

I am also grateful to my parents who supported me morally and without those prayers and wishes this journey could not have been completed. Furthermore, I would like to express my gratitude to my parents in law for all their support, emotions, and prayers. I want also to convey my appreciation to my siblings whom I counted on in helping me numerous times during this journey and for being source of comfort all the times.

Table of Contents

Impact of COVID-19	ii
Abstract.....	iii
Acknowledgements	v
List of Figures.....	x
List of Tables	xiii
List of Abbreviations	xiv
Chapter 1. Introduction.....	1
1.1 Background to Project.....	2
1.2 Urinary Tract infection (UTI) a global problem	3
1.2.1 Complicated and uncomplicated UTI	5
1.2.2 UTIs and mortality	6
1.3 Host response to UTI	6
1.3.1 Physical barriers.....	8
1.3.2 Pattern recognition receptors (PRRs).....	10
1.3.3 Toll like Receptors in the uroepithelium.....	10
1.3.4 Innate response signalling pathways activated by TLRs	12
1.3.5 Adaptive response signalling pathways in the bladder	15
1.4 Genetic Risk of Recurrent Urinary Tract Infections	16
1.5 UTI treatment.....	16
1.6 Uropathogens associated with UTIs	19
1.6.1 <i>Escherichia coli</i>	20
1.6.2 <i>E. coli</i> pathovars.....	20
1.6.3 Enteropathogenic <i>E. coli</i> (EPEC).....	20
1.6.4 <i>Enterohaemorrhagic E. coli</i> (EHEC).....	22
1.6.5 Enterotoxigenic <i>E. coli</i> (ETEC)	22
1.6.6 Enteroinvasive <i>E. coli</i> (EIEC).....	23
1.6.7 Enteroaggregative <i>E. coli</i> (EAEC).....	23
1.6.8 Diffusely adherent <i>E. coli</i> (DAEC).....	24
1.6.9 Adherent invasive <i>E. coli</i> (AIEC).....	24
1.6.10 Uropathogenic <i>E. coli</i> (UPEC).....	24
1.7 Virulence factors of UPEC	25
1.8 Flagellar components and their synthesis	27
1.8.1 The filament	29
1.9 Regulation of flagellar synthesis	33
1.10 Proteolytic control of the flagellar system	35

1.11 Population heterogeneity	35
1.12 Motility of Uro-associated <i>E. coli</i>	36
1.13 The urothelial innate response to Uro- associated <i>E. coli</i>	37
1.14 Urothelial responses to Flagellin serotypes	38
1.15 Urothelial responses to outer membrane preparations	39
1.16 Flagellar abundance	40
1.17 Hypothesis and Aims	42
Chapter 2. Material and Methods	43
2.1. Bacterial cell culture	44
2.1.1 Bacterial Media.....	44
2.1.2 Bacterial Strains	45
2.2 Tissue culture: RT4 epithelial cells.....	47
2.3 Polymerase chain reaction (PCR)	47
2.3.1 Primers	47
2.3.2 Primers list	48
2.3.3 DNA visualization:	49
2.3.4. Purification of PCR products	49
2.4 Gene expression	50
2.4.1 RNA Isolation	50
2.4.2 Reverse transcription.....	50
2.4.3 qRT-PCR.....	51
2.5 DNA isolation	52
2.5.1 Plasmid miniprep	52
2.5.2 Plasmid midiprep	52
2.5.3 Isolation of bacterial genomic DNA	53
2.6 DNA gel extraction	53
2.7 Bacterial Transformation by Electroporation	54
2.7.1 Preparation of electro-competent <i>E. coli</i> cells	54
2.7.2 Bacterial Electroporation	54
2.8 Constructing mutants using a lambda (λ) red recombinant system	55
2.8.1 Datsenko and Wanner method	55
2.8.2 Eliminating chloramphenicol resistance	56
2.9 Protein analysis using SDS-page	56
2.10 Immunoblotting.....	56
2.11 Motility Assay.....	57
2.12 RT4 Bladder Cell Challenges	58
2.12.1 Heat killing of bacteria.....	58

2.11.2 RT4 cell challenges with bacteria	58
2.12.3 IL-8 ELISA	58
2.13 Quantification of Flagellation	59
2.13.1 Labelling Flagella	59
2.13.2 Bacterial Staining with Maleimide	59
2.13.3 Capturing Pictures with Fluorescence microscopy	60
2.13.4 Processing Images using Image J.....	60
2.13.5 Randomization of chosen bacterial cells for Foci counting	60
2.14 Statistical analysis.....	61
Chapter 3. Impact of Uro-associated <i>Escherichia coli</i> motility on the innate response of RT4 Bladder Cells	62
3.1 Introduction.....	63
3.2 Results	64
3.2.1 Growth fitness of UPEC strains	64
3.2.2 Flagellar contamination residual levels.....	69
3.2.3 Overexpression of flhDC in clinical uro-associated <i>E. coli</i> isolates and analyses of bacterial motility	73
3.2.4 Using pSE_flhDC recombinant strains to explore the RT4 bladder innate response	78
3.3 Discussion	80
Chapter 4. The effect of manipulating the regulation of flagellar synthesis in UPEC and its impact on the innate response of RT4 Bladder cells.....	87
4.1 Introduction.....	88
4.2 Constructing deletion mutants of <i>flhDC</i> and <i>clpP</i> in <i>E. coli</i>	89
4.3 Comparing motility of the Δ <i>flhDC</i> and Δ <i>clpP</i> mutants to the wildtype strains	91
4.4 Defining the innate response to Δ <i>flhDC</i> and Δ <i>clpP</i> mutants	95
4.5. Detecting FlgE in the Δ <i>flhDC</i> and Δ <i>clpP</i> strains	97
4.6 Flagellar gene expression of the Δ <i>flhDC</i> and Δ <i>clpP</i> mutants	98
4.7 Comparing flagellar abundance in selected wildtype strains and the Δ <i>flhDC</i> and Δ <i>clpP</i> mutants.	102
4.7.1 Deletion of <i>flgE</i>	103
4.7.2 Quantification of Flagellar abundance using FlgEA240C Foci	106
4.8 Discussion.....	111
Chapter 5. The effects of Uro-associated <i>E. coli</i> isolates, grown in artificial urine medium (AUM), on the innate response(s) of RT4 bladder cells.....	117
5.1 Introduction.....	118
5.2 Motility in AUM.....	119
5.3 Innate responses of RT4 bladder cells to <i>E. coli</i> isolates cultured in AUM	123
5.3.1 IL-8 production: pH 6.5 and 5.5	124
5.4 Exploring FlgE expression in bacterial samples cultured in AUM and heat-killed.....	125

5.5 Discussion.....	131
Chapter 6. General Discussion.....	136
Chapter 7. Bibliography.....	146

List of Figures

Chapter 1

Figure 1.1 Bacterial migration in UTIs.....	4
Figure 1.2 ROS antimicrobial effect.....	8
Figure 1.3 Schematic of the urothelium.....	9
Figure 1.4 Schematic of host signalling pathways triggered by TLRs.	13
Figure 1.5 Schematics presenting the chemical structure of some antibiotics that commonly used to treat UTIs.	18
Figure 1.6 A schematic of T3SS.....	21
Figure 1.7 UPEC adhesion to epithelia.....	26
Figure 1.8 Schematic of the bacterial flagella.	27
Figure 1.9 Schematic of FliC structure.....	29
Figure 1.10 Schematic of the transcription hierarchy of flagellar.....	33
Figure 1.11 Quantification of motility assay of UTI isolates.....	36
Figure 1.12 NF- κ B induction in RT4 bladder cells following challenge with motile and non-motile UTI isolates.....	37
Figure 1.13 The induction of NF- κ B by different flagellin serotypes.....	38
Figure 1.14 IL-8 response following Outer membrane and whole cell challenges of RT4 bladder cells.	39
Figure 1.15 Flagellar abundance compared to innate response.....	40

Chapter 2

Figure 2.1 Schematic of Datsenko and Wanner method.....	54
Figure 2.2 Motility Assay.....	57

Chapter 3

Figure 3.1 Average doubling times (min) of motile and non-motile UTI isolates according to their source.....	66
Figure 3.2 Growth curves motile and non- motile strains..	67
Figure 3.3 Growth curves of fast and slow growing motile isolates.....	68
Figure 3.4 Fitness of motile and non-motile strains of <i>E. coli</i> defined by the maximum doubling time.	70

Figure 3.5 BLAST alignment of FliD and FlgE amino acids sequences comparing <i>E. coli</i> to Salmonella.....	71
Figure 3.6 Optimization of the Salmonella α -FliD and α -FlgE antibodies.....	73
Figure 3.7 Analyses of flagellar contamination in <i>E. coli</i> OM preparations.	74
Figure 3.8 Motility assay of <i>E. coli</i> isolates \pm pSE- <i>flhDC</i> \pm IPTG (Qualitative Data).	76
Figure 3.9 Motility assays comparing strains \pm pSE \pm <i>flhDC\pmIPTG.....</i>	77
Figure 3.10 Response of RT4 (bladder epithelial cells) to <i>E. coli</i> heat killed strains \pm pSE- <i>flhDC</i>	78

Chapter 4

Figure 4.1 Generating the chloramphenicol resistant cassettes which were to be used in replacing <i>flhDC</i> and <i>clpP</i> to construct Δ <i>flhDC</i> , and Δ <i>clpP</i> mutants.	89
Figure 4.2 PCR confirmation of the constructed Δ <i>flhDC</i> mutants.....	91
Figure 4.3 PCR confirmation of the constructed Δ <i>clpP</i> mutants.	92
Figure 4.4 Motility assays of <i>E. coli</i> isolates and their Δ <i>flhDC</i> , and Δ <i>clpP</i> mutants.	93
Figure 4.5 Quantification of motility in <i>E. coli</i> isolates compared to Δ <i>clpP</i> mutants.	94
Figure 4.6 Response of bladder epithelial RT4 cells to <i>E. coli</i> strains and their Δ <i>flhDC</i> & Δ <i>clpP</i> mutants.	95
Figure 4.7 indicating the expression of FlgE in the <i>E. coli</i> isolates and their Δ <i>flhDC</i> and Δ <i>clpP</i> mutants.	97
Figure 4.8 Flagellar genes expression of <i>E. coli</i> strains.	98
Figure 4.9 Flagellar genes expression of UPEC isolates.	99
Figure 4.10 Flagellar genes expression of UPEC isolates.	100
Figure 4.11 PCR confirmation of chloramphenicol resistant cassette removal from Δ <i>flhDC</i> and Δ <i>clpP</i> mutants.....	103
Figure 4.12 PCR confirmation of constructed Δ <i>flgE</i> mutants.	104
Figure 4.13 Motility assay confirming deletion of <i>flgE</i> and the transformation of <i>flgEA240C</i>	104
Figure 4.14 Example areas of phase contrast and fluorescent images of FlgEA240C foci...106	
Figure 4.15 Quantification of flagellar abundance.	107
Figure 4.16 Quantification of the number of flagella/bacterial cells.....	108

Chapter 5

Figure 5.1 Motility assay using AUM motility media pH 6.5.	119
---	-----

Figure 5.2 Motility assay using AUM motility media pH 5.5.	120
Figure 5.3 Quantification of Motility assay using AUM motility media.	121
Figure 5.4 IL-8 levels of RT4 bladder cells challenged with heat-killed <i>E. coli</i> UTI isolates grown in AUM pH 6.5.	124
Figure 5.5 IL-8 levels of RT4 bladder cells challenged with heat-killed <i>E. coli</i> UTI isolates grown in AUM pH 5.5.	125
Figure 5.6 Expression of FlgE in wild-type isolate 3408 and its $\Delta flhDC$ and $\Delta clpP$ mutants grown either in LB or AUM.	126
Figure 5.7 Expression of FlgE in wild-type isolate CFT073 & 5489 and their $\Delta flhDC$ and $\Delta clpP$ mutants grown either in LB or AUM.	127
Figure 5.8 Expression of FlgE in wild-type isolate 3408 and 5469 3 and their $\Delta flhDC$ and $\Delta clpP$ mutants grown either in LB or AUM.	128

List of Tables

Chapter 1

Table 1.1 List of innate immune system components functioning in the urinary tract.....	7
Table 1.2 Toll-Like receptors and their localization, ligands, and the origin of these Ligands.....	9
Table 1.3 Treatment strategies for UTI.....	16
Table 1.4 List of the conserved amino acids affecting the TLR5 recognition of flagellin.....	28

Chapter 2

Table 2.1 Preparation of AUM.....	44
Table 2.2 Antibiotic stock and working solution concentrations.....	45
Table 2.3 List of strains used in this study.....	45
Table 2.4 List of plasmids used in this study.....	46
Table 2.5 List of PCR components and volumes used in a 50 µL reaction mix (Taq).....	47
Table 2.6 List of PCR components and volumes used in a 50 µL reaction mix (Q5).....	47
Table 2.7 Lists the primers used in the experiments described in this thesis.....	47
Table 2.8 qPCR programme details.....	50

Chapter 3

Table 3.1 Motile strains used in the growth curve study.....	63
Table 3.2 Non-motile strains used in the growth curve study.....	64

Chapter 6

Table 6.1 Designing conditions variability	142
--	-----

List of Abbreviations

Abbreviation	Defenition
ALRs	(AIM2)-like receptors
TAK	(TGF)- β -activated kinase
Δ DC	Δ <i>flhDC</i>
AIM	Absent in melanoma
AIEC	Adherent invasive <i>E. coli</i>
Amp	Ampicillin
MyD88	An adaptor protein has a TIR domain
AMP	Antimicrobial peptide
AMR	Antimicrobial resistance
ASB	Asymptomatic bacteriuria
BLAST	Basic local alignment search tool
CAUTI	Catheter-associated UTI
Cm	Chloramphenicol
CAT	Chloramphenicol resistance gene
CLR	C-type lectin receptor
DAMP	Damage-associated molecular patterns
DC	Dendritic cells
DAEC	Diffusely adherent <i>E. coli</i>
<i>Dfr</i>	Dihydrofolate reductase
DSB	Double-stranded break
EC	<i>E. coli</i>
EAEC	Enterogaagregative <i>E. coli</i>
EHEC	Enterohaemorrhagic <i>E. coli</i>
EIEC	Enteroinvasive <i>E. coli</i>
EPEC	Enteropathogenic <i>E. coli</i>
ETEC	Enterotoxigenic <i>E. coli</i>
ELISA	Enzyme Linked Immunosorbent Assay
ExPEC	Extraintestinal pathogenic <i>E. coli</i>
Gent	Gentamycin
GAG	Glycosaminoglycan
HBB	hook-basal body
IgA	Immunoglobulin A
IFN	Interferon
IL	Interleukins
IBC	Intracellular bacterial colonies
Kan	Kanamycin
LRR	Leucine-rich repeat
LPS	Lipopolysaccharide
LBP	LPS-binding protein
LB	Luria broth
mRNA	Messenger RNA

Min	minutes
MAPK	Mitogen-activated protein kinases
MDR	Multi drug resistant
NICE	National Institute for Health and Care Excellence
NLR	NLR(NOD)-like receptor
NF- κ B	Nuclear factor- κ B
NOD	Nucleotide oligomerization domain
OLC	Overlap layout consensus
PRR	Pathogen recognition receptor
PAMP	Pathogen-associated molecular pattern
PBS	Phosphate-buffered saline
PCR	Polymerase chain reaction
rUTI	Recurrent urinary tract infection
RFP	Red fluorescent Protein
RIG-I	Retinoic acid-inducible gene I
RLR	RIG-I-like receptors
ST131	Sequence type 131
Stx	Shiga toxin
ShET	<i>Shigella</i> enterotoxin
σ^{28}	sigma factor 28
σ^{70}	sigma factor 70
sgRNA	Single guide RNA
SNP	Single nucleotide polymorphism
SDS	Sodium dodecyl sulphate
TAB	TAK-binding proteins
Tet	Tetracycline
TRAF	TNF receptor-associated factor
TLR	Toll-like receptor
TGF	transforming growth factor
TNF	Tumour necrosis factor
TTSS	Type III secretion system
TPF	Type P fimbriae
UTI	Urinary tract infection
UPEC	Uropathogenic <i>E. coli</i>
WT	Wild-type

Chapter 1. Introduction

1.1 Background to Project

Uropathogenic *Escherichia coli* (UPEC) are responsible for the majority of uncomplicated and complicated urinary tract infections (UTIs) suffered by patients worldwide (Flores-Mireles et al., 2015). Clinical treatments at present are limited to antibiotics and current National Institute for Health and Care Excellence (NICE) and Scottish Intercollegiate Guidelines Network (SIGN) treatment guidelines for UTIs recommend either Nitrofurantoin or Trimethoprim as first-line antibiotics (NICE, 2021). A consequence of such treatments is antimicrobial resistance (AMR) with resistance reported in 5 and >30% of uro-associated *E. coli* isolates respectively (Carter et al., 2023; Vallee et al., 2023). This resistance is driving global antibiotic stewardship programmes and the need for further understanding of UPEC/urothelial interactions that will help underpin the development of new UTI therapies.

A further concern is that over 25% of all UTI cases, particularly in females, are associated with recurrent infections. The success of UPEC, particularly in females, links to its motility and ability to ascend the urethra, which is shorter in females, into the bladder (Hickling et al., 2015). While flagella underpin UPEC motility this property can be costly as animal and bird tissues have evolved an innate defence mechanism to detect the flagellar filament subunit, flagellin. In humans, the recognition mechanism involves a membrane bound receptor known as Toll-like Receptor-5 (TLR5). TLR5 activation leads to the rapid release of inflammatory cytokines such as interleukin-8 (IL-8) that recruit macrophages and neutrophils to the site of infection, and host antimicrobial agents that directly kill bacteria. To further our understanding of UPEC/urothelial interactions this thesis describes experiments interrogating the interactions between UPEC flagella and the urothelial host responses (Ali et al., 2017).

1.2 Urinary Tract infection (UTI) a global problem

UTIs affect 150 million people around the world every year (O'Brien et al., 2016). UTIs are commonly associated with *Escherichia coli*, originating in the gut, contaminating the lower urinary tract and represent one of the most frequent reasons for those suffering a bacterial infection consulting their health care provider (Foxman, 2002). Women are particularly affected with data suggesting that during their lifetime up to 50% of women will experience at least one case of UTI (Foxman et al., 2003; Micali et al., 2014). While 11% of women over the age of 18 will suffer a case of UTI annually (Foxman & Brown, 2003), UK data suggests up to 57% of these experience three or more episodes, which clinically, is referred to as suffering from recurrent UTIs (rUTIs) (Butler et al., 2015). Recurrent UTIs are defined as two UTI episodes in six months or more than three episodes in 12 months (Sihra et al., 2018), with these repeated infections linking either to a relapse i.e., re-infection with the same strain or reinfection with a different microbe or strain (Kodner & Thomas Gupton, 2010). While rUTIs are debilitating for the patient, these infections also carry significant economic consequences, not only through lost productivity, due to absence from work, but also through the healthcare costs associated with treating the infections. Such costs were estimated at \$3.5 billion in the USA, \$1.5 billion in the European Union (Sihra et al., 2018), and \$26 million is the cost of only primary care in the UK in 1995 (Callan et al., 2014).

UTIs can be classed clinically as either symptomatic or asymptomatic. Symptomatic episodes are characterized by urinary urgency, frequency, pain during urination (dysuria), urine being contaminated by blood and the detection of $> 10^4$ CFU/mL microorganisms in a single voided midstream urine. If not treated, symptomatic UTIs can, particularly in older populations and the immunocompromised, lead to bacteraemia, sepsis, and death (Gonzalez & Schaeffer, 1999). In contrast, asymptomatic bacteriuria (ASB) infections are defined as the presence of bacteria in urine in the absence of clinical symptoms. Many individuals present

with asymptomatic bacteriuria, but particularly older populations, where up to 15% have been reported to be characterized by persistent bacteriuria (Ariathianto, 2011).

UTIs are also classified according to the localization of the infection. Urethritis describes an infection of the urethra, cystitis describes a bladder infection and pyelonephritis is the term used when a patient's kidneys are infected (Figure 1.1) (Stamm & Hooton, 1993).

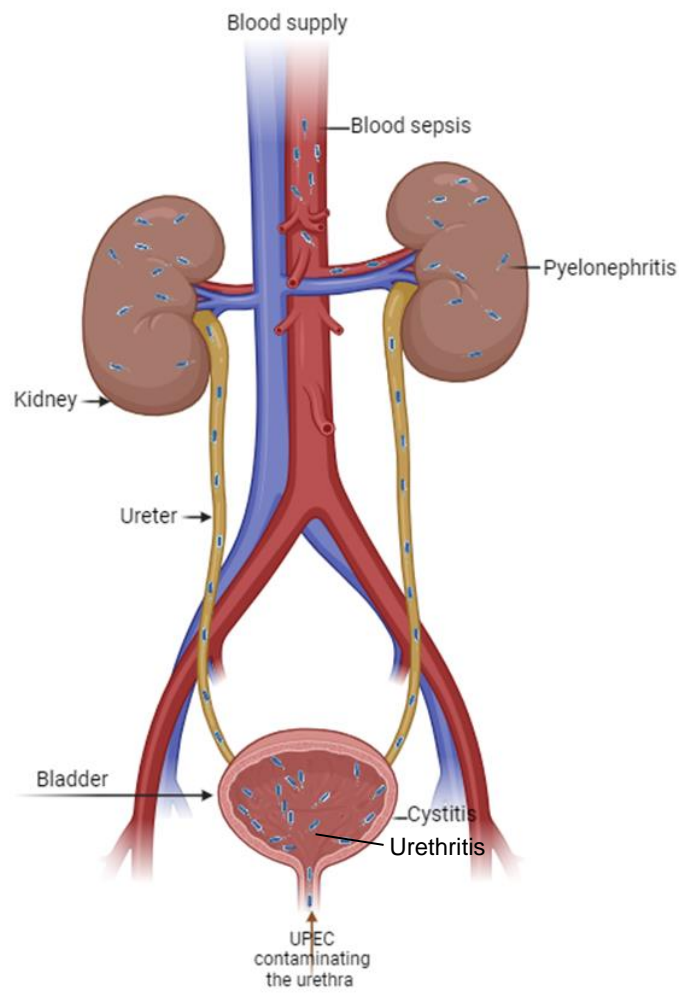


Figure 1.1: Bacterial migration in UTIs. *Escherichia coli* from the gut contaminate the urethra and ascend to the bladder causing Cystitis. In cases left untreated, UPEC may ascend to the kidney causing pyelonephritis. Untreated pyelonephritis may lead to tissue damage and bacteria contaminating the bloodstream causing urosepsis and bacteraemia. Adapted from (Aldridge et al., 2003; Foxman et al., 2003; Kaper et al., 2004).

1.2.1 Complicated and uncomplicated UTI

UTIs can be further described as either uncomplicated or complicated. Uncomplicated infections describe acute bladder infections or cystitis experienced by healthy individuals with no structural or functional urinary tract abnormalities (Sabih & Leslie, 2021). Women suffer more uncomplicated infections than males due to their anatomy i.e., the close proximity of urethral and anal openings, which allows microbes from the gut to contaminate, colonise and infect the urethral and bladder tissues (Heinz et al., 2020). On the other hand, UTIs in immunocompromised individuals, pregnant women, and those associated with fevers, stones, sepsis, urinary blockage, catheters, or involving the kidneys are classified as complicated UTIs (Sabih & Leslie, 2023). These link to either structural and/or functional abnormalities of the urinary tract and to individual cases where there are factors affecting the neurological and/or immunological responses of the patient e.g., damaged spinal cord and/or the use of immunosuppressive drugs (Sabih & Leslie, 2021; Zacche & Giarenis, 2016). Complicated UTI (cUTI) cause more morbidity, have a higher chance of treatment failure, and often necessitate longer antibiotic courses (Sabih & Leslie, 2023). CUTI are also associated with a broad spectrum of causative agents i.e., bacterial species (Wagenlehner et al., 2020).

Some of the most common infections acquired in health care are catheter acquired urinary tract infections (Magill et al., 2014). In the US, up to 80% of catheter acquired UTI are caused by the use of an indwelling urethral catheters (Nicolle, 2014). In long term care facilities, over 50% of episodes of bacteraemia link to catheter associated urinary tract infections (Hooton et al., 2010; Mylotte, 2005).

1.2.2 UTIs and mortality

In UTI paediatric patients, bacterial UTIs have been reported as a common cause of morbidity (Ching et al., 2020). Additionally, UTIs associate with a mortality rate of approximately 2.3% in hospitalized patients (Yang et al., 2022), while the mortality rates linking to severe urosepsis are between 20-42% (Rosser et al., 1999). Globally, 236,790 deaths were associated with an UTI in 2019, which represented a 2.4-fold increase compared to 1990 data (Yang et al., 2022). Such mortalities emphasise the significance of addressing UTIs as a public health concern.

1.3 Host response to UTI

The lower urinary tract tissues defend themselves from infection via their innate host defences. Such responses are rapid when compared to those of the adaptive immune response (Ching et al., 2020). Clinical symptoms, including long-term inflammation and/or infection, are evident when the innate immune system is either overwhelmed, for example by uropathogens, or is compromised immunologically (Zasloff, 2007). The innate immune system is generally composed of physical barriers, for example, the urothelium, pattern recognition receptors (PRR), antimicrobial peptides (AMPs), plasma proteins such as cytokines and phagocytes and molecules such as reactive oxygen species (ROS) (Spencer et al., 2014) (Table 1.1). ROS and reactive nitrogen species (RNS) play critical roles in bacteria death, both directly and indirectly. They are produced by a variety of cell types, including phagocytes, and can directly harm bacterial components like DNA, lipids, and proteins. Upon the ingestion of microorganisms, immune cells such as neutrophils and macrophages activate NADPH oxidase, which catalyses the production of superoxide anions. This process is a key component of the oxidative burst, which is essential for the microbicidal activity of these cells (Morris et al., 2022; Tavassolifar et al., 2020). Superoxide and its derivatives, including hydrogen peroxide and hypochlorous acid, exert direct toxic effects on microbial cells. These

ROS can damage critical components of microbial cells, such as DNA, proteins, and lipids, leading to cell death (Martinvalet & Walch, 2021; Tavassolifar et al., 2020). ROS can disrupt iron-sulfur centers in microbial respiratory chains, impairing their energy production and leading to cell dysfunction and death. Additionally, the increase in ionic strength within the phagosome can facilitate the proteolytic digestion of engulfed microorganisms (Tavassolifar et al., 2020; Wang et al., 2021). On the other hand, RNS can directly damage microbial cells. For instance, NO can inhibit bacterial respiration by affecting the function of heme-containing enzymes, leading to impaired energy production and eventual cell death. Peroxynitrite can modify proteins, lipids, and DNA, causing significant cellular damage. RNS also can inhibit key metabolic pathways in bacteria. For example, they can disrupt the electron transport chain, which is vital for ATP production, thereby compromising the bacterium's energy metabolism and leading to its death (Borisov & Forte, 2022; Martinvalet & Walch, 2021). However, certain bacteria have evolved ways to deal with ROS and RNS, such as antioxidant defence systems and iron sequestration. ROS generation can indirectly improve proteolytic elimination of microbes by increasing the activity of proteolytic enzymes. In rare situations, bacteria may benefit from ROS generation by using it as a metabolic supplement or to liberate iron from ferritin (Li et al., 2020; Zhao & Drlica, 2014) (Figure 1.2).

Table 1.1. List of innate immune system components functioning in the urinary tract

Component	Examples
Physical barriers	Urothelium & Uroplakins
Pattern Recognition Receptors (PRR)	Toll-like receptors (TLRs), and NOD-like receptors (NLRs)
Plasma Proteins	cytokines and phagocytes
Cellular Components	Natural killer cells, epithelial cells, dendritic cells, and bone marrow-derived
Toxic Molecules	Reactive nitrogen and reactive oxygen intermediates
Antimicrobial Peptides (AMP)	Defensins

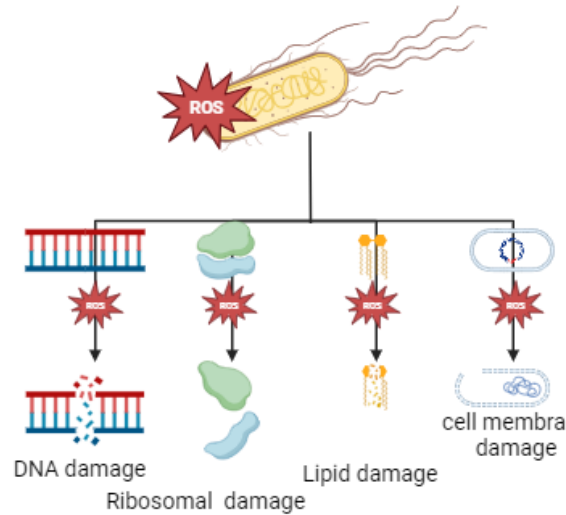


Figure 1.2 ROS antimicrobial effect. These reactive molecules exert antimicrobial effects by damaging bacterial proteins, lipids, and DNA, cell membrane, disrupting essential cellular functions, and ultimately leading to bacterial killing.

1.3.1 Physical barriers

Protection of the bladder from infection by UPEC and/or other potential uropathogens is mediated by physical barriers that include plaque uroplakins which are part of the epithelial barrier (Figure 1.3). Additionally, bladder transitional cells secrete glycosaminoglycans (GAG) (Wu et al., 2009), that create a surface coating of mucin, which works as an anti-adherence factor. These GAGs trap microorganisms, preventing them from destroying the epithelium and facilitate their removal during the urine voiding process (Mulvey et al., 1998). Urothelial cells are also decorated by pattern recognition receptors (PRR), such as Toll-like receptors (TLRs), that detect pathogen - associated molecular patterns (PAMPs). Activation of such receptors results in host defence agents being synthesised and secreted (Abraham & Miao, 2015). Bacterial cells overcome these barriers by adhering to the uroplakins via FimH in the type 1 fimbria also if these barriers got compromised due to other underlying symptoms or change in the pH of the bladder environment.

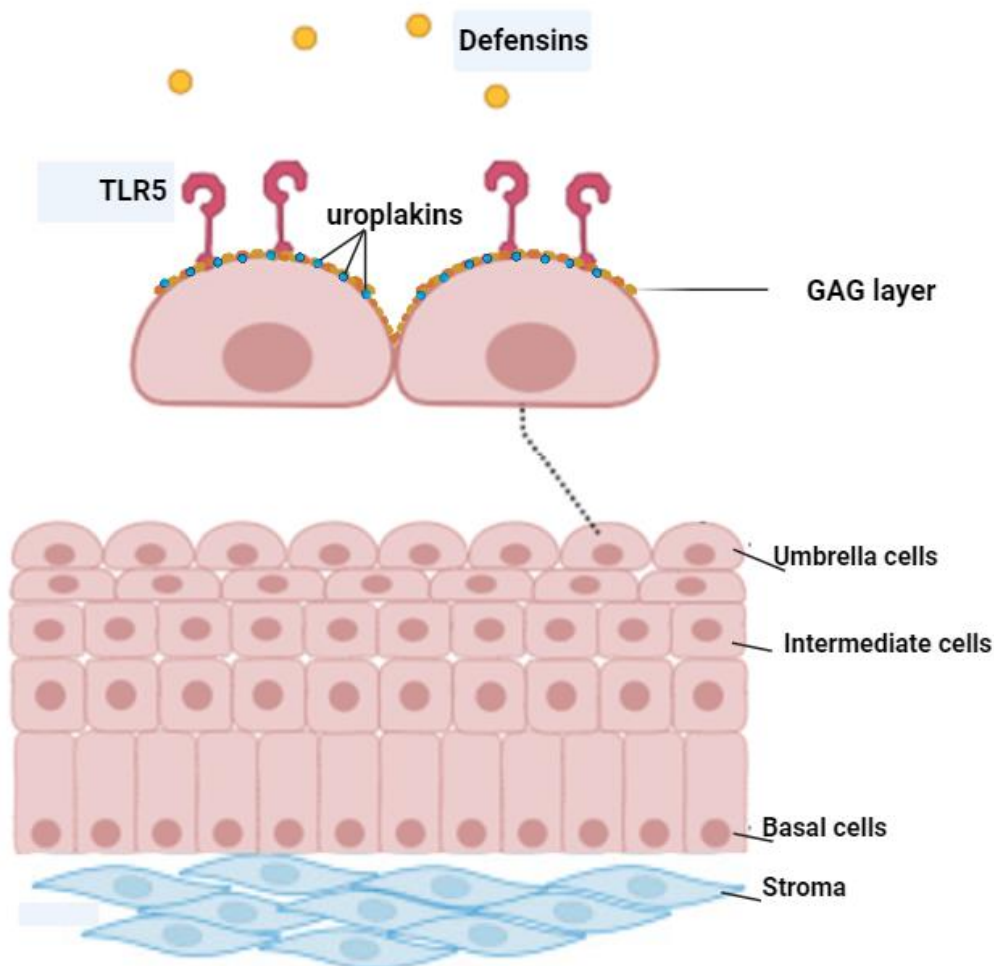


Figure 1.3: Schematic of the urothelium. It shows the components of the urothelium and the physical barrier including GAG layer and the uroplakins. It also shows an example of the PRR, (TLR5), and AMP, (defensins).

Several strategies have been developed by UPEC to ensure its survival and pathogenicity in the bladder environment. To overcome the physical barriers, bacterial cells adhere to the uroplakins via FimH in the type 1 fimbria also if these barriers got compromised due to other underlying symptoms or change in the pH of the bladder environment (Mann et al., 2017). Besides fimbriae, UPEC employs non-fimbrial adhesins that facilitate adhesion and stability on the epithelial surface, hence augmenting their capacity to withstand urinary flushing (Whelan et al., 2023). Once adhered, UPEC can enter bladder epithelial cells via endocytosis. This process is controlled by host cell signalling pathways that reorganise the cytoskeleton, allowing UPEC to be absorbed into vesicles (Mediati et al., 2024). Moreover, UPEC can form biofilms on the bladder epithelium, providing a barrier to

human defences and antibiotic therapy. Biofilms help bacteria survive by forming a barrier against immune reactions and antimicrobial drugs (Whelan et al., 2023).

1.3.2 Pattern recognition receptors (PRRs)

The ability of the host to detect external microorganisms and elicit an appropriate response is one of the most critical aspects of host-pathogen interactions. One of the host mechanisms, which is mediated by PRRs, is the identification of PAMPs or damage-associated molecular patterns (DAMPs) (Li & Wu, 2021). PRRs include TLRs, C-type lectin receptors (CLRs), nucleotide oligomerization domain (NOD)-like receptors (NLRs), absent in melanoma-2 (AIM2)-like receptors (ALRs), and Retinoic acid-inducible gene I (RIG-I)-like receptors (RLRs) (Li & Wu, 2021).

PRR can be expressed by both immune and non-immune cells; the latter includes the umbrella cells of the urothelium, which are decorated by TLRs (Takeuchi & Akira, 2010).

1.3.3 Toll like Receptors in the uroepithelium

Eleven receptors belonging to the TLR family have been described in mammals (Kawai & Akira, 2010). They have been identified in many different tissues including bladder, lung, kidney and gut (Uehara & Takada, 2007), and are typically found on cell surfaces (TLR1, 2, 4, 5, 6, and 11), but they can also be found intracellularly, in the cytoplasm and/or endosomes (TLR3, 7, 8, and 9) (Li & Wu, 2021) (Table 1.2). Interestingly while, TLR11 has been identified in mice and has a potential role in defending the urinary tract from infection (Song & Abraham, 2008) it is not synthesised in humans (Zhang et al., 2004). TLR receptors 1, 2, 4, 5 and 6 have been identified in tissues of the urinary tract (Behzadi & Behzadi, 2016). These recognise the following microbial ligands: lipopeptides (TLR1, 2, 6), LPS (TLR4), and bacterial flagellin (TLR5) (Uematsu & Akira, 2006). TLRs comprise an extracellular domain, to which ligands bind, and an intracellular domain called the Toll/IL-1R(TIR), which is

linked to signal transduction (Kawai & Akira, 2010). Following binding of ligands, TLRs form dimers and this dimer formation activates the signalling pathway.

Table 1.2 Toll-Like receptors and their localization, ligands, and the origin of these ligands.

TLR	Localization	Ligand	Origin of the Ligand
1	Plasma membrane	Triacyl lipoprotein	Bacteria
2	Plasma membrane	Lipoprotein	Bacteria, viruses, parasites, self
3	Endolysosome	dsRNA	Virus
4	Plasma membrane	LPS	Bacteria, viruses, self
5	Plasma membrane	Flagellin	Bacteria
6	Plasma membrane	Diacyl lipoprotein	Bacteria, viruses
7	Endolysosome	ssRNA	Virus, bacteria, self
8	Endolysosome	ssRNA	Virus, bacteria, self
9	Endolysosome	CpG-DNA	Virus, bacteria, protozoa, self
10	Endolysosome	Several	Bacteria, viruses, parasites, self
11	Plasma membrane	Profilin-like molecule	Protozoa

TLR4 function has been well studied in the urinary tract of mice (Beutler, 2000; Ching et al., 2020; Ragnarsdottir et al., 2010; Zhang et al., 2008). Studies have shown TLR4 activation following the binding of microbial lipopolysaccharide, but also following binding of FimH, the adhesin portion of the Type 1 fimbriae that secures UPEC attachment to urothelial cells (Song & Abraham, 2008).. The TLR4 receptors studied were located on the surface of bladder umbrella cells and, interestingly, Type 1 fimbriae binding was associated with exfoliation (Song & Abraham, 2008). While *in vitro* experiments suggest TLR4 plays a minor role in human bladder defences (Ali et al., 2017; Smith et al., 2011), has been shown using gene association studies that a TLR4 polymorphism, which leads to an LPS-hyporesponsive TLR4 is associated with a lower incidence of rUTI in adult women (Hawn, Scholes, Li, et al., 2009). TLR4 is also found expressed in the urethral cells lining the kidneys (Behzadi & Behzadi, 2016) where it plays a significant role in defending against infection (Zhang et al., 2008).

While TLR4 recognises multiple ligands, TLR5 proteins recognise only flagellin (FliC), the subunit forming the filament of the bacterial flagella, which is responsible for

bacterial motility (Hayashi et al., 2001). Clinical observations and *in vitro* experiments support TLR5 being the key PRR in protecting humans from lower UTIs (Ali et al., 2017) and these observations are strengthened by experiments involving wild-type and TLR5 knockout mice (Andersen-Nissen, *et al* , 2007). Additionally, in adult humans, a TLR5 gene polymorphism associated with the synthesis of a truncated receptor links to recurrent UTIs (Ali et al., 2017; Hawn, Scholes, Wang, et al., 2009).

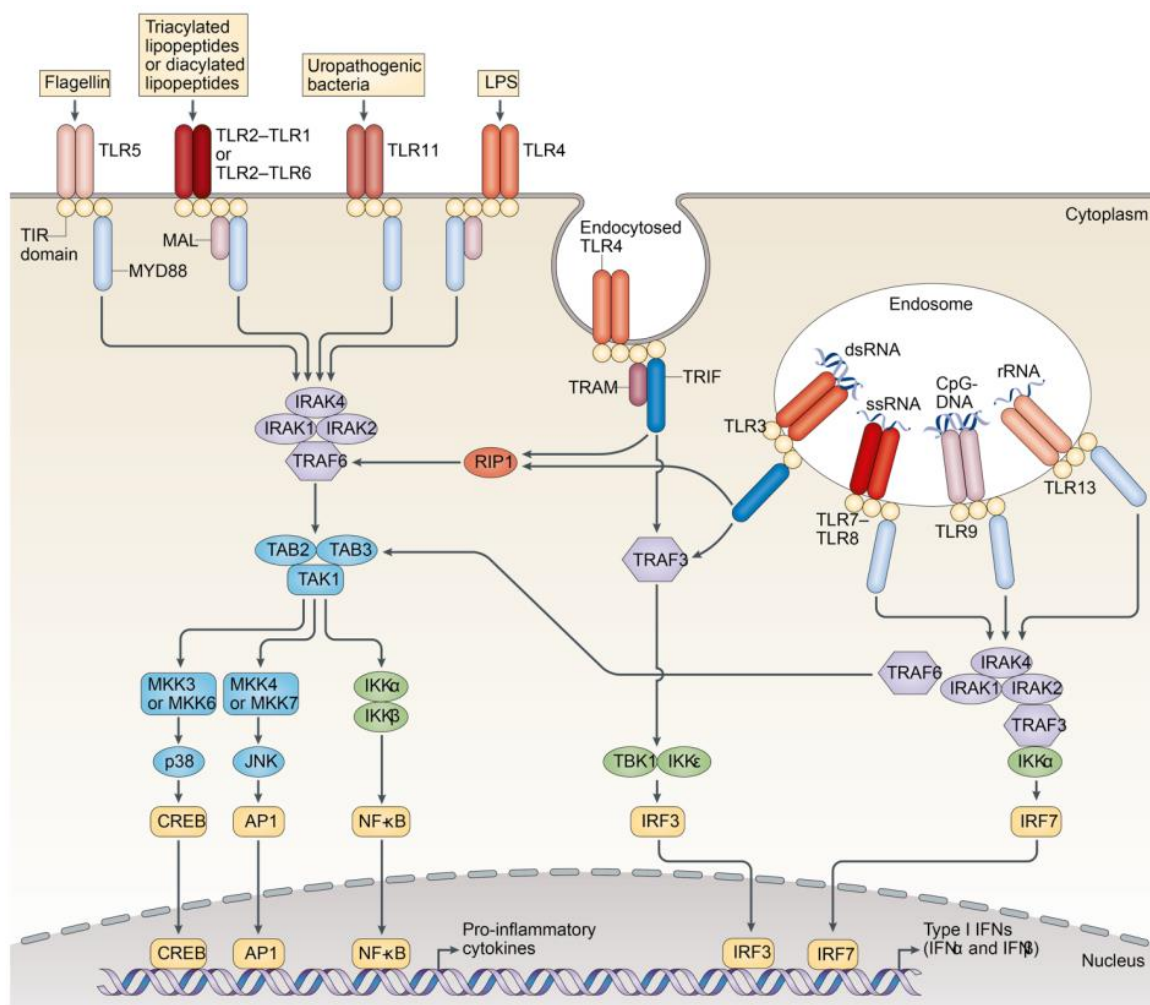
1.3.4 Innate response signalling pathways activated by TLRs

There are two key pathways, one being MyD88-dependant and the other MyD88-independent (O'Neill & Bowie, 2007; Satoh & Akira, 2016) (Figure 1.4). MyD88 binding to TLRs initiates a signalling cascade that activates NF- κ B and other transcription factors including CREB and API, resulting in the induction of genes involved in the inflammatory response (Cohen & Strickson, 2017; Kawai et al., 2004). TIRAP is a sorting adaptor that recruits MyD88 to cell surface TLRs including TLR5 (Figure 1.4) (O'Neill et al., 2013; von Bernuth et al., 2008). MyD88 binds to the TIR domain of TLRs, and it recruits IL-1R-related kinase 4 (IRAK4) and through autophosphorylation of its central domain it activates IRAK1 and IRAK2 (De Nardo et al., 2018). Then it recruits TNF receptor-associated factor 6 (TRAF6) forming a complex after combining with two TAK-binding proteins (TAB1 and TAB4) and transforming growth factor (TGF)- β -activated kinase 1 (TAK1) (Hacker et al., 2006; Verstak et al., 2009) (Figure 1.4). TRAF6 is degraded and the complex composed of TAK1–TAB1–TAB4 activates the I κ B kinase via phosphorylation (Kawai et al., 2004). Activation of the signalling pathway results in the translocation of the transcription factor Nuclear factor- κ B (NF- κ B), to the nucleus to regulate the transcription of genes encoding proteins involved in the host inflammatory response (Cohen & Strickson, 2017; Kawai et al., 2004).

In some cases, following the initiation by ligand binding to receptors (specifically TLR1,2,4,6), the TIR domains involve TIR domain-containing adaptor proteins (either TIR domain-containing adaptor protein inducing IFN β (TRIF) and TRIF-related adaptor molecule (TRAM), or MYD88-adaptor-like protein (MAL) and myeloid differentiation primary-response protein 88 (MYD88).

The pro inflammatory response includes the release of cytokines such as Interleukins 8 and 6 (IL-8; IL-6) that attract neutrophils and macrophages to the infection site. Other agents released include host defence peptides, e.g., defensins, that directly kill microbes and, for example, host defence proteins such as Neutrophil gelatinase associated lipocalin (NGAL) that chelate iron and impact microbial growth (Ali et al., 2017; Mowbray et al., 2018).

During an UTI, cytokine signalling is critical for the innate immune response (Abraham & Miao, 2015). Cytokines are small proteins that are released to facilitate cell-to-cell communication via autocrine, paracrine, and/or endocrine effects (Ching et al., 2020). Interleukins (ILs) are cytokines that are often produced by inflammatory cells and have action on immune cells, whereas chemokines are cytokines that have chemotactic features (Ragnarsdottir & Svanborg, 2012). The cytokine IL-6 plays multiple roles in UTI prevention (Ching et al., 2020; Khalil et al., 2000). To facilitate UPEC clearance, IL-6 not only stimulates AMP expression (Ching et al., 2020), but inhibits intramacrophage UPEC growth by regulating monocyte proliferation and altering iron homeostasis (Dixit et al., 2018; Owusu-Boaitey et al., 2016). Its role in protecting mice from UTIs is clearly shown in IL-6 knock-out (Δ IL-6) mice, which, when infected, with uropathogens are characterised by higher death rates and more severe renal histopathology, compared to their wild-type siblings (Ching et al., 2020; Khalil et al., 2000). In mice, IL-6 deficiency is also associated with the increased frequency of UPEC intracellular bacterial communities (IBC) during early cystitis, allowing UPEC to evade the innate immune system and contributing to recurrent UTIs (Ching et al., 2018).



(O'Neill et al., 2013)

Figure 1.4: Schematic of host signalling pathways triggered by TLRs. TLR1, 2, 4, 5, 6, 11 are exogenous TLRs while TLR3, 7, 8, 9, 13 are endocytosed. All TLRs signalling pathways are MyD88 dependant except TLR3 and endocytosed TLR4, which are TRIF dependant pathways. In case of flagellin, TLR5 utilizes MyD88 dependant signalling pathway leads to the activation of IRAK4,1,2 then the recruiting of TRAF6 leads to the combination of TAB1, TAB4 and TAK1 which leads to the activation of the I κ B kinase leading to the translocation of NF- κ B to the nucleus. NF- κ B regulate the transcription of genes encoding proteins involved in the host inflammatory response such as IL-8. IKK, inhibitor of NF- κ B kinase; MKK, MAP kinase kinase; RIP1, receptor-interacting protein 1; TAK, TGF β -activated kinase; TAB, TAK1-binding protein; TBK1, TANK-binding kinase 1.

Interestingly however, a study in our laboratory focussed on older populations of rUTI patients did not identify IL-6 as a major cytokine in rUTI. Data showed that the pro-inflammatory cytokines IL-1 β and IL-8, and the anti-inflammatory cytokines IL-5 and IL-10, were more clinically relevant (Drage et al., 2019).

IL-8 levels are elevated following UT infections with UPEC (Bien et al., 2012; Hedges et al., 1994; Mowbray et al., 2022). IL-8 plays a vital role in clearing the urogenital tract of UPEC by recruiting neutrophils (Agace, 1996; Bien et al., 2012; Hang et al., 1999). This is achieved through interactions with the IL-8 receptors CXCR1 and CXCR2 (Weichhart et al., 2008). This has been clearly shown in mice deficient in the IL-8 receptor; these mice were more susceptible to UTI with bacterial loads increased in the bladder and kidneys compared to wild type mice. This observation was linked to the reduced migration of neutrophils to the infection site (Freundt et al., 2000).

1.3.5 Adaptive response signalling pathways in the bladder

In contrast to kidney infections, lower UT infections are not associated with antibody production and the lack of an adaptive response is often used to explain why patients suffer from lower rUTIs (Abraham & Miao, 2015). The absence of an adaptive response in the bladder has been linked to IL-10 synthesis although these links relate to work in mice. Essentially mice deficient in IL-10 are characterised by antibody responses to a bladder infection (Chan et al., 2013). A source of IL-10 production in urothelial tissues following an infection is mast cells. While mast cells are known to induce a pro-inflammatory response early in a bladder infection this response is switched within 6 hours to an anti-inflammatory response, which involves IL-10 production. This switch happens, presumably, to help manage the inflammatory response to the infection. Moreover, IL-10 molecules are able to inhibit the expression of co-stimulatory molecules on dendritic cells (DC), which not only

prevents DC from functioning as antigen presenting cells, but additionally also conditions DCs to form suppressive T cells. These observations suggest that IL-10 molecules attenuate the innate and adaptive urothelial immune responses meaning the bladder cannot mount an antibody response to bacterial infection. This response to bacterial infection has been explained as a mechanism to prevent the occurrence of potentially harmful adaptive immune responses when urinary molecules make contact with the urothelium (Ortega Martell, 2020; Wiles et al., 2008).

1.4 Genetic Risk of Recurrent Urinary Tract Infections

As mentioned previously, clinical observations in females have suggested a genetic link to UTI susceptibility (Ali et al., 2009; Hawn, Scholes, Li, et al., 2009; Stauffer et al., 2004). As highlighted the polymorphism TLR4_A896G associates with protection from rUTI, while the polymorphism TLR5_C1174T, links to an increased risk of rUTI. *In vitro* and clinical studies within our laboratory further suggested that the TLR5 polymorphism, associated with a truncated TLR5 receptor, links to reduced innate host defences i.e., defensin and pro-inflammatory urinary responses, which helps explain patient susceptibility to rUTIs (Ali *et al.* 2017). Interestingly, an increased risk of ASB is associated with the TLR2_G2258A SNP although the mechanism(s) underpinning such risk is not known (Hawn, Scholes, Wang, et al., 2009; Tabel et al., 2007).

1.5 UTI treatment

The National Institute for Health and Care Excellence (NICE) guidelines recommend treating UTI cases with a course of antibiotics (NICE, 2018), but also advocate good patient hydration and hygiene practices (NICE, 2021). NICE guidelines (October 2018) advise a short, 3-day, course of antibiotics, specifically Nitrofurantoin or Trimethoprim for symptomatic uncomplicated UTIs. Nitrofurantoin is reduced to generate reactive

intermediates by flavoproteins and nitroreductases. These reactive intermediates interfere with ribosomal proteins, enzymes involved in biosynthesis like citric acid cycle, DNA, RNA, and protein synthesis. On the other hand, Trimethoprim blocks the metabolism of folate by inhibiting the bacterial enzyme, dihydrofolate reductase (DHFR), Which is responsible of catalysing the reduction of dihydrofolic acid (DHF) to tetrahydrofolic acid (THF). The later is essential for the synthesis of bacterial DNA and RNA. However, despite being prescribed antibiotics, up to 50% of women report further symptomatic infections within six months of their initial treatment leading to diagnosis of recurrent rUTI (Butler et al., 2015). In these cases, NICE guidelines suggest prophylactic antibiotic treatments (6-12 months) with the choice of antibiotics directed by local antimicrobial resistance data. However, many of these women suffer from a constant cycle of repeated infections and antibiotic therapies that select for multidrug-resistant bacteria, which colonise their urinary and faecal microflora, and worsen the problem. Essentially, antibiotic resistant urine infections compromise both patient safety and long-term treatment options, and clinically become challenging and expensive to manage (Lecky et al., 2020).

Urologists treating rUTI patients and needing to address antimicrobial resistance have introduced antibiotic stewardship programmes www.nice.org.uk/guidance/ng15 and reassessed non-antibiotic management options. Present alternative strategies are wide-ranging and primarily, but not always, preventative (Table 1.3). The clinical use of these treatments is also limited, compromised by the lack of randomised control trials (RCTs) (Sihra et al., 2018). However, NICE guidelines do allow medical practitioners discretion to recommend some unlicensed treatment options, including vaginal oestrogen creams, cranberry and D-mannose products. Of those products tested clinically via RCTs, some such as Methenamine Hippurate have shown positive outcomes (Harding et al., 2022). Other outcomes have been disappointing. For example, the use of oral probiotics, predicted to impact the gut microbiota

and hence reduce UPEC contamination, were not found to be beneficial in reducing UTI frequency in older populations residing in care homes (Butler et al., 2020). One more recent approach is the use of the sublingual vaccination, MV140. A recent report suggests this treatment reduces the risk of rUTIs, although the outcomes were observational and prospective (Nickel & Doiron, 2023), and need to be further verified by a RCT.

Antibiotics§	Nitrofurantoin
	Trimethoprim
Probiotics	<i>Lactobacillus</i>
	<i>Bifidobacterium</i>
	<i>avirulent E. coli*</i>
Others	Cranberry products
	Vaginal oestrogen
	Hyaluronic acid cream
	D-mannose
	Synthetic mannosides (GSK38823470- Phase1)
	Methenamine Hippurate
Vaccines	

Table 1.3: Treatment strategies for UTI § NICE guidelines * for complicated UTIs. Adopted from Barclay *et al.*, (2017) and Saini *et al.*, (2010).

A second line of antibiotics used in cases of first line failures include pivmecillinam hydrochloride and amoxicillin (NICE, 2021). Amoxicillin, however, is only prescribed for UTIs where sensitivity reports indicate resistance (NICE, 2021). Both of pivmecillinam and amoxicillin are beta-lactams which inhibit cell wall biosynthesis by binding to penicillin binding protein leading to disruption of cell wall and bacterial death (Dewar et al., 2014; Graninger, 2003).

A course of ciprofloxacin or cefalexin is used also to manage upper UTIs (NICE, 2018). Ciprofloxacin is a member of fluoroquinolone antibiotic family that kills bacteria by inhibiting their DNA gyrase and topoisomerase enzymes, which are essential for bacterial DNA replication and repair. On the other hand, cefalexin is a cephalosporin antibiotic which is a β -lactam antibiotic. The chemical structure of mentioned antibiotics is presented in

(Figure 1.5). Patients suffering from upper UTI, but at high risk of developing sepsis are usually treated with intravenous antibiotics (Poh et al., 2021).

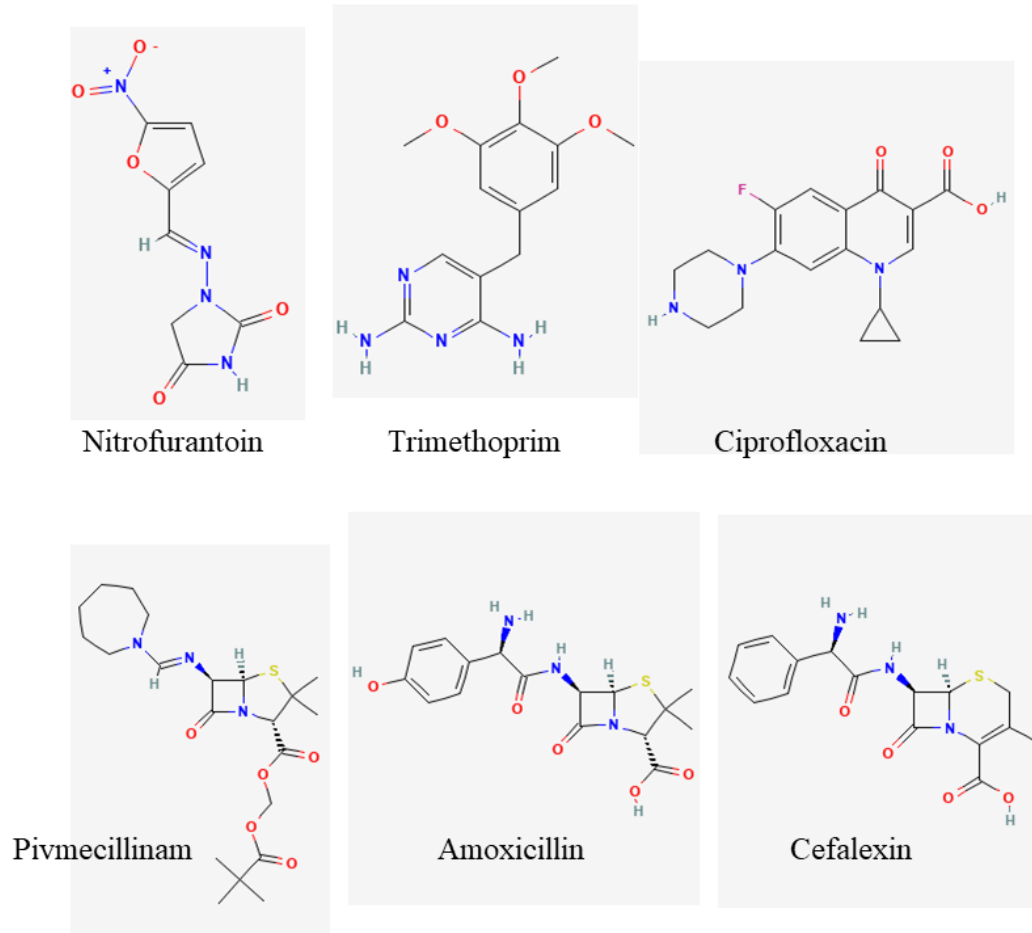


Figure 1.5 Schematics presenting the chemical structure of some antibiotics that commonly used to treat UTIs.

1.6 Uropathogens associated with UTIs

UTIs can be caused by either Gram negative or Gram-positive bacteria and more rarely *Candida* species (Serretiello et al., 2021). In both complicated and uncomplicated UTIs, UPEC is the most common agent, recovered in up to 90% of infections (Serretiello et al., 2021). However, other microbes including *Staphylococcus saprophyticus* (2-6% cases), *Proteus mirabilis* (2%), *Enterococcus faecalis* (5-11%), *Klebsiella pneumonia* (6-8%),

Pseudomonas aeruginosa (2%), and *Staphylococcus aureus* (1-3%) have also been identified (Flores-Mireles et al., 2015).

1.6.1 *Escherichia coli*

E. coli is a flagellated, non-spore-forming, rod-shaped, facultative anaerobic, Gram-negative bacteria, that ferments glucose (Berg, 1996). It is part of the intestinal commensal flora of humans, as well as other mammals, reptiles and birds, but *E. coli* strains can also cause diseases ranging from mild, self-limited gastroenteritis to renal failure and septic shock (Kaper et al., 2004; Lukjancenko et al., 2010; Mueller & Tainter, 2023; Tenailon et al., 2010). *E. coli* has an established phylogenetic classification, and *E. coli* isolates are classified into seven clades: A, B1, B2, C, D, E and F (Chaudhuri & Henderson, 2012).

1.6.2 *E. coli* pathovars

Pathogenic strains of *E. coli* are implicated in many human and animal diseases with pathovars classified as intestinal *E. coli* (IPEC) or extraintestinal *E. coli* (ExPEC) (Russo & Johnson, 2000). Enteroaggregative *E. coli* (EAEC), enterohaemorrhagic *E. coli* (EHEC), enteroinvasive *E. coli* (EIEC), enteropathogenic *E. coli* (EPEC), enterotoxigenic *E. coli* (ETEC), diffusely adherent *E. coli* (DAEC), and adherent invasive *E. coli* (AIEC) are the subgroups of the IPEC, while UPEC, neonatal meningitis *E. coli* (NMEC), and avian pathogenic *E. coli* (APEC) belong to the ExPEC (Crossman et al., 2010; Croxen & Finlay, 2010; Croxen et al., 2013). The *E. coli* strains, which belong to these pathovars, reside in clades A, B1, B2, C, D, and E respectively (Chaudhuri & Henderson, 2012; Hazen et al., 2016; Meza-Segura et al., 2020).

1.6.3 Enteropathogenic *E. coli* (EPEC)

There are around 1.7 billion cases of diarrhoea among children worldwide every year, with diarrhoea being the second leading cause of morbidity among children under 5 years of

age (WHO, 2017). A common causative agent of severe diarrhoea in infants under three years is EPEC (Lapointe et al., 2009; Nataro & Kaper, 1998).

EPEC is a member of the attaching and effacing (A/E) family of pathogens as attachment to gut epithelia leads to loss (effacement) of absorptive microvilli i.e. A/E lesions (Knutton et al., 1989). A/E lesions are produced in a three-stage process: initial non-intimate attachment, via bundle forming pilis, to the microvillus surface followed by the pathogens sinking into microvilli linked actin-rich pedestal structures forming beneath the adherent bacteria and finally the loss of absorptive microvilli (Knutton et al., 1989). A/E family members share a homologous region on their genome called the locus of enterocyte effacement (LEE) which encodes a type III secretion system (T3SS). This T3SS transfers ‘effector’ proteins from the bacterial cytoplasm to the host cytosol where their subversion of cellular processes leads to disease (Donnenberg et al., 1997; Jarvis & Kaper, 1996).

T3SSs are found in many Gram-negative bacterial pathogens (Buttner, 2012). The T3SS can be divided into three main parts: basal body, needle and translocon (Abrusci et al., 2014). The basal body is formed by protein forming rings, which span the inner and outer membranes, like a socket, with a central rod (Kubori et al., 1998) (Figure 1.6). Extending from the basal body is the needle component with a hollow core wide enough to accommodate unfolded proteins (Deane et al., 2006; Kubori et al., 1998). The needle is, in A/E pathogens, also extended by polymerization of a EPEC secreted/signalling protein (EspA). This filament is tipped by other translocon proteins, EspB and EspD, that insert into host membrane to complete an effector-delivery conduit (Hakansson et al., 1996; Holmstrom et al., 2001).

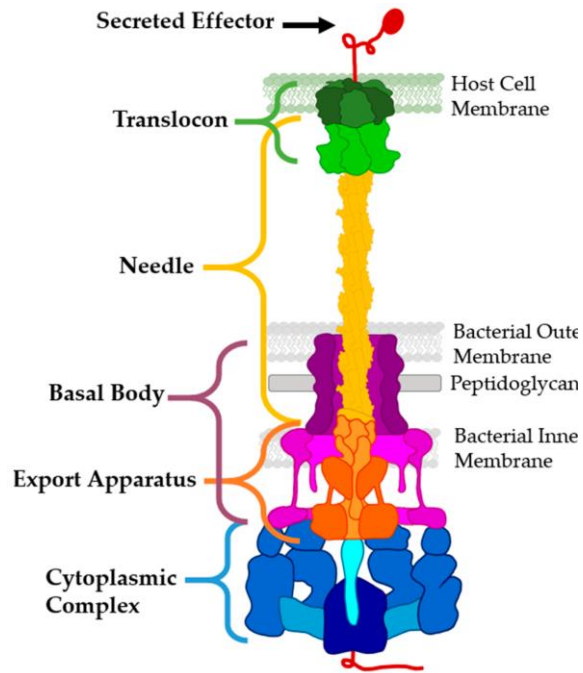


Figure 1.6 A schematic of T3SS. It shows cytoplasmic complex, Export apparatus, basal body, needle, and translocon. The T3SS cytoplasmic-associated proteins play control the timely secretion of rod proteins, then needle, then translocators. Taken from (Hotinger et al., 2021).

1.6.4 Enterohaemorrhagic *E. coli* (EHEC)

EHEC is also a member of the attaching and effacing (A/E) family (Knutton et al., 1989). EHEC produce Shiga-like toxins (Stx), which facilitate adhesion of the bacteria to ileal and large intestinal cells, as well as inactivation of NF- κ B leading to a repressed inflammatory response (Gobert et al., 2007). This results in severe gastroenteritis and bloody diarrhoea, which if not treated can lead to haemolytic uraemic syndrome (Kaper et al., 2004). Stx are also associated with haemolytic uraemic syndrome and acute renal failure (Eaton et al., 2008).

1.6.5 Enterotoxigenic *E. coli* (ETEC)

ETEC pathovar is mostly responsible for travellers' diarrhoea and deadly diarrhoea in piglets (Nataro & Kaper, 1998). ETEC attaches to host small intestinal cells through

synthesis of colonization factors called coli surface antigens, which include CFA/II and CFA/IV. These are expressed via virulence plasmids (Qadri et al., 2005). Two types of toxins are secreted by this pathovar: a heat-labile enterotoxin (LT), and a heat-stable enterotoxin (ST), which are involved in different virulence pathways (Croxen & Finlay, 2010). Another toxin secreted by ETEC is CylA, which is a cytotoxin that forms pores in target host cells (Turner et al., 2006).

1.6.6 Enteroinvasive *E. coli* (EIEC)

EIEC display the same pathogenicity mechanisms as *Shigella*, and infection with EIEC results in dysentery, invasive inflammatory colitis and watery diarrhoea (Kaper et al., 2004). A T3SS carried on a 220 Kbp plasmid facilitates infection of host gut cells (Schroeder & Hilbi, 2008). Additionally, this pathovar can cause the apoptosis of macrophages through invading them (Schroeder & Hilbi, 2008). *Shigella* enterotoxin 2 (ShET-2) is produced by EIEC and the genes encoding this toxin are chromosomally encoded (Farfan & Torres, 2012).

1.6.7 Enteroaggregative *E. coli* (EAEC)

The mucosa of both the large and small intestine are the infection sites of EAEC and infection is associated with mucoid, watery and bloody diarrhoea (Nataro & Kaper, 1998). A 100 Kbp plasmid encodes aggregative adherence fimbriae (AAFs) that are part of the Dr family of adhesions (Croxen & Finlay, 2010). A IncII plasmid also encodes type IV pili (Dudley et al., 2006). A toxin termed plasmid encoded toxin (Pet), one of multiple types of toxins produced by EAEC, causes exfoliation of host cells linked to the breakdown of the cytoskeleton protein, α -fodrin (Navarro-Garcia & Elias, 2011). EAEC also produces ShET-1 and the heat stable toxin EAST-1 (Croxen & Finlay, 2010).

1.6.8 Diffusely adherent *E. coli* (DAEC)

DAEC causes diarrhoea in children by infecting the small intestine and has been reported in adult rUTI cases (Nowicki et al., 2001) and pyelonephritis (Selvarangan et al., 2004). The bacterial cells attach to host cells using fimbrial and afimbrial adhesins (Servin, 2005) via carcinoembryonic antigen-related cell adhesion molecule (CEACAM) and decay accelerating factors (DAF) receptors (Le Bouguenec & Servin, 2006). Studies have shown that bacterial binding to such receptors is associated with IL-8 production. This attracts neutrophils to the infection site, which in turn leads to the expression of more DAF (CD55) receptors that enhance bacterial binding (Betis et al., 2003).

1.6.9 Adherent invasive *E. coli* (AIEC)

AIEC are able to adhere and invade intestinal epithelial cells via CEACAM6 receptors (Barnich et al., 2007). Interestingly, the ileal tissues of patients with Crohn's Disease (CD), a disease of the gastrointestinal tract, have been found to be colonized by AIEC. In such patients the first inflammatory lesions are often seen as microscopic erosions of the epithelium lining the Peyer's patches (PPs). Studies using mice and human tissues have shown that AIEC bacteria interact with the PPs via long polar fimbriae (LPF). Moreover, when analysed the number of AIEC strains carrying the *lpf* operon was markedly higher in CD patients compared to controls, which supports a role for AIEC in the pathogenesis of CD (Chassaing et al., 2011).

1.6.10 Uropathogenic *E. coli* (UPEC)

The majority of host commensal strains are found in the A and B1 phylogroups (Chakraborty et al., 2016). In contrast UPEC strains, based on their genetic diversity, can be sorted into phylogroups B2, D and less commonly, E (Chaudhuri & Henderson, 2012), with

laboratory UPEC isolates, including UTI89, CFT073 and NU14 characterised as members of the B2 family. In Europe and the United States most UPEC clinical strains affiliate to the B2 clade (Wiles et al., 2008).

1.7 Virulence factors of UPEC

UPEC are characterized by specific virulence factors which facilitate their infection of the urinary tract and these factors include, siderophores, toxins, pili and flagella.

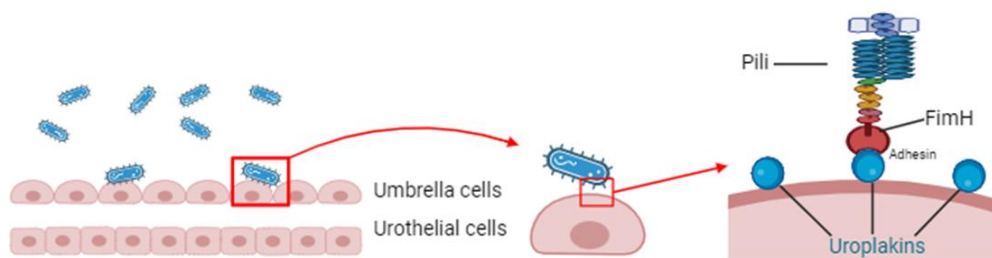
Siderophores enable UPEC to acquire free or protein-bound iron from either urine, the uroepithelium, or haem proteins (Robinson et al., 2018). Aerobactin, enterobactin and its glucosylated derivative salmochelin, and yersiniabactin are examples of functioning siderophores (Garcia et al., 2011). When compared to commensal *E. coli* strains isolated from faeces, the salmochelin and yersiniabactin siderophores are more frequently found among UPEC isolates (Henderson et al., 2009).

Another UPEC virulence factor facilitating infection of the urinary tract is the secretion of toxins; toxins include α -hemolysin, secreted autotransporter toxin (sat), and cytotoxic necrotising factor 1 and 2. α - Haemolysin (HlyA) is a key toxin that creates pores in host cells and causes their lysis, which releases iron and allows the infecting bacteria access to essential nutrients (Wang et al., 2020). Action of these toxins supports siderophore activities allowing these scavenging molecules better access to iron (Laestadius et al., 2002; Wang et al., 2020).

Pili or fimbriae are adherence proteins (Johnson, 1991) which are involved in attaching UPEC to the uroepithelium (Johnson, 1991). P-fimbriae and Type 1 fimbriae are the two major pili studied in UPEC isolates (Connell et al., 1996; Lane & Mobley, 2007). It has been observed that Type P fimbriae facilitate UPEC adhesion to the renal epithelium rather than the bladder epithelium (Wullt et al., 2000). P-fimbriae attach to renal cells through a PapG adherence molecule which recognises-D-galactopyranosyl-(1-4)-D-galactopyranoside, a

prominent glycolipid found in the renal epithelium. Interestingly, one study reported that only one-third of clinical isolates recovered from cystitis patients carried genes involved in P-fimbriae production (Tiba et al., 2008). Type 1 fimbriae facilitate bacterial attachment to urothelial tissues (Gunther et al., 2001). These fimbriae are helical rods of repeated FimA subunits with a FimH subunit at the distal tip. They attached to specific mannoseylated receptors on the urothelial cell surface, which results in an inflammatory response and exfoliation of the urothelial cells (Bouckaert et al., 2006; Schilling et al., 2001; Thumbikat et al., 2009) (Figure 1.7 A &B).

A



B

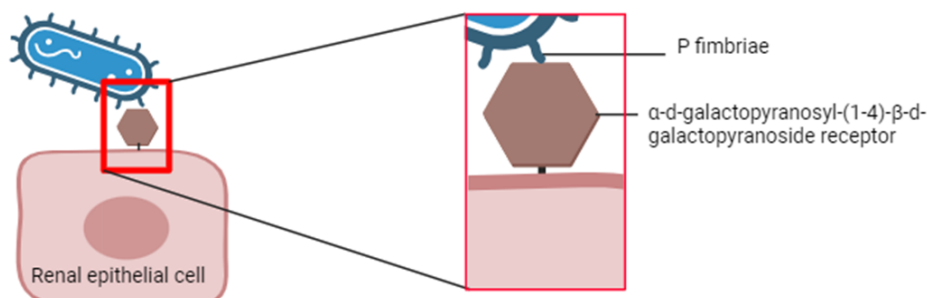


Figure 1.7 UPEC adhesion to epithelia. A) FimH adhesins found on pili bind to mannoseylated proteins called uroplakins that coat the urothelial surface in the bladder. B) Pyelonephritis-associated (P) pili (P fimbriae) interacts with glycolipid receptors (globosides) located on renal cell membranes in the kidney (Davis et al., 2010).

Uncomplicated UTIs are ascending infections. Ascension of the urinary tract by *E. coli* involves bacterial motility, which is driven by flagella (Kaper et al., 2004). Interestingly, UPEC motility and adherence to the urothelium appear interconnected (Lane et al., 2007; Simms & Mobley, 2008). This is supported by studies in vitro, using the UPEC strain CFT073, which have shown that constitutive expression of type 1 fimbriae is linked to reduced flagellin expression and bacterial motility (Lane et al., 2007). However, studies also suggest this relationship to be unidirectional as flagellar mutants did not upregulate type 1 fimbriae expression.

1.8 Flagellar components and their synthesis

The flagellum spans the bacterial membrane; assembly starts at the base embedded within the inner membrane and distal components are secreted by a type III secretion system through the base of the structure (Macnab, 1999). For a bacterial flagellum to be assembled and functional, over 50 genes are required to produce structural subunits, the chemosensory machinery, the motor force generators and regulatory proteins (Chilcott & Hughes, 2000). The flagellum is divided into two substructures: a hook-basal-body (HBB) that spans the bacterial membranes and an external filament (Figure 1.8).

The structure is assembled in a step-by-step procedure that begins with the insertion of the MS-ring into the inner membrane. After the assembly of an associated type III secretion system (T3SS), the individual extra cytoplasmic flagellar subunits are secreted through the MS-ring. The motor force generators, serve as stators against the C-ring, which is composed of three structural proteins connected with the cytoplasmic face of the MS-ring. The motor force generators act as proton pumps and the movement of protons generates the necessary energy to rotate the HBB structure (Lloyd et al., 1996).

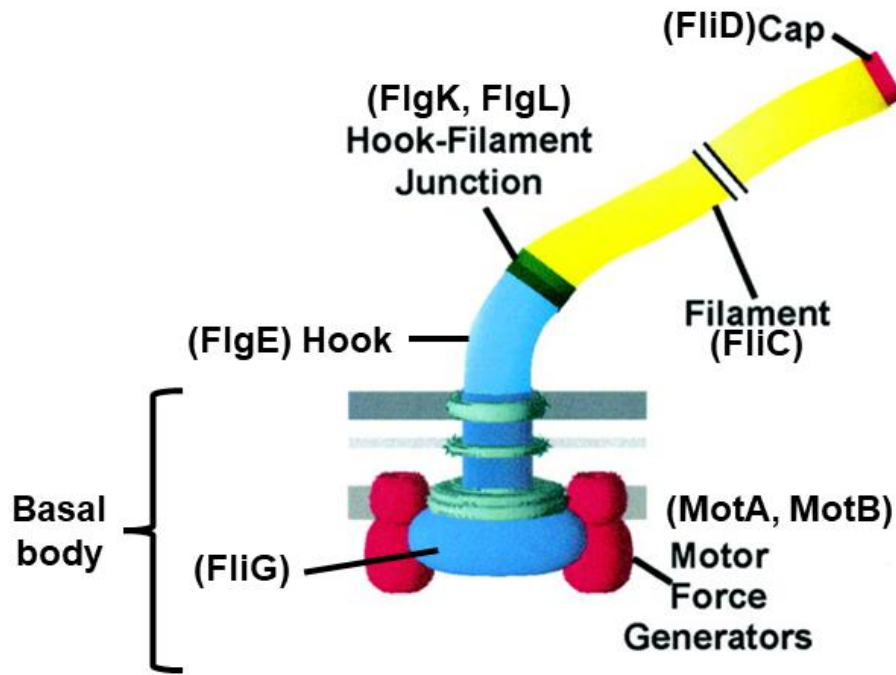


Figure 1.8: Schematic of the bacterial flagella. Schematic shows the basal body, the hook, and the filament. The filament is formed by subunits of FliC and capped by FliD while the junction between the filament and the hook comprises FlgK and FlgL. The hook is formed by FlgE subunits; MotA and MotB are part of the motor force generator, while FliG is part of the C-ring. Adopted from (Aldridge et al., 2003).

The link between the filament and the basal body is a cylindrical structure called the hook, formed by FlgE (Macnab, 2003). During assembly the growing extra cytoplasmic structure is always capped. For example, the rod that spans the periplasmic space in *E. coli* is capped by FlgJ, that facilitates the localised degradation of peptidoglycan to let the assembling flagellum pass through (Nambu et al., 1999). On rod completion FlgJ will be replaced by the hook cap, FlgD. On completion of the hook, FlgD is replaced by the filament cap, FliD. Once FliD is in place, the hook-filament junction is formed by FlgK and FlgL which allows filament formation to begin (Homma et al., 1984; Macnab, 2003).

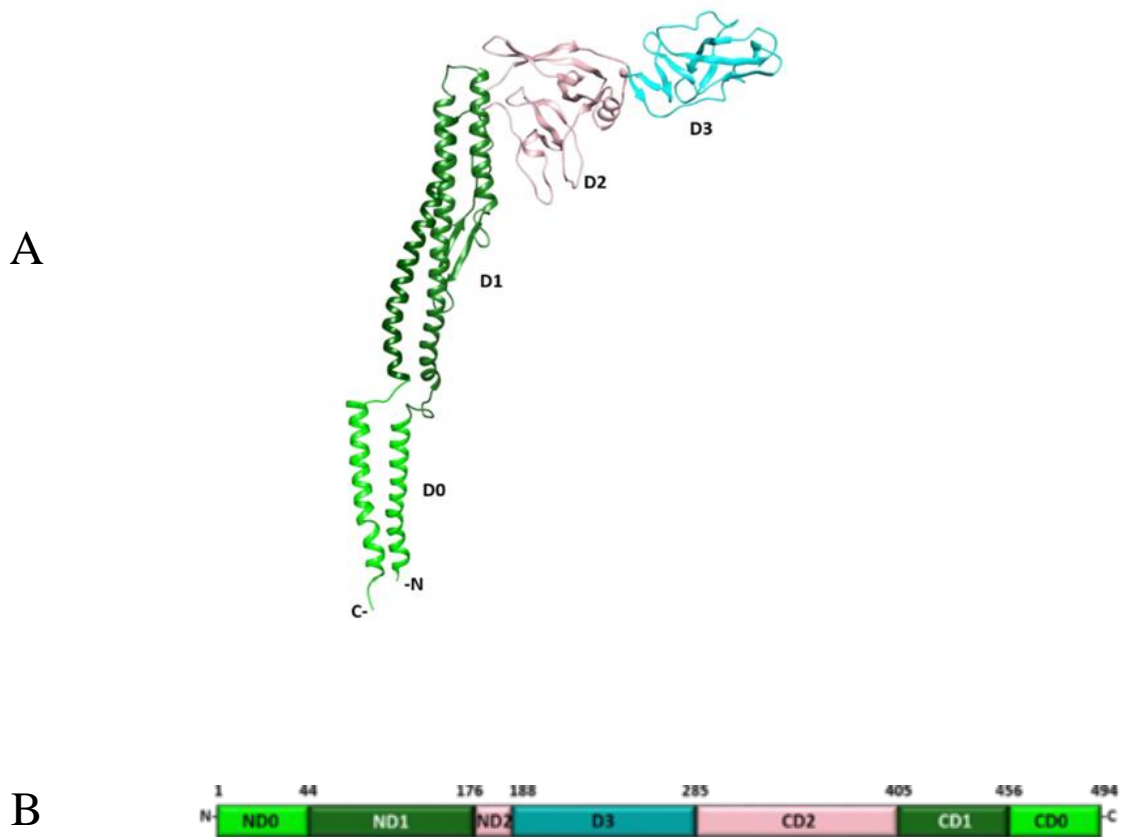
1.8.1 The filament

The filament is a helical structure with a central lumen running all the way along its length, synthesized from an approximately 20000 subunits of flagellin (FliC) (Macnab, 2003). The amino acid sequence of flagellin is remarkably conserved across different bacterial species, as is the quaternary structure of the filament (Maki-Yonekura et al., 2010). Significant sequence conservation is seen among *fliC* genes from closely related Enterobacteriaceae species. For example, *E. coli* FliC can show high degrees of similarity amongst different strains, often ranging from 92% to 100% within *E. coli* itself (Beutin et al., 2005). Studies have indicated that FliC of *E. coli* and Salmonella have a significant degree of sequence similarity. For example, precise comparisons of *fliC* alleles between *E. coli* and Salmonella spp. have revealed identity levels ranging from around 92.6% to 97.4% among closely related strains (Liu et al., 2017; Yamaguchi et al., 2020).

When the filament starts to grow, the hook-filament junction proteins FlgK and FlgL act as structural adapters between the hook and filament. Unlike the majority of flagellar subunits that are incorporated into the growing structure FliD (the filament cap) moves up, remaining at the tip of the filament, as flagellin subunits are added underneath it. The filament cap supports the polymerization of flagellin units by facilitating the insertion of one flagellin unit into a gap generated by contacts between FliD and the growing filament (Yonekura et al., 2000).

There are very few solved structures of FliC proteins from the bacterial kingdom. For many years the only structure available was from *Salmonella enterica* defined by Samatey *et al.*, (2001). The structural organisation of *S. enterica* FliC, is however conserved across motile bacterial species. *S. enterica* FliC folds into an upside-down L-shaped protein with four defined domains D0-D1-D2-D3 (Figure 1.9). The domains D0 and D1 are conserved across all FliC homologues and are generated from both the N- and C-terminal portions of the

protein (ND0, ND1, CD0, and CD1 are conserved across all FliC). They form the downward facing arm of the ‘L-shape’. These domains generate the required contacts that create the central hollow lumen within the filament by which TLR5 recognise flagellin. The domains D2-D3 do not exhibit conservation across the bacterial kingdom. In fact, the D2-D3 domains fold from the central region of the FliC protein and reflect the high level of antigenic variation associated with FliC homologues from different species and within a species like *E. coli* (Figure 1.9).



(Nedeljkovic et al., 2021)

Figure 1.9: Schematic of FliC structure. **A)** Characterization of FliC from *Salmonella Typhimurium* highlighting the Domains in the N- and C-termini, and the mid region of the polypeptide. **B)** The gene *fliC* showing regions encoding each of the domains. Domains in (A) colour correlate to (B).

As mentioned in section 1.3.3 FliC is the ligand that activates TLR5 receptors in immune and non-immune cells (Gewirtz et al., 2001). In fact, TLR5 is proposed to have

evolved to provide mammals with the capability of detecting flagellated bacteria (Hayashi et al., 2001). A variety of cells carry TLR5 including epithelial cells, dendritic cells (DC), lymph node stromal cells, NK cells, lymphocytes, neutrophils, macrophages, monocytes (Gewirtz et al., 2001; Tsujimoto et al., 2005; Vicente-Suarez et al., 2009). Moreover, flagellin possesses adjuvant activity associated with TLR5 presenting cells of the adaptive immune system: i.e. T and B cells (Hajam et al., 2017). Dendritic Cells are activated by TLR5 directly or indirectly through T cell interactions (Salazar-Gonzalez et al., 2007). Within the TLR5 amino acid sequence, 228 amino acids were identified to be crucial for the recognition of flagellin (Andersen-Nissen et al., 2007).

Earlier studies reported by Smith *et al* (2003), and Murthy *et al* (2004) showed that regions within the N and C-terminal regions of FliC were essential for TLR5 recognition. In their work they only perform N- and C- terminal deletions leading to them only being able to suggest that the recognition sequence was in D1 but where exactly they could not say. Further much more refined analysis located the recognition sequence to be between amino acids 95-108 and 441-449 respectively, as when any of these amino acids were deleted or altered, it abolished TLR5 recognition. They used alanine scanning to aid their search for the motif. Furthermore, TLR5 recognition was stronger for monomeric flagellin rather than polymerised filaments (Smith et al., 2003). The previous work had been done by deletion of parts of the genes leading to the reduction of binding or loss of binding and the difference in sizes between the fragments is about 10 bp. Further work by Anderson-Nissen *et al* (2007), then narrowed the recognition motif to be a stretch of amino acids between 89-96 in FliC. Moreover, as they suggested, this work independently verifies the position of the TLR5 recognition site on flagellin. Flagellin's TLR5-stimulatory action is mostly in the N-terminal D1 domain, centred around amino acids 89-96, but requires additional contribution from the

D2-D3 and C-terminal D1 domains. The deletions of DNA fragments need to be compensated to allow the appropriate amino acids to be in the optimum position.

In these experiments they used single point mutants identifying the most important amino acids required for affinity. Interestingly, many gut residing commensal motile species such as *Campylobacter jejuni*, *Helicobacter pylori*, and *Bartonella bacilliformis* have naturally mutated this motif to evade TLR5 recognition (Andersen-Nissen et al., 2005). Importantly to maintain a motility phenotype when engineering such changes in FliC 89-96 compensatory mutations at residue 411 were required (Table 1.4).

Table 1.4 List of the conserved amino acids affecting the TLR5 recognition of flagellin. Those in red are the most important ones for binding flagellin (Andersen-Nissen et al., 2007).

Amino acid	L	Q	R	I	R	E	L	T	V	Q	E	I	L	T	L
Site	88	89	90	91	92	93	94	95	96	97	114	411	415	420	425

Flagellin is a major antigen recognised by the adaptive immune system while also boosting adaptive immunity to other antigens. When mice models are infected with *Salmonella* species, flagellin is a prominent antigen promoting CD4⁺ and CD8⁺ T cell activation and humoral immunity (Bergman et al., 2005; McSorley et al., 2000; McSorley & Jenkins, 2000). In fact, the central region of the FliC protein (D2-D3) is known to activate the adaptive immune response. This area is hypervariable and contains motifs that contribute to serotype specificity and influence immunological recognition of distinct FliC variants. Furthermore, investigations have demonstrated that the central region of FliC is implicated in the release of inflammatory cytokines such as TNF- α , IFN- γ , and IL-4, which are critical for increasing both innate and specific adaptive immune responses. As a result, the FliC protein's core region is critical in activating and modifying the adaptive immune response, ultimately contributing to the host's defence against infection (Koosakulnirand et al., 2018).

1.9 Regulation of flagellar synthesis

The *flhDC* operon, which encodes the transcriptional regulator FlhD₄C₂, is one of the most important regulators of flagellar synthesis because it serves as the master regulator of the flagellar system (Liu & Matsumura, 1994; Wang et al., 2006), and is essential for the transcription of flagellar genes (Chilcott & Hughes, 2000). Flagellar gene expression follows a rigid hierarchy, resulting in the grouping of flagellar operons into three classes based on the promoters that drive their transcription: P_{class1}, P_{class2}, and P_{class3} (Figure 1.7) (Chilcott & Hughes, 2000). Transcription of genes *flhD* and *flhC* is driven by the P_{class1} promoter and the encoded proteins FlhD and FlhC combine to produce the hetero-hexameric complex FlhD₄C₂ (Wang et al., 2006). Global regulators are known to influence FlhD₄C₂ expression and activity in *E. coli*. Essentially, flagellar gene expression is coordinated via cellular and external regulatory signals including nutrition source, temperature, osmolarity, and envelope stress (Anderson et al., 2010). Furthermore, *flhDC* expression is known to fluctuate during cell growth, with the highest levels observed during the mid-log phase (Pruss & Matsumura, 1996). FlhD₄C₂ stimulates transcription by interacting directly with the RNA polymerase alpha subunit, allowing σ^{70} to activate transcription from FlhD₄C₂ specific promoters (Liu & Matsumura, 1995). FlhD₄C₂ has been shown to bind DNA through a direct interaction with FlhC while FlhD has a stability effect (Claret & Hughes, 2000; Wang et al., 2006). In *S. enterica* and *E. coli*, there are eight P_{class2} promoters under the direct influence of FlhD₄C₂. One of them is responsible for the transcription of the gene *fliA*, which encodes the flagellar-specific sigma factor σ^{28} , which is required for transcription involving P_{class3} promoters (Ohnishi et al., 1990). The transcription of *fliA* is essential for the flagellar filament synthesis as *fliC* transcription is driven from a P_{class3} promoter (Ohnishi et al., 1994).

Another regulator of flagellar transcription, transcribed from both a P_{class2} and P_{class3} promoter, is FlgM. FlgM is an anti-sigma factor that prevents the transcription of genes from

P_{class3} promoters by binding to σ^{28} until the HBB assembly is completed (Gillen & Hughes, 1991). On HBB completion, FlgM is secreted releasing σ^{28} leading to the activation of transcription from P_{class3} promoters (Hughes et al., 1993) (Figure 1.10).

There are two proteins, FliT and FliZ, which also play roles in regulating flagellar gene transcription (Kutsukake et al., 1999). FliT functions as an anti-FlhD₄C₂ factor, which regulates the activity of FlhD₄C₂ negatively by inhibiting the binding of FlhD₄C₂ to DNA (Yamamoto & Kutsukake, 2006). Interestingly, FlhD₄C₂: DNA complexes are insensitive to FliT regulation (Aldridge et al., 2010). FliT also interacts directly with FliD, and the flagellar-specific T3SS subunits FliI and FliJ (Evans et al., 2006; Fraser et al., 1999; Imada et al., 2010). The interaction between FliD and FliT inhibits FliT regulation of FlhD₄C₂ defining FliD as an anti-anti-FlhD₄C₂ factor (Yamamoto & Kutsukake, 2006). Upon the completion of HBB, FliD is secreted, which requires FliT and its interactions with the T3S apparatus, the outcome is that this frees FliT to inhibit FlhD₄C₂ activity (Yamamoto & Kutsukake, 2006).

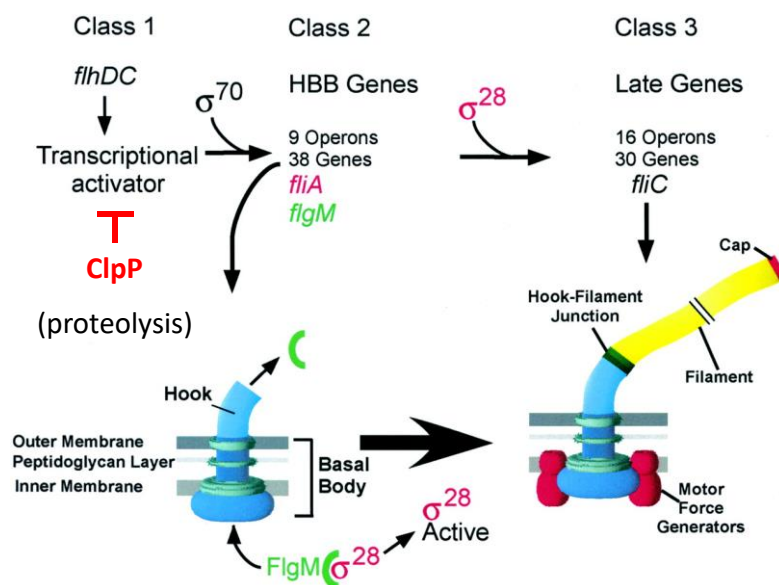


Figure 1.10: Schematic of the transcription hierarchy of flagellar synthesis promoter classes. The class 1 promoter regulates transcription of *flhC* and *flhD* following internal and external signals to form FlhD₄C₂, the master regulator of flagellar synthesis. FlhD₄C₂ alongside with σ^{70} activate P_{class2} promoters leading to structural units such as hook-basal body (HBB) to be synthesized. FlgM is secreted out of the cell after the completion of HBB freeing σ^{28} to activate the P_{class3} promoters. The P_{class3} promoters with the help of σ^{28} activate the expression of the late genes to synthesize other structural units such as FliC. Figure taken and modified from Chevance *et al.*, (2006).

1.10 Proteolytic control of the flagellar system

To limit the availability of regulatory proteins and clear the cell of abnormal and/or misfolded proteins proteolysis is an essential cellular pathway. In *E. coli*, more than 90 % of proteolysis is performed by ATP-dependant proteases including ClpP, ClpQ, Lon, and FtsH (Woo et al., 1992). ClpP associates with one of two ATPases ClpA or ClpX (Gottesman et al., 1993), while ClpQ associates with the ClpY ATPase (Kessel et al., 1995; Rohrwild et al., 1996). ClpP consists of two stacked heptameric rings, which form a central hollow containing the active sites of the peptidase (Baker & Sauer, 2006). ClpX associates with either ClpP to generate a macromolecular structure that allows proteins to thread into the central channel for degradation. Deletion of *clpXP* in *S. enterica* resulted in a hyper flagellated phenotype and analysis indicated that FlhD₄C₂ is negatively regulated by the ClpXP protease (Tomoyasu et al., 2002). In *S. enterica* and *E. coli*, a protein, here defined as YdiV, was also identified as a negative regulator of flagellar gene expression (Jonas et al., 2010; Wada, Morizane, et al., 2011). Sato *et al.*, (2014) demonstrated that YdiV accelerates the degradation of FlhD₄C₂ by ClpXP (Sato et al., 2014). FlhD and YdiV directly interact and deliver the FlhD₄C₂ complex to ClpXP protease for degradation (Takaya et al., 2012). Furthermore, unlike FliT, YdiV is able to release FlhD₄C₂ from DNA (Takaya et al., 2012). FliT has also been shown to enhance the proteolysis of FlhC by ClpXP (Sato et al., 2014). The outcome of the combined effect of YdiV and FliT on FlhD₄C₂ activity is that the flagellar system can respond rapidly to environmental and cellular signals.

1.11 Population heterogeneity

It has been shown in previous studies that expression of flagellar genes in *S. enterica* and *E. coli* is regulated by nutrient availability and growth rate (Sim et al., 2017; Wada, Morizane, et al., 2011). Not all bacteria respond to nutrients in the same way, for example, *S.*

enterica and *E. coli* respond inversely to nutrients with respect to flagellar synthesis (Koirala et al., 2014). A result of nutritional regulation of flagellar gene expression is an adjusted ratio of non-motile and motile cells within the same population, defined as population heterogeneity (Koirala et al., 2014). For *S. enterica* specifically, population heterogeneity of the flagellar system is controlled by the combined regulatory inputs of FliT and YdiV directed towards FlhD₄C₂ activity (Aldridge et al., 2010; Brown et al., 2008; Saini et al., 2011). In high nutrient conditions, nutrients negatively control *ydiV* expression freeing FlhD₄C₂ thus leading to upregulation of P_{class2} activity and increased number of flagellated cells in the population. In contrast, *ydiV* is highly expressed when nutrients are depleted preventing the activation of P_{class2} by preventing FlhD₄C₂ binding (Wada, Morizane, et al., 2011). However, the opposite is seen in *E. coli* (Takaya et al., 2012; Wada et al., 2012). Additionally, *ydiV* expression is regulated by FliZ, generating a network of regulatory circuits that all impact *flhDC* expression (Koirala et al., 2014; Wada, Tanabe, et al., 2011).

1.12 Motility of Uro-associated *E. coli*

Previous work in our laboratory focussed on uro- associated *E. coli* isolates recovered from patients suffering from either bacteraemia, pyelonephritis, cystitis or asymptomatic bacteriuria (ABU). The motility of these isolates alongside two control *E. coli* strains - NCTC10418 (Ali et al., 2017) and CFT073 (Welch et al., 2002) were assessed and 67% were identified as motile. Isolates, however, showed variable motilities; <2 to >7 cm swarming halos for isolates recovered from cystitis patients and <1 to >5 cm swarming halos for ABU isolates (Figure 1.11) (Tan et al., 2023).

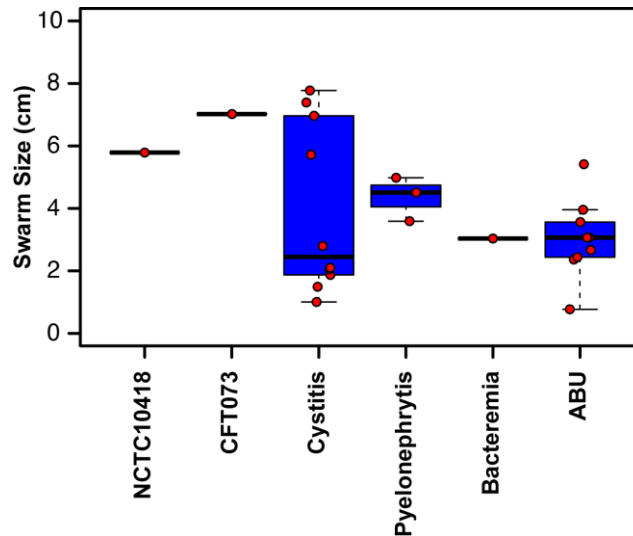


Figure 1.11: Quantification of motility assay of UTI isolates. Box and whisker plot of UTI clinical isolates recovered from UTI patients and categorized by infection type (Tan et al., 2023). The black lines represent the median value while red circles represent the swarm size values for each strain.

1.13 The urothelial innate response to Uro- associated *E. coli*

These uro-associated *E. coli* isolates were heat killed and (1×10^5 CFU/mL) inoculants used to challenge bladder RT4 cells stably transfected with a NF- κ B luciferase reporter for 24h (Tan et al., 2023). Data showed that 78% of the isolates induced NF- κ B signalling by 2-5 fold, supporting their ability to trigger an innate response. Interestingly, 30% of the motile strains, isolated from cystitis patients, increased NF- κ B signalling by >5 fold while two strains induced NF- κ B signalling by more than 30 fold (Tan et al., 2023) (Figure 1.12).

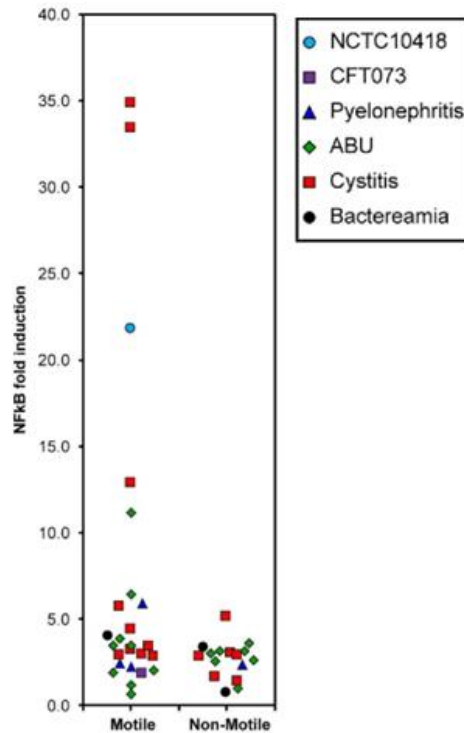


Figure 1.12: NF- κ B induction in RT4 bladder cells following challenge with motile and non-motile UTI isolates. (Tan *et al.*, 2023).

1.14 Urothelial responses to Flagellin serotypes

The urothelial response to an uro-associated *E. coli* assault is mediated via TLR5 signalling (Ali *et al.*, 2017). Flagellin is the ligand that activates TLR5 which leads to a pro-inflammatory response (Andersen-Nissen *et al.*, 2005). In *E. coli*, 53 flagellin serotypes have been identified with H1, H5, H6, H18, H27 serotypes being the most common serotypes (Wang *et al.*, 2003). Previous work in our laboratory exploring the bladder innate response to *E. coli* involved isolates carrying different flagellin serotypes (Tan *et al.*, 2023). This raised the question of whether serotype contributed to the observed variation in bacterial motilities. Using flagellin (50 or 250 ng/mL) purified from a selection of clinical isolates to challenge RT4 cells resulted in consistent NF- κ B induction data (Figure 1.13). These data suggested that flagellin serotype does not play a role in the bladder immune response.

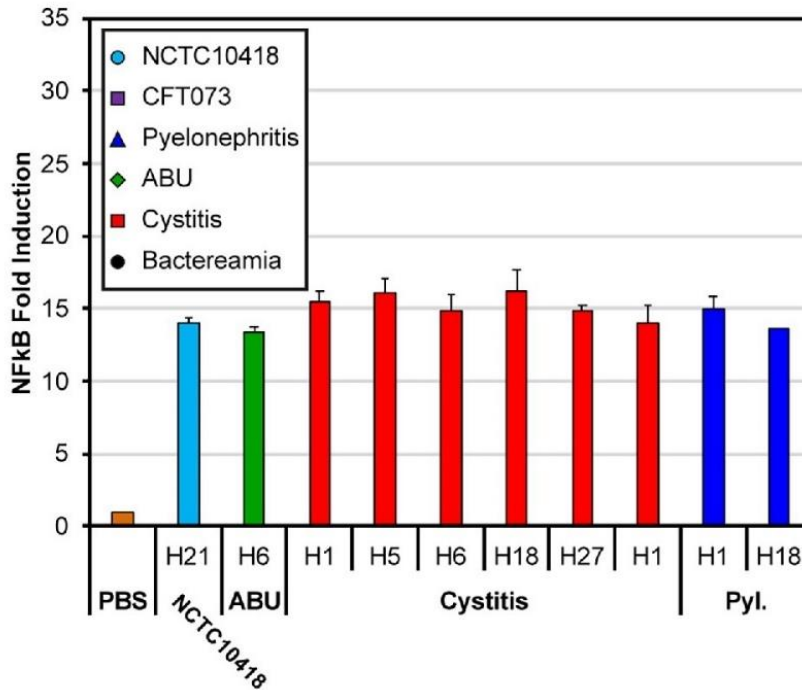


Figure 1.13: The induction of NF-κB by different flagellin serotypes. Isolated flagellin filaments representing common flagellin serotypes from 10 *E. coli* strains (250 ng/mL) were used to challenge RT4 bladder cells for 24h. NF-κB activity was measured by luciferase activity and data presented as fold induction (Tan et al., 2023).

1.15 Urothelial responses to outer membrane preparations

To explore whether outer membrane (OM) proteins could explain the variable innate (NF-κB) responses, OM preparations from the control strains NCTC10418 and CFT073, three motile isolates and one non motile isolate were used to challenge RT4 cells. These cells had been treated using siRNA to ‘Knock-down’ TLR4 and TLR5 gene expression. The innate response was quantified by measuring the concentration of the effector IL-8 (Figure 1.14). Data relating to TLR4 knock-down cells hinted of a potential role for LPS and TLR4, but it could not be ruled out that the OM membrane preparations were contaminated with flagellin (Tan et al., 2023)

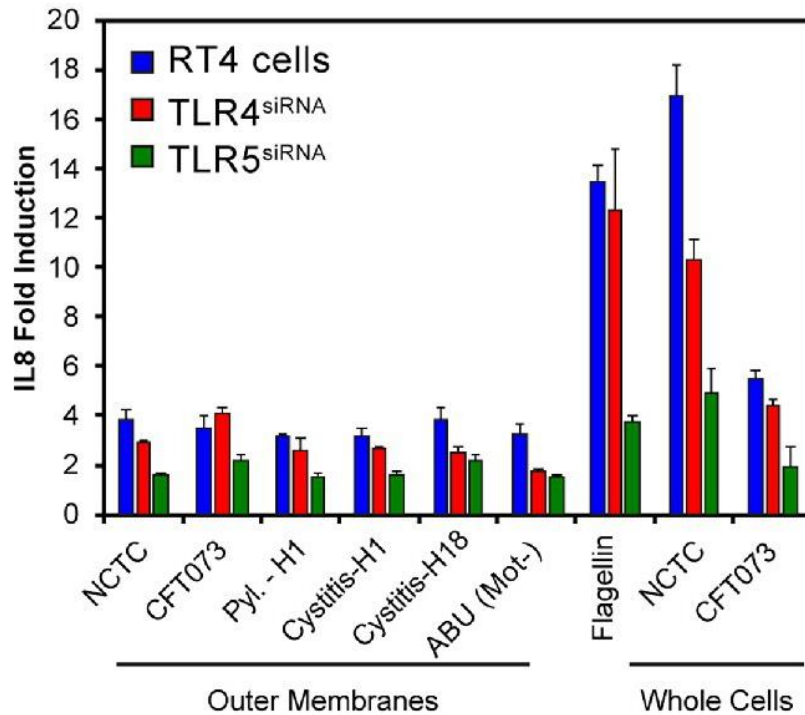


Figure 1.14: IL-8 response following Outer membrane and whole cell challenges of RT4 bladder cells. Outer membrane preparation from *E. coli* strain NCTC10418 and UTI isolates were used to challenged RT4 bladder cells and cells treated with siRNA to ‘knock-down’ TLR4 and TLR5 gene expression. IL-8 concentration were measured and reflected innate responses (Tan et al., 2023).

1.16 Flagellar abundance

Flagella abundance in *E. coli* is regulated by growth rate (Sim et al., 2017). According to Sim *et al* , (2017), faster-growing cells synthesise more flagella, whereas slower-growing cells produce fewer flagella. This association between flagellar abundance and growth rate was observed in steady-state chemostat cultures where the growth rates of the bacterial populations could be tightly controlled. *E. coli* is known to produce 5-10 flagella that are randomly dispersed around the cell surface and the growth rate of the cells influences the regulation of flagellar gene expression. As a result, *E. coli* growth rate has a direct impact on flagella abundance, with quicker growth resulting in a greater number of flagella. This link

between growth rate and flagellar abundance has ramifications for *E. coli* motility and pathogenicity (Sim et al., 2017).

Since flagellin is responsible for triggering the innate response, the amount of flagellin expressed by a bacterial population links to the percentage of the population carrying flagella as well as the numbers of flagella the bacterial cells carry. Analyses of the uro-associated *E. coli* isolates showed that less than 60% of the bacteria were flagellated (Tan et al., 2023) (Figure 1.15) while the numbers of flagella per cell were not known. This population heterogeneity was a potential explanation for the variable innate (NF- κ B) responses observed amongst the clinical isolates.

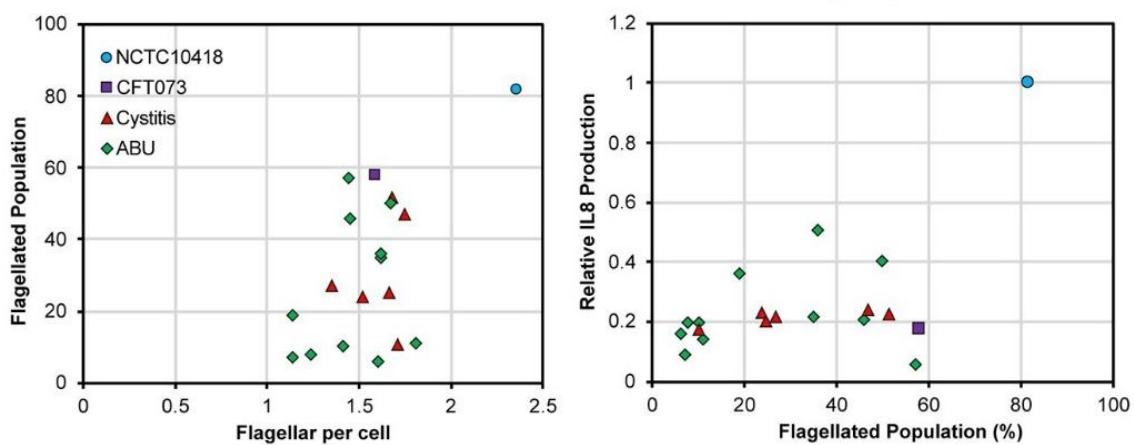


Figure 1.15: Flagellar abundance compared to innate response. A) The figure shows the comparison between the flagellated population percentage and the average flagella presented per cell. B) shows the relation between the percentage of flagellated bacteria in a population and its effect on the proinflammatory response by measuring the IL-8 levels. The *E. coli* control strain reach up to 80 % flagellated population and it has the highest impact on the production levels of IL- 8.

1.17 Hypothesis and Aims

Uro-associated *E. coli* clinical isolates recovered from cystitis, pyelonephritis, ABU and bacteraemia patients were characterised by their different motilities and abilities to induce variable innate responses when used to challenge RT4 bladder cells. These data underpinned the hypotheses that i) uro-associated *E. coli* motility is key in triggering the bladder innate response (ii) uro-associated *E. coli* strains control their motility by regulating flagellar synthesis (iii) such regulation allows uro-associated *E. coli* to evade recognition by host urothelial TLR5 receptors and avoid bacterial killing by host antimicrobial agents.

To explore these hypotheses this project aimed to:

- Investigate the impact of uro-associated *E. coli* motility on the innate responses of RT4 bladder cells, and to
- Investigate the effects of manipulating the regulation of uro-associated *E. coli* flagellar synthesis on the innate responses of RT4 bladder cells.

These investigations involved overexpressing *flhDC* in uro-associated *E. coli* isolates as well as engineering $\Delta flhDC$ and $\Delta clpP$ mutants, and investigating the impact of such mutations on RT4 bladder cell innate responses. In addition, flagellar abundance was determined in wild-type uro-associated and mutant strains ($\Delta flhDC$, and $\Delta clpP$), and compared.

Finally, these uro-associated isolates and their mutants were cultured in artificial urine medium to mimic the bladder environment and the impacts, if any, of changing the bacterial growing conditions on the bladder innate responses determined.

Chapter 2. Material and Methods

2.1. Bacterial cell culture

2.1.1 Bacterial Media

2.1.1.1 Luria-Bertani (LB) media

Bacteria were cultured in LB-media containing 1% (w/v) Bacto-tryptone, 0.5% (w/v) sodium chloride and 0.5% (w/v) Bacto-yeast extract, and prepared in deionized water. The LB-medium was sterilized for 20 min at 121°C and 15 PSI. For solid media, the LB medium was before sterilisation supplemented with 1.5% (w/v) Bacto-agar. After sterilizing, media was cooled to 55 °C and, if appropriate, antibiotics were added to achieve the optimal concentration (Table 2.1). Media was poured into petri dishes (~30 mL/plate). For motility assays, media contained 1% (w/v) Bacto-tryptone, 0.5% (w/v) NaCl and 0.3% (w/v) Bacto-agar.

2.1.1.2 Artificial Urine Media (AUM):

The protocol and composition for AUM was derived from a detailed protocol embedded in the supplementary materials of de Vos *et al.* (2017). To prepare AUM, piperazine-N,N'-bis (2-ethanesulfonic acid) (PIPES) was first dissolved in deionised water to achieve a final concentration of 50 mM, adjusting the pH to 6.0 using sodium hydroxide pellets. Solutions itemised in Table 2.1 were then added to the PIPES buffer, in the order shown. Bacto-peptone and yeast extract were aseptically added to the AUM solution and the solution sterilized by filtering (Nalgene filters 500 mL, 75 mm, 0.45 µM).

For AUM motility plates, 0.6% (w/v) agar was added to an amount of deionised water equal to 50% (v/v) of the intended final volume of media and sterilized. AUM was prepared in 50% of the intended final volume (2x concentrated) and added aseptically to the sterilised agar at 55°C.

Table 2.1; Preparation of AUM. Components were added as ordered. * was added aseptically.

Component	Final Concentration	Stock Concentration	Component	Final Concentration	Stock Concentration
Urea	153 mM	1 M	Creatine	8.4 mM	500 mM
NaCl	108 mM	1 M	NaHCO ₃	30 mM	1 M
KH ₂ PO ₄	8.4 mM	500 mM	CaCl ₂ .H ₂ O	0.24 mM	500 mM
K ₂ HPO ₄	8.4 mM	500 mM	FeSO ₄ .7H ₂ O	0.006 mM	100 mM
NH ₄ Cl	30 mM	1 M	MgSO ₄ .7H ₂ O	12 mM	500 mM
Uric Acid	0.48 mM	59.48 mM	NaSO ₄ .10H ₂ O	12 mM	500 mM
Lactic Acid	1.32 mM	500 mM	Bacto Peptone*	1.1 g/L	20 g/L
Citric Acid	2.4 mM	500 mM	Yeast Extract*	6 mg/L	5 g/L

2.1.2 Bacterial Strains

2.1.2.1 Bacterial standard growth conditions:

Strains were activated overnight on Luria-Bertani (LB) agar plates supplemented with the appropriate antibiotics at either 37 or 30 °C, according to their plasmid profile and optimal growing temperature. For overnight cultures, a single colony was picked under aseptic conditions, used to inoculate 5 mL LB and grown overnight at 37/30 °C using SANYO orbital shaker set at 160 rpm.

2.1.2.2 Bacterial strain storage:

Bacterial strains were numbered and catalogued before they were frozen at -80 °C in 10% (v/v) dimethyl sulfoxide (DMSO). Strains were activated from frozen by streaking on LB agar plates. These plates were stored at 4 °C for up to 4 weeks.

2.1.2.3 Antibiotics

Antibiotics were prepared and stored at 4°C at 200x stock solutions and either added to agar media at 55°C or to liquid cultures using aseptic techniques. The antibiotic working concentrations used in this research are shown in Table 2.2.

Table 2.2: Antibiotic stock and working solution concentrations.

Antibiotic	Stock Concentration (mg/mL) (200x)	Working Concentration (µg/mL)	Diluted in
Ampicillin (Amp)	20	100	H ₂ O
Kanamycin (Kan)	10	50	H ₂ O
Chloramphenicol (Cm)	2.5	12.5	50% Ethanol
Tetracycline (Tet) <i>light sensitive</i>	2.5	12.5	H ₂ O

2.1.2.3 List of plasmids & bacterial strains

Tables 2.3 & 2.4 identifies and lists the strains and plasmids (plus catalogue numbers) either used or engineered during this study.

Table 2.3: List of strains used in this study.

ID #	Strain description	Source
1	<i>Salmonella enterica</i>	(Popoff et al., 2000)
2743	<i>E. coli</i> (NCTC10418)	(Ali et al., 2017)
3373	<i>E. coli</i> (CFT073)	(Welch et al., 2002)
3408	<i>E. coli</i> UTI Clinical Isolate 100273D	(Drage et al., 2019)
3439	<i>E. coli</i> (MG1655)	(Blattner et al., 1997)
5469	UT115-D3 <i>E. coli</i> UTI isolate	(Drage et al., 2019)
5489	UT1675-D3 <i>E. coli</i> UTI isolate	(Drage et al., 2019)
5714	(NCTC10418)/ <i>pSE_flhDC</i>	This study
5716	(3408)/ <i>pSE_flhDC</i>	This study
5718	(MG1655)/ <i>pSE_flhDC</i>	This study
5816	3408Δ <i>clpP</i>	This study
5818	MG1655Δ <i>clpP</i>	This study
5820	MG1655Δ <i>flhDC</i>	This study
5902	NCTC10418Δ <i>flhDC</i>	This study
5904	NCTC10418Δ <i>clpP</i>	This study
5906	CFT073Δ <i>flhDC</i>	This study
5908	CFT073Δ <i>clpP</i>	This study
5910	3408Δ <i>flhDC</i>	This study
5912	5469Δ <i>flhDC</i>	This study
5914	5469Δ <i>clpP</i>	This study
5916	5489Δ <i>flhDC</i>	This study
5918	5489Δ <i>clpP</i>	This study
6000	NCTC10418 Δ <i>flgE</i> / <i>pBAD_kan_flgEA240C</i>	This study
6001	NCTC10418 Δ <i>flhDC</i> Δ <i>flgE</i> / <i>pBAD_kan_flgEA240C</i>	This study
6006	CFT073Δ <i>flgE</i> / <i>pBAD_kan_flgEA240C</i>	This study
6019	3408Δ <i>flgE</i> / <i>pBAD_kan_flgEA240C</i>	This study
6021	3408Δ <i>clpP</i> Δ <i>flgE</i> / <i>pBAD_kan_flgEA240C</i>	This study
6023	NCTC10418 Δ <i>clpP</i> Δ <i>flgE</i> / <i>pBAD_kan_flgEA240C</i>	This study
6036	CFT073Δ <i>flhDC</i> Δ <i>flgE</i> / <i>pBAD_kan_flgEA240C</i>	This study
6038	3408Δ <i>flhDC</i> Δ <i>flgE</i> / <i>pBAD_kan_flgEA240C</i>	This study
6040	CFT073Δ <i>clpP</i> Δ <i>flgE</i> / <i>pBAD_kan_flgEA240C</i>	This study

Table 2.4: List of plasmids used in this study.

Plasmid	Source
pkD3	(Datsenko & Wanner, 2000)
pSE380	Dr. Aldridge's lab
pKD46_kan	(Datsenko & Wanner, 2000)
pBAD_kan_flgEA240C	(Tan et al., 2023)
pCP20_Amp	(Datsenko & Wanner, 2000)
pCP20_Gent	(Datsenko & Wanner, 2000)

2.2 Tissue culture: RT4 epithelial cells

RT4 cells (ATCC-HTB-2, LGC Standards, UK), isolated from a transitional bladder cell papilloma, were employed to explore bladder innate responses. The cells were cultured at 5% CO₂ and 37 °C (Rao et al., 2001) in either 75 cm³ culture flasks (Corning, UK) or 6/12 well plates (Grenier Bio-one). Growth media comprised of RPMI 1640 media, modified by the addition of 2.5% (w/v) HEPES buffer, supplemented with 2 mM L-glutamine and 10% (v/v) Foetal Calf Serum (Sigma). Cells were passaged weekly using trypsin and 10⁵ cells seeded into a 75 cm³ culture flask.

2.3 Polymerase chain reaction (PCR)

2.3.1 Primers

Purified primers, designed using benchling.com, were purchased from Integrated DNA Technologies (IDT) Inc. The primers were resuspended in PCR grade water to make a stock solution of 200 µM and stored at -20°C. The stock primers were diluted 1:10 to give a working solution of 20 nmole/µL (20 µM) for PCR experiments and, 2.5 µL of each primer was added to a 50 µL PCR reaction.

A Biometra T3000 thermocycler was used for PCR reactions. Reactions utilised either Taq polymerase (NEB) or Q5 High Fidelity polymerase (NEB). The temperature of the thermocycler was set in accordance with the polymerase manufacturer's procedure and primer design.

Each PCR reaction consisted of the following components:

Table 2.5 PCR components and volumes used in 50 μ L reaction mix (Taq polymerase)

Component /concentration	Volume(μ L)
5 x Reaction buffer	10
dNTPs (Final concentration of 250 μ M)	5
Forward primer (working concentration of 20 μ M)	2.5
Reverse primer (working concentration of 20 μ M)	2.5
Template DNA	2
DNA polymerase (Final concentration of 1 U/ μ L)	0.2
MilliQ water	Top to 50

Table 2.6 PCR components and volumes used in 50 μ L reaction mix (Q5 polymerase)

Component /concentration	Volume(μ l)
10 X Reaction buffer	5
dNTPs (Final concentration of 250 μ M)	5
Forward primer (working concentration of 20 μ M)	2.5
Reverse primer (working concentration of 20 μ M)	2.5
Template DNA	2
DNA polymerase (Final concentration of 0.2 U/ μ L)	0.5
MilliQ water	Top to 50

2.3.2 Primers list

Table 2.7 Lists the primers used in the experiments described in this thesis.

#	Primer Name	Sequence
13	test-cl	ttatacgcaaggcgacaagg
877	clpP1	atgtcatacagcggcgaacgagataactttgcacccatattggcgGTGTAGGCTGGAGCTGCTTC
878	clpPP2	tcaattacgatgggtcagaatcgaatcgaccagaccgtattccacCATATGAATATCCTCCTTA
893	clpP_CFT073-212chk	ggcccgccaccgccaggtgggtggg
894	clpP_CFT073+848chk	ggatggaccggcaatcagcttgcg
1023	flhC+616REco	gaattcGTTACCGCTGCTGGAATGTT
1031	flhD-42Feco CFT073	gaattcgggtgcggtgagaccgcata
1303	pKD4_F	TCAATAATATTGAAAAAGGAAGAGTATGattgaacaagatggattgcacg
1304	pKD4_R	TATATGAGTAAACTTGGTCTGACAGTTAgaagaactcgtcaagaaggcga
1305	pBADbla_F	tcgcttcttgacgagttcttcTAACTGTCAGACCAAGTTTACTCATATA
1306	pBADbla_R	cgtgcaatccatctgttcaatCATACTCTTCCTTTTTTCAATATTATTGA

#	Primer Name	Sequence
1322	pSE_DCCFT-198_F	catccggctcgataatgtgtggGATTTAGGAAAAATCTTAGATAAG
1323	pSE_DCCFT-198_R	CTTATCTAAGATTTTTCTAAATCccacacattacgagccggatg
1324	DCCFT+963pSEF	GTGTGGCGAAACATTCCAGCAGCtgccctggcggcagtagcgggtgg
1325	DCCFT+963pSER	ccaccgctactgccgccaggcaGCTGCTGGAATGTTTCGCCACAC
1611	flhD-39P1	accgcataaaaaataaagtgggttattctgggtgggaataatgcatGTGTAGGCTGGAGCTGCTTC
1612	flhC+618_P2	tcgttaccgctgctggaatgttgcgcctcaccgtatcagttaaacCATATGAATATCCTCCTTAG
1617	flhC+358-fw	GCCTGGACATTGGTGC GG
1618	flhC+543-rv	TGGGATAATATCGGCAGG
1619	fliCMG+1318-fw	ACCAACCTGAACAACACC
1620	fliCMG+1401-rv	ATTGGACACTTCGGTCGC
1621	fliG+153-fw	GCTAACCGATGTGCTGGC
1622	fliG+325-rv	TTTCAATACCGCTGGCGG
1625	gmk+423-fw	CAGCGAAGAGGTCATTGC
1626	gmk+599-rv	AAAGCGTCATGACGCTGC
1627	gyrB+1994-fw	GCGTGCGTACCCACGGTG
1628	gyrB+2175-rv	CCAGTCCAGCGCCTGCTC
1629	motA+767-fw	CGCCGTTGAGTTTGGTCG
1630	motB+77-rv	CACGATCCATGTGCTGCC
1631	rpoB+563-fw	TCGATCCGAAGGACAACC
1632	rpoB+746-rv	TCACCACGCAGGCGTTCC

2.3.3 DNA visualization:

To prepare agarose gels, agarose (final concentration 0.8 – 2% (w/v)) was dissolved in 1 x TAE buffer (40 mM Tris-Acetate/ 1 mM EDTA) by heating. Following cooling, SafeView (NBS) Biologicals, UK) (5 µL) was added to each 100mL gel. Gels were prepared on casting trays until solidified and then placed in electrophoresis tanks containing 1x TAE running buffer. DNA samples were combined with 6x Loading Buffer (NEB UK) in a 5:1 ratio and loaded onto the agarose gel. A DNA ladder solution (New England Biolabs UK) (5 µL) was used as a marker to identify band sizes. Gels were electrophoresed at 100V for 60-120 min according to the size of either the DNA bands and/or the gels.

2.3.4. Purification of PCR products

PCR products used for mutagenesis were treated with the DpnI restriction enzyme before being purified. PCR product DNA was purified, using the Monarch PCR & DNA Cleanup Kit (NEB) following the manufacturer instructions, except the purified material was

eluted with PCR grade water. A Nanodrop 2000 spectrophotometer was used to evaluate the concentration and purity of the eluted PCR DNA. The DNA was either utilised immediately or stored at -20 °C.

2.4 Gene expression

2.4.1 RNA Isolation

The Promega SV Total RNA Extraction Kit (Promega, USA) was used to extract RNA from bacterial cultures (1 mL and OD₆₀₀ 0.6-0.8). After pelleting the bacterial cells and discarding the supernatant the cells were resuspended in the lysis buffer supplied in the kit. RNA from each sample was extracted as directed by the manufacturer's instructions. The RNA samples were washed, DNase treated, passed through a Spin Column and eluted into Milli-Q water. RNA concentrations were measured using a Thermo Scientific Nanodrop 2000. Milli-Q water was used as blank. 1 µL of the sample then was loaded and the software was set to measure RNA samples under 230 nm wavelength. The Nanodrop is capable of assessing nucleic acids concentrations between 1 pg/µL and 15,000 ng/µL. Purified RNA was stored at -80°C.

2.4.2 Reverse transcription

RNA was reverse transcribed into complementary (c) DNA. For each reaction 1 µg of RNA was diluted in 25 µL of Milli-Q water, 1 ng of random hexamers (Roche, Switzerland) added and the reaction heated at 65°C for 5 min. Tubes containing the reactions were kept on ice for 2 min before the following chemicals were added to each tube; 10 µL of 5x Moloney murine leukaemia virus (MMLV) buffer (Promega, UK); 12.5 µL of 2 mM dNTPs (Bioline, UK); 0.5 µL RNase inhibitor (Promega, UK) (20 units); 1 µL Reverse transcriptase (Promega, UK) (100 units). The samples were centrifuged briefly and then incubated at 42°C for 2 hours, followed by 3 min at 70°C. The resultant cDNA was stored at -80°C.

2.4.3 qRT-PCR

SYBR Green I, a fluorescent dye that binds to double-stranded DNA and fluoresces, was used in qPCR assays. Samples were prepared by adding the following volumes of reagents into each 0.1 mL QIAGEN qPCR tube: 5 μ L Lightcycler 480 SYBR Green I Master (Roche, Switzerland); 2.5 μ L Forward primer; 2.5 μ L Reverse primer; 2.5 μ L Sample cDNA; 1.5 μ L Milli-Q water. SYBR-green-based qPCR primers were designed to be 20 base pairs long, a melting temperature between 55°C and 60°C, a GC content of approximately 50% and a product size of approximately 100 base pairs. The qPCR program (Rotor-Gene Q, QIAGEN) was as follows:

Table 2.8 qPCR programme details (Rotor-Gene Q, QIAGEN)

Step	Temperature (°C)	Time (min:sec)	Cycles
Preincubation	95	10:00	1
Denaturation	95	00:20	45
Annealing	60	00:30	
Elongation	72	00:20	

Samples were analysed in triplicate and the melt curves of each sample were checked to ensure the amplification of a single DNA product. Mean data from each run were analysed to calculate the concentration of target cDNA in each sample using internal positive (housekeeping genes; *gmk*, *gyrB*, and *rpoB*) and negative (distilled water) controls. A mathematical approach was used to calculate the relative quantification of the target genes in comparison to the reference gene (Pfaffl, 2001; Singer et al., 2013). The relative expression ratio (R) of a target gene was determined using $\Delta\Delta CT/Geomean(\Delta\Delta CT \text{ of the house keeping genes})$. $\Delta\Delta CT$ was calculated using ΔCT and efficiency of the PCR reaction. ΔCT was calculated from the average of the CT values of the three biological repeats.

2.5 DNA isolation

2.5.1 Plasmid miniprep

Plasmid miniprep Kit (NEB) was used to extract plasmid DNA from 5 mL of an overnight bacterial culture and the DNA eluted in 50 μ L of PCR grade water. The concentration of DNA was determined using a Nanodrop NA1000 spectrophotometer. The plasmid DNA was either utilised immediately or stored at -20 $^{\circ}$ C for future studies.

2.5.1.2 Crude plasmid miniprep

This method was used to isolate crude plasmid preparations from bacterial cells (Sambrook *et al.*, 1989). Bacterial cultures (3-5 mL) were grown overnight, centrifuged in microfuge tubes for 1 min and 13000 xg to pellet the bacteria, and the supernatants decanted off. The pellets were each treated with three solutions: 300 μ L of solution I (50 mM Glucose, 25 mM Tris HCl, and 10 mM EDTA with 250 μ L RNase for each 50 mL of solution I) was added to resuspend the pellet; solution II, 600 μ L (2 mL NaOH 1 M, 1 mL 10% SDS, and 7 mL water), was then added, the solution mixed and incubated 5 minute incubation at room temperature (RT), then 250 μ L of solution III (5 M potassium acetate, glacial acetic acid, and water) was added the solutions mixed and centrifuged for 20 min at 13000 xg. The sample supernatants were collected, and the plasmid DNAs precipitated using isopropanol (600 μ L). Plasmid DNA was collected following 15 min of centrifugation at 13000 xg, each pellet was washed with 500 μ L 70% ethanol and resuspended in 50 μ L of PCR grade water.

2.5.2 Plasmid midiprep

When either a large quantity of plasmid DNA was required or the plasmid was low copy number, a midiprep procedure was used (Sigma Aldrich midi-prep kit). Plasmid DNA was prepared from 50 mL of overnight bacterial culture according to the manufacturer's instructions and eluted using 1 mL of PCR grade water. The DNA was concentrated to 100

µL using ethanol precipitation. The concentration of the plasmid DNA was quantified using the Thermo Scientific Nanodrop 2000. The software was set to measure DNA samples under 260 nm wavelength. The plasmid was used immediately or stored at -20 °C.

2.5.3 Isolation of bacterial genomic DNA

2.5.3.1 Colony-PCR Preparation

A bacterial colony was taken from an agar plate and re-suspended in 30 µL PCR MilliQ water in a microfuge tube. The suspension was heated for 10 min at 100 °C in a heat block, vortexed and a 2 µL aliquot used as the template for PCR.

2.5.3.2 Culture-PCR Preparation

An aliquot (20 µL) of an overnight bacterial culture was mixed with 180 µL of PCR grade water in a microfuge tube. The suspension was centrifuged for 1 min at 13000 xg, the supernatant discarded and the pellet resuspended in 100 µL PCR grade water. The suspension was heated for 10 min at 100 °C, vortexed and 2 µL used as a template for PCR.

2.5.3.3 Whole bacterial genomic DNA isolation

Bacterial genomic DNA was extracted using a GenElute Bacterial Genomic DNA kit (Sigma Aldrich) according to the manufacturer's instructions. In this procedure, a 5 mL overnight bacterial culture was used and the DNA eluted using 100 µL PCR grade water. The genomic DNA samples were either used immediately or stored at -20 °C.

2.6 DNA gel extraction

DNA bands were excised from agarose gels, transferred to microfuge tubes and the DNA purified from the gels using a Monarch DNA Gel Extraction Kit (New England

Biolabs), as directed by the manufacturer. DNA was eluted using 30 μ L of PCR grade water and either used immediately or stored at -20 °C.

2.7 Bacterial Transformation by Electroporation

2.7.1 Preparation of electro-competent *E. coli* cells

Single colony bacterial cultures, 5 mL LB \pm an antibiotic, were grown at the appropriate temperature overnight with gentle shaking. This overnight culture was used to inoculate 30 mL LB to achieve a starting OD₆₀₀ of 0.05 and the culture grown with shaking to an OD₆₀₀ of 0.6-0.8. At this OD the culture was transferred to a 50 mL falcon tube and centrifuged at 4 °C for 20 min and 4000 xg. The supernatant was discarded and the bacterial pellet washed x2 each in 25 mL of chilled sterile water re-centrifuging each time. The final bacterial pellet (electro-competent bacterial cells) was resuspended in the leftover liquid and stored on ice until the electroporation step.

2.7.2 Bacterial Electroporation

For each electroporation, 50 μ L of the electro-competent bacterial cell suspension was transferred to a 1.5 mL microfuge tube and up to 5 μ L of PCR or plasmid DNA added to the suspension with mixing. This DNA-cell suspension was transferred to a chilled sterile electroporation cuvette (Flowgen Bioscience) and placed in the electroporator (BIO-RAD MicroPulser) using programme Ec1 (1.8 kV, one pulse, no time constant). The cells were electrically pulsed, and 1 mL of LB was immediately added to the mixture. This LB cell mix was shaken in a SANYO rotatory incubator for 45-60 min at 160 rpm and at the appropriate temperature. After this period 200 μ L and 500 μ L aliquots were plated onto LB agar plates containing the appropriate antibiotic. Plates were incubated overnight at the appropriate temperature.

2.8 Constructing mutants using a lambda (λ) red recombinant system

2.8.1 Datsenko and Wanner method

The Datsenko and Wanner's one-step chromosomal gene inactivation method was used to delete targeted genes (Datsenko & Wanner, 2000). Primers were designed to amplify a cassette encoded on plasmid pKD3 that contains a chloramphenicol resistance gene (*cat*) flanked by FLP recognition target (FRT) sites. Each primer contained a 20 nucleotide sequence complementary to pKD3 and a 45 nucleotide 5' overhang complementary to sequences targeting upstream and downstream sequences of the gene targeted for deletion (Figure 2.1). Bacterial cells, targeted for gene deletion were transformed, using

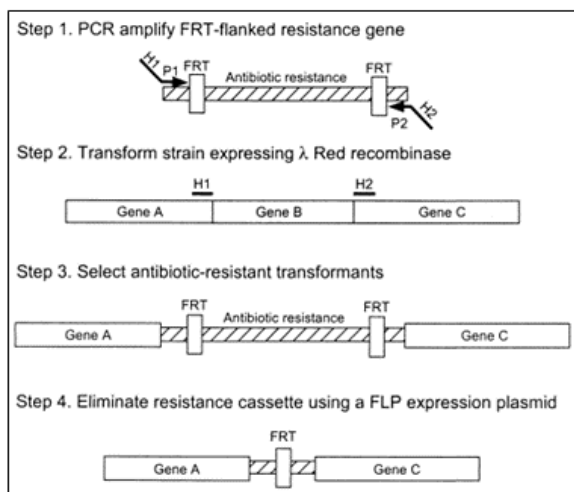


Figure 2.1: Schematic of Datsenko and Wanner method. Step 1: Primers anneal to the flanking region of the antibiotic resistance cassette and are compatible with the region flanking the targeted gene. Step 2: The amplified antibiotic cassette with the λ red recombinase replaces the targeted gene with the Ab^R cassette. Step 3: The antibiotic cassette is eliminated using a FLP plasmid (Datsenko & Wanner, 2000).

electroporation, with the plasmid pKD46-kan. Transformant cells carrying pKD46-kan, were selected on kanamycin plates following an overnight incubation at 30°C. Cultures of strains carrying pKD46-kan were grown overnight in LB+Kanamycin at 30°C from a single colony. These cultures were used to inoculate 30 mL LB+Kanamycin cultures to a starting OD_{600} nm of 0.02 and grown until OD_{600} nm 0.1 at which time 0.1% (w/v) arabinose was added. At an OD_{600} nm 0.6-0.8, cultures were made electro-competent and transformed with the PCR product, amplified from pKD3. Following a 45–60-minute recovery incubation period at

37°C, recombinant colonies were selected using LB agar plates supplemented with chloramphenicol and incubated overnight at 37 °C.

2.8.2 Eliminating chloramphenicol resistance

The chloramphenicol resistance gene was removed using a helper plasmid, pCP20-Gent encoding a FLP recombinase and carrying gentamycin resistance (Figure 2.1). Electrocompetent mutant cells were transformed with the pCP20-Gent and plated onto LB+Gentamycin and incubated at 30°C. Two to 4 transformants were streaked on LB with no selection and incubated at 37°C. After the two passages on LB the colonies were screened for loss of Chloramphenicol and Gentamycin resistance. Any Cm^S Gent^S colonies were confirmed to have lost the pKD3 derived cassette by PCR.

2.9 Protein analysis using SDS-page

For protein electrophoresis commercially available NOVEX® NuPAGE® precast gels (Life Technologies Carlsbad, USA) were used. Sample preparation was as follows: one mL of bacterial culture was harvested at OD₆₀₀ nm 0.6-0.8 pelleted and the supernatant discarded. The cell pellet was resuspended in 50 µL of SDS sample buffer (100 mM Tris-Cl (pH 6.8), glycerol (50% (w/v)), SDS (10% (w/v)), bromophenol blue (0.5% (w/v)), 4% (v/v) β-mercaptoethanol) and the mixture incubated at 100°C for 10 min. A quick centrifugation step (pulse) was performed, and the sample loaded equivalent to (200OD) onto the stacking gel. Samples were electrophoresed for 55-60 min at 200 V.

2.10 Immunoblotting

Following electrophoresis, proteins were transferred to a nitrocellulose membrane using the Trans-Blot Turbo system (BioRad) according to the manufacturer's protocol. The nitrocellulose membrane was blocked overnight in 1x PBS (pH 7.4) + 5% Milk + 0.1% Tween (PMT). The membrane was washed twice in PMT before being incubated for 1-2

hours at room temperature with the primary antibody at a pre-determined concentration. Following this incubation, the membrane was washed 4 x 5 min with PMT, and then incubated for 60 min with secondary antibody (goat anti-rabbit IgG-horseradish peroxidase (HRP)-conjugated, diluted 1:5,000, Southern Biotech, #4030-05). Following this incubation, the membrane was washed 4 x 5 min in 1x PBS. After the final wash, the membrane was incubated for 5 min in a mixture of Clarity Max™ Western ECL Substrate (BioRad). Images were captured via an iBright FL1500 Imaging System.

2.11 Motility Assay

Bacterial strains were tested for motility using a motility assay. To facilitate this a bacterial colony was stabbed into motility agar and the plate incubated for up to 24 h at 37°C. Images of the plates after the respective incubation period were captured using a Syngene Bioimaging cabinet and GeneSnap software at a 75 ms shutter speed. A ruler was photographed alongside the plates and used in combination with Image J software analysis to determine and compare the swarming sizes of the colonies. When possible one batch of motility agar was used per experiment and motility assays were always done in triplicate.

Bacterial motility was quantified by the size of the halo observed on each agar plate (Figure 2.2). For every inoculated colony, the resulting halo size was measured in mm. Using ImageJ, at least three measurements through the centre of the halo, the inoculation point, were collated and the mean value calculated.

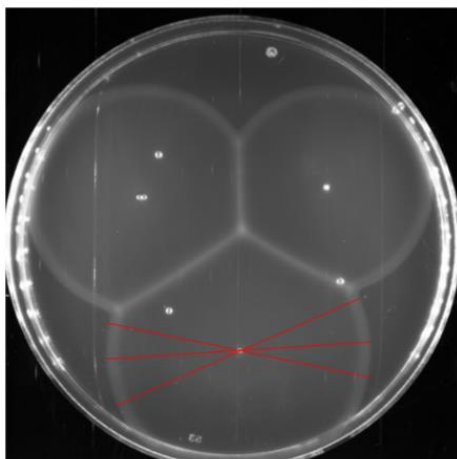


Figure 2.2: Motility Assay: Three inoculations of a motility plate, following a 6 h incubation at 37 °C, are shown. The red lines through the halo show how the size of the halos were measured.

2.12 RT4 Bladder Cell Challenges

2.12.1 Heat killing of bacteria

Bacterial colonies were inoculated into 5 mL LB +/- antibiotic aliquots and incubated overnight on an SANYO orbital shaker set at the appropriate temperature with shaking. Thirty mL of LB +/- antibiotic were inoculated using the overnight culture to a starting OD₆₀₀ of 0.05 and the culture incubated to an OD₆₀₀ of 0.6. An aliquot of the culture was removed, serially diluted and these dilutions plated onto LB agar plates to determine the CFU/mL. Ten mL of the 30 mL culture was centrifuged for 10-12 min at 4,500 RPM and 4 °C, and the supernatant discarded. The bacterial pellet was washed by resuspending in 10 mL PBS and centrifuging for 10 min at 1788 xg and 4 °C. The supernatant was decanted off and the pellet resuspended in 1 mL PBS. This bacterial suspension was treated at 100°C for 20 min. The heat killed bacterial aliquots were stored at -20°C until used.

2.11.2 RT4 cell challenges with bacteria

RT4 cells were seeded into 12-well plates at 2×10^5 cells/well. When the cells reached 100% confluence (48 h), the growth medium was removed, the cells were washed with PBS, and 900ul of cell culture medium containing either 10 µL of heat killed bacteria (1×10^5 CFU) in PBS or PBS alone was added. The RT4 cells were incubated with the heat-killed bacteria for 24 hours at 37°C and 5% CO₂. Following challenge, the media bathing the RT4 cells was collected and stored frozen at -20 °C until analysed for innate effectors. Where appropriate *E. coli* flagellin (50 ng) was used as a positive control (Tan et al., 2023).

2.12.3 IL-8 ELISA

IL-8 concentrations in the RT4 cell bathing media were measured using either the Invitrogen IL-8 Human Uncoated ELISA kit or the Human IL-8/CXCL8 Quantikine ELISA

Kit following the manufacturer's instructions. All ELISA studies were performed using Nunc MaxiSorp 96-well flat-bottom plates and sample ODs measured using a BMG Labtech FLUOstar OMEGA microplate reader.

2.13 Quantification of Flagellation

2.13.1 Labelling Flagella

Maleimide flagella staining is a method allowing visual observation of flagella in bacteria. Maleimide dyes react with the thiol groups found in cysteines, which when oxidised form disulphide bonds in proteins (Turner *et al* , 2010; Sim *et al* , 2017). To count flagella a plasmid pBAD_kan_ *flgEA240C* carrying *flgE* in which an arginine (A) had been replaced with a cysteine (C), by single point mutation, was introduced by electroporation into targeted strains in which the *flgE* had been deleted. Strains carrying pBAD_kan_ *flgEA240C* were then subjected to maleimide staining to quantify flagella abundance.

2.13.2 Bacterial Staining with Maleimide

Bacterial colonies were picked, inoculated into 5 mL LB + Kan and incubated overnight at 37°C at 160 rpm in a SANYO rotary shaker. The overnight cultures were diluted to 0.05 OD₆₀₀ nm and grown to OD₆₀₀ nm of 0.5. An aliquot (0.5 mL) of bacterial culture was pelleted in a microfuge (Eppendorf Mini Spin Plus Centrifuge) at 3000 xg for 2 min. Staining solution was prepared by mixing 5 µL of Alexa Fluor 488 maleimide (1 mg/mL), in DMSO, with 0.5 mL PBS. 50 µL of this staining solution was used to gently resuspend the pellet by pipetting and this was incubated at room temperature for 5 min. 1 mL of PBS was added and the mix centrifuged (Eppendorf Mini Spin Plus Centrifuge) at 3000 xg for 2 min. The supernatant was discarded and the pellet resuspended in 0.5 mL of PBS. The labelled flagella were observed using fluorescence microscopy.

2.13.3 Capturing Pictures with Fluorescence microscopy

Multispot microscope slides (Hendley-Essex) containing 1% agarose pads were used for the fluorescence microscopy. Stained bacterial suspensions (2 μ l), prepared as described in section 2.12.2, were spotted onto the slides, allowed to air dry on the agarose surface and sealed using a coverslip. A Nikon Ti inverted microscope with a Sutter Instruments Lambda LS light source and a Nikon 100 1.30 oil objective linked to a Photometrics CoolSNAP HQ CCD camera was used to view the stained bacteria and capture images. NIS elements software was used to control the device and capture images aided by the Nikon Perfect Focus system. Images of phase contrast and red fluorescence staining were captured using exposure periods of 100 ms and 1000 ms respectively. Files of the phase contrast and the fluorescent images were saved as.ND2 files.

2.13.4 Processing Images using Image J

A copy of the phase contrast picture of the targeted field had its threshold adjusted to identify the bacterial cells. Bacterial cells were analysed using ellipses to generate regions of interest (ROI) and a drawing image was generated. Fluorescent foci measurements reflecting flagella numbers were saved on an Excel file and ROIs saved as a Zip file. Fluorescent images detecting the FlgE foci were merged with the phase contrast images detecting the bacterial cells resulting in images showing the bacterial cells with the foci in red.

2.13.5 Randomization of chosen bacterial cells for Foci counting

After bacterial cells were identified with designated numbers according to the ROI, 50 bacterial cells from every field were chosen randomly using “Random.org”. The chosen bacterial cells were analysed to determine flagellar abundance by quantifying the foci using multi-point cell counter of imageJ. Every counter (10 counters in total) represented the number of foci per bacterial cell (0-9+).

2.14 Statistical analysis

Microsoft Excel software was used for statistical analysis. Data were analysed using either one-way ANOVA and appropriate T-tests or explained in the text.

Chapter 3. Impact of Uro-associated *Escherichia coli* motility on the innate response of RT4 Bladder Cells

3.1 Introduction

Research reported by Lane *et al.* (2005) and Wright *et al.* (2005) demonstrated that motility provides uro-associated *E. coli* a competitive advantage over non-motile UPEC strains in relation to UTIs, at least in mouse models. Motility is driven by flagella, hence flagella are virulence factors in the aetiology of an UTI. However, flagella are recognised by host TLR5 receptors, which once activated trigger a signalling cascade that releases host defence agents to facilitate bacterial killing.

Uro-associated *E. coli* isolates recovered from the urines of patients suffering lower and upper UTIs as well as asymptomatic bacteriuria revealed a mixture of motile and non-motile phenotypes (M. L. Lanz, 2013). Indeed, only 23 of the 39 clinical isolates tested by motility agar assays, which measured bacterial motility based on swarm size after 8 hours, were shown to be motile (Tan *et al.*, 2023). These data suggested that uro-associated *E. coli* regulate their motility, potentially, to allow colonisation, but avoid the host innate defences.

To explore this, further experiments reported in Tan *et al.*, (2023), were performed *in vitro*, to determine if bacterial motility affected the innate response of the bladder. RT4 bladder cells were used to model the urothelium and reporter cells had been engineered by stably transfecting the RT4 cells with an NF- κ B luciferase reporter (Ali *et al.*, 2017). When these cells were challenged with the clinical isolates, heat killed and 1×10^5 CFU/mL/challenge, only two of the motile isolates caused significant (30-35 fold) increases in luciferase activity, reflecting robust innate responses (Figure 1.8). To explore whether this response reflected antigenic variation flagellin filaments were purified from isolates recovered from different clinical pathologies including ABU, cystitis and pyelonephritis, and of varying H-serotype. These flagellin preparations were used to challenge the RT4 cells (250 ng/mL flagellin/challenge), and the challenges resulted in comparable NF- κ B data. These

data suggested that the source of the flagellin itself was not key in explaining the variability of the host responses (Tan et al., 2023).

Synthesising flagella is an energy-consuming process for bacteria, so it is only initiated when motility is advantageous. Interestingly, the growth rate of *E. coli* strain RP437 was shown to be correlated with flagellar abundance (Sim et al., 2017). This observation led to the initial hypothesis that growth fitness is important in the recognition of uro-associated *E. coli* by the host urothelial cells. To address this new hypothesis experiments were initially performed to compare the fitness of the motile and non-motile clinical strains.

3.2 Results

3.2.1 Growth fitness of UPEC strains

The maximal doubling times of the uro-associated *E. coli* clinical isolates used in the host challenge experiments (Figure 1.9) were investigated to determine bacterial fitness. Information related to the source and laboratory ID number of each isolate is presented in Tables 3.1 and 3.2 respectively. Growth experiments to determine bacterial fitness were performed in collaboration with P. Aldridge.

Table 3.1. Motile strains used in the growth curve study in collaboration with P. Aldridge. Doubling time is calculated in min. * ABU: asymptomatic bacteriuria.

Infection	Strain #	Doubling time (min)	Infection	Strain #	Doubling time (min)
ABU*	3406	15.3 ± 2.3	NON-UTI	NCTC10418	23.4 ± 7.3
	3695	19.1 ± 8.7	Cystitis	3408	15.3 ± 3.6
	3697	14.5 ± 2		3409	16.6 ± 4.3
	3698	14.7 ± 1.4		3411	26.9 ± 10
	3699	15.8 ± 0.9		3412	18.7 ± 4.3
	3694	22.1 ± 8		3414	16.1 ± 0.8
	3710	15.1 ± 2.9		3701	21.5 ± 4.1
	4738	21.2 ± 8.4		3702	16.8 ± 1.7
	4739	20.6 ± 5.7		3703	17.8 ± 5.3
	4740	16.1 ± 2.8		3704	16.7 ± 3
	4741	19.7 ± 10.4		3417	17.7 ± 6.6
	4742	14.4 ± 2.3	Pyelonephritis	3398	19.3 ± 6.5
	4743	15.9 ± 0.3		3424	14.1 ± 2.9
	3419	15.2 ± 3.9		3425	21.6 ± 8.1
	3692	13.9 ± 1.7	Bacteraemia	CFT073	15.6 ± 3.2
	3693	14.2 ± 0.4		3415	15.6 ± 3.7

Table 3.2. Non-motile strains used in the growth curve study in collaboration with P. Aldridge. Doubling time is calculated in min. * ABU: asymptomatic bacteriuria.

Infection	Strain #	Doubling time (min)	Infection	Strain #	Doubling time (min)
ABU*	3399	14.7 ± 1.4	Cystitis	3401	21.2 ± 6.9
	3400	25.3 ± 7.9		3403	19.8 ± 10.2
	3413	16.4 ± 1.3		3407	18.9 ± 7.1
	3416	18.9 ± 7.6		3701	19.6 ± 4.7
	3418	18.4 ± 1.9		3706	23.4 ± 6.7
	3420	20.5 ± 1.9		3707	17.5 ± 6
	3696	21.3 ± 7		Bacteraemia	3402
Pyelonephritis	3422	18.5 ± 7.4	3410		20.2 ± 5.3

Briefly, the growth curves of 30 motile clinical uro-associated *E. coli* isolates, 16 non-motile clinical isolates and two control strains, NCTC10418 and CFT073 were analysed to determine their maximum doubling times. These growth experiments were performed in LB media at 37°C. Initially the strains were grown overnight and diluted to a starting OD₆₀₀ nm of 0.02. Two hundred microliters of each culture were aliquoted into a 96-well plate, the plate sealed with a BreatheEasy membrane and OD₆₀₀ nm readings taken every 400 s for 10 h, with shaking between the readings, using a BMG Fluostar microplate reader. All growth experiments were performed in triplicate and used independent colonies. When analysing data negative values were set to 0.02, which reflected the starting OD₆₀₀ nm. The maximum slope for each strain was derived from log (OD₆₀₀ nm) using a sliding sub-set of 10 time points (~60 min) across the timeline of the growth experiment (Tan et al., 2023). The maximum doubling time was derived from the calculated maximum slope before the mean value was determined. Growth data, presented as calculated doubling times, are presented in Tables 3.1 and 3.2 respectively.

The maximum calculated doubling times for the motile strains ranged from 13.9 min (ABU isolate) to 26.9 min (Cystitis isolate) (Table 3.1). The maximum calculated doubling times for non-motile isolates ranged between 14.7 min and 25.3 min (ABU isolates) (Table 3.2).

The 16 motile ABU isolates, showed doubling times ranging from 13.9 to 22.1 min with an average of 16.7 min. In contrast, the doubling times of the 6 non-motile ABU isolates ranged from 14.7 to 25.3 min with an average of 19.0 min. These doubling times were not significantly different ($p=0.13$). Furthermore, the 10 cystitis motile isolate doubling times ranged from 15.3 to 26.9 min with an average of 18.4 min whereas the 6 non motile cystitis isolates doubling times ranged from 17.5 to 23.4 min with an average of 20.0 min. Again, these data were not significantly different ($p=0.3$). The doubling times for the pyelonephritis motile isolates ranged from 14.1 to 21.6 min with an average doubling time of 18.3 min; the study included only one non-motile pyelonephritis isolate with a doubling time of 18.5 min. On the other hand, the two bacteraemia motile isolates each displayed doubling times of 15.6 min respectively, while the non-motile strains showed doubling times of 19.9 and 20.2 min respectively, with an average of 20.0 min (Figure 3.1).

The individual growth curves of four motile isolates (3406 ABU; 3408 Cystitis; 3415 Bacteraemia; and 3424 Pyelonephritis) and four non-motile isolates (3400 ABU; 3401 Cystitis; 3410 Bacteraemia; and 3422 Pyelonephritis) are presented in Figure 3.2. Growth curves all appear similar. Additionally, presenting mean growth data for two isolates characterised by a fast doubling time (ABU 3693- 14.2 min) and a slow doubling time (cystitis 3706- 23.4 min) revealed similar growth profiles (Figure 3.3). However, the range of maximal doubling times between the two groups was similar (motile 13.9 - 26.9 min; non-motile 14.7 - 25.3 min). These data therefore strongly argued against the hypothesis that fitness underpins the variability in host recognition observed within the motile strain collection. However, comparing the doubling time data for the motile and non-motile isolates collectively and statistically,

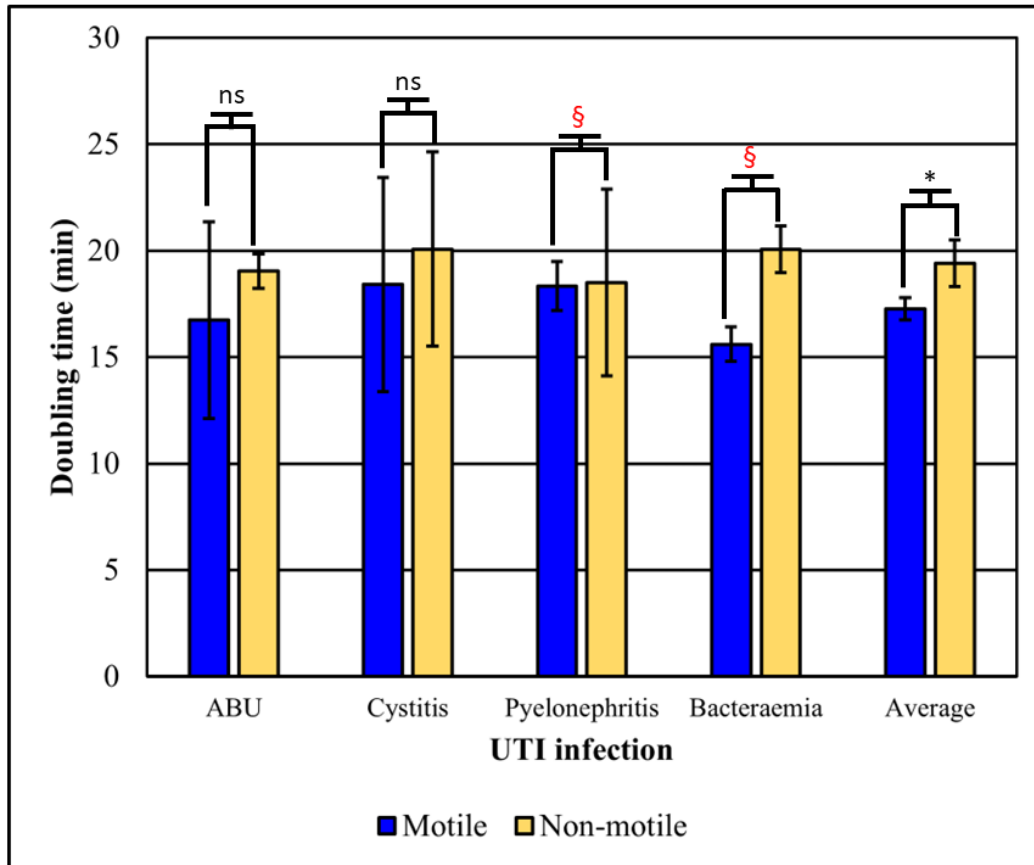


Figure 3.1 Average doubling times (min) of motile and non-motile UTI isolates according to their source. Error Bar = SEM. ns = not significant; § = low numbers: statistics not applicable; (* = p<0.05).

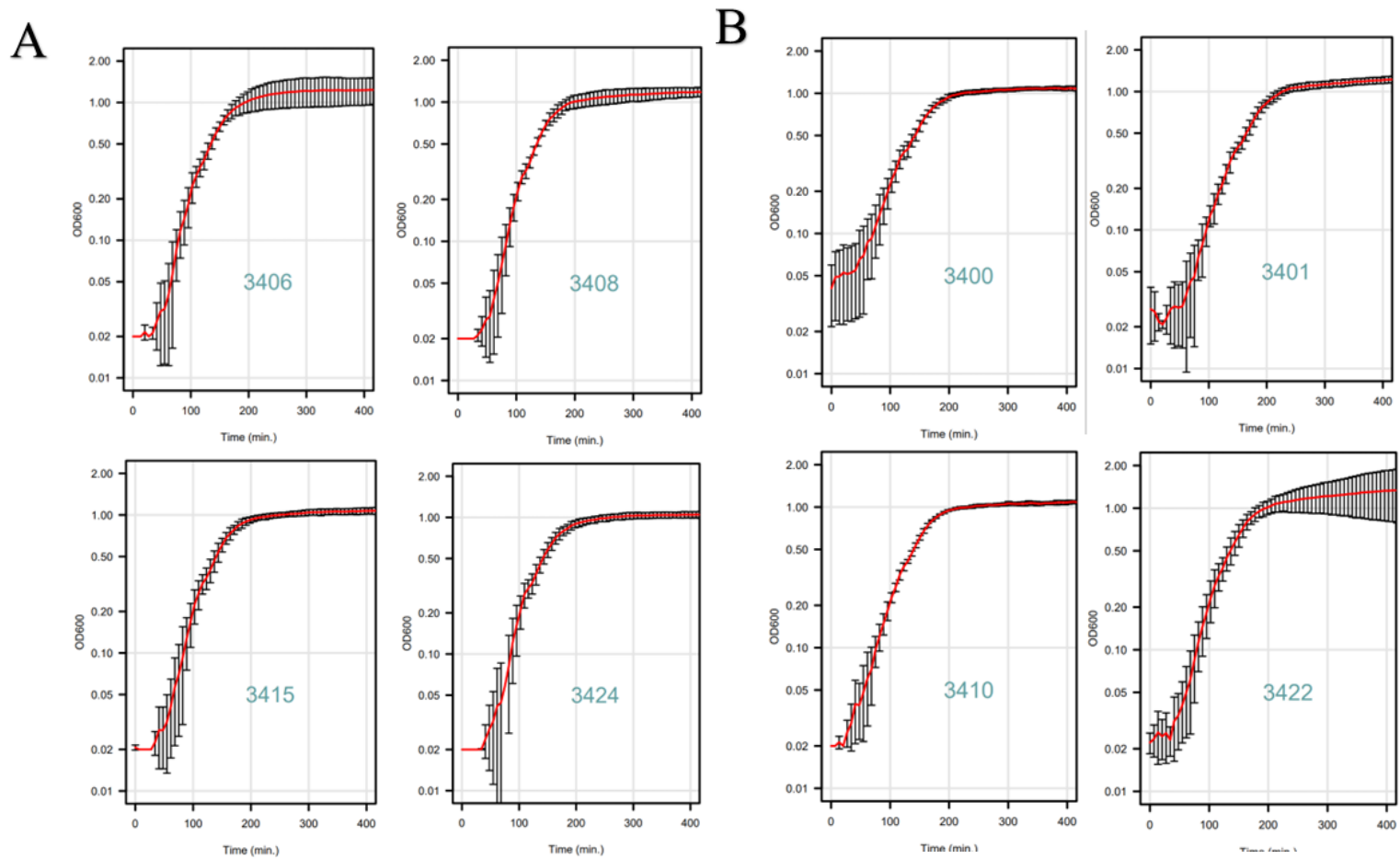


Figure 3.2 Growth curves motile and non- motile strains. A) Growth rates of motile UTI isolates.3406 ABU; 3408 Cystitis; 3415 Bacteraemia; and 3424 Pyelonephritis (Table 3.1). **B)** Growth rates of several non-motile UTI isolates. 3400 ABU; 3401 Cystitis; 3410 Bacteraemia; and 3422 Pyelonephritis (Table 3.2).

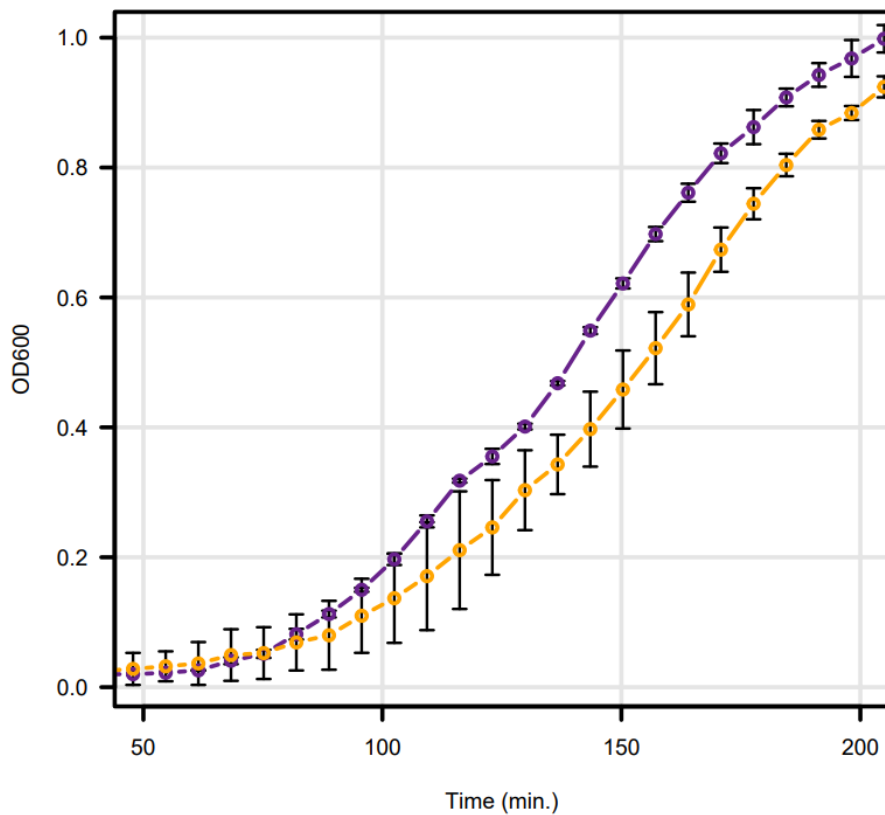


Figure 3.3 Growth curves of fast and slow growing motile isolates. Isolate 3693, an ABU motile strain, with a fast doubling time (14.2 ± 0.4) min compared to isolate 3706, a

identified a significant difference in growth rates between the groups. The average doubling time for the non-motile bacteria was 19.7 ± 2.5 min which was significantly different from that of the motile strains, calculated as 17.4 ± 3.0 min (ANOVA $p = 0.011$). This difference was clearly shown using a density plot analysis (Figure 3.4) that identified a significant shift between the two groups of isolates.

3.2.2 Flagellar contamination residual levels

Previously reported studies (Ali et al., 2017) have shown that TLR5 is the key bladder host receptor activated in response to an uro-associated *E. coli* challenge with activation triggering an innate response involving IL-8 release. There are data however, involving mice

studies and genotype analyses (Jerde et al., 2000), that suggest a role for LPS and TLR4 in the bladder innate defences. It was therefore hypothesised that TLR4 and LPS may help explain the varying responses of the RT4 cells to the clinical *E. coli* isolates. To address this, outer membrane preparations from three motile isolates ID 3398 (pyelonephritis), 3408 (Cystitis) and 3412 (Cystitis) were used to challenge wild-type RT4 cells and RT4 cells, where expression of either TLR5 or TLR4 had been knocked-down or silenced using siRNA (Mowbray et al., 2018). IL-8 responses, measured using ELISA (Mowbray et al., 2018), supported a potential role for LPS and TLR4. It was possible however, that the OM membrane preparations were contaminated with flagellin.

To explore this further, antibodies raised against FliD and FlgE of *S. enterica* (Minamino & Namba, 2008), were available and used to examine the OM preparations for flagellin contamination. These antibodies were raised against *Salmonella* proteins but comparing the FlgE (hook protein) amino acid sequences of *Salmonella* and *E. coli* indicated 87% identity and 92% similarity, while that of FliD (Filament cap) revealed 52% identity and 70% similarity (Figure 3.5 A & B) (Minamino & Namba, 2008).

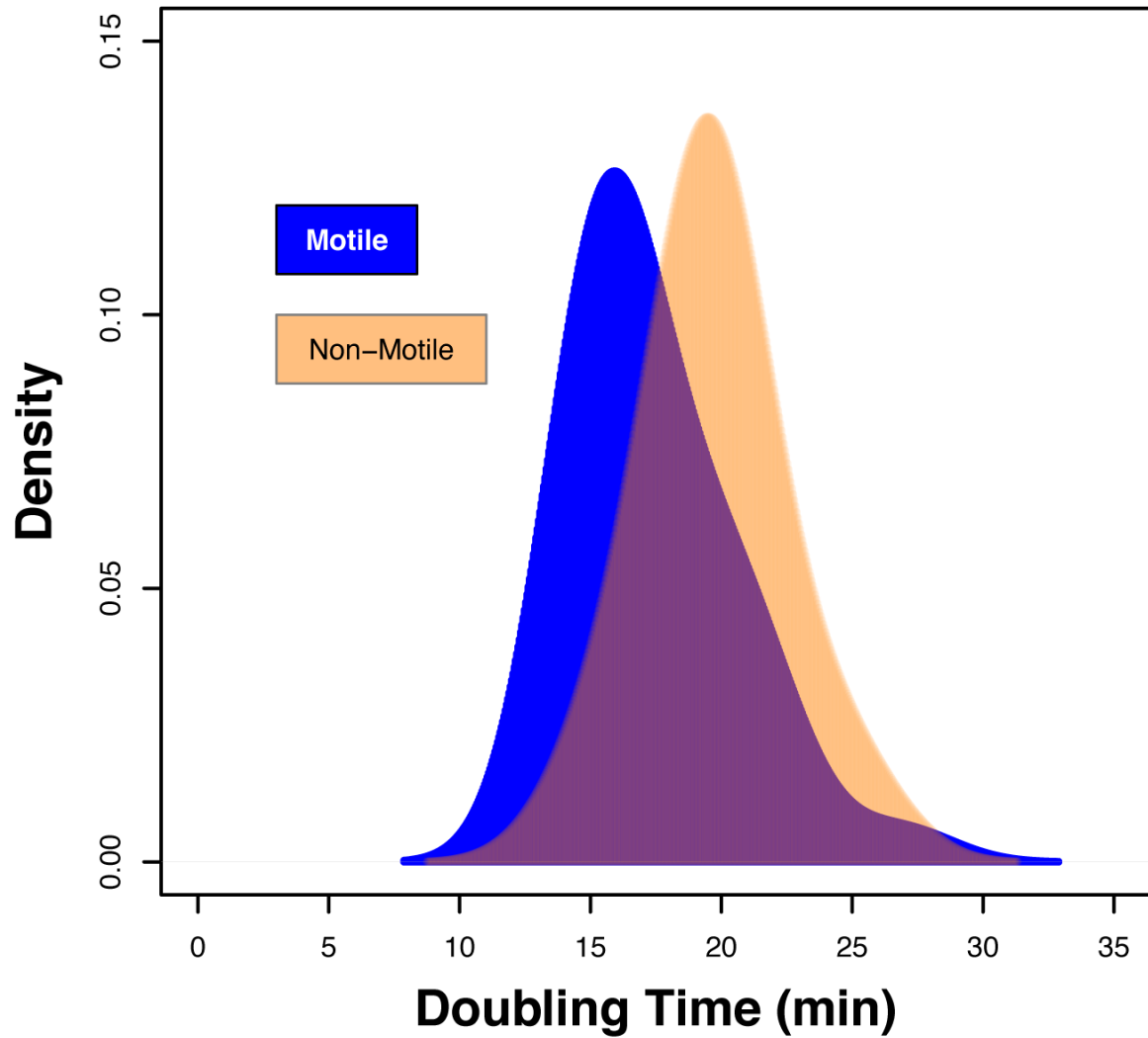


Figure 3.4 Fitness of motile and non-motile strains of *E. coli* defined by the maximum doubling time. The range of doubling time (min) for motile and non-motile isolates exploited in density plot. Isolates 3398 to 4745 (Table 3.1) represent the motile strains while isolates 3399 to 3707 (Table 3.2) represent non-motile strains. Data are based on $n=3$ for each isolate.

FlgE

	1	10	20	30	40	50
E. coli	MAFSQAVSGLNAAATNLDVIGNNIANSATYGFKSGTASFADMFAGSKVGLGVKVGAGIT					
S. enterica	MSFSQAVSGLNAAATNLDVIGNNIANSATYGFKSGTASFADMFAGSKVGLGVKVGAGIT					
	60	70	80	90	100	110
E. coli	ODFTDGTNTTNTGRGLDVAISQNGFFRLVDSNGSVFYSRNGQFKLDENRNLVNMQGLQL					
S. enterica	ODFTDGTNTTNTGRGLDVAISQNGFFRLVDSNGSVFYSRNGQFKLDENRNLVNMQGLQL					
	120	130	140	150	160	170
E. coli	TGYPATGTPPTIQGANPTNLSIPNTLMAAKTTTASMQINLNSDPLPTVTPFSASN					
S. enterica	TGYPATGTPPTIQGANPAPITIPNTLMAAKSTTTASMQINLNSDDEVPSKTPFSVSD					
	180	190	200	210	220	230
E. coli	ADSYNKKGSVTVFDSQGNADHMSVYFVKTDGNNWQVYTDSSDPNSIAKT..ATTLEF					
S. enterica	ADSYNKKGTVTVMDSQGNADHMNVYFVKTDNEWAVYTDSSDPAAATPTTASTTLKF					
	240	250	260	270	280	
E. coli	NANGTLVDGAMANNIATGAINGAEPATFSLSFLNSMQONTGANNIVATTONGYKPGDL					
S. enterica	NENGLLESGGTVLNIITGTINGATAATFSLSFLNSMQONTGANNIVATNONGYKPGDL					
	290	300	310	320	330	340
E. coli	VSYQINDDGTVVGNYSNEQTLGQIVLANFANNEGLASEGDNVWATQSSGVALLGT					
S. enterica	VSYQINDDGTVVGNYSNEQEQVQLGQIVLANFANNEGLASQGDNVWATQASGVALLGT					
	350	360	370	380	390	400
E. coli	AGTGNFGTLTNGALEASNVDLSKELVNMIVAQRNYQSNAQTIKTQDQILNTLVNLR					
S. enterica	AGSGNFGKLTNGALEASNVDLSKELVNMIVAQRNYQSNAQTIKTQDQILNTLVNLR					

FliD

	1	10	20	30	40	50
E. coli	MASISLGVGSGLDLSILDSLTAAQKATLTPISNQSSFTAKLSAYGTLKSALITTFQ					
S. enterica	MASISLGVGSGLDLQLLTDLTKNEKGRITPITKQSSANSKALTAAYGTLKSALTEKFQ					
	60	70	80	90	100	110
E. coli	TANTALSADLFSATSTSSSTAFSATTAGNAIAGKYTISVTHLAAQQLTITRTRRDD					
S. enterica	TANTALNKADLFSKSTVASSSTEDLKVSTTAGAAAGTYRINVTQLAAQSLATKTTFAT					
	120	130	140	150	160	170
E. coli	TKTAIAT...SDSKLTIQGGDKDPIITIDISAANSLSLGGIRDAINNAKAGVSASTINLV					
S. enterica	TKEQLGDTSVTSRITLIEQGRKEPLEIKLIDKGDTSMEAIRDAINDADSGLIASIVKVV					
	180	190	200	210	220	
E. coli	GNGEYRISVTSNDTGLDNAMTLVSQDGLQSFMGYDASASSNGMEVSVAAQNAQLTV					
S. enterica	KENEFOVLTANSGTDNMTKIVVEGDKLMDLLAYDSTTNTGNMQELVKAENAKLNV					
	230	240	250	260	270	280
E. coli	NNVAIENSNTISDALENITLNLNDVITGNQTLTITODTSKAQTAIKDWNAYNSLID					
S. enterica	NGIDIERQSNTVTDAPQGITLTLTKKVT.DATVTVTKDDTKAKEAIRSWVDAYNSLVD					
	290	300	310	320	330	340
E. coli	TFSSLTKYTAVDAGADSSNGALLGDSITRTIQTQLKSMLSNTVSSSSYKTEAOLIG					
S. enterica	TFSSLTKYTAVEPGEA.SDKNGALLGDSVVRTIQTGIRAQFANSQNSAFKTMALIG					
	350	360	370	380	390	400
E. coli	ITTDPSDGLKLELDADKLTAAALKDASGVGALIVGDGKKTGITTITGNSLTSWLSSTGI					
S. enterica	ITQDGTSGKLELDADKLTAAALKDASGVGALIVGDGKKTGITTITGNSLTSWLSSTGI					
	410	420	430	440	450	460
E. coli	IKAAATDGVSKTLNKLTKDYNAASDRIDAQVARYKEQFTQLDVLMTSLNSTSSYLTDQF					
S. enterica	IDNAQDNVNATLKLTKQYLSVNSIDEIVARYKAQFTQLDMMSEKLNNTSSYLTDQF					
E. coli	ENNSNSK					
S. enterica	TA.MNRS					

Figure 3.5 BLAST alignment of FliD and FlgE amino acids sequences comparing *E. coli* to *Salmonella*. The upper line shows *E. coli* sequence and the lower shows *Salmonella* sequence. In the alignment, amino acids with black background represent identity while bold letters represent similarity; the rest mean neither similarity nor identity.

These data showed >50 amino acid identity between the proteins so it was predicted that the Salmonella antibodies would cross-react with the *E. coli* proteins and hence could be used to test the OM preparations for flagellin contamination. Cross-reaction was first tested by immuno-probing *E. coli* whole cell lysates and flagellin preparations from *E. coli*, *Proteus* and *Salmonella* with each of the antibodies. Using the FliD_{ST} antibody protein bands of 50 kDa were observed in the flagellin preparation from Salmonella, but no bands were observed either in the *Proteus*, *E. coli* flagellin preparations or the *E. coli* cell lysate preparations. When FlgE_{ST} antibody was used protein bands of 42 kDa were observed in the *E. coli* flagellin and cell lysate preparations (Figure 3.6). FlgE antibodies were therefore used to analyse the *E. coli* outer membrane preparations for flagellin contamination.

Probing with FlgE_{ST} antibody detected FlgE only in the *E. coli* cell lysates and flagellar preparations (Figure 3.7). No signals were detected in the OM preparations indicating no contamination of these samples with flagellin. These data suggested that the observed IL-8 responses to the OM preparations were not due to flagellin contamination. However, as the IL-8 responses to the OM preparations were relatively constrained (2-4 fold) and very comparable, these data also suggested a minor role for LPS in the bladder innate response to *E. coli*. Hence, it was unlikely that the observed variability in the bladder RT4 innate responses to motile uro-associated *E. coli* was linked to LPS. To summarize, the *E. coli* OM preparations did not contain flagellin contamination, so this did not explain IL-8 variable responses.

3.2.3 Overexpression of flhDC in clinical uro-associated *E. coli* isolates and analyses of bacterial motility

The next hypothesis to explain the observed variability addressed the roles of flagellar numbers or abundance. To explore this hypothesis *E. coli* strains were engineered to overexpress the *flhDC* gene and create hyperflagellated bacteria.

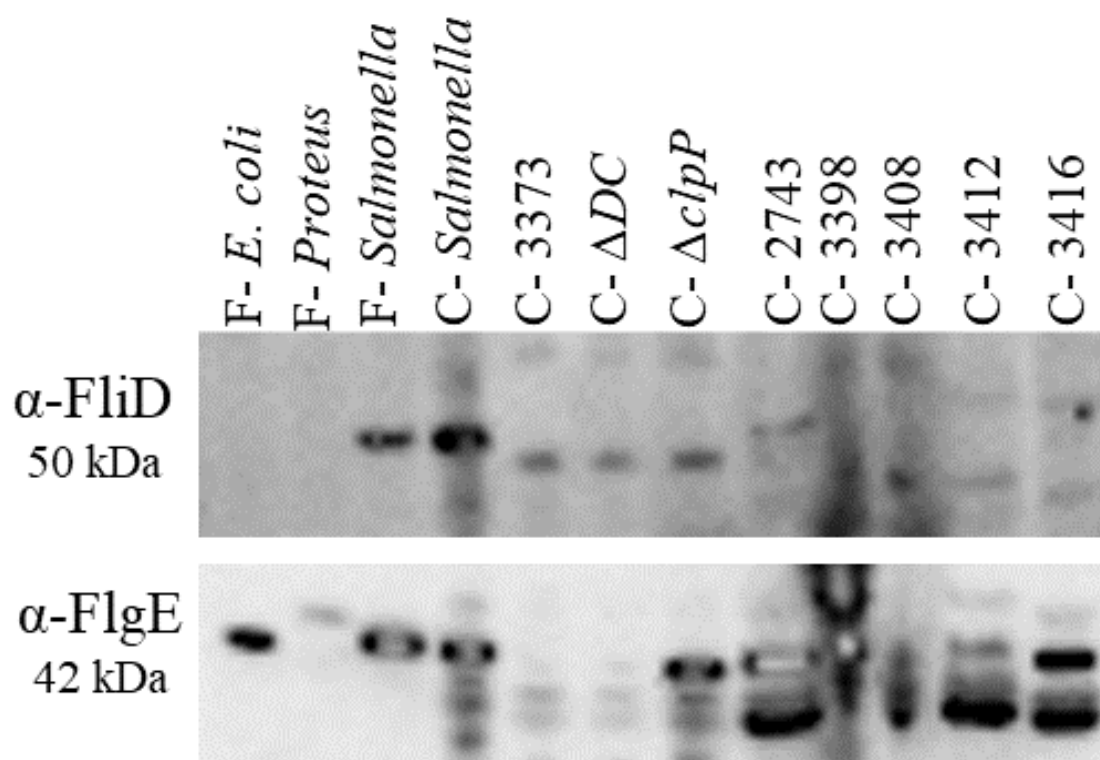


Figure 3.6 Optimization of the *Salmonella* α -FliD and α -FlgE antibodies. Antibodies raised against *S. Typhimurium* FlgE and FliD (Minamino and Namba, 2008) were tested on flagellin isolates (F) from several species as well as *E. coli* cell lysates (C) to explore cross reaction. The strains used were mix of motile (NCTC10418, CFT073, 3398, 3408, 3412) and non-motile strain (3416). Δ DC represents a mutant (CFT073) that lacks the master regulator of flagellar synthesis (negative control) while Δ clpP (CFT073) represents a mutant lacking a repressor of *flhDC* and hence hyper-flagellated (positive control).

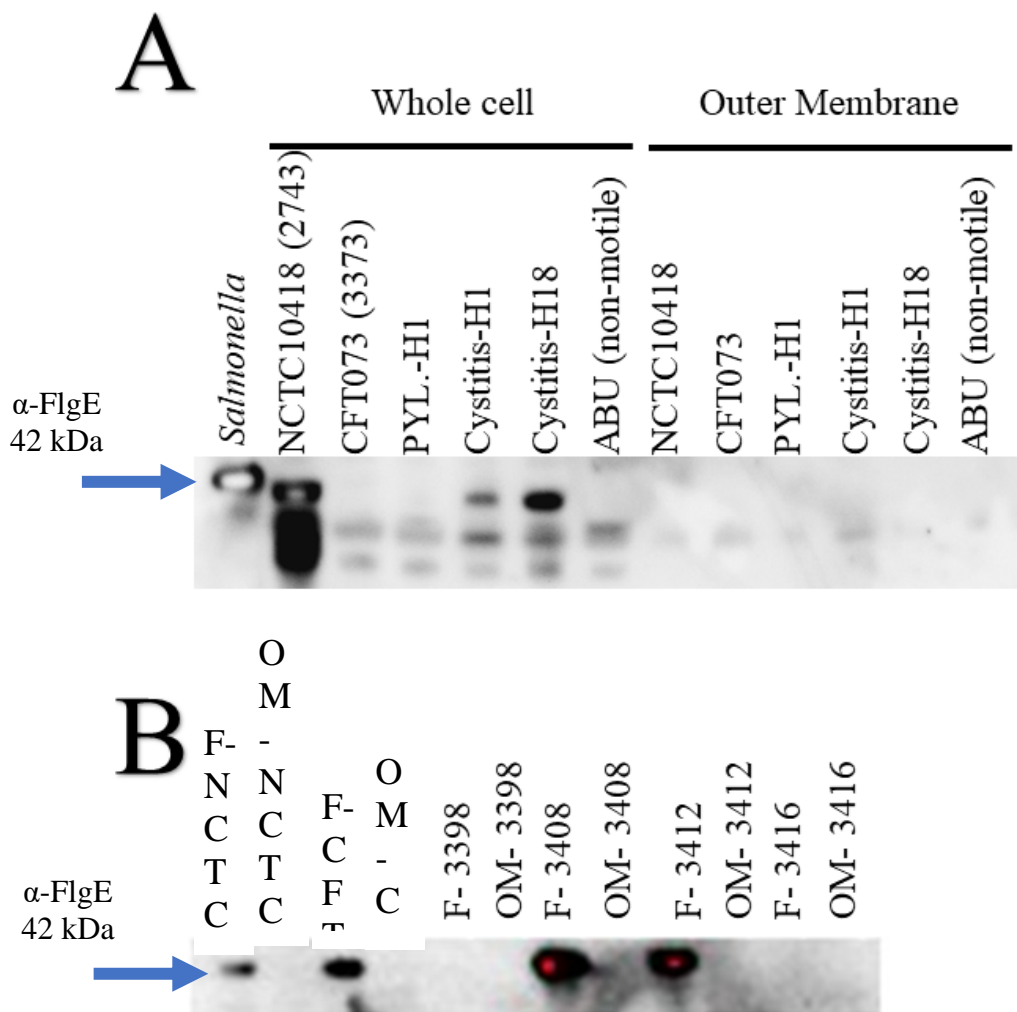


Figure 3.7 Analyses of flagellar contamination in *E. coli* OM preparations. **A)** Whole cell lysates and the OM isolations were immunoblotted with α -FlgE. The *Salmonella* strain was utilised as the positive control. Outer membrane preparations showed no FlgE. **B)** Comparison of the OM preparation and flagellar filament preparations (F) of the strains utilised in panel (A). Because the filaments were isolated by shearing, FlgE is typically visible in the flagellar preparations as expected. The antibody used was raised against FlgE from *Salmonella*.

The laboratory already had a plasmid (pSE_*flhDC*), containing the *flhDC* operon (*Salmonella*) with selection determined by ampicillin resistance. This plasmid, as well as a control plasmid pSE280 (no *flhDC*), were each transformed into three strains NCTC10418 which is a non-UTI strain, 3408 (UTI clinical isolate), and MG1655 which is a laboratory strain of *E. coli* K-12), by electroporation as described in M&M section 2.7.2 resulting in six recombinant strains. The choice of strains was limited as the ampicillin resistance marker of pSE_*flhDC* constrained the transformation of this plasmid into the majority of clinical strains as most of these strains were already ampicillin resistant.

A typical approach for quantifying swarming motility is the halo size, which refers to the region of bacterial motion on a solid surface. The size of the halo can be used to estimate the extent of swarming behaviour displayed by bacteria. Swarming motility is defined as the rapid and coordinated movement of a bacterial population across solid or semi-solid surfaces, and halo size gives a quantitative assessment of this behaviour. The size of the halo can be regulated by a variety of parameters, including nutritional composition, culture medium viscosity, and agar concentration.

Three independent recombinant colonies were used from each strain on two different days (n= 6 colonies) to test for motility (6 h at 30°C). As *flhDC* gene expression was under the control of the lac promoter, IPTG (0.1 mM) was added to the motility agar. Qualitative motility data are presented in Figures 3.8A & B while quantitative data, as determined by measuring halo diameters, are shown in Figure 3.9. The motility of NCTC10418, transformed with pSE_*flhDC*, was not significantly different from the wild-type strain although motility was significantly increased in strains 3408 and MG1655 respectively (p<0.001).

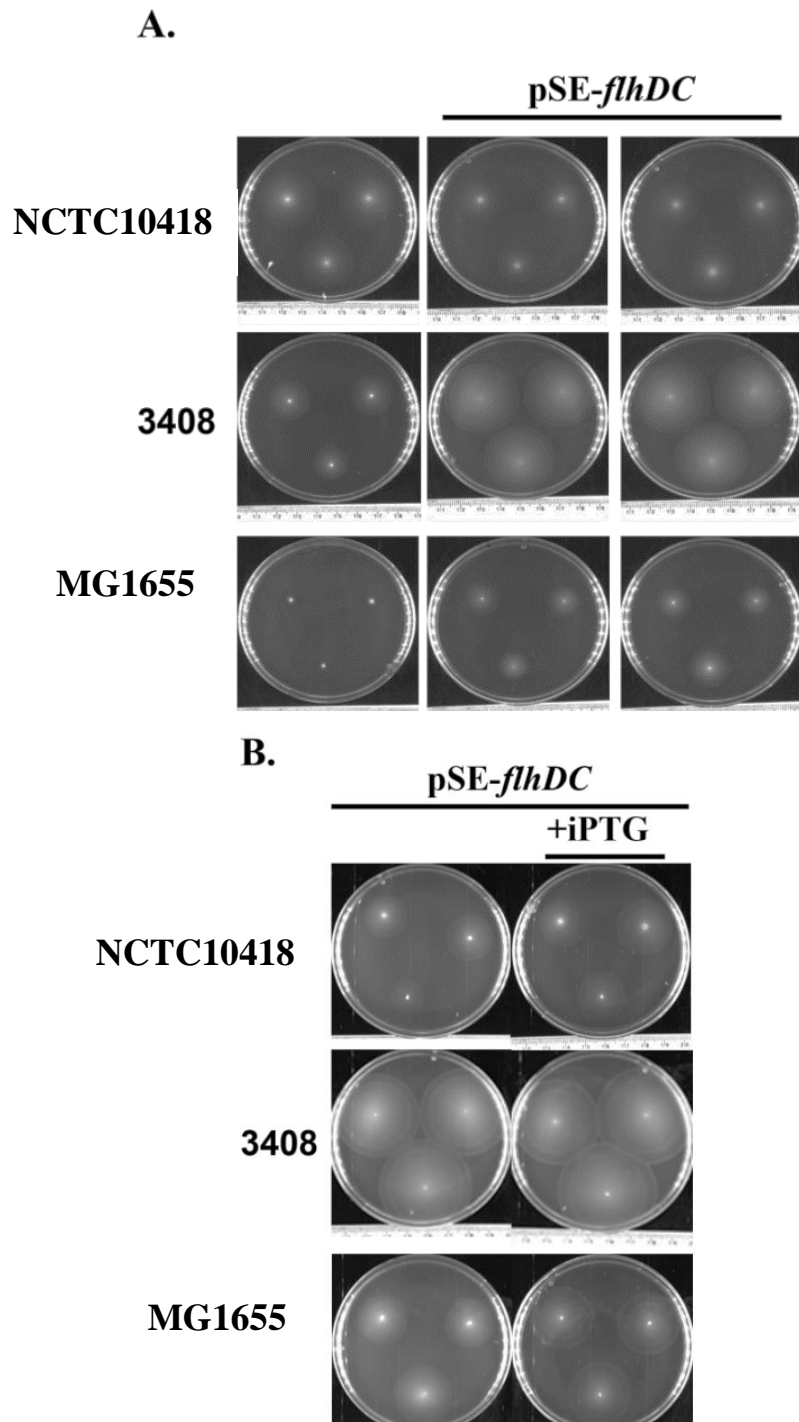


Figure 3.8 Motility assay of *E. coli* isolates \pm pSE-*flhDC* \pm IPTG (Qualitative Data).
A) *E. coli* strains \pm pSE-*flhDC*. **B)** Motility of the *E. coli* strains carrying the pSE-*flhDC* \pm IPTG.

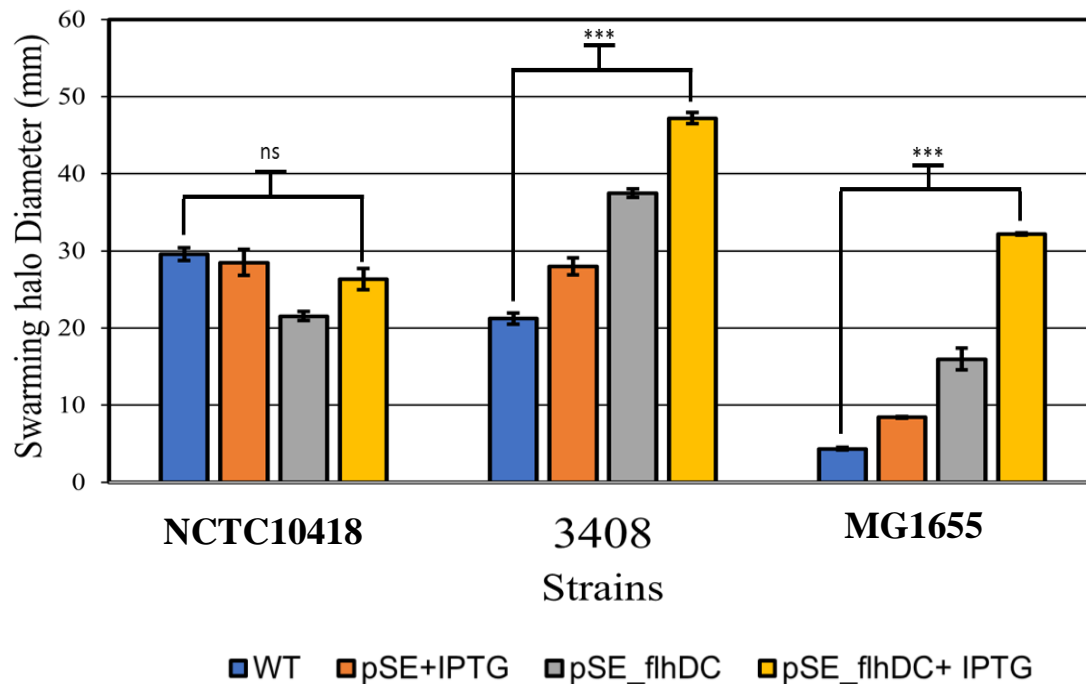


Figure 3.9 Motility assays comparing strains \pm pSE \pm *flhDC \pm IPTG.* Quantification of halo size resulting from the motility assays. error bars (SEM). Statistical analysis was performed by ANOVA. ns=not significant, ***= $p < 0.001$.

3.2.4 Using pSE_flhDC recombinant strains to explore the RT4 bladder innate response

Hyper-expression of *flhDC* significantly increased the motility of isolates 3408 and MG1655. To examine whether this increased motility affected the bladder innate response, the wild-type and transformed *E. coli* strains were cultured, heat killed as described in 2.11.1 and used (1×10^5 CFU/mL) to challenge 100 % confluent RT4 bladder cells for 24 h at 37°C. RT4 cells were also challenged with PBS and purified *E. coli* flagellin (50 ng/mL). Media bathing the RT4 cells were assayed, using neat and 1:100 dilutions, by ELISA for IL-8 concentrations (section 2.11.3). Data are shown in Figure 3.10.

Results demonstrated that the increased motility observed in strains 3408 and MG1655 transformed with pSE_ *flhDC*, was associated with an increase in IL-8 in the media

($p < 0.001$). However, the IL-8 concentrations measured in the media bathing the wild-type and transformed.

NCTC10418 strain were not significantly different, Figure 3.10. These data showed that for two strains, 3408 and MG1655, the innate response correlated to the motility data i.e. when the flagellar synthesis was increased the host innate response was also increased. These data suggest that the variability in the host response is linked to fluctuations in flagellar abundance and hence motility within the uro-associated *E. coli* clinical isolates.

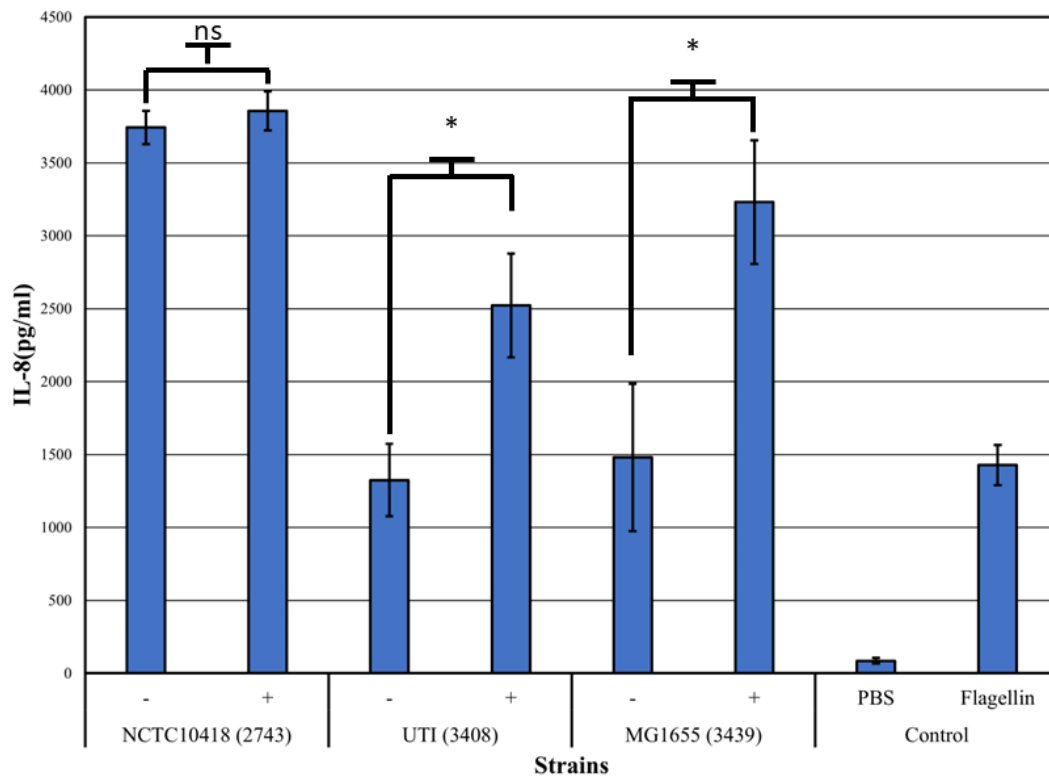


Figure 3.10 Response of RT4 (bladder epithelial cells) to *E. coli* heat killed strains \pm pSE_ *flhDC*. *E. coli* strains NCTC10418 (NCTC10418), 3408 (UTI), and 3439 (MG1655) \pm pSE_ *flhDC* were heat-killed and used to challenge RT4 cells for 24 hours. The negative control was (PBS), and the positive control was flagellin 50 ng/mL. IL-8 levels were quantified using ELISA. (ANOVA *: $p < 0.05$)

3.3 Discussion

Uro-associated *E. coli* isolates recovered from the urines of patients suffering lower and upper UTIs as well as asymptomatic bacteriuria revealed a mixture of motile and non-motile phenotypes (M. L. Lanz, 2013). When the motile strains were used to challenge RT4 bladder cells the innate responses, measured by NF- κ B activation were, surprisingly, variable, ranging from 2 fold to >30 fold. The studies reported in this Chapter were performed to attempt to understand the reasons underlying such variability.

Forsyth *et al.*, (2018), stated that infecting bacteria causing an UTI must multiply quickly in order to circumvent the host defences. This is supported by studies that show higher cell densities allow bacteria to overpower the host defences (Sintsova *et al.*, 2019). Additionally, it has been reported that faster growing *E. coli* produce more flagella, (Sim *et al.*, 2017), which in the case of an UTI will facilitate UPEC ascension of the urinary tract and infection of the bladder. However, in the lower urinary tract, potential uropathogens are detected via their flagella via TLR5 receptors. Therefore, it can be hypothesised that the growth rates of infecting bacteria need to be fast to saturate the host TLR5 receptors and innate defences, and ensure survivability. In support, a faster than average doubling time has been reported in clinical isolates from patients suffering UTIs (Forsyth *et al.*, 2018). However, data in this study also suggested that uro-associated *E. coli* motility was linked to variable NF- κ B responses, hence variable innate responses, which was surprising. To explore this further the uro-associated *E. coli* isolates, which were a mix recovered from ABU, cystitis and pyelonephritis patients, were examined for their growth rates ie fitness.

Comparing the growth rates of the motile and non-motile strains showed a significant difference (ANOVA $p = 0.011$). However, when the growth rates of motile and non-motile isolates were compared according to the source of the infection, no significant differences in

growth rate were identified. Yet, it could be argued that some of these data (pyelonephritis and bacteraemia related) were compromised by isolate numbers meaning more isolates need to be analysed to confirm this data. However, the range of doubling times measured between the motile and non-motile strains led to the overall conclusion that bacterial fitness was not underpinning the variability in host recognition observed within the motile strain collection.

Interestingly, an investigation determining the doubling times of *E. coli* strains showed a similar outcome with doubling times varying between strains (Gibson et al., 2018). Being motile is one of the most energy expensive bacterial activities with flagellar synthesis typically increased during periods of stress. For example, Ni *et al.*, (2020), showed that in poor nutritional conditions *E. coli* invests in motility, rather than cell division, to exploit nutritional resources. Interestingly, these authors also reported that motility was exploited in homogeneous bacterial cultures, presumably to allow utilisation of excreted metabolites, such as amino acids, sugars and organic acids. In relation to UTIs it is presumed that flagellar synthesis provides access to better nutritional conditions, but motility has to be balanced against detection by the host and subsequent microbial death.

Constructing mutants in genes involved in chemotaxis will help explain their involvement in motility and innate immunity. Deleting all the genes involved in chemotaxis will give an idea whether they are impacting both the motility and impacting the innate immune response. In case of any effect then a systematic mutation series targeting those genes individually will help identify the level of involvement of each gene in such impact. All these mutants should undergo a series of experiments testing motility, gene expression, protein expression, impacting the innate response, and flagellar abundance.

On the other hand, chemotaxis is a microorganism's capacity to recognise chemical gradients and direct their movement either up or down the gradient. Motility, on the other hand, refers to the active movement of cells in a liquid environment, frequently aided by

flagella or other extracellular appendages. Chemotaxis and motility play critical roles in bacterial infection establishment and maintenance, as well as nutrition uptake. *E. coli*, for example, can demonstrate chemotaxis towards hormones or repulsion from indole, which can help it connect to host cells and establish infection. Other harmful bacteria, including *H. pylori*, *C. jejuni*, *S. Typhimurium*, *V. cholerae*, and *P. aeruginosa*, can demonstrate chemotactic responses to different metabolites, allowing them to identify and colonise their hosts. The regulation of motility and chemotaxis is intricate, including numerous genetic and metabolic pathways. In *Sinorhizobium meliloti*, *Agrobacterium fabacearum*, and *Rhizobium leguminosarum*, transcriptional activation of flagellar and chemotaxis genes is controlled by a distinct cluster encoding a second copy of the *cheY* and *cheZ* genes (Aroney et al., 2021). Chemotaxis clusters in *B. diazoefficiens* include core genes like *cheY*, *cheA*, *cheR*, *cheB*, and *cheW*, as well as additional genes like *cheB* and *cheW* that are linked to specific chemoreceptors (Mediati et al., 2024). Overall, chemotaxis and motility play important roles in bacterial behaviour and interactions, and knowing these mechanisms can shed light on the ecology and pathogenicity of diverse microbial systems.

E. coli chemotaxis is the movement of bacteria towards attractants and away from repellents. *E. coli*'s chemotaxis system is made up of five transmembrane proteins, each of which detects a different type of attractant or repellent chemical (Hadjidemetriou et al., 2022). When attractants are absent or repellents are present, these receptors send out a signal that causes CheA autophosphorylation. Increased CheA phosphorylation raises the level of phosphorylated CheY, a response regulator that interacts with the flagellar motor to govern swimming direction. *E. coli*'s chemotaxis system is extremely complex, with 10,000 potential states for these receptors due to methylation at four different locations. This intricacy results in individuality among genetically identical bacteria within a community, with no two bacteria responding exactly the same manner to attractant and repellent stimuli. Cryo-electron

microscopy has been utilised to investigate the structure and function of *E. coli* chemotaxis receptor arrays, resulting in a more complete understanding of their structure and function (Burt et al., 2021). Molecular modelling and simulation techniques have also been used to supplement structure determination, resulting in a better understanding of the mechanisms underpinning chemotaxis signalling pathways. Chemotaxis pathways have historically been studied in the model organism *E. coli* because of its relative tractability in terms of signalling components (Hadjidemetriou et al., 2022). Individual *E. coli* cells' chemotactic adaptation kinetics have been investigated, with the chemotactic response providing as a model for how living cells respond and adapt to changes in their environment. Chemotaxis in bacteria, particularly *E. coli*, has been demonstrated to play an important role in regulating bacterial colonisation and pathogenesis in the gastrointestinal tract (Lopes & Sourjik, 2018).

Bacterial LPS is detected by urothelial TLR4 proteins (Freundt et al., 2001). TLR4, in the murine model, is a key part of the bladder innate immune response to UPEC (Ragnarsdottir et al., 2010), playing a crucial role in clearing the bladder of bacterial cells by triggering exfoliation (Cheng et al., 2016). In the human bladder the role of TLR4 in protecting the urinary tract appears much less important with TLR5 being the key innate receptor (Ali et al., 2017; Smith et al., 2011).

A NF- κ B response was observed in bladder cells challenged with *E. coli* isolates OM material, which contained LPS + PG PAMPs. These responses were low and equivalent to those of bladder cells in which the TLR5 receptor expression had been 'knocked-down'. To exclude flagellin contamination of the OM preparations the OM samples were probed for flagellar proteins. Our laboratory supplies included antibodies raised against *Salmonella* flagellar proteins. FliD and FlgE, which share identities of 52% and 87% and similarities of 70% and 92%, respectively to the *E. coli* proteins. It was predicted that the α -FlgE_{ST} antibody was the most likely to show cross-reaction between the two bacterial species and this proved

to be the case (Figure 3.6). Despite showing 52% and 70% similarity with the *E. coli* protein the protein identity, data indicated that the FlhD antibody only detected the *Salmonella* protein. Thus, suggested that key immuno-reactive amino acids were either not part of the *E. coli* protein or were buried within the protein (structural difference). In contrast the FlgE_{ST} antibody showed cross-reaction with the *E. coli* proteins which reflected the >70% amino acid identity and similarity data. Use of this antibody, led to the conclusion that the observed variability in the innate responses of the motile bacteria was not linked to flagellin contamination of the OM preparations. It could be argued that the antibody approach was not sensitive enough to detect flagellin contamination of the OM preparations. Another technique that could have been used with increased sensitivity is mass spectrophotometry. Recently, this technique has been used to identify and characterise proteolytic flagellin (flagellinolysins) in the bacterium, *Hylemonella gracilis*, a Gram negative found in pond water (Eckhard et al., 2020).

To investigate the potential roles of flagella numbers in modulating motility and hence the innate, NF- κ B, response *E. coli* strains were manipulated to alter their flagella numbers. The plasmid pSE_ *flhDC* carrying *flhDC* from *Salmonella* was used to test the hypothesis that changing bacterial motility will change the innate response. This plasmid is ampicillin resistant which compromised the analyses scientifically as only strains sensitive to ampicillin (NCTC10418, UTI isolate #3408, and MG1655) could be engineered. The use of this plasmid again raised potential issues as *Salmonella* and not *E. coli* was the source of the *flhDC* operon. However, the *Salmonella* system exhibits 94% similarity and 92% identity to *E. coli*, which arguably justified the use of the plasmid (Albanna et al., 2018). The ideal approach, had time allowed, would have been to construct a plasmid carrying *flhDC* from *E. coli* and containing a range of appropriate antibiotic resistant markers to allow the use of the plasmid in clinical isolates carrying different antibiotic resistance.

Engineering NCTC10418 did not change its motility nor its impact on the bladder innate response, however, the motility of *E. coli* strains, MG1655 and the UTI isolate, were increased after pSE_ *flhDC* transformation. These findings indicate that overexpressing *flhDC* in the UTI isolate and MG1655 strain, resulted in increased flagellin production, which contributed to the high levels of the proinflammatory response i.e., increased, IL-8 production. These findings showed that uropathogenic *E. coli* have the ability to activate flagella production, leading to increased motility. However, as mentioned previously this comes at a cost as these bacterial cells are readily identified by host TLR5 receptors. Activation of these receptors activates the innate response involving NF- κ B and the production of the proinflammatory cytokines, including IL-8 that attract macrophages to eliminate the bacteria. In relation to NCTC10418, it can be predicted that is already exceeding the percentage of flagellated bacterial cells threshold (>60%) which explains why no changes in motility were observed (Tan et al., 2023).

Overexpressing bacterial genes by inserting a plasmid carrying a gene from another species presents both advantages and disadvantages. On the positive side, this approach provides precise control over gene expression, allowing researchers to modulate protein production levels using inducible promoters or regulatory elements. This enhanced control facilitates functional studies to elucidate the roles of specific proteins in bacterial physiology, metabolism, or pathogenesis (Ijaq et al., 2022; Mahlich et al., 2023). Additionally, overexpressing foreign genes can lead to increased production of desired proteins, which is beneficial for industrial applications requiring large quantities of recombinant proteins. Moreover, introducing genes from other species into bacterial hosts can confer advantageous traits, such as the degradation of environmental pollutants or the synthesis of valuable compounds, with applications in bioremediation, biotechnology, and biofuel production.

However, there are notable disadvantages associated with this approach. Overexpressing foreign genes may impose a metabolic burden on bacterial hosts, resulting in reduced growth rates, decreased viability, or altered physiological states. This burden arises from the diversion of cellular resources towards protein synthesis, leading to energy depletion or the accumulation of toxic intermediates. Plasmids carrying foreign genes may also exhibit instability within bacterial hosts, leading to the loss of inserted DNA over time. This instability can result from plasmid segregation during cell division or selective pressure against plasmid maintenance. Additionally, exogenous proteins produced by overexpressed genes may elicit immune responses or exert toxic effects on bacterial hosts, impacting cell viability and productivity. In this chapter, an overexpression of the master regulator has been performed leading to the upregulating of the expression of the flagella system. the flagellar system has a significant metabolic burden so overexpressing it would have an overall metabolic impact that may bias the observed response of RT4 cells. In summary, while overexpressing bacterial genes via plasmid-mediated gene transfer offers significant advantages, careful consideration of the associated disadvantages is essential to maximize benefits and minimize potential drawbacks. The next phase of this project was to explore how UPEC strains control their flagellar synthesis to evade the bladder innate defences. In this approach no foreign genes would be used.

Chapter 4. The effect of manipulating the regulation of flagellar synthesis in UPEC and its impact on the innate response of RT4 Bladder cells.

4.1 Introduction

The information in Chapter three demonstrated that plasmid-based overexpression of *S. enterica flhDC* in uro-associated *E. coli* isolates results in increased motility and a reciprocal increase in the innate immune response, defined by IL-8 concentrations, of challenged RT4 bladder cells. The hypothesis demonstrated in (Tan et al., 2023), suggests that UPEC strains regulate flagellar synthesis to evade the recognition by host TLR5 receptors. In this chapter, two mutants $\Delta flhDC$, and $\Delta clpP$ were constructed to further explore the effect of gene regulation on the motility phenotype of *E. coli* clinical isolates and model strains, and the impact on the bladder innate response. To achieve this objective, UPEC strains and mutants used in this chapter, were assessed for motility, flagellar gene expression, flagellar protein expression, flagella abundance and their ability to induce an innate response.

The master regulator of flagellar synthesis in *Enterobacteriaceae*, including *E. coli*, is FlhD₄C₂ (Shi et al., 1993). The transcription of all flagellar genes depends on the expression of *flhDC*, located in the class1 flagellar operon at the top of the three-tier transcriptional hierarchy that controls flagellar synthesis (Chilcott & Hughes, 2000). To control flagellar synthesis and coordinate gene expression in *E. coli*, FlhD₄C₂ interacts with σ^{70} (Helmann & Chamberlin, 1987). FlhC and FlhD from *E. coli* and *S. enterica* exhibit 92 and 94% identity respectively (Albanna et al., 2018). To maintain optimal flagella numbers *E. coli* requires a specific transcription rate of *flhDC*. FlhD₄C₂ is affected negatively by both transcriptional and post-transcriptional regulatory mechanism, one post-transcriptional regulatory pathway is the degradation of FlhD₄C₂ by ClpXP (Kitagawa et al., 2011).

The majority of bacterial intracellular proteolysis activities are triggered by ATP-dependent proteases, such as Clp and Lon (Goldberg, 1992). ClpXP is a protease that is involved in numerous cellular processes, one being the control of flagellar synthesis.

Phenotypic characterization of *S. enterica* lacking the ClpXP protease resulted in a hyper-flagellated phenotype (Tomoyasu et al., 2002). Two mechanisms are used by the ClpXP protease to control the expression of flagellar genes in *E. coli*. One mechanism includes the degradation of the FlhC and FlhD proteins by ClpXP, which results in the downregulation of flagellar gene expression (Sato et al., 2014). Only after the cells have reached stationary phase in a culture media is the ClpXP protease active in controlling the transcription of the *flhD* promoter (Kitagawa et al., 2011). Within the flagellar regulon, FlhD₄C₂ is the primary target of ClpXP. While ClpX does not directly interact with FlhD₄C₂, it does increase affinity of ClpXP against the FlhD₄C₂ complex. ClpXP acts through the complex FlhD₄C₂, but not on the FlhC or FlhD as individuals (Takaya et al., 2012).

Although, the flagellar synthesis system of *E. coli* performed as predicted when under the control of FlhDC from *S. enterica* (Albanna et al., 2018) - Chapter 3, section 3.2.3 - it was important to further test the regulation of the *E. coli* flagellar system. This was achieved by manipulating known regulators of *E. coli* flagellar synthesis by constructing mutants. The mutants constructed included one that resulted in no expression of flagellar synthesis: $\Delta flhDC$, while the other mutant lacked a repressor of flagellar synthesis: $\Delta clpP$ and resulted in hyper-flagellated strains. These mutants were used to examine motility and to challenge RT4 bladder cells to explore the impact on the urothelial innate response.

4.2 Constructing deletion mutants of *flhDC* and *clpP* in *E. coli*

Deletion mutants were constructed to the *flhDC* operon and *clpP* using a lambda (λ) red recombinase system that allowed the targeted genes to be replaced with a gene fragment encoding a chloramphenicol (Cm) resistant cassette (Datsenko & Wanner, 2000). To construct the mutants, primers were designed with compatible sequences to the chloramphenicol (Cm) resistant cassette in pKD3 and 5' overhangs to the primers designed to

the flanking regions of *flhDC* and *clpP* consecutively (Chapter 2, Section 2.8). The primers #1611, and # 1612 (Table 2.5) were used to generate a fragment to replace *flhDC*, while primers #877 and #878 generated a fragment to replace *clpP*. The expected PCR fragments were 1.1 Kbp in length, and these are shown in Figure 4.1. The PCR fragments were extracted and cleaned as described (Chapter 2, Section 2.6).

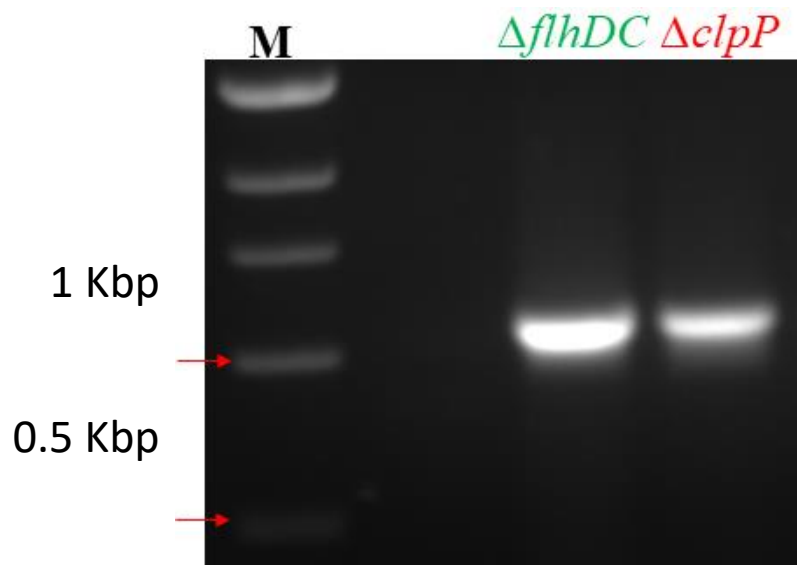


Figure 4.1 Generation of the chloramphenicol resistant cassettes used in constructing the $\Delta flhDC$ and $\Delta clpP$ mutants. The generated fragments are 1.1 Kb in size. M: marker lane using the 1 Kb NEB DNA ladder #B7025 (New England Biolabs).

The strains chosen for this chapter included CFT073, MG1655, and NCTC10418, described in Tan *et al.* (2023), and three uro-associated clinical *E. coli* isolates: 3408, 5469 and 5489. These uro-associated *E. coli* isolates represented sequence types ST1126, ST131 and ST69 respectively. Sequence type ST131 and ST69, along with ST73 represented by CFT073, are common genotypes of *E. coli* associated with UTIs. To construct $\Delta flhDC$ and $\Delta clpP$ in the above-mentioned strains, plasmid pKD46_Kan was introduced into the strains by electroporation and selected for on LB plates supplemented with kanamycin at 30°C. PCR fragments (chloramphenicol resistant cassette) for *flhDC* and *clpP* were introduced into the

strains carrying pKD46_Kan by a second round of electroporation and transformants selected for on LB plates supplemented with chloramphenicol at 37 °C.

Construction of each mutant was confirmed genetically by PCR. Insertion of the Cm cassette in the generation of $\Delta flhDC$ lead to a PCR fragment size of 1.1 Kbp compared to the 1 Kbp parental gene (Figure 4.2 A). Using primers #1031 and #1023 led to the expected increase in PCR fragment size (Figure 4.2 B). In relation to $\Delta clpP$, primers #893 and #894 were used for strains 3408, and MG1655 generating a 1.5 Kbp fragment compared to 1Kbpp for an intact *clpP* gene (Figure 4.3 A & B). The remainder of the strains (NCTC10418, CFT073, 5469, and 5498) were analysed using the primers #893 and #13. Primer #13's recognition site was within the Cm cassette with amplification resulting in a PCR fragment of 472 bp, but only in the mutants; no bands were observed when parental wild type DNA was used (Figure 4.3C).

4.3 Comparing motility of the $\Delta flhDC$ and $\Delta clpP$ mutants to the wildtype strains

After the mutants were successfully generated and confirmed by PCR, motility assays were performed for 6 hours at 37 °C using semi-solid motility media. As predicted all $\Delta flhDC$ mutants were non-motile (Figure 4.4). In contrast all $\Delta clpP$ mutants showed increased motility compared to the respective wildtype (Figure 4.4). These motilities were quantified, and the parental wild type *E. coli* isolate data compared to their respective $\Delta clpP$ mutant data (Figure 4.5). Significance was measured by using individual t-tests of each pairing. For NCTC10418, the difference in motility between the wildtype and its $\Delta clpP$ mutant was not significant. Interestingly the $\Delta clpP$ mutant exhibited similar motility behaviour to that observed in relation to *flhDC* overexpression in Chapter 3 (Figures 3.8 & 3.9). However, statistical significance was detected for all other strain pairings with each $\Delta clpP$ mutant showing increased motility compared to its wild-type (p value <0.001; Figure 4.5).

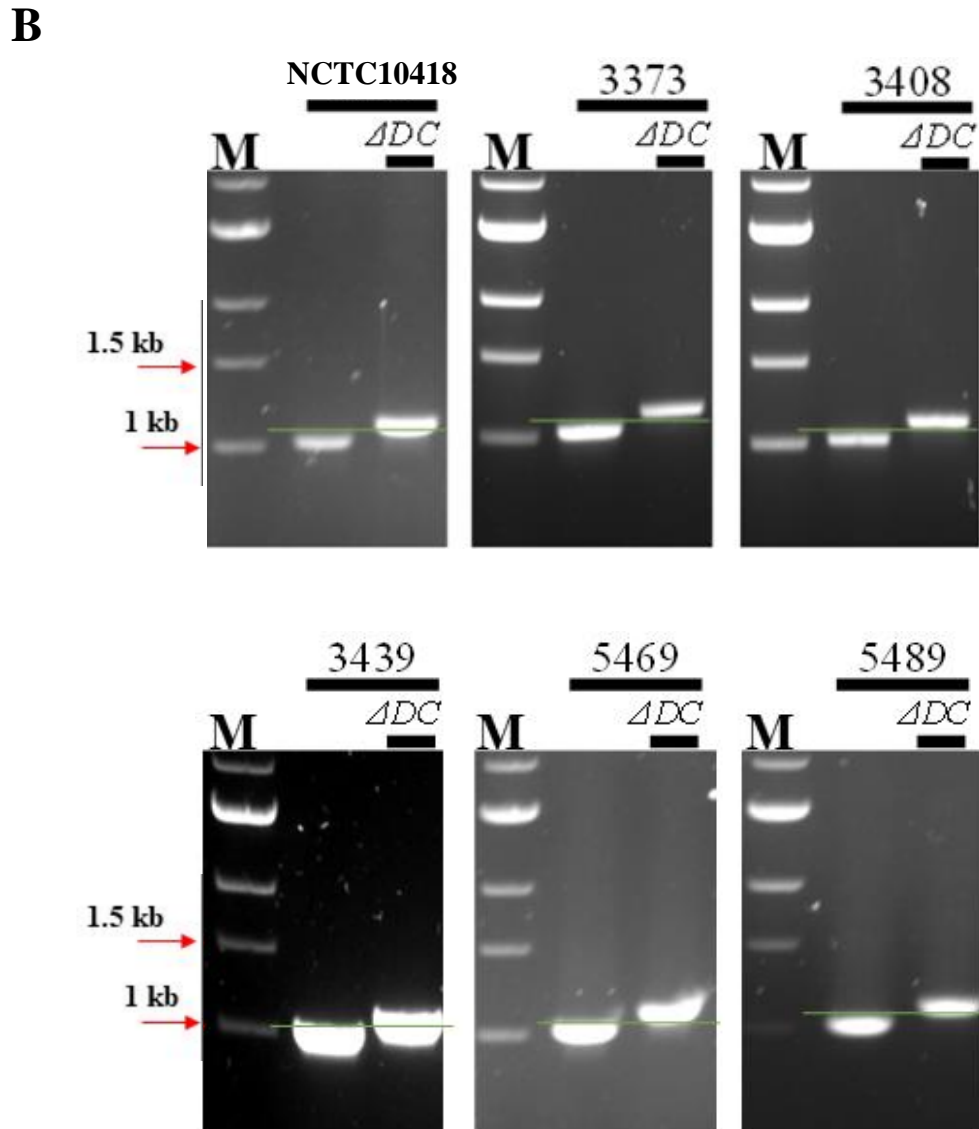
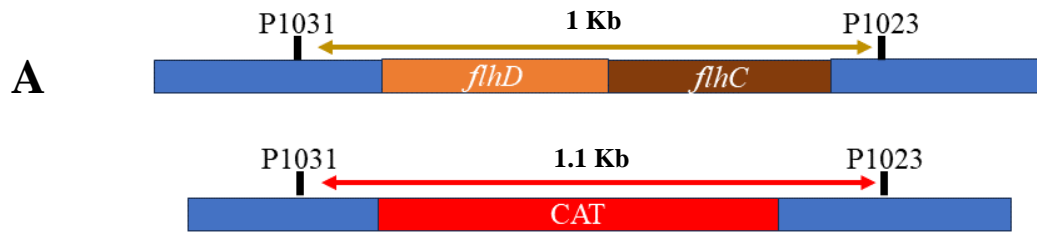


Figure 4.2 PCR confirmation of the $\Delta flhDC$ mutants: **A)** Schematic of the primer annealing sites and the expected PCR fragment sizes. **B)** Gel images of the amplified PCR fragments relating to the wildtype and $\Delta flhDC$ mutants. M: marker lane using the 1 Kb NEB DNA ladder #B7025 (New England Biolabs).

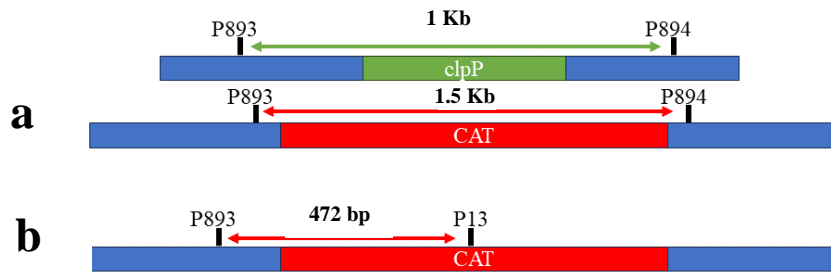
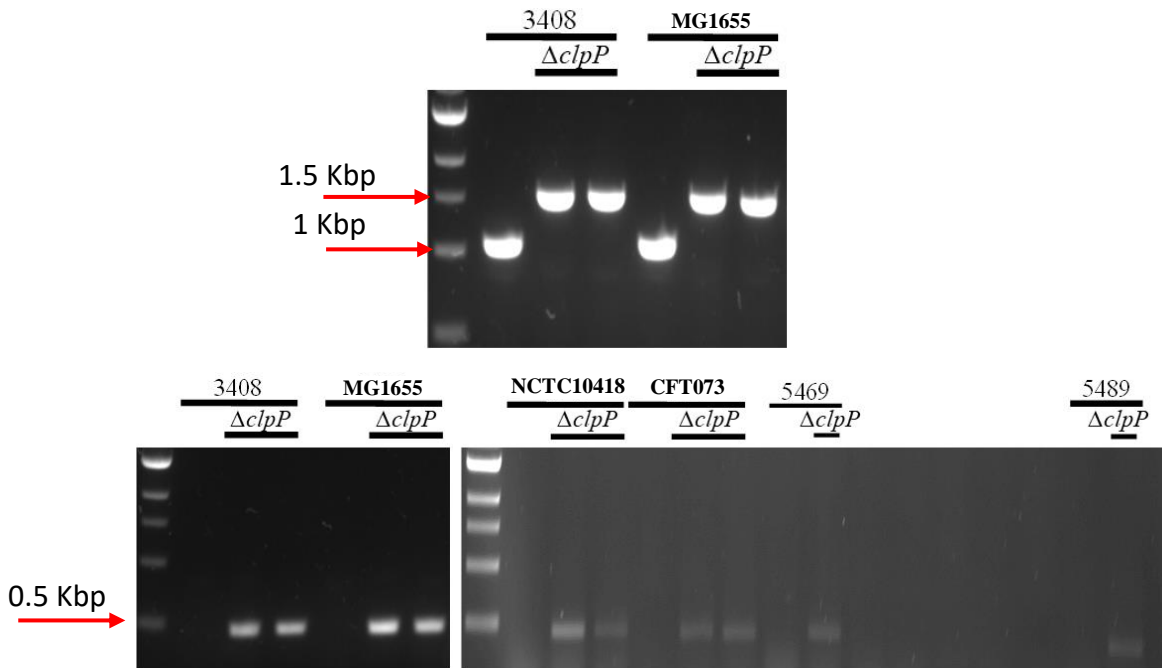
A**B**

Figure 4.3 PCR confirmation of the $\Delta clpP$ mutants. A) Schematic of the primer annealing sites and the expected PCR fragment sizes. Panel (a) represents the expected sizes generated using reverse primer #894, which anneals downstream the gene. Panel (b) represents the expected sizes generated using reverse primer #13, which anneals to the middle of the insert. B) Gel images of the amplified PCR fragments produced using primers #893-894 showing the expected 1.5 Kb bands for $\Delta clpP$ while the wild type produced a 1 Kb band. M: marker lane using the 1 Kb NEB DNA ladder #B7025 (New England Biolabs)

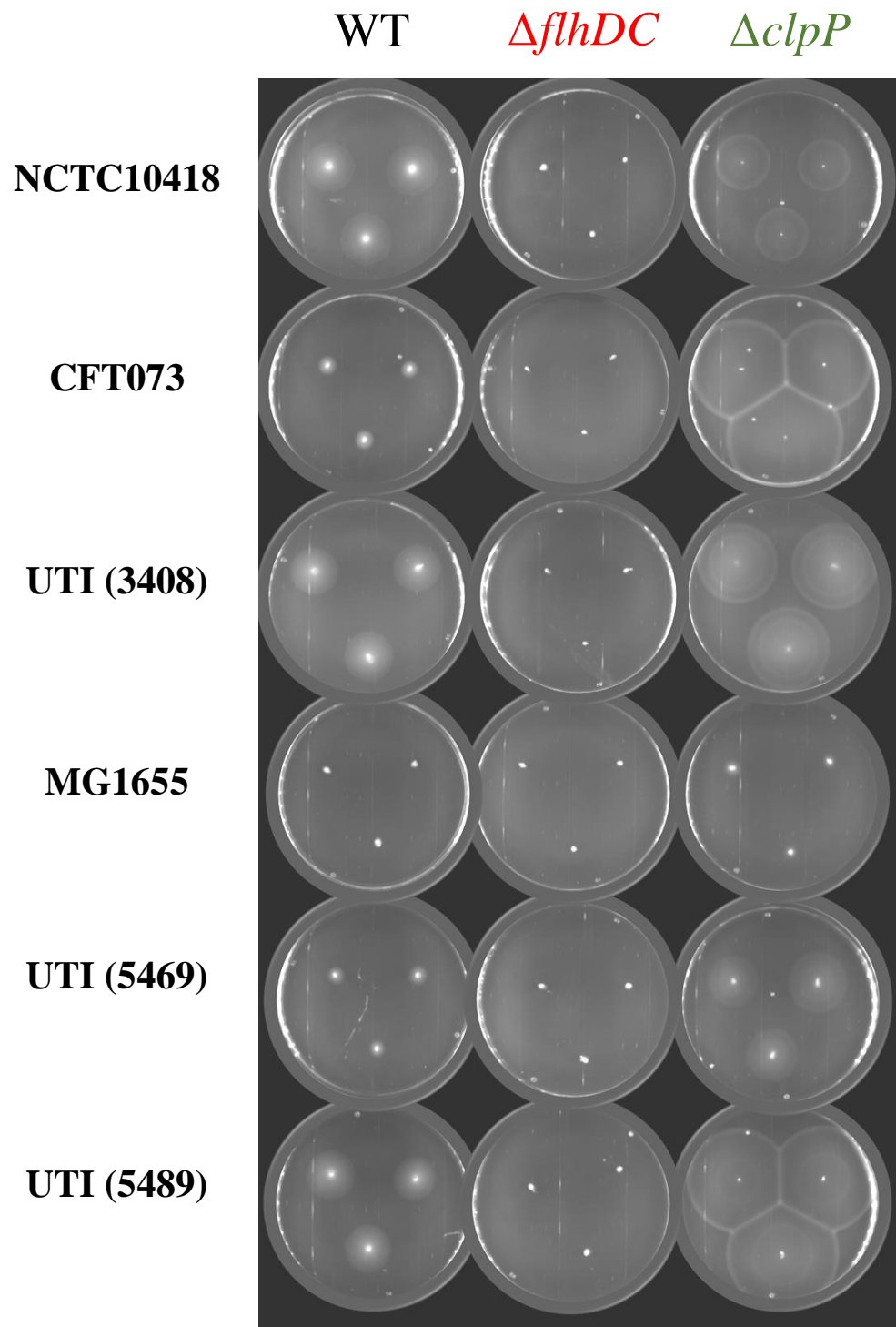


Figure 4.4 Motility assays of *E. coli* wild-type isolates and their respective $\Delta flhDC$ and $\Delta clpP$ mutants. Motility assays were performed at 37 °C for 6 h.

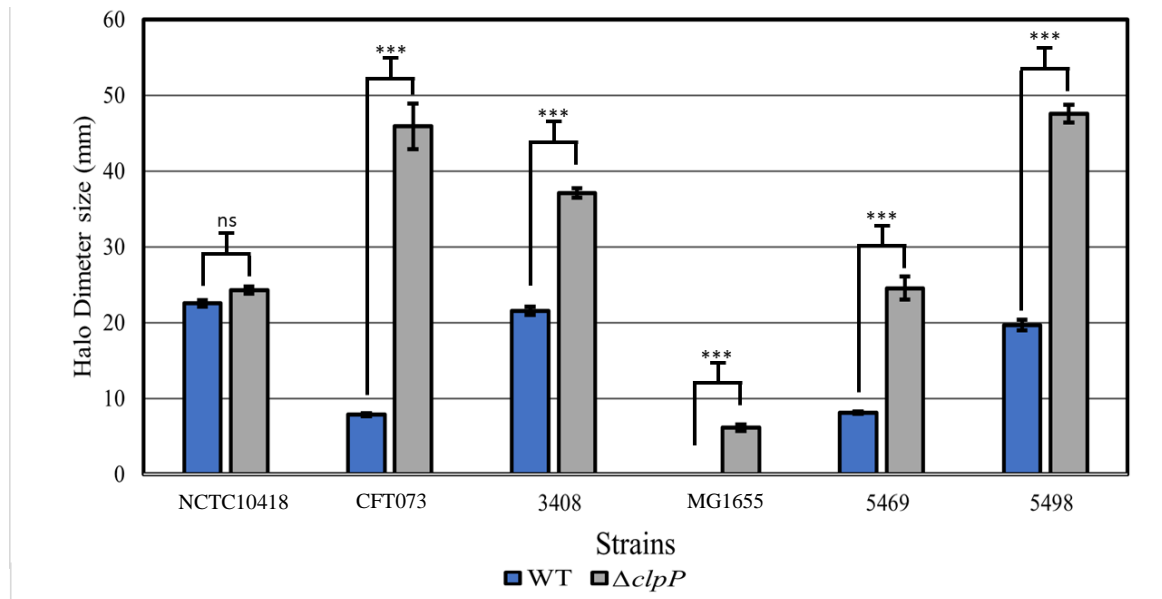


Figure 4.5 Quantification of motility in wild-type *E. coli* isolates compared to their $\Delta clpP$ mutants. Halo sizes were measured in mm using imageJ (Section 2.11). Error bars represent standard error of mean (SEM). Statistical analysis was performed by t-test. ns=not significant, ***= $p < 0.001$.

Calculating the ratio of motility for each pair identified CFT073 as showing the largest increase in swarm size, 5.5-fold.

4.4 Defining the innate response to $\Delta flhDC$ and $\Delta clpP$ mutants

Previous research in Chapter 3 indicated that overexpression of *flhDC* was associated with a stronger IL-8 RT4 bladder cell host response. To explore these responses further the mutants described in this Chapter were also used to challenge RT4 cells. As previous all challenges were performed for 24h using heat killed samples (10^5 CFU/mL). PBS was used as the negative control while purified flagellin was used as the positive control. Twenty-four hour IL-8 data are presented in Figure 4.6. Deletion of *flhDC* lead to a 4-fold reduction in IL-8 production in NCTC10418 (Figure 4.6).

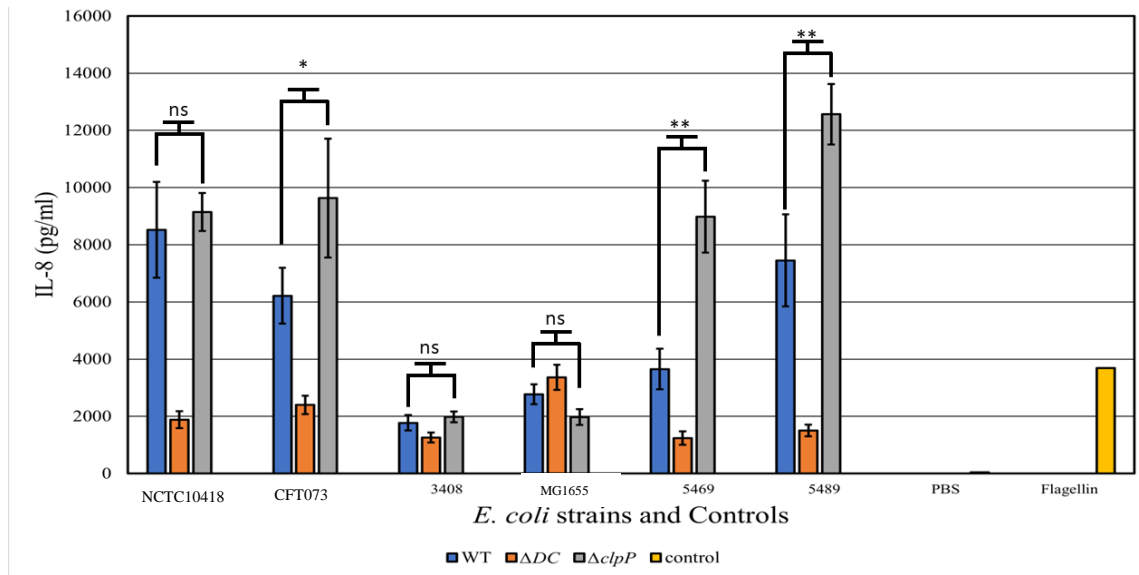


Figure 4.6 IL-8 concentrations following challenge of bladder RT4 cells to wild-type *E. coli* strains and their $\Delta flhDC$ & $\Delta clpP$ mutants. PBS was the negative control and Flagellin (500 ng) the positive control (Yellow). Data show IL-8 concentrations (pg/mL) following exposure of the RT4 cells to wild type (Blue), $\Delta flhDC$ (orange), and $\Delta clpP$ (Grey) strains. Ns : not significant; *= $p < 0.05$; **= $p < 0.01$.

Data represent three independent biological repeats for each strain and two technical repeats. Statistical analysis was performed by t-test.

While the $\Delta flhDC$ mutants were associated with IL-8 concentrations of between 1235-3362 pg/mL these were in fact significantly reduced compared to their respective parental strains CFT073, 5469 and 5489.

In contrast, significant increases in IL-8 concentrations were detected for the $\Delta clpP$ mutants, CFT073, 5469, and 5489. As with overexpression of *flhDC* in NCTC10418, and the motility phenotype of the $\Delta clpP$ mutant, no significant increase in IL-8 was observed for NCTC10418 $\Delta clpP$ compared to its wildtype parent.

The mutants and wild types of strains 3408 and MG1655 showed similar IL-8 responses (Figure 4.6), hence these strains did not behave as expected. Additionally, these data were reproducible as further repeats of the challenges for these two strains did not alter the observed outcome shown in Figure 4.6 – data not shown. This IL-8 response pattern does

not correlate with the motility phenotypes of these strains and justified further investigation of flagellar protein levels and flagellar gene expression. While the $\Delta flhDC$ mutants were associated with IL-8 concentrations of between 1235-3362 pg/mL these were in fact significantly reduced compared to their respective parental strains CFT073, 5469 and 5489. In contrast, significant increases in IL-8 concentrations were detected for the $\Delta clpP$ mutants, CFT073, 5469, and 5489.

As with overexpression of *flhDC* in NCTC10418, and the motility phenotype of the $\Delta clpP$ mutant, no significant increase in IL-8 was observed for NCTC10418 $\Delta clpP$ compared to its wildtype parent.

4.5. Detecting FlgE in the $\Delta flhDC$ and $\Delta clpP$ strains

To further investigate the behaviour of the 3408 and MG1655 $\Delta flhDC$ and $\Delta clpP$ mutants with respect to the flagellar system, FlgE protein synthesis was explored. Immunoblots were performed as described in Chapter 2, using α -FlgE_{ST}, with the results shown in Figure 4.7. The $\Delta flhDC$ mutants were characterised by the lack of FlgE bands indicating no flagellar gene synthesis. On the other hand, qualitative assessment of the $\Delta clpP$ mutant isolates indicated, as expected, strong FlgE bands consistent with flagellar synthesis. These data supported enhanced FlgE synthesis in the $\Delta clpP$ mutants compared to their parental wild type strains. When viewed qualitatively these immunoblot data suggested comparable synthesis of FlgE in the MG1655 parental and $\Delta clpP$ strains, but reduced synthesis in the wild-type 3408 strain compared to its $\Delta clpP$ mutant. These data correlated with the motility data for 3408 ($\Delta clpP$ mutant associated with increased motility (Figure 4.5)), but not the IL-8 data (no change in IL-8 concentrations between the wild-type and mutant strains). In relation to strain MG1655 the immunoblot data neither explained the motility data (flagella, but no motility) nor the IL-8 data (flagella, but no IL-8 response). To

try and understand this further flagellar gene expression of all the isolates was quantified and compared.

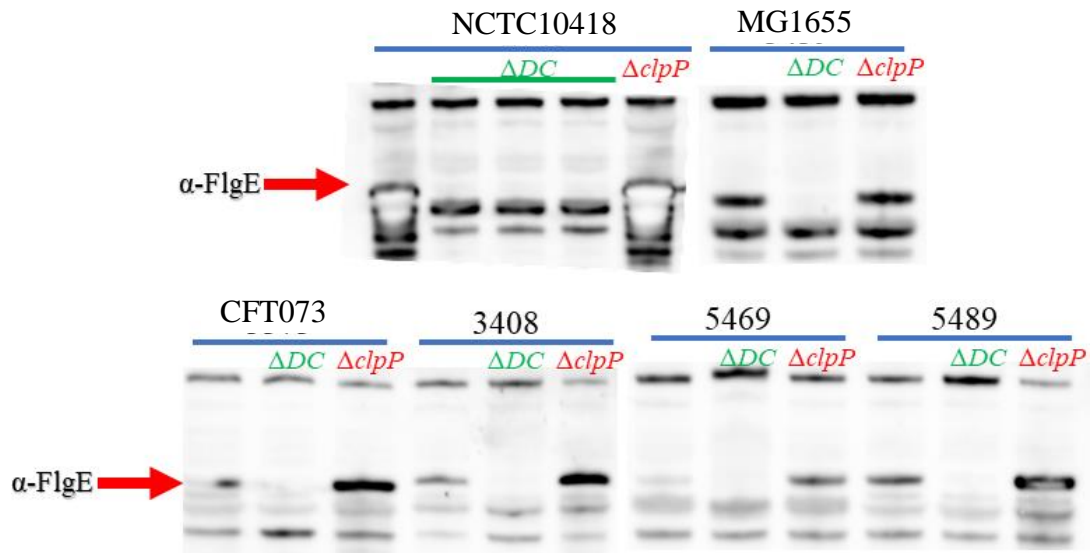


Figure 4.7 FlgE synthesis in the wild-type *E. coli* isolates and their respective $\Delta flhDC$ and $\Delta clpP$ mutants. Immuno blotting of cell lysates prepared from isolates NCTC10418, 3439, CFT073, 3408, 5469 and 5489 and their respective mutants using 200 OD for each sample and α -FlgE_{ST}

4.6 Flagellar gene expression of the $\Delta flhDC$ and $\Delta clpP$ mutants

There is evidence to suggest that ClpP can indirectly regulate *flhDC* transcription via degradation of other transcription factors in *E. coli* (Kitagawa et al., 2011; Takaya et al., 2012). So, to further investigate the effect of deleting the *flhDC* and *clpP* in *E. coli*, flagellar expression was measured using RT-qPCR as detailed in sections 2.4.1-3 and using the housekeeping genes *gyrB*, *rpoB* and *gmk*. Flagellar genes relating to different promoter classes were targeted including *flhC*-(class1), *fliG* (class2), *motA* and *fliC* (class3). Gene expression data are shown in Figures 4.8, 4.9 and 4.10 respectively.

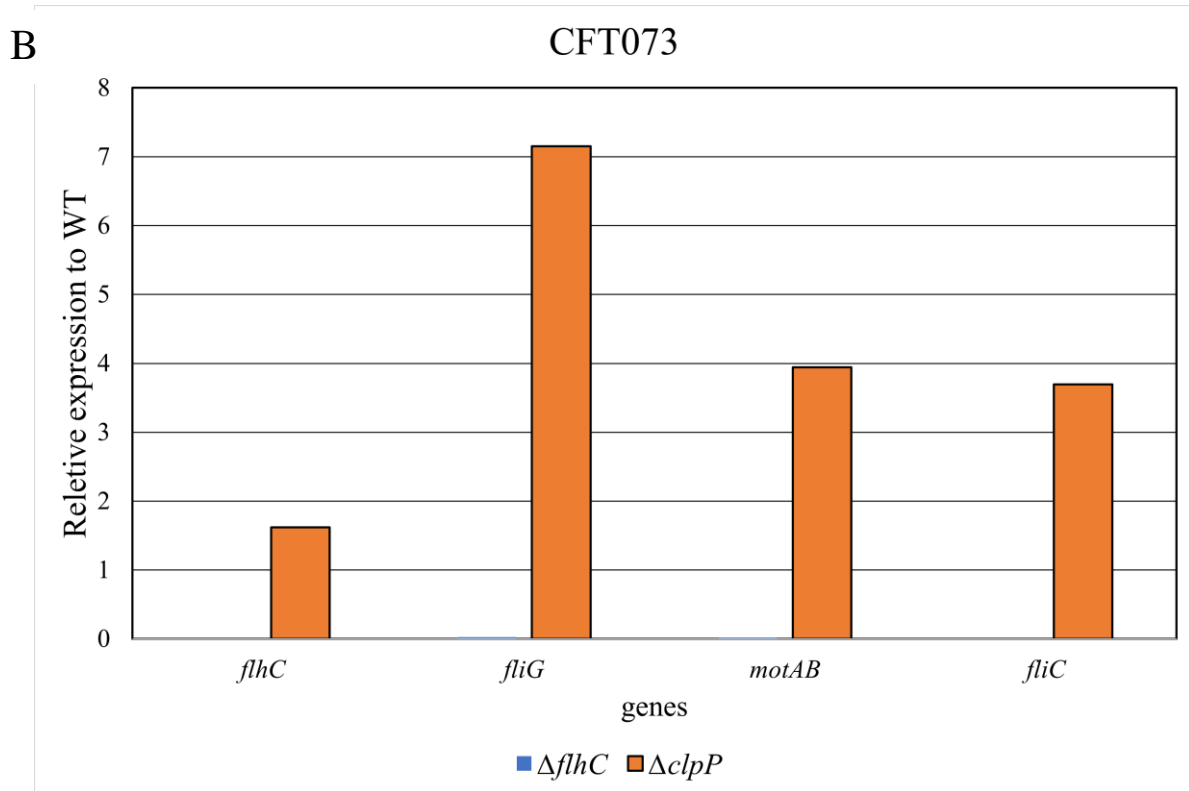
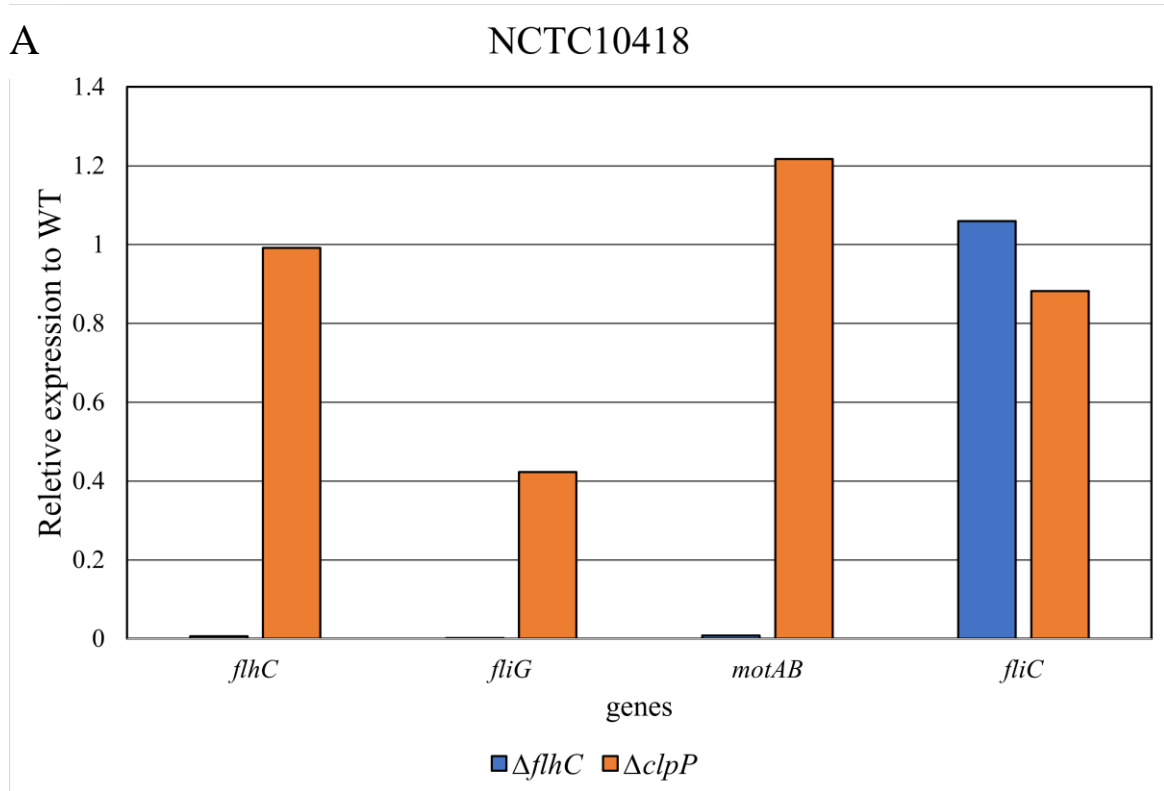


Figure 4.8 Flagellar gene expression of *E. coli* strains **A. NCTC10418** and **B. CFT073**, and their respective mutants. Data represent 3 biological repeats and 3 technical repeats for each biological measurement and are presented.

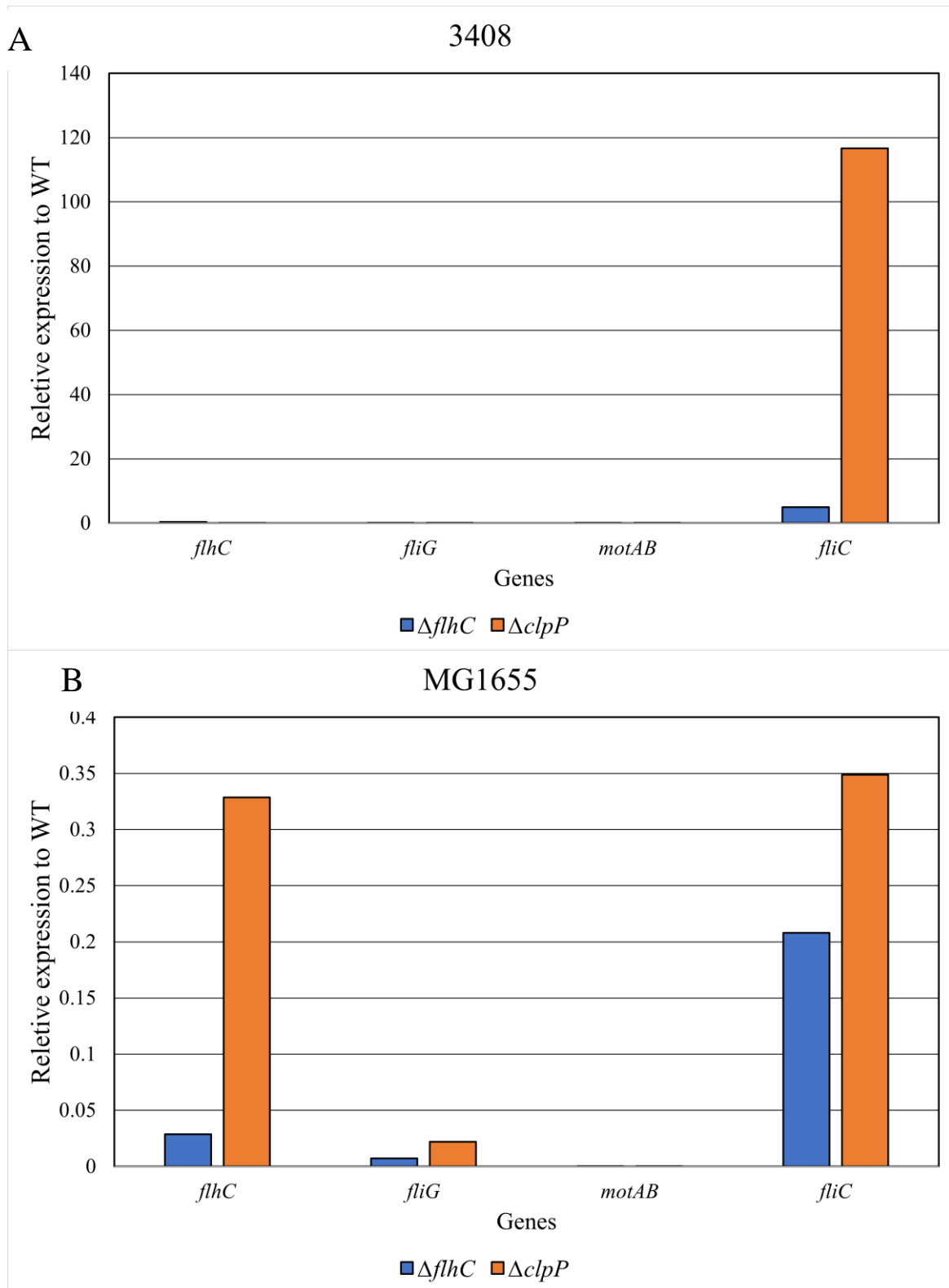


Figure 4.9 Flagellar gene expression of *E. coli* strains A. 3408 and B. 3439, and their respective mutants. Data represent 3 biological repeats and 3 technical repeats for each biological measurement and are presented.

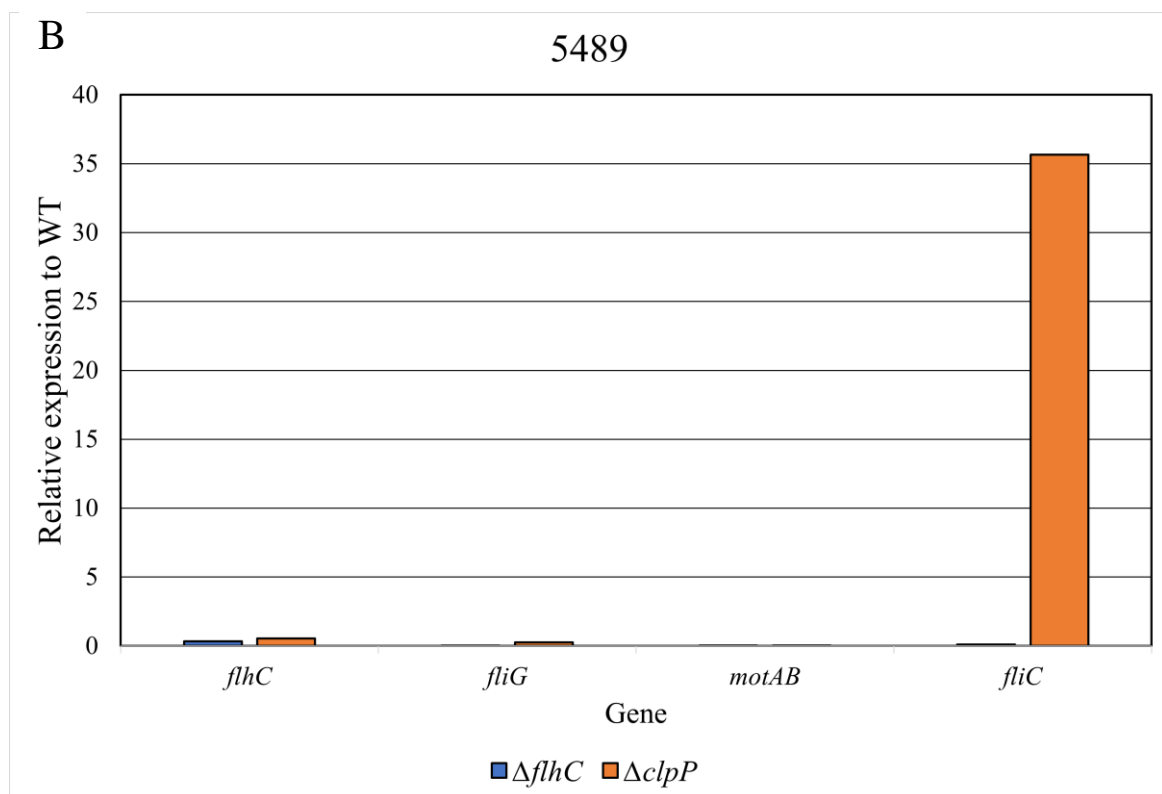
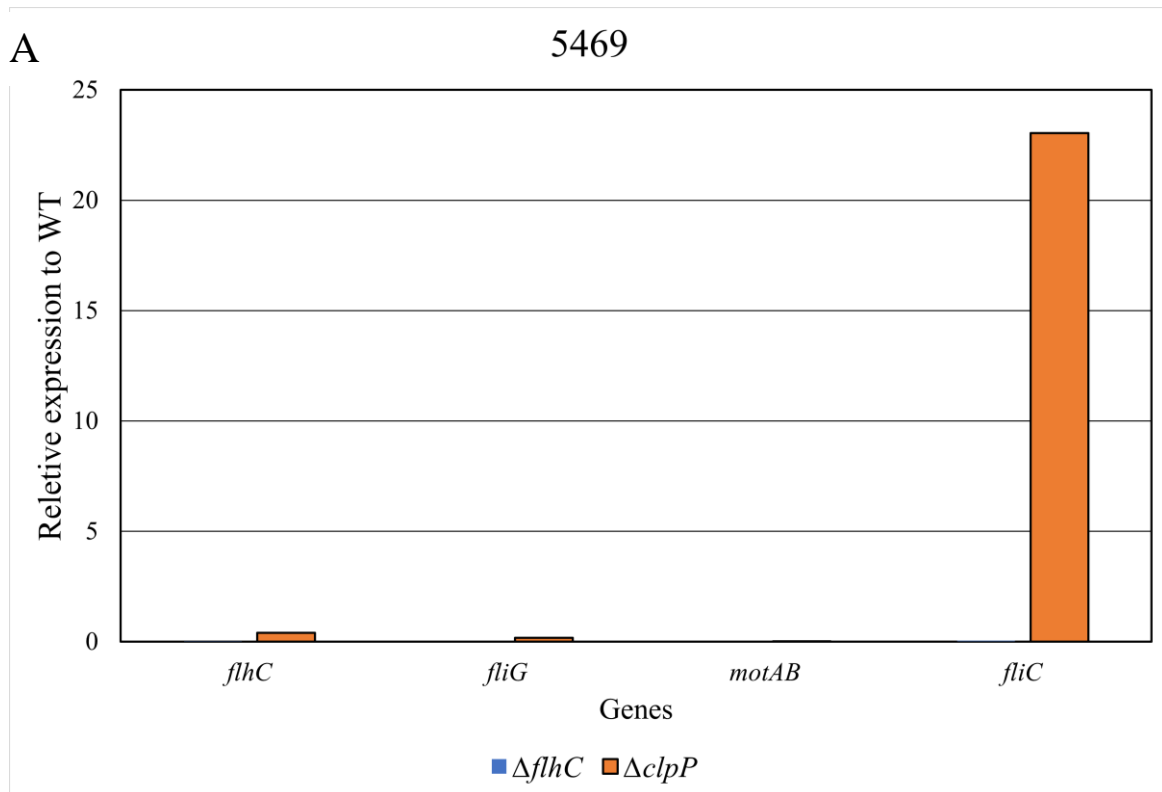


Figure 4.10 Flagellar gene expression of *E. coli* strains A. 5469 and B. 5489, and their respective mutants. Data represent 3 biological repeats and 3 technical repeats for each biological measurement and are presented.

These results showed that flagellar gene expression was variable between the strains analysed, with no obvious shared gene expression patterns. Starting with the control strain NCTC10418, the increase in tested genes expression did not exceed 1.3 folds comparing the *clpP* mutant to the wild type with an only increase of *fliC* expression in *flhDC* mutant reaching over a fold. The other strain that shows increase in all tested genes expressions was the UTI model strain CFT073. The expression of *fliG* in *clpP* mutants compared to the wildtype reached over 7 folds while *motAB* and *fliC* were less than 4 folds, and *flhC* increased 1.5 folds. On the other hand the *clpP* mutants of the three UTI strains 3408, 5469, and 5489 was associated with an increase only in the *fliC* expression reaching 116, 23, and 35 folds respectively. For MG1655 the increase in gene expression if there is any did not exceed 0.35 folds in *flhC* and *fliC*. The increase in *fliC* expression in the *clpP* mutants of the UTI isolates correlate with the motility data and with the IL-8 data leaving 3408 as an anomaly.

The lack of consistent gene expression data was challenging to comprehend and as such did not really help explain the motility and IL-8 observations relating to each strain. A different approach was therefore taken which focussed on determining the number of actual flagellar each strain was synthesising. To do this FlgEA240C was employed to visualise flagellar structures using fluorescent microscopy (Section 2.12).

4.7 Comparing flagellar abundance in selected wildtype strains and the $\Delta flhDC$ and $\Delta clpP$ mutants.

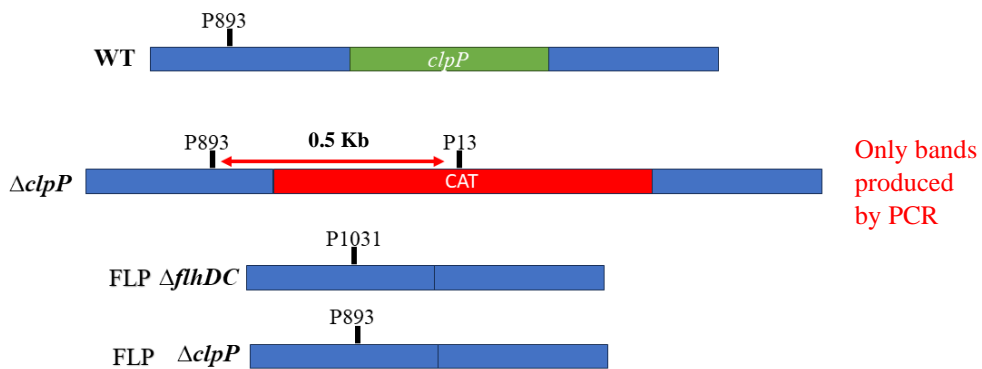
To study the effect these mutations had on flagellar abundance it was necessary to count and compare the number of flagella in the wildtype $\Delta flhDC$ and $\Delta clpP$ mutants. This was achieved by replacing *flgE* with a flgEA240C variant, expressed on a plasmid. For FlgEA240C to be the only copy of FlgE, *flgE* had to be deleted from all the *E. coli* strains and their $\Delta flhDC$, and $\Delta clpP$ mutants. Three strains were chosen for this experiment, NCTC10418 as a control and two uro-associated strains CFT073, and 3408 respectively.

Selection was based on their phenotypic profiles and the experience of genetically manipulating these strains. For example, NCTC10418 was the control strain as deletion of *clpP* did not impact either motility or induction of IL-8; in contrast the 3733 $\Delta clpP$ mutant showed improved motility and recognition, while the 3408 $\Delta clpP$ mutant showed improved motility but not recognition.

4.7.1 Deletion of *flgE*

The *flgE* genes of the parental strains were replaced with the chloramphenicol resistant cassette (CAT) using the lambda red recombinase system as described previously for the construction of the $\Delta flhDC$ and $\Delta clpP$ mutants. Conversely, the mutants, $\Delta flhDC$, and $\Delta clpP$, required their chloramphenicol resistant cassettes to be deleted, which was done using the FLP expression plasmid, pCP20 carrying gentamicin resistance. This plasmid was introduced into the mutated strains by electroporation and colonies were picked from gentamicin plates after incubation at 30°C overnight. Strains were cured by subculturing colonies on LB plates at 37°C until no longer resistant to either gentamicin and chloramphenicol. Loss of the cassette was confirmed by PCR (Figure 4.11). pKD46_Kan was introduced into the mutants to allow for the replacement of *flgE* with a chloramphenicol resistance cassette. To achieve this PCR fragments were generated from pKD3 using primers flanking the chloramphenicol resistance cassette and with a complementary sequence to the chromosomal regions flanking *flgE*. Once amplified the PCR fragments were introduced into the mutants carrying pKD46_Kan and selected on chloramphenicol LB plates. Deletion of *flgE* was confirmed by PCR (Figure 4.12). A plasmid carrying *flgEA240C* was introduced by electroporation followed by curing of pKD46_Kan. The new engineered strains $\Delta flgE$ / *pBADflgEA240C* were subjected to motility assays to determine if complementation had been achieved (Figure 4.13).

A



B

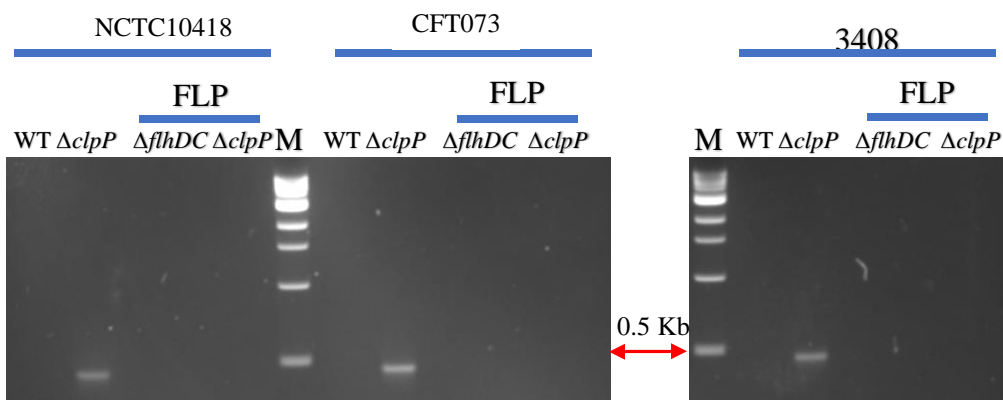


Figure 4.11 PCR confirmation of chloramphenicol resistant cassette deletion from $\Delta flhDC$ and $\Delta clpP$ mutants. Confirmation PCR with primers annealing upstream to the insertion site of $\Delta flhDC$ and $\Delta clpP$ (primers #1031, and 893 respectively) and the reverse primer annealing within the insertion (primer#13). **A)** Schematic of the expected PCR fragments amplified by the primers annealing to flanking *clpP* sites. **B)** PCR fragments with the insert ($\Delta clpP$) being approximately 500 bp; wild type did not produce any fragments (positive control). Samples showing deleted chloramphenicol resistant cassette (FLP). M: marker lane using the 1 Kb NEB DNA ladder #B7025 (New England Biolabs).

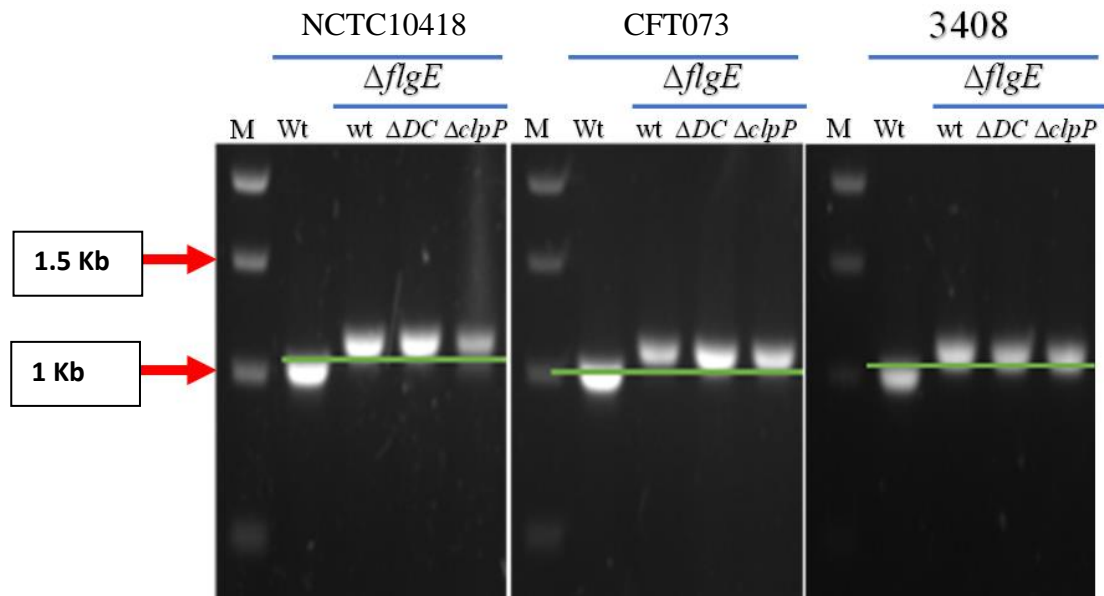


Figure 4.12 PCR confirmation of constructed $\Delta flgE$ mutants. Confirmation PCR with primers annealing to insertion sites flanking *flgE*. PCR fragments with the insert produced a 1.1 Kb band while the wild type produced a 1 Kb band. M: marker lane using the 1 Kb NEB DNA ladder #B7025 (New England Biolabs).

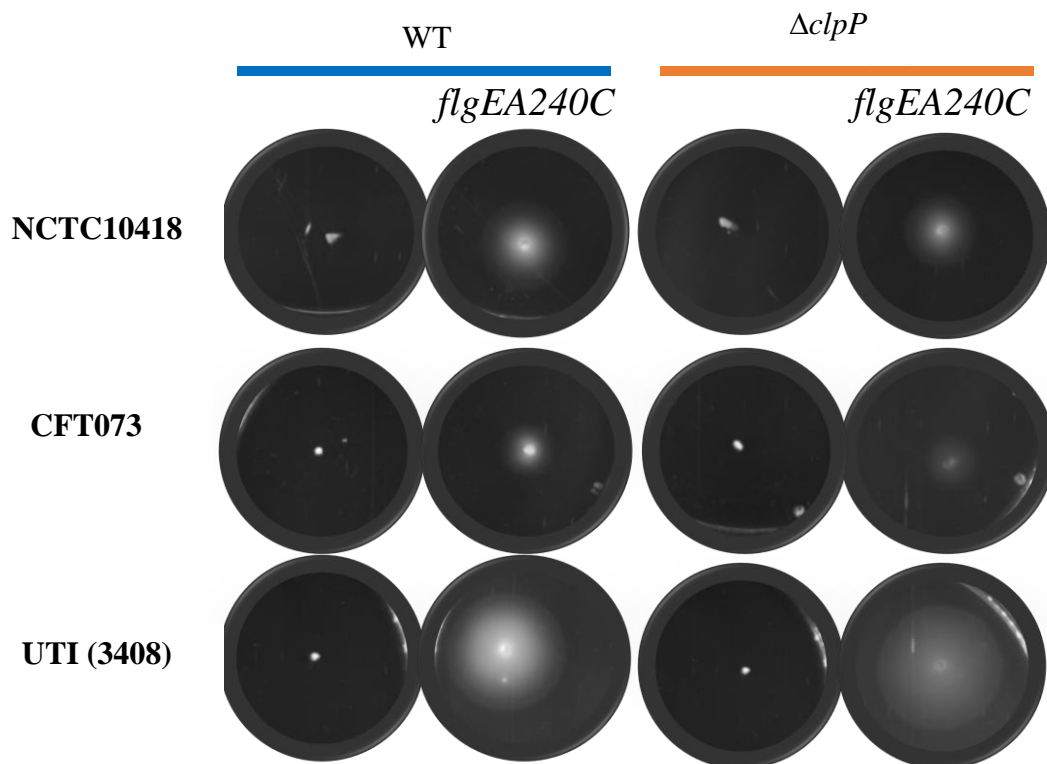


Figure 4.13 Motility assay confirming deletion of *flgE* and the transformation of *flgEA240C*. WT (blue) and $\Delta clpP$ mutants (orange): Loss of motility when *flgE* was replaced with a chloramphenicol resistant cassette and restoration of the motility phenotype by complementation with *flgEA240C*.

4.7.2 Quantification of Flagellar abundance using FlgEA240C Foci

To examine flagellar numbers the strains were grown to 0.5 OD₆₀₀ nm and stained for foci as described in Chapter 2, section 2.8. Stained cells were examined using fluorescent and phase contrast microscopy. Every strain was examined using three biological repeats and in five random fields. Each field contained ~200 bacterial cells and images were captured in two ways, phase contrast (showing the bacterial cell), and fluorescent excitation (red channel) that enabled the foci of FlgEA240C to be visualised. The two images for each field were merged to facilitate the counting and definition of cells to be included in the quantification (Figure 4.14). The number of flagella on each bacterial cell were quantified for fifty randomly chosen cells in each captured picture (Aldridge et al., 2010). The data generated for each strain provided the extent of flagellation i.e. how many cells have flagella, the range of flagella per cell and the average number of flagella per cell (Figures 4.15 and 4.16 respectively).

In case of strain NCTC10418, there was a consistent theme in that motility did not change significantly when either *flhDC* was overexpressed or *clpP* was deleted. A similar pattern emerged from the analysis of flagellar abundance with the percentage of flagellated cells in the wildtype defined as 73.1% and in the $\Delta clpP$ mutant as 79.5% (Figure 4.15). In contrast, CFT073 and 3408 had noticeable changes in the flagellated population when comparing the parental strains to the $\Delta clpP$ mutants (Figure 4.15).

Parent strain CFT073 had 29.3% flagellated bacterial cells while its $\Delta clpP$ mutant had 83.5% flagellated bacterial cells. This was a significant increase and correlated to the CFT073 $\Delta clpP$ mutant motility phenotype and IL-8 induction data (Figures 4.5 and 4.6 respectively). Isolate 3408 was characterised by a larger proportion of the population being flagellated (52.9 %), which increased to 78.9% in the $\Delta clpP$ mutant. Again, these data were

A

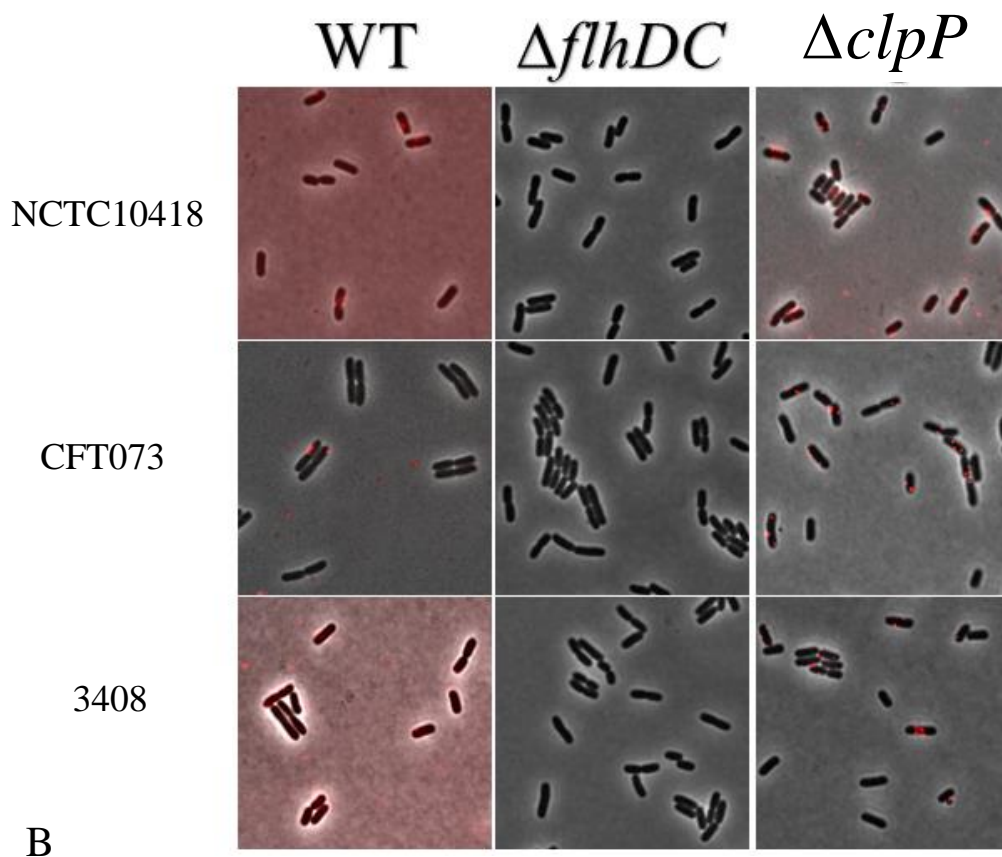
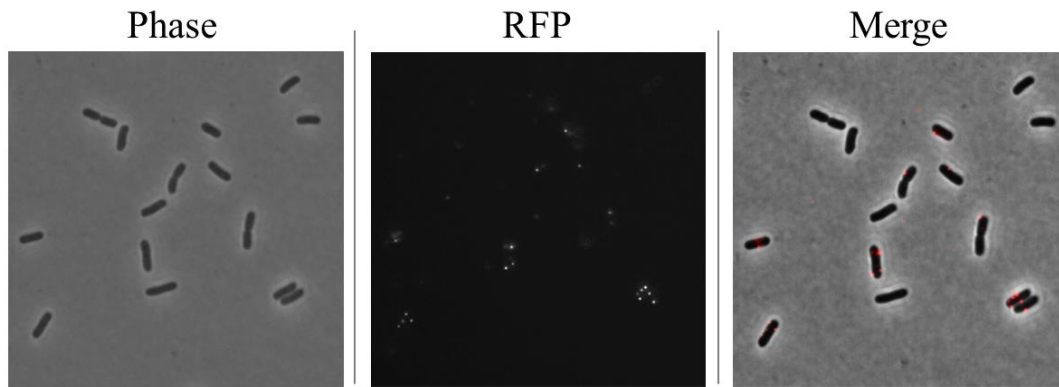


Figure 4.14 Phase contrast and fluorescent images of FlgEA240C foci. A) Example of images phase contrast (phase), and red fluorescent channel (RFP), and the merging of the two images using imageJ. B) Examples of final merged images of all the strains, NCTC10418, CFT073 and 3408, and their mutants $\Delta flhDC$ and $\Delta clpP$.

consistent with the motility results (Figure 4.5) but did not explain the lack of the RT4 IL-8 response to 3408 (Figure 4.6).

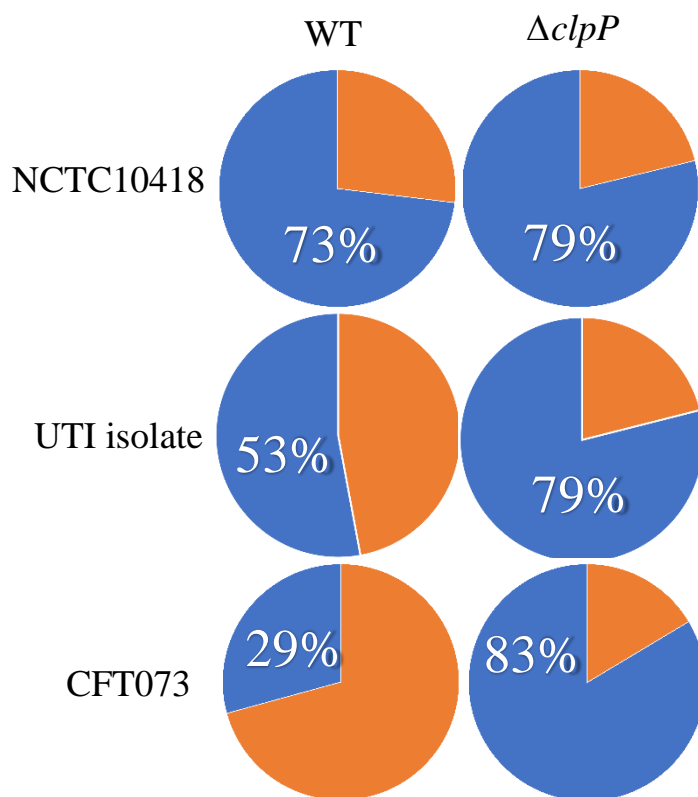


Figure 4.15 Quantification of flagellar abundance. The pie charts show the flagellation percentage of wildtype strains and $\Delta clpP$ mutants for (NCTC10418), 3408(UTI isolate) and CFT073 (CFT073). Percentage of flagellated bacterial cells (blue) compared to non-flagellated bacterial cells (orange).

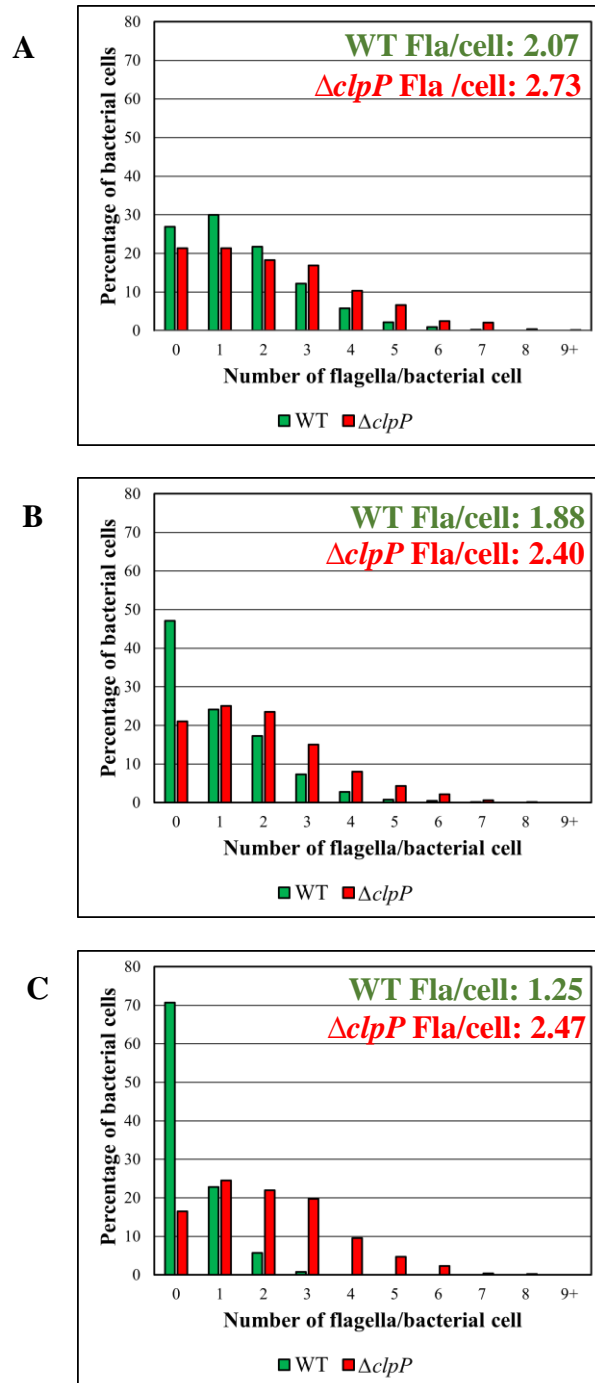


Figure 4.16 Quantification of the number of flagella/bacterial cells. **A)** NCTC10418 control strain: Percentage of flagellated cells in the wildtype (green) and $\Delta clpP$ (red) populations. The average number of flagella per cell in the wildtype (green) strain was 2.07 while the $\Delta clpP$ (red) was 2.73. **B)** Isolate 3408: The average number of flagella per cell in the wildtype strain (green) was 1.88 while the $\Delta clpP$ (red) was 2.4. **C)** CFT073: The average number of flagella per cell in the wildtype strain (green) was 1.25 while the $\Delta clpP$ (red) was 2.47.

When comparing the impact of $\Delta clpP$ deletion on the number of flagella per cell a pattern emerged. In the case of strain NCTC10418, the wild type averaged 2.07 flagella per cell compared to the $\Delta clpP$ mutant where 2.73 flagella per cell was recorded (Figure 4.6). While this was not associated with a significant change of motility due to the percentage of cells flagellated remaining >70% it shows that the $\Delta clpP$ mutant did exhibit a weak $\Delta clpP$ phenotype. In contrast, in strains CFT073 and 3408 there was a stronger shift in the distribution of flagella per cell (Figure 4.16). In these cases, the parental strains were recorded as having 1.25 and 1.88 flagella per cell, but the $\Delta clpP$ mutants had an average of 2.47 and 2.40 flagella per cell respectively. Hence not only were the number of flagella per cell increased but also the percentage population of cells carrying flagella.

4.8 Discussion

In this chapter, the regulation of flagellar synthesis was studied by the construction of two mutants one lacking *flhDC* and the other *clpP*. The resulting mutants were evaluated by comparing them to their parental wildtype strains for motility, flagellar gene expression, flagellar protein expression and flagella abundance. Additionally, RT4 cell challenges were performed to measure and compare induction of an innate bladder (IL-8) response. Data were consistent across the several assays described in this chapter showing that the mutants behaved in similar manners. For example, in relation to motility, the *flhDC* mutants lost motility while the *clpP* mutants showed increased motility when compared to their wild type parental strains. The motility was assessed by halo size of bacterial growth in motility agar. The exception was strain NCTC10418, whose results were consistent with the *flhDC* overexpression data reported in Chapter 3.

As predicted according to the results of chapter 3 in 3.2.4, increasing motility and challenging RT4 bladder cells was associated with an elevated innate response as determined by increased IL-8 concentrations. There were exception however – strain 3408 – for while its *clpP* mutant showed increased motility no comparable IL-8 induction was observed. According to (Tan et al., 2023), the percentage of flagellated bacterial cells in a population should exceed 60% for the bacteria to be recognized by the host facilitating TLR5 activation and the release of antimicrobial agents including the pro-inflammatory cytokine IL-8. Investigations (Figure 4.16 B) showed the 3408 $\Delta clpP$ mutant to have approximately 2-3 flagellar per cell (range 0-6) and in excess of 70% of the population flagellated, but despite this did not cause an innate response.

When further investigation performed on the protein expression of the strains and their mutants via probing with α -FlgEST, the two control strains NCTC10418 and MG1655,

which did not significantly increase motility comparing $\Delta clpP$ to WT, have similar levels of FlgE expression in WT and $\Delta clpP$. On the other hand, the UTI isolates show less expression of FlgE in their wildtype in comparison with $\Delta clpP$. All *flhDC* mutants did not express FlgE. These results correlate with the motility data and the IL-8 data except 3408.

The reasons why 3408 did not induce an innate response despite its motility remain unknown. However, microbes can inhibit the host responses by numerous mechanisms one of which includes the synthesis of a TcpC protein. This virulence factor binds to MyD88 and dysregulates the innate signalling pathway resulting in a dampened innate response (Yadav et al., 2010). Interestingly, recent research has also shown TcpC to impact neutrophil extracellular trap formation (Ou et al., 2021) and M1(pro-inflammatory)/M2(ant-inflammatory) polarisation (Fang et al., 2022). Future analyses will use PCR to screen 3408 and other isolates, particularly MG1655, which also did not induce an innate response, for TcpP gene expression to identify if this is the mechanism by which this uro-associated isolate is able to evade the innate immune response.

The impacts of deleting *clpP* on gene expression patterns were explored by RT-qPCR and as highlighted the data relating to the different isolates were variable (Figures 4.8-4.10). The target genes were chosen as they encoded proteins involved in flagellar synthesis, but were regulated by different promoters, class1(*flhC*), class2 (*fliG*) and class3 (*fliC* and *motAB*). The rationale behind such choices was to potentially identify common gene expression patterns. The variability could not be explained by growth differences as the bacterial cells were all grown in the same media and harvested at the same OD values. However, if viewed globally these data did suggest a decrease in gene expression in the *flhDC* mutants and an increase in the *clpP* mutants compared to wild-type, but there were notable exceptions, the increased of *fliC* expression in $\Delta clpP$ of all UTI strains. The change of gene expression in the strain MG1655 correlate with the motility, IL-8 and FlgE

expression data. In reality these analyses need to be repeated ensuring good quality RNA and using different sets of primers.

Moreover, genes effecting the chemotaxis activities could be tested to help explain if they have an impact on the recognition. Testing the gene expression of the five transmembrane proteins, *cheA*, and *cheY* could help explain if they effect the impact on the innate response or not. Alternative ways of evaluating flagellar gene expression could have been utilised as well. These include engineering strains with *flhDC* either under the influence of promoter induced by tetracycline or by using flagellar transcriptional reporters that involve, for example, *luxCDABE*, which is the luciferase operon from *P. luminescens* (Aldridge et al., 2010; Brown et al., 2008; Goodier & Ahmer, 2001; Karlinsey et al., 2000). However, as these tools are associated with *Salmonella* research new plasmids and strains would have to be engineered for use in *E. coli*. This was not possible for this project due to time constraints. Moreover, as clinical isolates are characterised by plasmids carrying antibiotic resistance any plasmid reporters would have to be customised specifically in relation to each isolate's antibiotic resistance profile.

In a final attempt to understand the varying NF- κ B responses of the clinical uro-associated isolates their number of flagella were counted. It has been reported that *E. coli* carry multiple flagella (Macnab, 1999), but data from this project suggested that up to 50% of wild-type uro-associated *E. coli* isolates had no flagella and up to 50% were characterised by only 1-2 flagella (Figure 4.16). Presumably this population heterogeneity allows the bacteria to retain motility and colonise tissues, but remain undetectable by the host TLR5 defences. Switching on flagella synthesis synthetically through deleting *clpP*, resulted in strains synthesising up to seven flagella per cell, but whether this would occur naturally in the urinary tract is not known.

Another way of investigating the effects the deletion of *flhDC* and *clpP* was assessing flagellar abundance. To be able of performing this assessment, strains had to undergo a mutation deleting *flgE* using the λ red system. To perform that, the previously made mutants, *flhDC* and *clpP*, should lose the antibiotic cassette replacing these genes. The plasmid used for such a purpose has an Amp^r cassette and some of the previously tested UTI isolates are Ampicillin resistant strains. This kind of limitation prevented those strains from this assessment. Ideally, another plasmid should have been either ordered or engineered but due to time restraints the assessment proceeded on plausible strains. This restraint led to only testing a control strain, NCTC10418, with two UTI isolates, CFT073 and 3408. The *clpP* mutants had over 70 % flagellated populations and the average number of flagella per bacterial cell exceeded 2.4.

One of the other approaches is to construct a mutant deleting *ydiV* which is another repressor of FlhD₄C₂ activity to compare their behaviour to the wildtype, Δ *flhDC*, and Δ *clpP*. Further investigation will be done by constructing a double deletion mutant in *clpP* and *ydiV* and compare their behaviour as well.

In approaching the aspect of flagellar abundance, manual counting was one of the disadvantages due to being time consuming. Counting the number of bacterial flagella automatically, which would have helped much, involves the application of image processing and analysis techniques. Initially, images of bacterial cells are acquired under a microscope, with a clear focus on flagella. These images are then subjected to pre-processing steps aimed at enhancing image quality and flagella visibility. Pre-processing techniques typically include noise reduction, contrast adjustment, and sharpening to optimize the images for subsequent analysis. Following pre-processing, segmentation algorithms are employed to isolate individual bacterial cells from the background (Zhang et al., 2022). This step is crucial for accurately analysing flagella on a per-cell basis. Once segmentation is completed, feature

extraction techniques are utilized to identify flagella-like structures within each bacterial cell. These techniques may encompass edge detection, Hough transform, or template matching, which highlight potential flagella locations based on specific image characteristics. With features extracted, the next step involves implementing counting algorithms to tally the number of flagella present within each bacterial cell. These algorithms may utilize thresholding methods or rule-based approaches to distinguish genuine flagella from other cellular structures or artifacts. During this stage, it's essential to account for variations in flagella appearance, such as length, thickness, and orientation, to ensure accurate counting. Validation of the automated counting results is paramount to assess the reliability and accuracy of the approach. This validation typically involves comparing automated counts against manual counts performed by trained observers or ground truth data. Discrepancies are addressed by refining algorithms or adjusting parameters to improve performance. Post-processing steps are applied to refine the counting results and eliminate potential errors or false positives. This may include filtering out noise, merging adjacent flagella belonging to the same bacterial cell, or correcting misclassifications. Once the automated counting process is completed, the data are analysed to extract relevant statistics and patterns. These may include the average number of flagella per bacterial cell, distribution of flagella lengths, or correlations with other bacterial characteristics. The results are then presented in a clear and interpretable format for further analysis or publication.

In summary, automating the counting of bacterial flagella requires a combination of image processing techniques, algorithm development, validation steps, and post-processing procedures to ensure accurate and reliable results. Mastering such a technique would help since flagellar abundance correlate mostly with the recognition by TLR5. A further limitation is that all these analyses were performed using bacteria grown in enriched media, which does not model the environment of the urinary tract. In the next chapter, this was addressed with

the uro-associated isolates and their *flhDC* and *clpP* mutants grown in artificial urine media (AUM) to try and mimic the host bladder environment.

Chapter 5. The effects of Uro-associated *E. coli* isolates, grown in artificial urine medium (AUM), on the innate response(s) of RT4 bladder cells

5.1 Introduction

Analyses of the innate response in Chapter 4 showed that, generally, increased *E. coli* motility was associated with an enhanced bladder cell innate response as measured by IL-8 concentrations. However, the research presented and discussed in Chapter 4 was performed using bacteria cultured in enriched media, so the next step was to try and mimic bacterial growth in urine to model the bladder environment. To model urine, artificial urine media (AUM) was prepared in the laboratory and used for all growth and motility analyses (Brooks & Keevil, 1997).

AUM provides a stable and regulated environment for examining bacterial responses in relation to UTI pathologies. AUM has been used to research urinary pathogen proliferation, urinary crystal formation and encrustations similar to those found in clinical cases of UTIs, and the behaviour of uropathogenic bacteria in the urinary tract (Benramdane et al., 2008; Ebrahim, 2019; Zandbergen et al., 2021). AUM has also been used in testing and identification procedures, including the rapid detection of *E. coli* in UTIs, utilising a virulence gene-based PCR methodology (Brons et al., 2020). These applications emphasise the use of AUM in providing a more relevant, yet controlled growth media, for researching urinary pathogens and UTIs, allowing for more accurate and reproducible data.

Urine pH varies according to factors that include a person's diet, drug usage and overall health (Welch et al., 2008). Generally however, the acidic, average and alkaline pH values of urine are characterised as 4.5-5.5, 5-6 and 6.5-8 respectively (Brendler & Gerber, 2016). In view of such variability in pH it is possible that uro-associated *E. coli* adopt distinct uropathogenic characteristics in response to the host conditions (Simerville et al., 2005), and in using conventional growth media these characteristics are missed.

To address this, experiments were performed using AUM media used at different pH. An acid pH of 5.5 close to the average pH and an alkaline pH of 6.5 also close to the average were selected. The strains used were the model UTI strain CFT073 (CFT073), the UTI isolates 3408, 5469, and 5489 and their $\Delta flhDC$ and $\Delta clpP$ mutants. The aim of the studies was to explore whether culturing these strains in AUM at an acid (5.5) and more alkaline urine pH (6.5), to mimic conditions in the urinary tract, impacted bacterial motility and the host bladder innate responses.

5.2 Motility in AUM

Motility assays were carried out for 24 hours at 37 °C, in triplicate, using semisolid AUM motility plates (0.3% agar) with pHs adjusted to 6.5 and 5.5 respectively (Figures 5.1 & 5.2). Strains CFT073, and the UTI isolates 3408, 5469, and 5489, and their $\Delta flhDC$ and $\Delta clpP$ mutants were inoculated onto these plates and swarming (motility) observed after 24 hours. Swarming halo diameters were measured as described in section 2.11. The mean of the three measurements was calculated and mean data presented (Figure 5.3).

In AUM pH 6.5 motility plates, the halo diameters of the control UTI strain CFT073 were <2 mm in both the wildtype and $\Delta flhDC$ strains (1.7 ± 0.2 mm and 1.8 ± 0.1 mm) (NS), respectively. In contrast the halo diameter of the $\Delta clpP$ mutant was 6.5 ± 0.3 mm ($p < 0.001$). The halo diameters of the UTI isolate 3408 wildtype, $\Delta flhDC$, and $\Delta clpP$ strains were 6.5 ± 0.4 mm, 2.8 ± 0.5 mm and 5.8 ± 0.3 mm, respectively. While comparable data for the UTI isolate 5469 were 3.5 ± 0.3 mm, 3.2 ± 0.3 mm, and 2.8 ± 0.5 mm (NS). Finally, isolate 5489 was associated with halo sizes of 4.7 ± 0.2 mm, 3.6 ± 0.4 mm and 2.6 ± 0.3 mm relating to the wildtype, $\Delta flhDC$, and $\Delta clpP$ strains respectively.

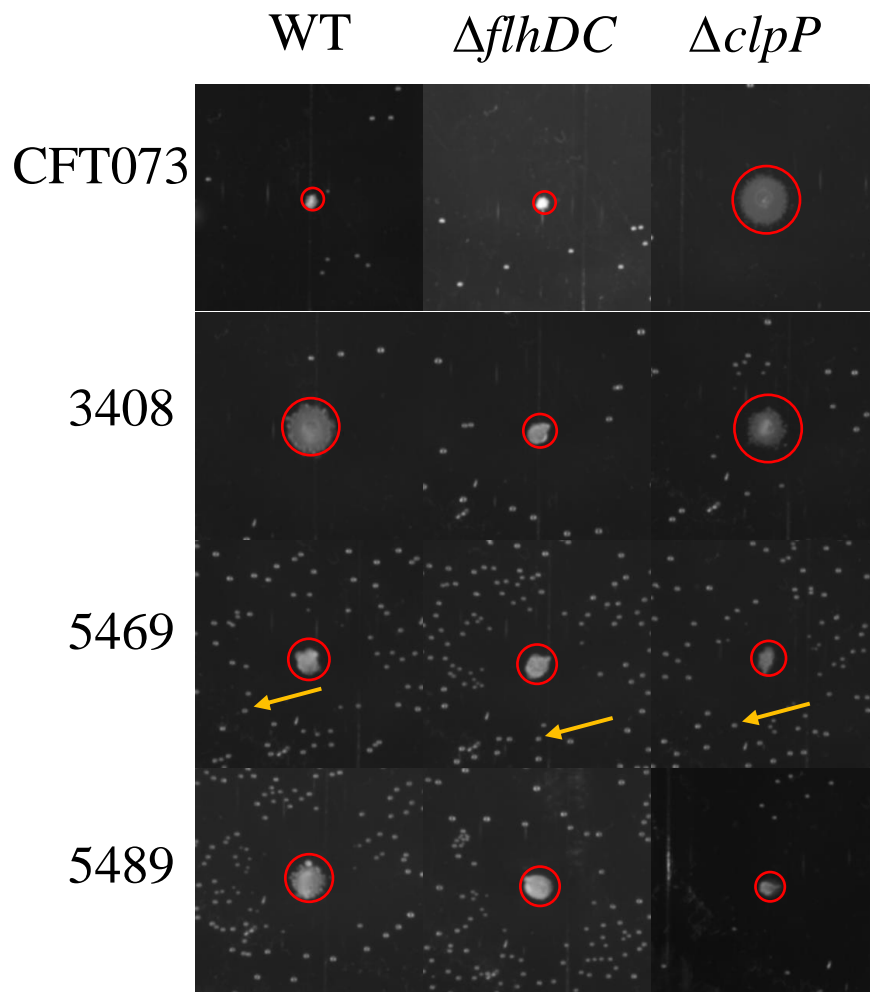


Figure 5.1 Motility assay using AUM motility media pH 6.5. Motility assays were performed using UTI isolates CFT073, 3408, 5469, 5489 and their $\Delta flhDC$, and $\Delta clpP$ mutants at 37 °C for 24 h in semisolid AUM media, pH 6.5. The motility halos (inside red circles) were measured and quantified as described in section 2.11. Air bubbles in the media are identified by yellow arrows.

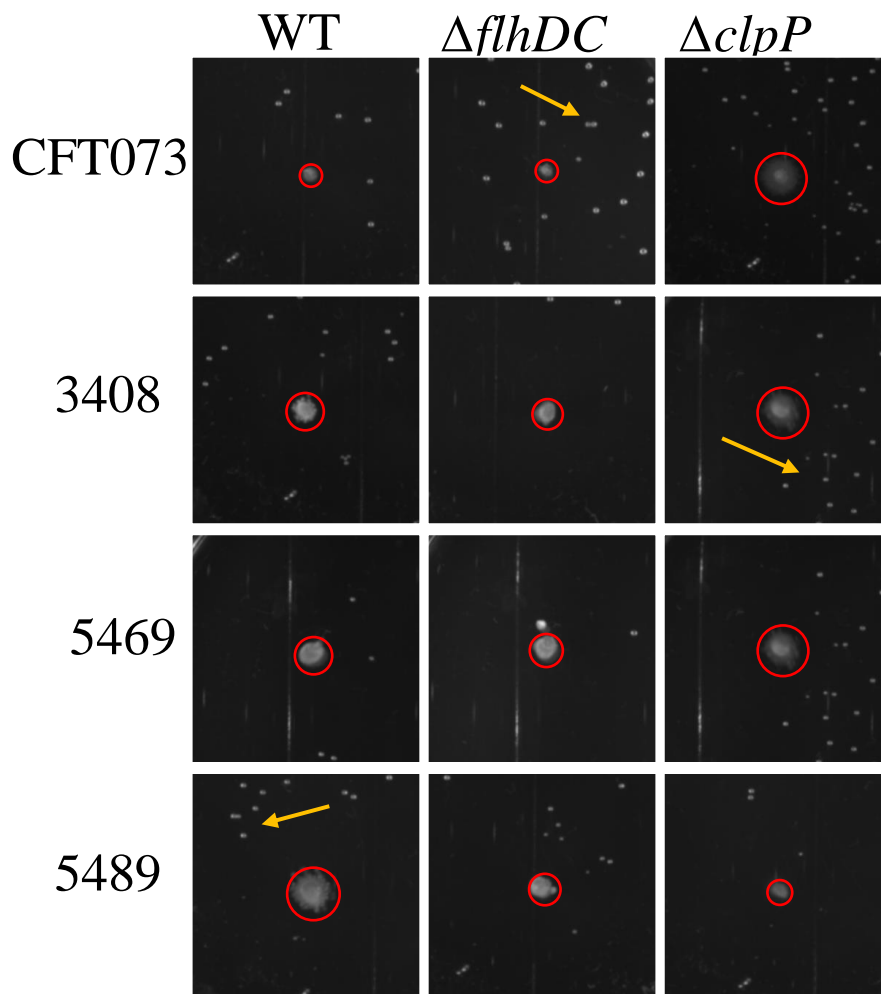


Figure 5.2 Motility assay using AUM motility media pH 5.5. Motility assays were performed using UTI isolates CFT073 (CFT073), 3408, 5469, 5489 and their $\Delta flhDC$, and $\Delta clpP$ mutants at 37 °C for 24 h in semisolid AUM media, pH 5.5. The motility halos were measured and quantified as described in section 2.11. Air bubbles in the media are identified by yellow arrows.

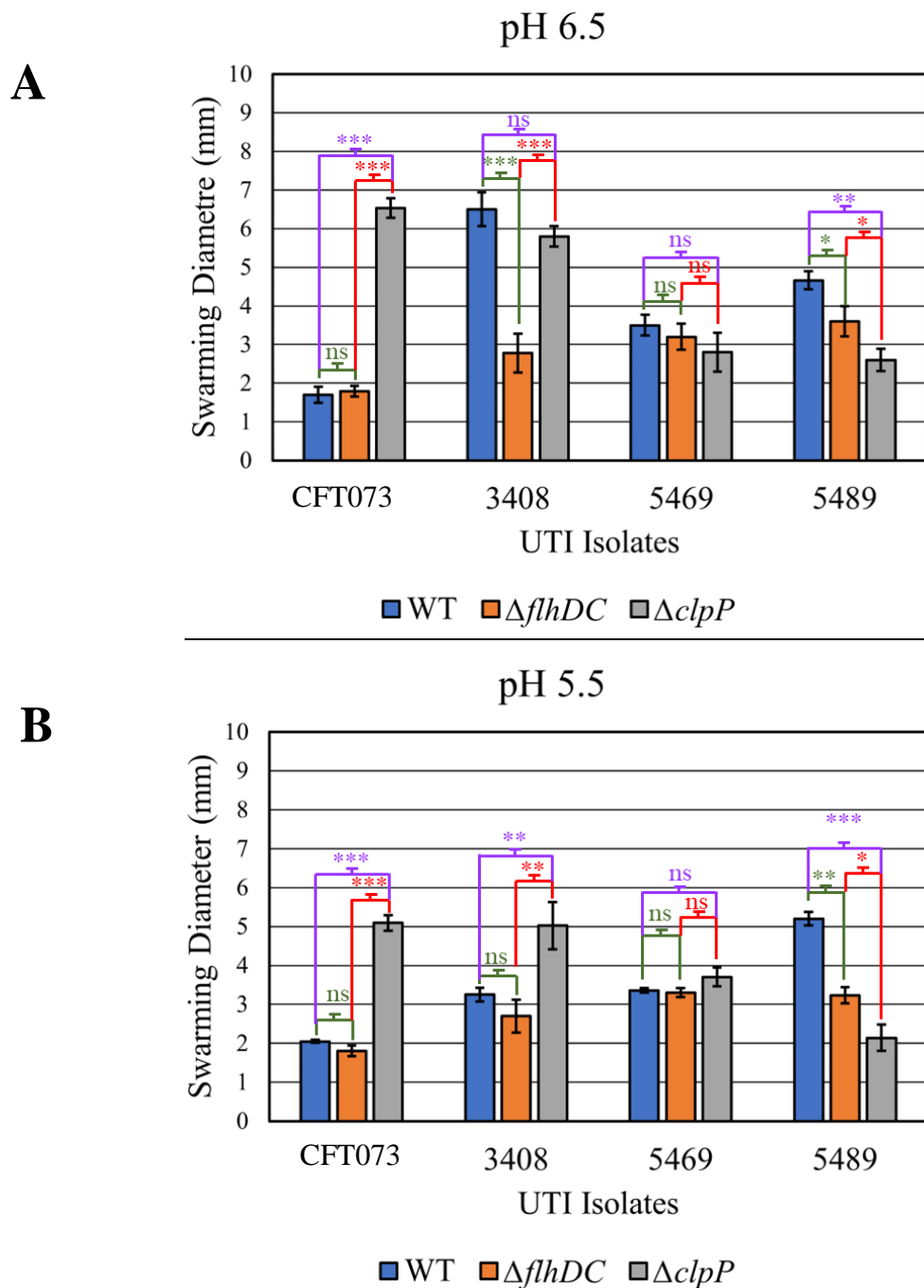


Figure 5.3 Quantification of Motility assay using AUM motility media. Motility assays were performed using UTI isolates CFT073 (CFT073), 3408, 5469, 5489 and their $\Delta flhDC$, and $\Delta clpP$ mutants at 37 °C for 24 h in semisolid AUM media. A) Bar chart reflecting the halo diameter measurements for UTI isolates inoculated into motility AUM plates pH 6.5 (N=3). B) Bar chart reflecting the halo diameter measurements for isolates inoculated into motility AUM plates pH 5.5. Three different colonies were used to perform the assays and at least three diameter readings per colony were measured. ns=not significant, *=p<0.05, **=p<0.01, ***=p<0.001.

In AUM pH 5.5 motility plates, the halo diameters of the control UTI strain CFT073 were again ≤ 2 mm in both the wildtype and $\Delta flhDC$ strains (2.0 ± 0.4 mm and 1.8 ± 0.1 mm (NS)) respectively. As previous the halo diameter of the $\Delta clpP$ mutant had increased to 5.1 ± 0.2 mm ($p < 0.001$). The halo diameters of the UTI isolate 3408, wildtype, $\Delta flhDC$, and $\Delta clpP$ strains were 3.3 ± 0.04 mm; 2.7 ± 0.4 mm; 5.0 ± 0.6 mm respectively.

Motility data for the UTI isolate 5469, again did not differ between its wildtype, $\Delta flhDC$ and $\Delta clpP$ strains. Finally isolate 5489 was associated with halo sizes of 5.2 ± 0.2 mm, 3.2 ± 0.2 mm and 2.1 ± 0.3 mm relating to the wildtype, $\Delta flhDC$, and $\Delta clpP$ strains respectively.

Data presented in Figure 5.3 suggests that the halo sizes of the strains inoculated onto motility plates at pH 5.5 and 6.5 were comparable suggesting pH did not appear to impact bacterial motility. However, there was an exception as while the wildtype isolate 3408 supported a motility of 6.5 ± 0.4 mm at pH 6.5 this was reduced by 50% at the more acidic pH 5.5 to a motility of 3.3 ± 0.04 mm. Interestingly the motilities of the 3408 $\Delta flhDC$ and $\Delta clpP$ strains appeared unchanged at pHs of 6.5 and 5.5 respectively.

It should be noted that the motilities of the UTI isolates inoculated into AUM media were reduced when compared to data collated and reported using traditional motility media (Chapter 4). This was despite motility assay data using AUM and reported in this Chapter being recorded after 24 hours compared to 8 hours when using traditional media (Chapter 4).

5.3 Innate responses of RT4 bladder cells to *E. coli* isolates cultured in AUM

These experiments were performed to examine whether the motility data reported in Section 5. 2 affected the host bladder cell innate responses. In these experiments the wild-type isolates and their mutants were cultured in AUM buffered to pH of either 5.5 or 6.5 and used (1×10^5 CFU/mL) to challenge monolayers of RT4 cells. The bladder epithelial cell

innate responses were determined by collecting the media bathing the RT4 cells and measuring the IL-8 concentrations.

5.3.1 IL-8 production: pH 6.5 and 5.5

Heat killed inoculants of isolates 3733, 3408, 5469 and 5489, and their $\Delta flhDC$ and $\Delta clpP$ mutants cultured in AUM at pH of 6.5 and 5.5 were prepared as described in Section 2.1.1.2. RT4 cells cultured to confluence in 12-well plates were challenged for 24 hours with 1×10^5 heat-killed bacterial cells in a volume of 1 mL. PBS was used as a negative control while 500 ng of purified flagellin prepared from the strain 3408 (Ali et al., 2017) was used as the positive control. Two independent experiments were performed and the isolate challenges were each performed in triplicate. IL-8 data are shown in Figures 5.4.& 5.5 respectively.

Data (Figure 5.4) indicated that for the strains 3408, 5469, and 5489 cultured in AUM at pH 6.5 there were no significant differences between the IL-8 concentrations measured in the media bathing the RT4 cells challenged with either wild-type or their corresponding $\Delta clpP$ isolates. However, an increase in IL-8 was observed in the media of the cells challenged with the CFT073 $\Delta clpP$ mutant ($p < 0.01$) compared to either the wild-type or the $\Delta flhDC$ mutant. These data were reproduced when the challenges were performed using isolates cultured at pH 5.5. However, when the 5469 $\Delta flhDC$ mutant cultured at pH 5.5 was used, it produced significantly lower levels of IL-8 ($p < 0.05$ and $p < 0.01$) compared to wildtype and its $\Delta clpP$ mutant respectively. Essentially the IL-8 challenge data patterns appeared consistent regardless of whether the bacteria had been cultured in AUM buffered at either pH 5.5 or 6.5.

5.4 Exploring FlgE expression in bacterial samples cultured in AUM and heat-killed

Bladder epithelial cells respond to bacterial flagellin by releasing pro-inflammatory cytokines such as IL-8 and anti-microbial agents such as NGAL to kill potential uropathogens (Ali et al., 2017). The IL-8 data summarised in Figures 5.4 and 5.5 respectively, were therefore confusing as the measured RT4 bladder innate responses were comparable between wild-type bacteria and selected mutations designed to either prevent ($\Delta flhDC$) or increase ($\Delta clpP$) flagellin expression and hence flagellar synthesis. Additionally, as changes in motility had been identified between strains, for example, isolate 3408 wildtype, $\Delta flhDC$ and $\Delta clpP$ at both pH 5.5 and 6.5 (Figure 5.3) this further challenged the validity of the IL-8 data.

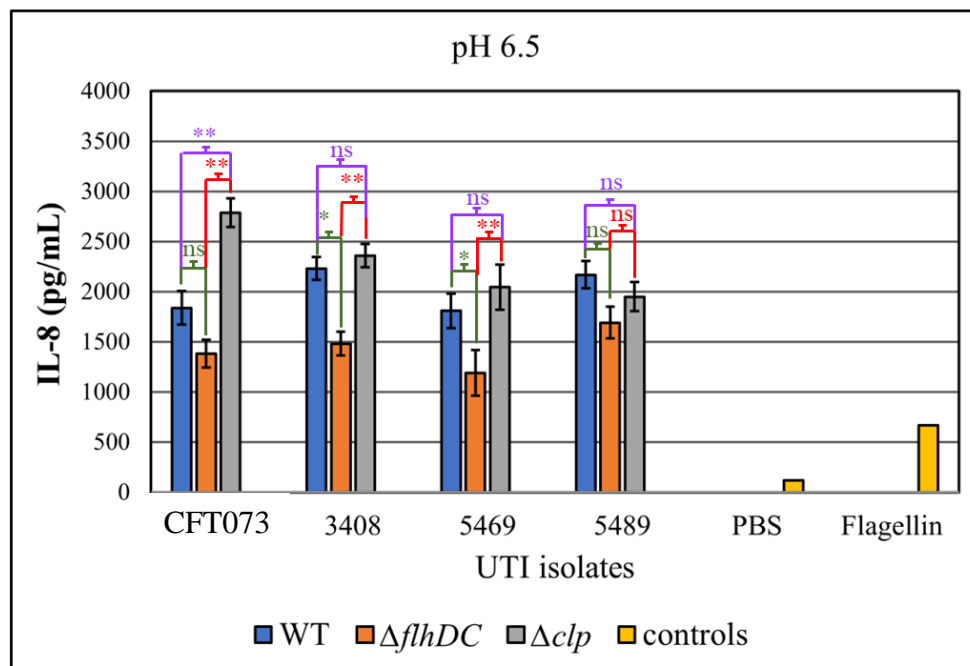


Figure 5.4) IL-8 levels of RT4 bladder cells challenged with heat-killed *E. coli* UTI isolates grown in AUM pH 6.5. Data \pm SEM show IL-8 concentrations measured via ELISA in media bathing the RT4 cells following the bacterial challenges. PBS was used as a negative control and Flagellin (500 ng) as a positive control (Yellow). IL-8 concentrations after exposing the RT4 cells to wild-type bacteria (blue); $\Delta flhDC$ (orange) and $\Delta clpP$ (Grey). N=2; n=6. T-tests performed for statistical analysis: ns = $p > 0.05$, * = $p < 0.05$, ** = $p \leq 0.01$.

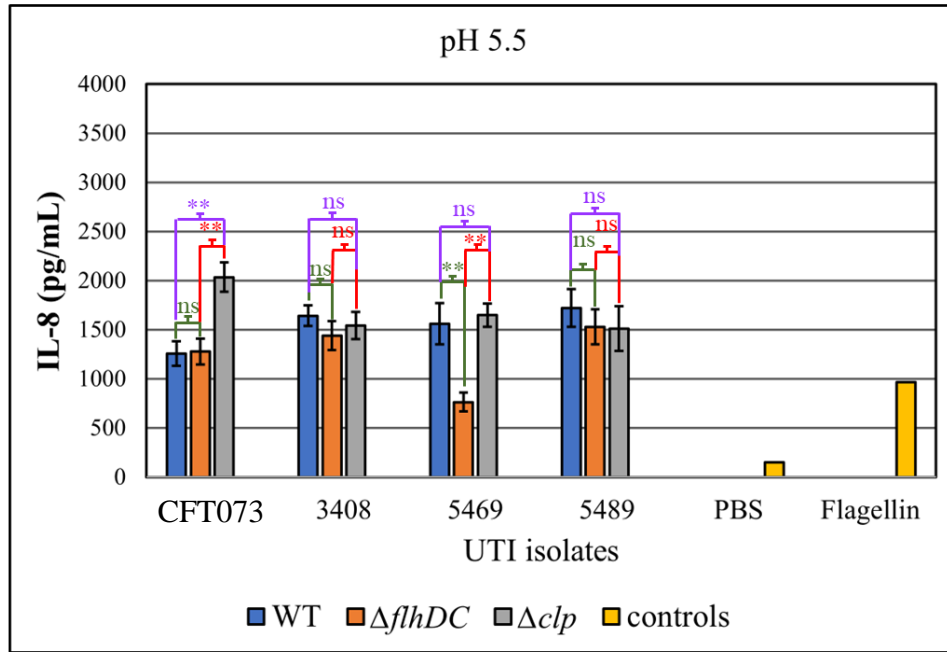


Figure 5.5) IL-8 levels of RT4 bladder cells challenged with heat-killed *E. coli* UTI isolates grown in AUM pH 5.5. Data \pm SEM show IL-8 concentrations measured via ELISA in media bathing the RT4 cells following the bacterial challenges. PBS was used as a negative control and Flagellin (500 ng) as a positive control (Yellow). IL-8 concentrations after exposing the RT4 cells to wild-type bacteria (blue); $\Delta flhDC$ (orange) and $\Delta clpP$ (Grey). N=2; n=6. T-tests performed for statistical analysis: ns = $p > 0.05$, *= $p < 0.05$, **= $p \leq 0.01$, ***= $p < 0.001$.

To investigate this further flagellar protein synthesis in the 3408 isolate and its mutant, 3408 $\Delta flhDC$, cultured in AUM and LB to 0.2 OD600, was explored using immunoblotting and the FlgEST antibody. Cell lysates from these bacterial isolates either heat treated or not heat treated were probed for FlgE protein. A cell lysate from the *Salmonella enterica* strain TPA1 was used as the positive control. Results are shown in Figure 5.6. FlgE expression was detected in the positive control sample, TPA1, and the cell lysate of the wild type isolate 3408 grown in LB. Signal i.e. a FlgE band was not detected in the 3408 $\Delta flhDC$ cell lysate, nor the heat killed 3408 cell lysate samples. Additionally, FlgE was not detected in the cell lysate of either 3408 or 3408 $\Delta flhDC$ grown in AUM, or in any of the heat killed cell lysate samples.

To explore whether these results could explain the bladder challenge data immunoblotting was performed using cell lysates of all the strains used in the AUM innate response experiment - CFT073, 3408, 5469, 5489- as well their $\Delta flhDC$ and $\Delta clpP$ mutants. Heat killed cell lysate samples of the wild-type isolates cultured in both LB and AUM were prepared and probed. Immunoblotting data are shown in Figures 5.7 and 5.8 respectively. Bands supporting FlgE synthesis were observed in the LB grown cell lysates of isolates 5489, 3408 and 5469 (wild type), with strong 42 kDa bands characterising their corresponding $\Delta clpP$ mutants. A FlgE band was observed in the cell lysate of the CFT073 $\Delta clpP$ mutant cultured in LB, but no band was observed in the CFT073 wild-type cell lysate. No bands were detected in any of the cell lysates from isolates cultured in AUM suggesting reduced or no expression of flagella, although there was the hint of a band in the wild-type 5489 AUM sample and in the CFT073 $\Delta clpP$ mutant sample. Additionally, no bands were detected in cell lysates from isolates grown either in LB or AUM and heat killed.

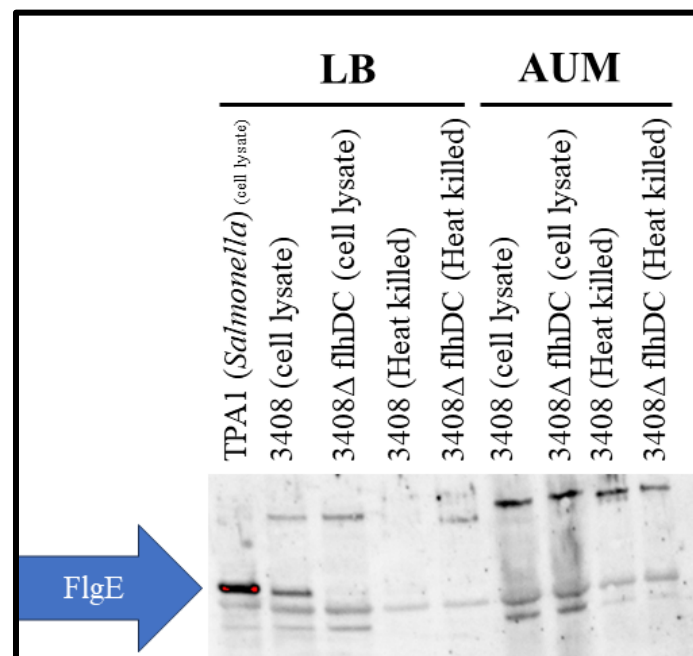


Figure 5.6 Expression of FlgE in wild-type isolate 3408 and its $\Delta flhDC$ and $\Delta clpP$ mutants grown either in LB or AUM. Strain 3408 cell lysates were probed with α -FlgE_{ST} antibody. Cell lysate of *Salmonella enterica* grown in LB was used as a positive control.

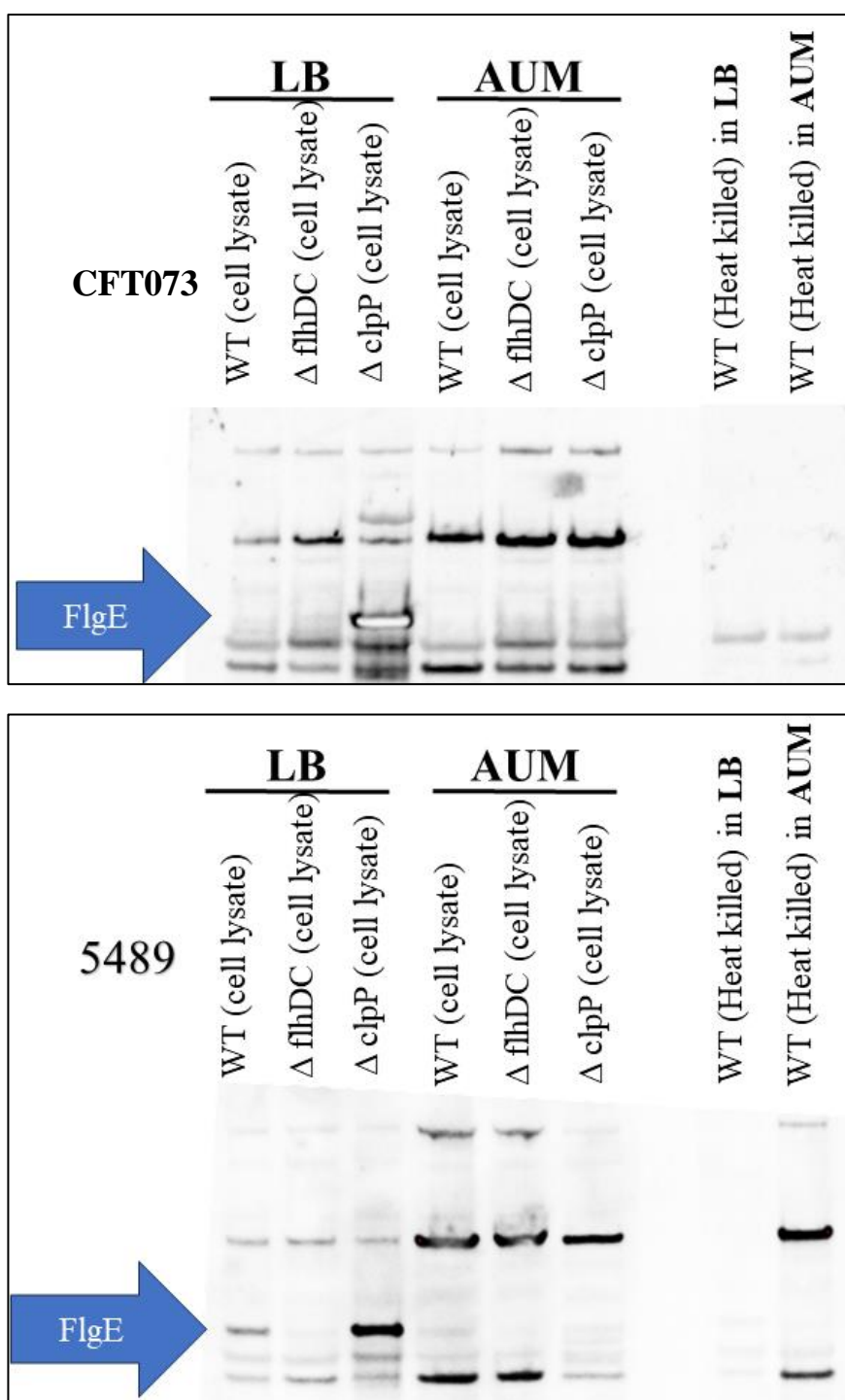


Figure 5.7 Expression of FlgE in wild-type isolate CFT073 & 5489 and their Δ flhDC and Δ clpP mutants grown either in LB or AUM. Cell lysates were probed with α -FlgE_{ST} antibody. Cell lysate of *Salmonella enterica* grown in LB was used as a positive control.

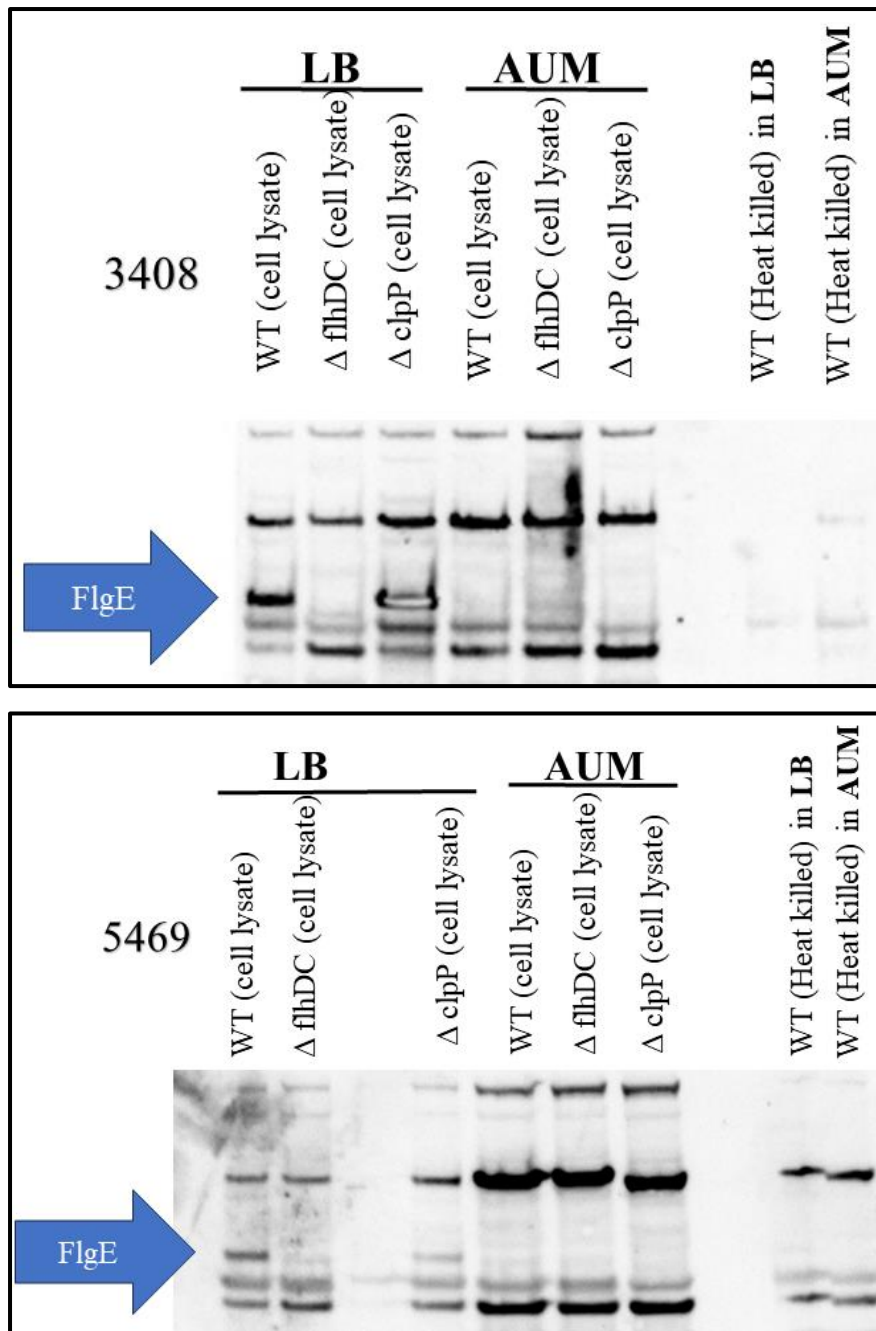


Figure 5.8 Expression of FlgE in wild-type isolate 3408 and 5469 3 and their $\Delta flhDC$ and $\Delta clpP$ mutants grown either in LB or AUM. Cell lysates were probed with α -FlgE_{ST} antibody. Cell lysate of *Salmonella enterica* grown in LB was used as a positive control.

These results indicated no or reduced synthesis of flagella in isolates cultured in AUM. However, it could not be excluded that harvesting the bacterial cells at 0.2 OD₆₀₀, flagellar synthesis was not optimal.

5.5 Discussion

Using AUM to investigate the impact of UTI isolates and their *flhDC* and *clpP* mutants on the bladder innate response was a tactic employed to help explain the role of the flagellar system in pathogenesis of an UTI. AUM is used to mimic the environment of the bladder replicating the physiological characteristics of human urine and the conditions of the urinary tract (Sarigul et al., 2019). Two different pH conditions, both are at the end of normal ranges for healthy people, 5.5 (modelling an acidic urine) and 6.5 (modelling an alkaline urine) (Brendler & Gerber, 2016), were selected and their impact(s), if any, on bacterial motility and the bladder pro-inflammatory response examined.

UTI isolates grew slowly in AUM, which in line with the literature (Sim et al., 2017), predicts a lower number of flagella per cell. This was evidenced by the experimental data as the motility activities of UTI strains and their *flhDC* and *clpP* mutants were reduced in AUM when compared to LB. Motility assays using AUM resulted in halo sizes of between 2 and 7 mm and after a 24 h incubation. In comparable assays using LB, halo sizes of up to 50 mm were observed and after only 8 h incubations. Interestingly isolates and strains linked to motility halos of >20 mm diameter were the ones associated with increased IL-8 concentrations, which arguably reflected a triggering of the bladder innate response via TLR5. Upon looking back on the way that the motility assays were performed, the inoculation points have diameters of 1-3 mm. For accurate measurements of halo sizes, imageJ was used, but the diameter of the inoculation points were not deducted from the halo sizes. This could result in error of measurements ranging between 1-3 mm.

UTI isolates grown in AUM were harvested for the bladder challenge experiments at 0.2 OD₆₀₀ nm, which was reached after growing the isolates for approximately five hours. It was feasible that the bacterial inoculants used in the challenge experiments had not switched

on flagellar synthesis. This was supported by the immunoblotting data (Figures 5.7 and 5.8) in which FlgE was not detected in the bacteria grown in AUM. Interestingly, where FlgE was detected, for example, the CFT073 $\Delta clpP$ mutant an IL-8 response was recorded (Fig 5.4 and 5.5).

The slow growth rate of the *E. coli* strains in AUM is presumably linked to reduced gene expression. Further investigation of the flagellar gene expression profiles would have provided more data to help explain how the AUM growth media impacts bacterial motility. This could be achieved by repeating the qPCR analyses described in Chapter 4 targeting genes such as *flhC*, *fliG*, *motAB* and *fliC* (Figure 4.9) as well as novel ones including *gyrB*, *rpoB* and *gmk*, to examine gene expression. Another option is to use the Datsenko and Wanner's one-step chromosomal gene inactivation method described in Chapter 2 to delete regulatory genes (Datsenko & Wanner, 2000). Experiments would be designed to construct mutants lacking the regulatory genes involved in flagellar synthesis, such as *fliT*, *fliZ*, *fliA*, *flgM*, and *csrA*, and then use these mutants to compare the growth and motilities of the wild-type and mutant strains in LB and AUM.

Conventionally, the acidic, average, and alkaline pH of urine is defined as 4.5 - 5.5, 5 - 6, and 6.5 - 8 (Brendler & Gerber, 2016). These experiments reported examined the impacts of two pH values 5.5 (borderline acidic) and 6.5 (borderline alkaline). Interestingly in a study focussed on paediatric patients (<18 years of age), (Ibrahim et al., 1984) suffering UTIs the urines of those infected with *E. coli* or the gram negative *Klebsiella pneumoniae* were recorded as 6.21 (n=3825) and 6.18 (n=209) respectively. The urine pHs of those negative for infection were 6.24 (n=4729), which suggests that infection with *E. coli* does not significantly impact the urine pH. This raises the question of whether pH plays any role in a lower UTI *in vivo* and the *in vitro* AUM data presented here suggests not. However, studies have shown that a very acidic pH (3-4), will damage flagella (Adler & Templeton, 1967)

although physiologically it is unlikely that such a low urine pH would be tolerated in humans. Interestingly exposing *E. coli* to an acidic environment of pH 4.6 (lower end of urine pH scale) was shown to be associated with de-flagellation and reduced motility (Soutourina et al., 2002) with *flhDC* expression reduced three fold at pH 4.6 compared to pH 7. Hence these data suggest a low acidic pH may protect from an ascending UTI.

Data from the experiments reported in this Chapter suggest a key factor is the constitution of the urine itself. However, while AUM was used to mimic the composition of urine other *in vivo* factors, including osmolality, cell breakdown products and dietary constituents were not modelled *in vitro* hence their impact on bacterial growth and motility cannot be excluded. The AUM used in these experiments resembles dilute human urine and models a low osmolality (<371 mOsm/kg) (Brooks & Keevil, 1997).

One of the alternatives to AUM is actual urine which should be collected from healthy people. The urine collection should be tested to eliminate any defected samples. The rest should be pooled together to be normalized as one sample so the pool will have the same characteristics. One of the advantages of such samples that they could be frozen and stored for consistency of the results. For more measures of quality control, the frozen urine should be tested before usage. This step will ensure consistency of the results and does not add variables changing the out-come of the results.

A criticism of these AUM challenge experiments was that they not only used a narrow selection of isolates, but also used killed rather than live bacteria. The advantage of using live bacteria is that the bacterial challenge mimics an UTI, but the disadvantage is that in the RT4 bathing media the bacterial cells tend to outgrow the bladder cells, characterised by longer doubling times of 40 – 65h, (Masters et al., 1986; Vallo et al., 2015) and kill them. It would,

however, have been interesting to observe the infection process and bladder innate responses using AUM grown live bacteria and compare these data to that using the heat-killed bacteria.

Using artificial urine media for growing urinary tract infection (UTI) isolates offers both advantages and disadvantages in research and diagnostic settings. Artificial urine media provide a standardized and controlled environment for culturing UTI isolates, ensuring consistency in experimental conditions. Unlike natural urine, which can vary significantly in composition and nutrient content between individuals, artificial urine can be precisely formulated to mimic the chemical composition of human urine. This allows researchers to conduct experiments under reproducible conditions, facilitating accurate comparisons between different bacterial strains and experimental setups. Additionally, artificial urine media offer a cost-effective alternative to using natural urine for bacterial culture. Natural urine collection can be logistically challenging and may require ethics, specialized storage and handling procedures to maintain sample integrity (Burton et al., 2019; Hasandka et al., 2022). In contrast, artificial urine can be prepared in large quantities using readily available chemicals, reducing the logistical and ethical concerns associated with handling human biological samples. Moreover, artificial urine media provide a versatile platform for studying bacterial growth and metabolism in the context of UTIs. Researchers can manipulate the composition of artificial urine to simulate different physiological conditions within the urinary tract, such as variations in pH, osmolality, or nutrient availability. This flexibility allows for the investigation of specific aspects of bacterial physiology and pathogenesis, providing insights into the mechanisms underlying UTI development and persistence (Ipe & Ulett, 2016; Rosen et al., 2007; Schreiber et al., 2017).

Despite their advantages, artificial urine media have some limitations that researchers must consider. One drawback is the potential lack of complexity compared to natural urine. Artificial urine formulations may not fully replicate the diverse array of nutrients,

metabolites, and host-derived factors present in human urine (Abbott et al., 2020; Psotta et al., 2023). As a result, bacterial growth and behaviour in artificial urine may not accurately reflect the conditions encountered in vivo, limiting the translational relevance of experimental findings. Furthermore, artificial urine media may not support the growth of all UTI-causing bacteria or accurately represent the diversity of microbial communities present in clinical samples. Some bacterial species or strains may have specific nutritional requirements or metabolic preferences that are not adequately met by artificial urine formulations. This can lead to biased results and hinder the identification of novel pathogens or virulence factors associated with UTIs. Additionally, the use of artificial urine media may overlook important interactions between bacteria and host cells or other microorganisms present in the urinary tract. UTIs are complex polymicrobial infections involving interactions between multiple bacterial species and the host immune system. Artificial urine media may fail to capture these intricate dynamics, limiting our understanding of UTI pathogenesis and potentially overlooking important therapeutic targets (Josephs-Spaulding et al., 2021; Psotta et al., 2023).

In summary, while artificial urine media offer several advantages for growing UTI isolates in research settings, researchers must carefully consider their limitations and ensure that experimental findings are interpreted within the context of these constraints. Integrating complementary approaches, such as in vivo models or clinical studies, can help overcome some of these limitations and provide a more comprehensive understanding of UTI pathogenesis and treatment strategies.

The original aim of this work was to explore whether uro-associated *E. coli* adopt distinct uropathogenic characteristics in response to the host conditions with a focus on mimicking urine by growing the bacteria in AUM and altering the pH. Data suggested that a physiological urine pH did not impact pathogenicity, but that the host environment, essentially urine composition probably does play a role.

Chapter 6. General Discussion

Work described in this thesis was focussed on determining links between bacterial (uro- associated *E. coli*) motility and the innate response of the host (mammalian) bladder. These analyses stemmed from observations that motilities within clinical uro-associated *E. coli* were variable (non-motile to very motile), but that motility was not always associated with a bladder innate response (Figure 1.9) (Tan et al., 2023). Experiments focussed on bacterial fitness suggested that the doubling times of the motile and non-motile clinically sourced isolates were significantly different (Figure 3.4), which suggested bacterial fitness played a role in inducing an innate response. However, additional analyses indicated that the range of maximum doubling times within each grouping was comparable (Motile: 13.9–26.9min.; Non-Motile: 14.7– 25.3 min.). As such these data suggested that bacterial fitness was not a key factor in determining the variable host responses observed following challenge of RT4 bladder cells with motile isolates.

The fitness data was none-the-less intriguing especially in respect to colonisation and UTIs. In future it would be interesting to perform *in vitro* competition experiments between the fast and slow growing strains to determine if there exists a hierarchy and whether a fast-growing bacterium has an advantage or not in relation to colonisation and infection. While *in vitro* data are useful the conditions are not always reflective of *in vivo* conditions, hence it would be exciting to repeat these competition experiments using bladder 3D models (Jafari & Rohn, 2023) and/or mouse models (Barber et al., 2016) and to compare the outcomes.

To further explore the motility of these uro-associated *E. coli* strains the regulation of flagellar gene expression was studied. In general mutants lacking *flhDC* resulted in non-motile strains while those in which *clpP* had been deleted (*clpP* is a repressor of *flhDC* activities), showed enhanced motility. There were exceptions, however, namely strains 3408 and MG1655. For example, while the motility of strain MG1655 $\Delta clpP$ did increase it was minimal. In contrast the motility of 3408 $\Delta clpP$ changed significantly, but despite this

increase it did not, surprisingly, induce a host response when used to challenge RT4 cells (Figure 4.6). This was despite further analyses showing that the mutation increased the flagellated population of 3408 to more than 75%. The model suggested by Tan *et al.*, (2023), argues that over 60 % of the population being flagellated triggers TLR5 signalling suggesting strain 3408 was behaving as an outlier. The behaviour of strain 3408, recovered from a cystitis patient, was therefore not typical of that predicted and needs further investigation. Comparing the genome of 3408 with those of other UTI isolates may give an insight into its unique characteristics, for example, the encoding of known or novel TLR signalling inhibitors that allow it to evade the host innate immune system. RNA seq analyses following challenges of host bladder cells *in vitro* and *in vivo* could also be performed to compare and identify novel gene expression patterns associated with evasion of the bladder innate immune defences. The isolate 3408 appeared unique, but the number of isolates examined in this project was minimal. The laboratory has over 1000 uro-associated clinical isolates banked hence it would be interesting to know if others, comparable to 3408 exist.

Analysing plasmids between Uropathogenic Escherichia coli (UPEC) strains involves examining the genetic makeup and characteristics of plasmids present within these bacterial populations. This analysis can provide valuable insights into the diversity, distribution, and potential virulence factors carried by these plasmids.

Another approach to investigate the UTI isolates is transcriptome analysis, with its ability to comprehensively capture gene expression profiles, presents numerous advantages (Hogins et al., 2023). By examining the entirety of RNA transcripts produced by a cell or tissue under specific conditions, researchers gain deep insights into the dynamic nature of cellular processes. This comprehensive view extends beyond the coding RNAs to encompass non-coding RNAs, including microRNAs and long non-coding RNAs, shedding light on their regulatory roles. Through transcriptome analysis, researchers can unravel intricate regulatory

networks and understand how gene expression patterns change in response to developmental cues, environmental stimuli, or disease states. Such insights offer valuable opportunities for deciphering the molecular mechanisms underlying complex biological phenomena.

However, transcriptome analysis also poses certain challenges and limitations. One significant challenge lies in the computational complexity associated with processing and interpreting transcriptome data (Deshpande et al., 2023; Gondane & Itkonen, 2023). Analysing large datasets generated from RNA sequencing experiments requires sophisticated bioinformatics tools and computational resources. Researchers must navigate through complex algorithms for data normalization, differential expression analysis, and functional annotation to extract meaningful biological insights (Jiang et al., 2015). Moreover, incomplete annotation of the transcriptome presents hurdles in accurately identifying novel transcripts and regulatory elements. Poorly annotated transcripts may hinder the interpretation of transcriptome data, potentially overlooking critical biological information. Technical variability introduces another layer of complexity in transcriptome analysis. Factors such as RNA extraction methods, library preparation protocols, and sequencing platforms can introduce biases and inconsistencies, impacting the reproducibility and reliability of transcriptome data. Addressing these technical challenges requires careful experimental design, stringent quality control measures, and validation strategies to ensure the robustness of findings (Deshpande et al., 2023). Additionally, the cost associated with transcriptome analysis, particularly high-throughput RNA sequencing, can be prohibitive for researchers with limited funding or resources. The financial burden may limit the accessibility of transcriptome analysis to certain research groups, potentially hindering broader scientific advancements. Despite these challenges, transcriptome analysis remains a powerful tool for understanding gene expression dynamics and unravelling the complexities of cellular biology. By leveraging the advantages of transcriptome analysis while addressing

its limitations, researchers can continue to unravel the intricate molecular mechanisms governing cellular processes and disease pathogenesis, paving the way for innovative therapeutic interventions and precision medicine approaches.

Utilizing urinary tract infection (UTI) isolates for fitness data and competition experiments offers a valuable approach to understanding the dynamics between fast growers and slow growers both in vitro and in animal models (Schreiber et al., 2017). By comparing the growth rates and competitive abilities of different bacterial strains, researchers can gain insights into how these characteristics influence colonization and infection in the urinary tract. Expanding the fitness experiments by increasing the number of isolates included with taking in consideration the variability of infection sites. Moreover, competition experiments in vitro involve co-culturing different UTI isolates and monitoring their interactions over time. By assessing the relative abundance of competing strains, researchers can determine the competitive fitness of each isolate. This approach allows for the identification of strains that outcompete others for resources, potentially leading to dominance within the urinary tract environment. In addition to in vitro experiments, studying fast and slow growers in animal models provides valuable insights into their behaviour during colonization and infection (Schreiber et al., 2017). Mouse models of UTI offer a controlled environment to assess bacterial virulence, host-pathogen interactions, and the impact of bacterial fitness on disease outcomes (Hannan & Hunstad, 2016). By inoculating mice with different UTI isolates and monitoring bacterial colonization and infection dynamics, researchers can evaluate the ability of fast growers to establish infection and cause disease compared to slow growers. Furthermore, studying fast and slow growers in animal models allows researchers to explore the host immune response and bacterial adaptation strategies. Fast growers may elicit stronger inflammatory responses and exhibit enhanced virulence factors, leading to more severe infections. Conversely, slow growers may rely on stealthier mechanisms to evade

immune detection and persist within the host. Overall, combining fitness data and competition experiments with in vitro and in vivo models provides a comprehensive understanding of the factors influencing bacterial colonization and infection in the urinary tract. By elucidating the characteristics of fast and slow growers, researchers can identify potential targets for therapeutic intervention and develop strategies to combat UTIs more effectively.

A criticism of these studies was that the bacteria studied were cultured using a nutrient rich growth medium, which does not reflect the bladder environment. To mimic the bladder environment, an artificial urine medium (AUM) was prepared in the laboratory. It was used to grow the UTI isolates, and their *flhDC* and *clpP* mutants, and investigate their motility and ability to induce an innate response. The motility studies revealed an altered phenotype with motility significantly affected (Figure 5.3) linked to reduced flagellar synthesis as determined by probing with FlgE_{ST}. Whether this occurs in the bladder is not known but it would be interesting to repeat these experiments using either the bladder 3D models and/or mouse models, or natural urine. While mimicking the urinary tract environment the latter has a disadvantage in that to collect sufficient volumes for experimentation, urine would have to be pooled from multiple donors, meaning a lack of quality control, which may impact data reproducibility.

The composition of urine often reflects a person's diet and one urinary constituent is D-serine (Huang et al., 1998), which is consumed via processed foods (Friedman, 1999) and excreted via urine. The detoxification of D-serine requires a genetic locus (*dsdCXA*), which is encoded by UPEC giving these bacteria the advantage of being able to grow in its presence (Connolly et al., 2021). UPEC strains can catabolise the metabolite via a D-serine deaminase DsdA, hence D-serine is proposed to play a role in UTI susceptibility. Interestingly work has shown that a CFT073 *dsdA* mutant is hyperflagellated and more motile than wild-type

suggesting that D-serine may influence expression of the flagella (Roesch et al., 2003). Additionally in a mixed-infection murine model using CFT073 wild-type and *dsdA* mutant strains these authors reported the mutant in the bladder at levels 270 times higher than wild-type. These data strongly support a role for D-serine and *dsdA* expression in UPEC flagellar regulation and it would be interesting to pursue this concept using the curated uro-associated *E. coli* clinical isolates available in the laboratory. The hypothesis would be that D-serine represents an important environmental signal in UTIs and its effects could initially be investigated using AUM media.

Another alternative way of assessing the impact of media on the innate response resulting from the UTI isolates would be accomplished by changing one element at a time instead of several ones at the same time. This could be achieved by systematically using LB with different pH values or changing the concentration of nutrients in the media. After that changing two elements at the same time and assess the strains behaviour accordingly. Designing these experiments to go steadily helps explain which element of the media is more responsible of the change in bacterial behaviour.

On the other hand, the time for the incubation should be tested as well. OD₆₀₀ 0.2 does not seem to be enough for the bacteria to express flagellar genes so the incubation time should be tested in further and longer incubation times leading for the culture to grow up to 0.4 - 0.6 OD₆₀₀. Another way of exploring whether the change in conditions could lead to the flagellar synthesis would be changing the conditions in the middle of the experiments. The bacteria might change the behaviour by synthesising flagella in case of sudden change in the environmental conditions (Table 6.1). All these suggestions should be assessed by comparing motility, detecting flagellar protein expression, measuring flagellar genes expression, and comparing flagellar abundance of the strains and their mutants.

Table 6.1 Designing conditions variability to examine their effect on UTI isolates' behaviour.

Experiment	A	B	C	D	E	F	G	H	I
Tryptone conc.	low	low	low	Optimum	Optimum	Optimum	High	High	High
pH	Acidic	Neutral	Alkaline	Acidic	Neutral	Alkaline	Acidic	Neutral	Alkaline

Previous research using mouse models has revealed that UPEC strains missing flagella had reduced virulence, indicating a critical role for flagella during ascending UTIs. According to the findings, flagella play an important role in the colonisation and progression of UTIs, particularly in the context of UPEC infections (Acharya et al., 2019; Ali et al., 2017). A further step in our research would be testing the effect of the UTI isolates and their mutants such as $\Delta flhDC$ & $\Delta clpP$ mutants in vivo using the mice module. Furthermore, the results could help explain the significance of flagellar expression during IBC development, demonstrating the in vivo dynamics of flagella expression and its impact on IBC physiological states. Findings of previous experiments indicated that flagella may help to maintain UPEC in the intestinal or genitourinary tracts, allowing them to emerge into periurethral areas and ascend into the urethra to cause UTIs.

Improved in vitro models that better mimic the human urothelium hold significant potential for studying the cellular alterations associated with infection. These models should ideally encompass at least four distinct structural and biophysical characteristics believed to play a crucial role in host-pathogen interactions, including tissue architecture, exposure to urine at the apical surface, dynamic fluid flow, and stretching of the urothelium (Murray et al., 2021). The following discussion expands on these essential features within the context of bladder physiology, their relevance to urinary tract infections (UTIs), and relevant models or platforms. using commercial primary cells or spontaneously immortalized cells such as HBEP and HBLAK in research involving UPEC has both advantages and disadvantages (Horsley et al., 2018). Commercially available primary cells or immortalized cell lines offer consistent

characteristics and behaviour, reducing variability in experimental results compared to primary cells isolated from different donors. Additionally, these cell lines are readily available and easy to maintain in laboratory settings, saving time and effort in culturing and establishing cell cultures. Purchasing commercial cell lines can also be more cost-effective than isolating and maintaining primary cells from tissues, especially considering the resources required for cell culture. Furthermore, commercially available cell lines often come with detailed protocols and standardized culture conditions, ensuring reproducibility across different experiments and laboratories. Spontaneously immortalized cell lines like HBEP and HBLAK provide an unlimited supply of cells, eliminating the need for continuous isolation from primary sources (Hagan et al., 2010; Russell et al., 2023). However, there are also disadvantages to using these cell lines. Immortalized cell lines may not fully retain the characteristics of primary cells, potentially affecting the relevance of findings to in vivo conditions. Additionally, they may accumulate genetic alterations during the immortalization process, leading to changes in cellular behavior and response to stimuli. Immortalized cell lines may also have limited differentiation potential compared to primary cells, affecting their suitability for studying specific cellular processes or differentiation pathways. There is also a risk of cross-contamination or misidentification with commercially available cell lines, which can lead to unreliable results if not properly authenticated. Ethical concerns arise regarding the use of immortalized cell lines, especially if derived from human tissues, raising questions about their origin and potential exploitation. Ultimately, the choice between using commercial primary cells or immortalized cell lines depends on the specific research objectives, balancing factors such as reproducibility, relevance to in vivo conditions, and practical considerations (Giron et al., 2002; He et al., 2009).

In summary this project has attempted to interrogate the variable motility phenotypes of uro-associated clinical *E. coli* isolates alongside their abilities to avoid and/or induce the

bladder host TLR5 defences. Results have shown that these isolates, in the main, can regulate flagellar synthesis to allow colonisation or infection, but appear to exploit population heterogeneity to prevent recognition by urothelial cell TLR5 receptors and bacterial killing. The next steps are to identify the signals, environmental or otherwise, that trigger flagella synthesis in an urinary tract infection.

Chapter 7. Bibliography

References:

- Abbott, I. J., van Gorp, E., Wijma, R. A., Meletiadis, J., Mouton, J. W., & Peleg, A. Y. (2020). Evaluation of pooled human urine and synthetic alternatives in a dynamic bladder infection in vitro model simulating oral fosfomycin therapy. *J Microbiol Methods*, 171, 105861. <https://doi.org/10.1016/j.mimet.2020.105861>
- Abraham, S. N., & Miao, Y. (2015). The nature of immune responses to urinary tract infections. *Nat Rev Immunol*, 15(10), 655-663. <https://doi.org/10.1038/nri3887>
- Abrusci, P., McDowell, M. A., Lea, S. M., & Johnson, S. (2014). Building a secreting nanomachine: a structural overview of the T3SS. *Curr Opin Struct Biol*, 25(100), 111-117. <https://doi.org/10.1016/j.sbi.2013.11.001>
- Acharya, D., Sullivan, M. J., Duell, B. L., Goh, K. G. K., Katupitiya, L., Gosling, D., Chamoun, M. N., Kakkanat, A., Chattopadhyay, D., Crowley, M., Crossman, D. K., Schembri, M. A., & Ulett, G. C. (2019). Rapid Bladder Interleukin-10 Synthesis in Response to Uropathogenic Escherichia coli Is Part of a Defense Strategy Triggered by the Major Bacterial Flagellar Filament FlhC and Contingent on TLR5. *mSphere*, 4(6). <https://doi.org/10.1128/mSphere.00545-19>
- Adler, J., & Templeton, B. (1967). The effect of environmental conditions on the motility of Escherichia coli. *J Gen Microbiol*, 46(2), 175-184. <https://doi.org/10.1099/00221287-46-2-175>
- Agace, W. W. (1996). The role of the epithelial cell in Escherichia coli induced neutrophil migration into the urinary tract. *Eur Respir J*, 9(8), 1713-1728. <https://doi.org/10.1183/09031936.96.09081713>
- Albanna, A., Sim, M., Hoskisson, P. A., Gillespie, C., Rao, C. V., & Aldridge, P. D. (2018). Driving the expression of the Salmonella enterica sv Typhimurium flagellum using flhDC from Escherichia coli results in key regulatory and cellular differences. *Sci Rep*, 8(1), 16705. <https://doi.org/10.1038/s41598-018-35005-2>
- Aldridge, C., Poonchareon, K., Saini, S., Ewen, T., Soloyva, A., Rao, C. V., Imada, K., Minamino, T., & Aldridge, P. D. (2010). The interaction dynamics of a negative feedback loop regulates flagellar number in Salmonella enterica serovar Typhimurium. *Mol Microbiol*, 78(6), 1416-1430. <https://doi.org/10.1111/j.1365-2958.2010.07415.x>
- Aldridge, P., Karlinsey, J., & Hughes, K. T. (2003). The type III secretion chaperone FlgN regulates flagellar assembly via a negative feedback loop containing its chaperone substrates FlgK and FlgL. *Mol Microbiol*, 49(5), 1333-1345. <https://doi.org/10.1046/j.1365-2958.2003.03637.x>
- Ali, A. S., Townes, C. L., Hall, J., & Pickard, R. S. (2009). Maintaining a sterile urinary tract: the role of antimicrobial peptides. *J Urol*, 182(1), 21-28. <https://doi.org/10.1016/j.juro.2009.02.124>
- Ali, A. S. M., Mowbray, C., Lanz, M., Stanton, A., Bowen, S., Varley, C. L., Hilton, P., Brown, K., Robson, W., Southgate, J., Aldridge, P. D., Tyson-Capper, A., Abraham, S., Pickard, R. S., & Hall, J. (2017). Targeting Deficiencies in the TLR5 Mediated Vaginal Response to Treat Female Recurrent Urinary Tract Infection. *Sci Rep*, 7(1), 11039. <https://doi.org/10.1038/s41598-017-10445-4>
- Andersen-Nissen, E., Smith, K. D., Bonneau, R., Strong, R. K., & Aderem, A. (2007). A conserved surface on Toll-like receptor 5 recognizes bacterial flagellin. *J Exp Med*, 204(2), 393-403. <https://doi.org/10.1084/jem.20061400>
- Andersen-Nissen, E., Smith, K. D., Strobe, K. L., Barrett, S. L., Cookson, B. T., Logan, S. M., & Aderem, A. (2005). Evasion of Toll-like receptor 5 by flagellated bacteria. *Proc Natl Acad Sci U S A*, 102(26), 9247-9252. <https://doi.org/10.1073/pnas.0502040102>
- Anderson, J. K., Smith, T. G., & Hoover, T. R. (2010). Sense and sensibility: flagellum-mediated gene regulation. *Trends Microbiol*, 18(1), 30-37. <https://doi.org/10.1016/j.tim.2009.11.001>
- Ariathianto, Y. (2011). Asymptomatic bacteriuria - prevalence in the elderly population. *Aust Fam Physician*, 40(10), 805-809. <https://www.ncbi.nlm.nih.gov/pubmed/22003486>

- Aroney, S. T. N., Poole, P. S., & Sanchez-Canizares, C. (2021). Rhizobial Chemotaxis and Motility Systems at Work in the Soil. *Front Plant Sci*, *12*, 725338. <https://doi.org/10.3389/fpls.2021.725338>
- Baker, T. A., & Sauer, R. T. (2006). ATP-dependent proteases of bacteria: recognition logic and operating principles. *Trends Biochem Sci*, *31*(12), 647-653. <https://doi.org/10.1016/j.tibs.2006.10.006>
- Barber, A. E., Norton, J. P., Wiles, T. J., & Mulvey, M. A. (2016). Strengths and Limitations of Model Systems for the Study of Urinary Tract Infections and Related Pathologies. *Microbiol Mol Biol Rev*, *80*(2), 351-367. <https://doi.org/10.1128/MMBR.00067-15>
- Barnich, N., Carvalho, F. A., Glasser, A. L., Darcha, C., Jantscheff, P., Allez, M., Peeters, H., Bommelaer, G., Desreumaux, P., Colombel, J. F., & Darfeuille-Michaud, A. (2007). CEACAM6 acts as a receptor for adherent-invasive E. coli, supporting ileal mucosa colonization in Crohn disease. *J Clin Invest*, *117*(6), 1566-1574. <https://doi.org/10.1172/JCI30504>
- Behzadi, E., & Behzadi, P. (2016). The role of toll-like receptors (TLRs) in urinary tract infections (UTIs). *Cent European J Urol*, *69*(4), 404-410. <https://doi.org/10.5173/ceju.2016.871>
- Benramdane, L., Bouatia, M., Idrissi, M. O. B., & Draoui, M. (2008). Infrared Analysis of Urinary Stones, Using a Single Reflection Accessory and a KBr Pellet Transmission. 72-80. <https://doi.org/10.1080/00387010801943806>
- Berg, R. D. (1996). The indigenous gastrointestinal microflora. *Trends Microbiol*, *4*(11), 430-435. [https://doi.org/10.1016/0966-842x\(96\)10057-3](https://doi.org/10.1016/0966-842x(96)10057-3)
- Bergman, M. A., Cummings, L. A., Alaniz, R. C., Mayeda, L., Fellnerova, I., & Cookson, B. T. (2005). CD4+T-cell responses generated during murine Salmonella enterica serovar Typhimurium infection are directed towards multiple epitopes within the natural antigen FliC. *Infect Immun*, *73*(11), 7226-7235. <https://doi.org/10.1128/IAI.73.11.7226-7235.2005>
- Betis, F., Brest, P., Hofman, V., Guignot, J., Kansau, I., Rossi, B., Servin, A., & Hofman, P. (2003). Afa/Dr diffusely adhering Escherichia coli infection in T84 cell monolayers induces increased neutrophil transepithelial migration, which in turn promotes cytokine-dependent upregulation of decay-accelerating factor (CD55), the receptor for Afa/Dr adhesins. *Infect Immun*, *71*(4), 1774-1783. <https://doi.org/10.1128/IAI.71.4.1774-1783.2003>
- Beutin, L., Strauch, E., Zimmermann, S., Kaulfuss, S., Schaudinn, C., Mannel, A., & Gelderblom, H. R. (2005). Genetical and functional investigation of fliC genes encoding flagellar serotype H4 in wildtype strains of Escherichia coli and in a laboratory E. coli K-12 strain expressing flagellar antigen type H48. *BMC Microbiol*, *5*, 4. <https://doi.org/10.1186/1471-2180-5-4>
- Beutler, B. (2000). Tlr4: central component of the sole mammalian LPS sensor. *Curr Opin Immunol*, *12*(1), 20-26. [https://doi.org/10.1016/s0952-7915\(99\)00046-1](https://doi.org/10.1016/s0952-7915(99)00046-1)
- Bien, J., Sokolova, O., & Bozko, P. (2012). Role of Uropathogenic Escherichia coli Virulence Factors in Development of Urinary Tract Infection and Kidney Damage. *Int J Nephrol*, *2012*, 681473. <https://doi.org/10.1155/2012/681473>
- Blattner, F. R., Plunkett, G., 3rd, Bloch, C. A., Perna, N. T., Burland, V., Riley, M., Collado-Vides, J., Glasner, J. D., Rode, C. K., Mayhew, G. F., Gregor, J., Davis, N. W., Kirkpatrick, H. A., Goeden, M. A., Rose, D. J., Mau, B., & Shao, Y. (1997). The complete genome sequence of Escherichia coli K-12. *Science*, *277*(5331), 1453-1462. <https://doi.org/10.1126/science.277.5331.1453>
- Borisov, V. B., & Forte, E. (2022). Bioenergetics and Reactive Nitrogen Species in Bacteria. *Int J Mol Sci*, *23*(13). <https://doi.org/10.3390/ijms23137321>
- Bouckaert, J., Mackenzie, J., de Paz, J. L., Chipwaza, B., Choudhury, D., Zavialov, A., Mannerstedt, K., Anderson, J., Pierard, D., Wyns, L., Seeberger, P. H., Oscarson, S., De Greve, H., & Knight, S. D. (2006). The affinity of the FimH fimbrial adhesin is receptor-driven and quasi-independent of Escherichia coli pathotypes. *Mol Microbiol*, *61*(6), 1556-1568. <https://doi.org/10.1111/j.1365-2958.2006.05352.x>
- Brendler, C. B., & Gerber, G. S. (2016). Evaluation of the urologic patient : history, physical examination, and urinalysis. *Campbell-Walsh Urology (11th ed.)*, *1*, 1-25.

- Brons, J. K., Vink, S. N., de Vos, M. G. J., Reuter, S., Dobrindt, U., & van Elsas, J. D. (2020). Fast identification of *Escherichia coli* in urinary tract infections using a virulence gene based PCR approach in a novel thermal cycler. *J Microbiol Methods*, *169*, 105799. <https://doi.org/10.1016/j.mimet.2019.105799>
- Brooks, T., & Keevil, C. W. (1997). A simple artificial urine for the growth of urinary pathogens. *Lett Appl Microbiol*, *24*(3), 203-206. <https://doi.org/10.1046/j.1472-765x.1997.00378.x>
- Brown, J. D., Saini, S., Aldridge, C., Herbert, J., Rao, C. V., & Aldridge, P. D. (2008). The rate of protein secretion dictates the temporal dynamics of flagellar gene expression. *Mol Microbiol*, *70*(4), 924-937. <https://doi.org/10.1111/j.1365-2958.2008.06455.x>
- Burt, A., Cassidy, C. K., Stansfeld, P. J., & Gutsche, I. (2021). Alternative Architecture of the *E. coli* Chemosensory Array. *Biomolecules*, *11*(4). <https://doi.org/10.3390/biom11040495>
- Burton, R. J., Albur, M., Eberl, M., & Cuff, S. M. (2019). Using artificial intelligence to reduce diagnostic workload without compromising detection of urinary tract infections. *BMC Med Inform Decis Mak*, *19*(1), 171. <https://doi.org/10.1186/s12911-019-0878-9>
- Butler, C. C., Hawking, M. K., Quigley, A., & McNulty, C. A. (2015). Incidence, severity, help seeking, and management of uncomplicated urinary tract infection: a population-based survey. *Br J Gen Pract*, *65*(639), e702-707. <https://doi.org/10.3399/bjgp15X686965>
- Butler, C. C., Lau, M., Gillespie, D., Owen-Jones, E., Lown, M., Wootton, M., Calder, P. C., Bayer, A. J., Moore, M., Little, P., Davies, J., Edwards, A., Shepherd, V., Hood, K., Hobbs, F. D. R., Davoudianfar, M., Rutter, H., Stanton, H., Lowe, R., Fuller, R., & Francis, N. A. (2020). Effect of Probiotic Use on Antibiotic Administration Among Care Home Residents: A Randomized Clinical Trial. *JAMA*, *324*(1), 47-56. <https://doi.org/10.1001/jama.2020.8556>
- Buttner, D. (2012). Protein export according to schedule: architecture, assembly, and regulation of type III secretion systems from plant- and animal-pathogenic bacteria. *Microbiol Mol Biol Rev*, *76*(2), 262-310. <https://doi.org/10.1128/MMBR.05017-11>
- Callan, A., O'Shea, E., Galvin, S., Duane, S., Corry, O., T, S. I. T., & Vellinga, A. (2014). The Economic Cost Of Urinary Tract Infections In The Community: Results From Ireland. *Value Health*, *17*(7), A468. <https://doi.org/10.1016/j.jval.2014.08.1319>
- Carter, C., Hutchison, A., Rudder, S., Trotter, E., Waters, E. V., Elumogo, N., & Langridge, G. C. (2023). Uropathogenic *Escherichia coli* population structure and antimicrobial susceptibility in Norfolk, UK. *J Antimicrob Chemother*, *78*(8), 2028-2036. <https://doi.org/10.1093/jac/dkad201>
- Chakraborty, S., Harro, C., DeNearing, B., Ram, M., Feller, A., Cage, A., Bauers, N., Bourgeois, A. L., Walker, R., & Sack, D. A. (2016). Characterization of Mucosal Immune Responses to Enterotoxigenic *Escherichia coli* Vaccine Antigens in a Human Challenge Model: Response Profiles after Primary Infection and Homologous Rechallenge with Strain H10407. *Clin Vaccine Immunol*, *23*(1), 55-64. <https://doi.org/10.1128/CVI.00617-15>
- Chan, C. Y., St John, A. L., & Abraham, S. N. (2013). Mast cell interleukin-10 drives localized tolerance in chronic bladder infection. *Immunity*, *38*(2), 349-359. <https://doi.org/10.1016/j.immuni.2012.10.019>
- Chassaing, B., Rolhion, N., de Vallee, A., Salim, S. Y., Prorok-Hamon, M., Neut, C., Campbell, B. J., Soderholm, J. D., Hugot, J. P., Colombel, J. F., & Darfeuille-Michaud, A. (2011). Crohn disease--associated adherent-invasive *E. coli* bacteria target mouse and human Peyer's patches via long polar fimbriae. *J Clin Invest*, *121*(3), 966-975. <https://doi.org/10.1172/JCI44632>
- Chaudhuri, R. R., & Henderson, I. R. (2012). The evolution of the *Escherichia coli* phylogeny. *Infect Genet Evol*, *12*(2), 214-226. <https://doi.org/10.1016/j.meegid.2012.01.005>
- Cheng, Y., Chen, Z., Gawthorne, J. A., Mukerjee, C., Varetas, K., Mansfield, K. J., Schembri, M. A., & Moore, K. H. (2016). Detection of intracellular bacteria in exfoliated urothelial cells from women with urge incontinence. *Pathog Dis*, *74*(7). <https://doi.org/10.1093/femspd/ftw067>

- Chilcott, G. S., & Hughes, K. T. (2000). Coupling of flagellar gene expression to flagellar assembly in *Salmonella enterica* serovar typhimurium and *Escherichia coli*. *Microbiol Mol Biol Rev*, *64*(4), 694-708. <https://doi.org/10.1128/MMBR.64.4.694-708.2000>
- Ching, C., Schwartz, L., Spencer, J. D., & Becknell, B. (2020). Innate immunity and urinary tract infection. *Pediatr Nephrol*, *35*(7), 1183-1192. <https://doi.org/10.1007/s00467-019-04269-9>
- Ching, C. B., Gupta, S., Li, B., Cortado, H., Mayne, N., Jackson, A. R., McHugh, K. M., & Becknell, B. (2018). Interleukin-6/Stat3 signaling has an essential role in the host antimicrobial response to urinary tract infection. *Kidney Int*, *93*(6), 1320-1329. <https://doi.org/10.1016/j.kint.2017.12.006>
- Claret, L., & Hughes, C. (2000). Functions of the subunits in the FlhD(2)C(2) transcriptional master regulator of bacterial flagellum biogenesis and swarming. *J Mol Biol*, *303*(4), 467-478. <https://doi.org/10.1006/jmbi.2000.4149>
- Cohen, P., & Strickson, S. (2017). The role of hybrid ubiquitin chains in the MyD88 and other innate immune signalling pathways. *Cell Death Differ*, *24*(7), 1153-1159. <https://doi.org/10.1038/cdd.2017.17>
- Connell, I., Agace, W., Klemm, P., Schembri, M., Marild, S., & Svanborg, C. (1996). Type 1 fimbrial expression enhances *Escherichia coli* virulence for the urinary tract. *Proc Natl Acad Sci U S A*, *93*(18), 9827-9832. <https://doi.org/10.1073/pnas.93.18.9827>
- Connolly, J. P. R., Turner, N. C. A., Hallam, J. C., Rimbi, P. T., Flett, T., McCormack, M. J., Roe, A. J., & O'Boyle, N. (2021). d-Serine induces distinct transcriptomes in diverse *Escherichia coli* pathotypes. *Microbiology (Reading)*, *167*(10). <https://doi.org/10.1099/mic.0.001093>
- Crossman, L. C., Chaudhuri, R. R., Beatson, S. A., Wells, T. J., Desvaux, M., Cunningham, A. F., Petty, N. K., Mahon, V., Brinkley, C., Hobman, J. L., Savarino, S. J., Turner, S. M., Pallen, M. J., Penn, C. W., Parkhill, J., Turner, A. K., Johnson, T. J., Thomson, N. R., Smith, S. G., & Henderson, I. R. (2010). A commensal gone bad: complete genome sequence of the prototypical enterotoxigenic *Escherichia coli* strain H10407. *J Bacteriol*, *192*(21), 5822-5831. <https://doi.org/10.1128/JB.00710-10>
- Croxen, M. A., & Finlay, B. B. (2010). Molecular mechanisms of *Escherichia coli* pathogenicity. *Nat Rev Microbiol*, *8*(1), 26-38. <https://doi.org/10.1038/nrmicro2265>
- Croxen, M. A., Law, R. J., Scholz, R., Keeney, K. M., Wlodarska, M., & Finlay, B. B. (2013). Recent advances in understanding enteric pathogenic *Escherichia coli*. *Clin Microbiol Rev*, *26*(4), 822-880. <https://doi.org/10.1128/CMR.00022-13>
- Datsenko, K. A., & Wanner, B. L. (2000). One-step inactivation of chromosomal genes in *Escherichia coli* K-12 using PCR products. *Proc Natl Acad Sci U S A*, *97*(12), 6640-6645. <https://doi.org/10.1073/pnas.120163297>
- Davis, M. A., Baker, K. N., Orfe, L. H., Shah, D. H., Besser, T. E., & Call, D. R. (2010). Discovery of a gene conferring multiple-aminoglycoside resistance in *Escherichia coli*. *Antimicrob Agents Chemother*, *54*(6), 2666-2669. <https://doi.org/10.1128/AAC.01743-09>
- De Nardo, D., Balka, K. R., Cardona Gloria, Y., Rao, V. R., Latz, E., & Masters, S. L. (2018). Interleukin-1 receptor-associated kinase 4 (IRAK4) plays a dual role in myddosome formation and Toll-like receptor signaling. *J Biol Chem*, *293*(39), 15195-15207. <https://doi.org/10.1074/jbc.RA118.003314>
- Deane, J. E., Roversi, P., Cordes, F. S., Johnson, S., Kenjale, R., Daniell, S., Booy, F., Picking, W. D., Picking, W. L., Blocker, A. J., & Lea, S. M. (2006). Molecular model of a type III secretion system needle: Implications for host-cell sensing. *Proc Natl Acad Sci U S A*, *103*(33), 12529-12533. <https://doi.org/10.1073/pnas.0602689103>
- Deshpande, D., Chhugani, K., Chang, Y., Karlsberg, A., Loeffler, C., Zhang, J., Muszynska, A., Munteanu, V., Yang, H., Rotman, J., Tao, L., Balliu, B., Tseng, E., Eskin, E., Zhao, F., Mohammadi, P., P, P. L., & Mangul, S. (2023). RNA-seq data science: From raw data to effective interpretation. *Front Genet*, *14*, 997383. <https://doi.org/10.3389/fgene.2023.997383>

- Dewar, S., Reed, L. C., & Koerner, R. J. (2014). Emerging clinical role of pivmecillinam in the treatment of urinary tract infection in the context of multidrug-resistant bacteria. *J Antimicrob Chemother*, *69*(2), 303-308. <https://doi.org/10.1093/jac/dkt368>
- Dixit, A., Bottek, J., Beerlage, A. L., Schuettpeitz, J., Thiebes, S., Brenzel, A., Garbers, C., Rose-John, S., Mittrucker, H. W., Squire, A., & Engel, D. R. (2018). Frontline Science: Proliferation of Ly6C(+) monocytes during urinary tract infections is regulated by IL-6 trans-signaling. *J Leukoc Biol*, *103*(1), 13-22. <https://doi.org/10.1189/jlb.3HI0517-198R>
- Donnenberg, M. S., Zhang, H. Z., & Stone, K. D. (1997). Biogenesis of the bundle-forming pilus of enteropathogenic Escherichia coli: reconstitution of fimbriae in recombinant E. coli and role of DsbA in pilin stability--a review. *Gene*, *192*(1), 33-38. [https://doi.org/10.1016/s0378-1119\(96\)00826-8](https://doi.org/10.1016/s0378-1119(96)00826-8)
- Drage, L. K. L., Robson, W., Mowbray, C., Ali, A., Perry, J. D., Walton, K. E., Harding, C., Pickard, R., Hall, J., & Aldridge, P. D. (2019). Elevated urine IL-10 concentrations associate with Escherichia coli persistence in older patients susceptible to recurrent urinary tract infections. *Immun Ageing*, *16*, 16. <https://doi.org/10.1186/s12979-019-0156-9>
- Dudley, E. G., Abe, C., Ghigo, J. M., Latour-Lambert, P., Hormazabal, J. C., & Nataro, J. P. (2006). An Inc11 plasmid contributes to the adherence of the atypical enteroaggregative Escherichia coli strain C1096 to cultured cells and abiotic surfaces. *Infect Immun*, *74*(4), 2102-2114. <https://doi.org/10.1128/IAI.74.4.2102-2114.2006>
- Eaton, K. A., Friedman, D. I., Francis, G. J., Tyler, J. S., Young, V. B., Haeger, J., Abu-Ali, G., & Whittam, T. S. (2008). Pathogenesis of renal disease due to enterohemorrhagic Escherichia coli in germ-free mice. *Infect Immun*, *76*(7), 3054-3063. <https://doi.org/10.1128/IAI.01626-07>
- Ebrahim, H. (2019). *Pseudomonas aeruginosa Pathogenesis in Urinary Tract Infections* [Doctor in Philosophy, University of Liverpool].
- Eckhard, U., Blochl, C., Jenkins, B. G. L., Mansfield, M. J., Huber, C. G., Doxey, A. C., & Brandstetter, H. (2020). Identification and characterization of the proteolytic flagellin from the common freshwater bacterium Hylemonella gracilis. *Sci Rep*, *10*(1), 19052. <https://doi.org/10.1038/s41598-020-76010-8>
- Evans, L. D., Stafford, G. P., Ahmed, S., Fraser, G. M., & Hughes, C. (2006). An escort mechanism for cycling of export chaperones during flagellum assembly. *Proc Natl Acad Sci U S A*, *103*(46), 17474-17479. <https://doi.org/10.1073/pnas.0605197103>
- Fang, J., Ou, Q., Wu, B., Li, S., Wu, M., Qiu, J., Cen, N., Hu, K., Che, Y., Ma, Y., & Pan, J. (2022). TspC Inhibits M1 but Promotes M2 Macrophage Polarization via Regulation of the MAPK/NF-kappaB and Akt/STAT6 Pathways in Urinary Tract Infection. *Cells*, *11*(17). <https://doi.org/10.3390/cells11172674>
- Farfan, M. J., & Torres, A. G. (2012). Molecular mechanisms that mediate colonization of Shiga toxin-producing Escherichia coli strains. *Infect Immun*, *80*(3), 903-913. <https://doi.org/10.1128/IAI.05907-11>
- Flores-Mireles, A. L., Walker, J. N., Caparon, M., & Hultgren, S. J. (2015). Urinary tract infections: epidemiology, mechanisms of infection and treatment options. *Nat Rev Microbiol*, *13*(5), 269-284. <https://doi.org/10.1038/nrmicro3432>
- Forsyth, V. S., Armbruster, C. E., Smith, S. N., Pirani, A., Springman, A. C., Walters, M. S., Nielubowicz, G. R., Himpsl, S. D., Snitkin, E. S., & Mobley, H. L. T. (2018). Rapid Growth of Uropathogenic Escherichia coli during Human Urinary Tract Infection. *mBio*, *9*(2). <https://doi.org/10.1128/mBio.00186-18>
- Foxman, B. (2002). Epidemiology of urinary tract infections: incidence, morbidity, and economic costs. *Am J Med*, *113 Suppl 1A*, 5S-13S. [https://doi.org/10.1016/s0002-9343\(02\)01054-9](https://doi.org/10.1016/s0002-9343(02)01054-9)
- Foxman, B., & Brown, P. (2003). Epidemiology of urinary tract infections: transmission and risk factors, incidence, and costs. *Infect Dis Clin North Am*, *17*(2), 227-241. [https://doi.org/10.1016/s0891-5520\(03\)00005-9](https://doi.org/10.1016/s0891-5520(03)00005-9)

- Foxman, B., Klemstine, K. L., & Brown, P. D. (2003). Acute pyelonephritis in US hospitals in 1997: hospitalization and in-hospital mortality. *Ann Epidemiol*, *13*(2), 144-150. [https://doi.org/10.1016/s1047-2797\(02\)00272-7](https://doi.org/10.1016/s1047-2797(02)00272-7)
- Fraser, G. M., Bennett, J. C., & Hughes, C. (1999). Substrate-specific binding of hook-associated proteins by FlgN and FliT, putative chaperones for flagellum assembly. *Mol Microbiol*, *32*(3), 569-580. <https://doi.org/10.1046/j.1365-2958.1999.01372.x>
- Freundus, B., Godaly, G., Hang, L., Karpman, D., Lundstedt, A. C., & Svanborg, C. (2000). Interleukin 8 receptor deficiency confers susceptibility to acute experimental pyelonephritis and may have a human counterpart. *J Exp Med*, *192*(6), 881-890. <https://doi.org/10.1084/jem.192.6.881>
- Freundus, B., Wachtler, C., Hedlund, M., Fischer, H., Samuelsson, P., Svensson, M., & Svanborg, C. (2001). Escherichia coli P fimbriae utilize the Toll-like receptor 4 pathway for cell activation. *Mol Microbiol*, *40*(1), 37-51. <https://doi.org/10.1046/j.1365-2958.2001.02361.x>
- Friedman, M. (1999). Chemistry, nutrition, and microbiology of D-amino acids. *J Agric Food Chem*, *47*(9), 3457-3479. <https://doi.org/10.1021/jf990080u>
- Garcia, E. C., Brumbaugh, A. R., & Mobley, H. L. (2011). Redundancy and specificity of Escherichia coli iron acquisition systems during urinary tract infection. *Infect Immun*, *79*(3), 1225-1235. <https://doi.org/10.1128/IAI.01222-10>
- Gewirtz, A. T., Navas, T. A., Lyons, S., Godowski, P. J., & Madara, J. L. (2001). Cutting edge: bacterial flagellin activates basolaterally expressed TLR5 to induce epithelial proinflammatory gene expression. *J Immunol*, *167*(4), 1882-1885. <https://doi.org/10.4049/jimmunol.167.4.1882>
- Gibson, B., Wilson, D. J., Feil, E., & Eyre-Walker, A. (2018). The distribution of bacterial doubling times in the wild. *Proc Biol Sci*, *285*(1880). <https://doi.org/10.1098/rspb.2018.0789>
- Gillen, K. L., & Hughes, K. T. (1991). Molecular characterization of flgM, a gene encoding a negative regulator of flagellin synthesis in Salmonella typhimurium. *J Bacteriol*, *173*(20), 6453-6459. <https://doi.org/10.1128/jb.173.20.6453-6459.1991>
- Giron, J. A., Torres, A. G., Freer, E., & Kaper, J. B. (2002). The flagella of enteropathogenic Escherichia coli mediate adherence to epithelial cells. *Mol Microbiol*, *44*(2), 361-379. <https://doi.org/10.1046/j.1365-2958.2002.02899.x>
- Gobert, A. P., Varelle, M., Glasser, A. L., Hindre, T., de Sablet, T., & Martin, C. (2007). Shiga toxin produced by enterohemorrhagic Escherichia coli inhibits PI3K/NF-kappaB signaling pathway in globotriaosylceramide-3-negative human intestinal epithelial cells. *J Immunol*, *178*(12), 8168-8174. <https://doi.org/10.4049/jimmunol.178.12.8168>
- Goldberg, A. L. (1992). The mechanism and functions of ATP-dependent proteases in bacterial and animal cells. *Eur J Biochem*, *203*(1-2), 9-23. <https://doi.org/10.1111/j.1432-1033.1992.tb19822.x>
- Gondane, A., & Itkonen, H. M. (2023). Revealing the History and Mystery of RNA-Seq. *Curr Issues Mol Biol*, *45*(3), 1860-1874. <https://doi.org/10.3390/cimb45030120>
- Gonzalez, C. M., & Schaeffer, A. J. (1999). Treatment of urinary tract infection: what's old, what's new, and what works. *World J Urol*, *17*(6), 372-382. <https://doi.org/10.1007/s003450050163>
- Goodier, R. I., & Ahmer, B. M. (2001). SirA orthologs affect both motility and virulence. *J Bacteriol*, *183*(7), 2249-2258. <https://doi.org/10.1128/JB.183.7.2249-2258.2001>
- Gottesman, S., Clark, W. P., de Crecy-Lagard, V., & Maurizi, M. R. (1993). ClpX, an alternative subunit for the ATP-dependent Clp protease of Escherichia coli. Sequence and in vivo activities. *J Biol Chem*, *268*(30), 22618-22626. <https://www.ncbi.nlm.nih.gov/pubmed/8226770>
- Graninger, W. (2003). Pivmecillinam--therapy of choice for lower urinary tract infection. *Int J Antimicrob Agents*, *22 Suppl 2*, 73-78. [https://doi.org/10.1016/s0924-8579\(03\)00235-8](https://doi.org/10.1016/s0924-8579(03)00235-8)
- Gunther, N. W. t., Lockatell, V., Johnson, D. E., & Mobley, H. L. (2001). In vivo dynamics of type 1 fimbria regulation in uropathogenic Escherichia coli during experimental urinary tract infection. *Infect Immun*, *69*(5), 2838-2846. <https://doi.org/10.1128/IAI.69.5.2838-2846.2001>

- Hacker, H., Redecke, V., Blagoev, B., Kratchmarova, I., Hsu, L. C., Wang, G. G., Kamps, M. P., Raz, E., Wagner, H., Hacker, G., Mann, M., & Karin, M. (2006). Specificity in Toll-like receptor signalling through distinct effector functions of TRAF3 and TRAF6. *Nature*, *439*(7073), 204-207. <https://doi.org/10.1038/nature04369>
- Hadjidemetriou, K., Kaur, S., Cassidy, C. K., & Zhang, P. (2022). Mechanisms of E. coli chemotaxis signaling pathways visualized using cryoET and computational approaches. *Biochem Soc Trans*, *50*(6), 1595-1605. <https://doi.org/10.1042/BST20220191>
- Hagan, E. C., Lloyd, A. L., Rasko, D. A., Faerber, G. J., & Mobley, H. L. (2010). Escherichia coli global gene expression in urine from women with urinary tract infection. *PLoS Pathog*, *6*(11), e1001187. <https://doi.org/10.1371/journal.ppat.1001187>
- Hajam, I. A., Dar, P. A., Shahnawaz, I., Jaume, J. C., & Lee, J. H. (2017). Bacterial flagellin-a potent immunomodulatory agent. *Exp Mol Med*, *49*(9), e373. <https://doi.org/10.1038/emm.2017.172>
- Hakansson, S., Schesser, K., Persson, C., Galyov, E. E., Rosqvist, R., Homble, F., & Wolf-Watz, H. (1996). The YopB protein of Yersinia pseudotuberculosis is essential for the translocation of Yop effector proteins across the target cell plasma membrane and displays a contact-dependent membrane disrupting activity. *EMBO J*, *15*(21), 5812-5823. <https://www.ncbi.nlm.nih.gov/pubmed/8918459>
- Hang, L., Haraoka, M., Agace, W. W., Leffler, H., Burdick, M., Strieter, R., & Svanborg, C. (1999). Macrophage inflammatory protein-2 is required for neutrophil passage across the epithelial barrier of the infected urinary tract. *J Immunol*, *162*(5), 3037-3044. <https://www.ncbi.nlm.nih.gov/pubmed/10072556>
- Hannan, T. J., & Hunstad, D. A. (2016). A Murine Model for Escherichia coli Urinary Tract Infection. *Methods Mol Biol*, *1333*, 159-175. https://doi.org/10.1007/978-1-4939-2854-5_14
- Harding, C., Chadwick, T., Homer, T., Lecouturier, J., Mossop, H., Carnell, S., King, W., Abouhajar, A., Vale, L., Watson, G., Forbes, R., Curren, S., Pickard, R., Eardley, I., Pearce, I., Thiruchelvam, N., Guerrero, K., Walton, K., Hussain, Z., Lazarowicz, H., & Ali, A. (2022). Methenamine hippurate compared with antibiotic prophylaxis to prevent recurrent urinary tract infections in women: the ALTAR non-inferiority RCT. *Health Technol Assess*, *26*(23), 1-172. <https://doi.org/10.3310/QOIZ6538>
- Hasandka, A., Singh, A. R., Prabhu, A., Singhal, H. R., Nandagopal, M. S. G., & Mani, N. K. (2022). Paper and thread as media for the frugal detection of urinary tract infections (UTIs). *Anal Bioanal Chem*, *414*(2), 847-865. <https://doi.org/10.1007/s00216-021-03671-3>
- Hawn, T. R., Scholes, D., Li, S. S., Wang, H., Yang, Y., Roberts, P. L., Stapleton, A. E., Janer, M., Aderem, A., Stamm, W. E., Zhao, L. P., & Hooton, T. M. (2009). Toll-like receptor polymorphisms and susceptibility to urinary tract infections in adult women. *PLoS One*, *4*(6), e5990. <https://doi.org/10.1371/journal.pone.0005990>
- Hawn, T. R., Scholes, D., Wang, H., Li, S. S., Stapleton, A. E., Janer, M., Aderem, A., Stamm, W. E., Zhao, L. P., & Hooton, T. M. (2009). Genetic variation of the human urinary tract innate immune response and asymptomatic bacteriuria in women. *PLoS One*, *4*(12), e8300. <https://doi.org/10.1371/journal.pone.0008300>
- Hayashi, F., Smith, K. D., Ozinsky, A., Hawn, T. R., Yi, E. C., Goodlett, D. R., Eng, J. K., Akira, S., Underhill, D. M., & Aderem, A. (2001). The innate immune response to bacterial flagellin is mediated by Toll-like receptor 5. *Nature*, *410*(6832), 1099-1103. <https://doi.org/10.1038/35074106>
- Hazen, T. H., Leonard, S. R., Lampel, K. A., Lacher, D. W., Maurelli, A. T., & Rasko, D. A. (2016). Investigating the Relatedness of Enteroinvasive Escherichia coli to Other E. coli and Shigella Isolates by Using Comparative Genomics. *Infect Immun*, *84*(8), 2362-2371. <https://doi.org/10.1128/IAI.00350-16>
- He, X. R., Chen, P. Y., Wang, T., Xie, Z. D., Hu, J. T., Bo, T., & Ge, J. F. (2009). [Comparison of therapeutic effect of different doses of ganciclovir for neonatal congenital cytomegalovirus

- infection]. *Zhongguo Dang Dai Er Ke Za Zhi*, 11(8), 641-644.
<https://www.ncbi.nlm.nih.gov/pubmed/19695189>
- Hedges, S., Agace, W., Svensson, M., Sjogren, A. C., Ceska, M., & Svanborg, C. (1994). Uroepithelial cells are part of a mucosal cytokine network. *Infect Immun*, 62(6), 2315-2321.
<https://doi.org/10.1128/iai.62.6.2315-2321.1994>
- Heinz, J., Rover, C., Furaijat, G., Kaussner, Y., Hummers, E., Debray, T., Hay, A. D., Heytens, S., Vik, I., Little, P., Moore, M., Stuart, B., Wagenlehner, F., Kronenberg, A., Ferry, S., Monsen, T., Lindbaek, M., Friede, T., & Gagyor, I. (2020). Strategies to reduce antibiotic use in women with uncomplicated urinary tract infection in primary care: protocol of a systematic review and meta-analysis including individual patient data. *BMJ Open*, 10(10), e035883.
<https://doi.org/10.1136/bmjopen-2019-035883>
- Helmann, J. D., & Chamberlin, M. J. (1987). DNA sequence analysis suggests that expression of flagellar and chemotaxis genes in *Escherichia coli* and *Salmonella typhimurium* is controlled by an alternative sigma factor. *Proc Natl Acad Sci U S A*, 84(18), 6422-6424.
<https://doi.org/10.1073/pnas.84.18.6422>
- Henderson, J. P., Crowley, J. R., Pinkner, J. S., Walker, J. N., Tsukayama, P., Stamm, W. E., Hooton, T. M., & Hultgren, S. J. (2009). Quantitative metabolomics reveals an epigenetic blueprint for iron acquisition in uropathogenic *Escherichia coli*. *PLoS Pathog*, 5(2), e1000305.
<https://doi.org/10.1371/journal.ppat.1000305>
- Hickling, D. R., Sun, T. T., & Wu, X. R. (2015). Anatomy and Physiology of the Urinary Tract: Relation to Host Defense and Microbial Infection. *Microbiol Spectr*, 3(4).
<https://doi.org/10.1128/microbiolspec.UTI-0016-2012>
- Hogins, J., Xuan, Z., Zimmern, P. E., & Reitzer, L. (2023). The distinct transcriptome of virulence-associated phylogenetic group B2 *Escherichia coli*. *Microbiol Spectr*, 11(5), e0208523.
<https://doi.org/10.1128/spectrum.02085-23>
- Holmstrom, A., Olsson, J., Cherepanov, P., Maier, E., Nordfelth, R., Pettersson, J., Benz, R., Wolf-Watz, H., & Forsberg, A. (2001). LcrV is a channel size-determining component of the Yop effector translocon of *Yersinia*. *Mol Microbiol*, 39(3), 620-632.
<https://doi.org/10.1046/j.1365-2958.2001.02259.x>
- Homma, M., Kutsukake, K., Iino, T., & Yamaguchi, S. (1984). Hook-associated proteins essential for flagellar filament formation in *Salmonella typhimurium*. *J Bacteriol*, 157(1), 100-108.
<https://doi.org/10.1128/jb.157.1.100-108.1984>
- Hooton, T. M., Bradley, S. F., Cardenas, D. D., Colgan, R., Geerlings, S. E., Rice, J. C., Saint, S., Schaeffer, A. J., Tambayh, P. A., Tenke, P., Nicolle, L. E., & Infectious Diseases Society of A. (2010). Diagnosis, prevention, and treatment of catheter-associated urinary tract infection in adults: 2009 International Clinical Practice Guidelines from the Infectious Diseases Society of America. *Clin Infect Dis*, 50(5), 625-663. <https://doi.org/10.1086/650482>
- Horsley, H., Dharmasena, D., Malone-Lee, J., & Rohn, J. L. (2018). A urine-dependent human urothelial organoid offers a potential alternative to rodent models of infection. *Sci Rep*, 8(1), 1238. <https://doi.org/10.1038/s41598-018-19690-7>
- Hotinger, J. A., Pendergrass, H. A., & May, A. E. (2021). Molecular Targets and Strategies for Inhibition of the Bacterial Type III Secretion System (T3SS); Inhibitors Directly Binding to T3SS Components. *Biomolecules*, 11(2). <https://doi.org/10.3390/biom11020316>
- Huang, Y., Nishikawa, T., Satoh, K., Iwata, T., Fukushima, T., Santa, T., Homma, H., & Imai, K. (1998). Urinary excretion of D-serine in human: comparison of different ages and species. *Biol Pharm Bull*, 21(2), 156-162. <https://doi.org/10.1248/bpb.21.156>
- Hughes, K. T., Gillen, K. L., Semon, M. J., & Karlinsey, J. E. (1993). Sensing structural intermediates in bacterial flagellar assembly by export of a negative regulator. *Science*, 262(5137), 1277-1280. <https://doi.org/10.1126/science.8235660>

- Ibrahim, A., Musa, B., & Zein, M. (1984). Changes in urinary pH and glomerular filtration rate in partially obstructed canine kidney. *J Urol*, *131*(1), 143-145. [https://doi.org/10.1016/s0022-5347\(17\)50247-5](https://doi.org/10.1016/s0022-5347(17)50247-5)
- Ijaq, J., Chandra, D., Ray, M. K., & Jagannadham, M. V. (2022). Investigating the Functional Role of Hypothetical Proteins From an Antarctic Bacterium *Pseudomonas* sp. Lz4W: Emphasis on Identifying Proteins Involved in Cold Adaptation. *Front Genet*, *13*, 825269. <https://doi.org/10.3389/fgene.2022.825269>
- Imada, K., Minamino, T., Kinoshita, M., Furukawa, Y., & Namba, K. (2010). Structural insight into the regulatory mechanisms of interactions of the flagellar type III chaperone FliT with its binding partners. *Proc Natl Acad Sci U S A*, *107*(19), 8812-8817. <https://doi.org/10.1073/pnas.1001866107>
- Ipe, D. S., & Ulett, G. C. (2016). Evaluation of the in vitro growth of urinary tract infection-causing gram-negative and gram-positive bacteria in a proposed synthetic human urine (SHU) medium. *J Microbiol Methods*, *127*, 164-171. <https://doi.org/10.1016/j.mimet.2016.06.013>
- Jafari, N. V., & Rohn, J. L. (2023). An immunoresponsive three-dimensional urine-tolerant human urothelial model to study urinary tract infection. *Front Cell Infect Microbiol*, *13*, 1128132. <https://doi.org/10.3389/fcimb.2023.1128132>
- Jarvis, K. G., & Kaper, J. B. (1996). Secretion of extracellular proteins by enterohemorrhagic *Escherichia coli* via a putative type III secretion system. *Infect Immun*, *64*(11), 4826-4829. <https://doi.org/10.1128/iai.64.11.4826-4829.1996>
- Jerde, T. J., Bjorling, D. E., Steinberg, H., Warner, T., & Saban, R. (2000). Determination of mouse bladder inflammatory response to *E. coli* lipopolysaccharide. *Urol Res*, *28*(4), 269-273. <https://doi.org/10.1007/s002400000114>
- Jiang, Z., Zhou, X., Li, R., Michal, J. J., Zhang, S., Dodson, M. V., Zhang, Z., & Harland, R. M. (2015). Whole transcriptome analysis with sequencing: methods, challenges and potential solutions. *Cell Mol Life Sci*, *72*(18), 3425-3439. <https://doi.org/10.1007/s00018-015-1934-y>
- Johnson, J. R. (1991). Virulence factors in *Escherichia coli* urinary tract infection. *Clin Microbiol Rev*, *4*(1), 80-128. <https://doi.org/10.1128/CMR.4.1.80>
- Jonas, K., Edwards, A. N., Ahmad, I., Romeo, T., Romling, U., & Melefors, O. (2010). Complex regulatory network encompassing the Csr, c-di-GMP and motility systems of *Salmonella Typhimurium*. *Environ Microbiol*, *12*(2), 524-540. <https://doi.org/10.1111/j.1462-2920.2009.02097.x>
- Josephs-Spaulding, J., Krogh, T. J., Rettig, H. C., Lyng, M., Chkonia, M., Waschina, S., Graspentner, S., Rupp, J., Moller-Jensen, J., & Kaleta, C. (2021). Recurrent Urinary Tract Infections: Unraveling the Complicated Environment of Uncomplicated rUTIs. *Front Cell Infect Microbiol*, *11*, 562525. <https://doi.org/10.3389/fcimb.2021.562525>
- Kaper, J. B., Nataro, J. P., & Mobley, H. L. (2004). Pathogenic *Escherichia coli*. *Nat Rev Microbiol*, *2*(2), 123-140. <https://doi.org/10.1038/nrmicro818>
- Karlinsey, J. E., Tanaka, S., Bettenworth, V., Yamaguchi, S., Boos, W., Aizawa, S. I., & Hughes, K. T. (2000). Completion of the hook-basal body complex of the *Salmonella typhimurium* flagellum is coupled to FlgM secretion and fliC transcription. *Mol Microbiol*, *37*(5), 1220-1231. <https://doi.org/10.1046/j.1365-2958.2000.02081.x>
- Kawai, T., & Akira, S. (2010). The role of pattern-recognition receptors in innate immunity: update on Toll-like receptors. *Nat Immunol*, *11*(5), 373-384. <https://doi.org/10.1038/ni.1863>
- Kawai, T., Sato, S., Ishii, K. J., Coban, C., Hemmi, H., Yamamoto, M., Terai, K., Matsuda, M., Inoue, J., Uematsu, S., Takeuchi, O., & Akira, S. (2004). Interferon-alpha induction through Toll-like receptors involves a direct interaction of IRF7 with MyD88 and TRAF6. *Nat Immunol*, *5*(10), 1061-1068. <https://doi.org/10.1038/ni1118>
- Kessel, M., Maurizi, M. R., Kim, B., Kocsis, E., Trus, B. L., Singh, S. K., & Steven, A. C. (1995). Homology in structural organization between *E. coli* ClpAP protease and the eukaryotic 26 S proteasome. *J Mol Biol*, *250*(5), 587-594. <https://doi.org/10.1006/jmbi.1995.0400>

- Khalil, A., Tullus, K., Bartfai, T., Bakhiet, M., Jaremko, G., & Brauner, A. (2000). Renal cytokine responses in acute Escherichia coli pyelonephritis in IL-6-deficient mice. *Clin Exp Immunol*, 122(2), 200-206. <https://doi.org/10.1046/j.1365-2249.2000.01377.x>
- Kitagawa, R., Takaya, A., & Yamamoto, T. (2011). Dual regulatory pathways of flagellar gene expression by ClpXP protease in enterohaemorrhagic Escherichia coli. *Microbiology (Reading)*, 157(Pt 11), 3094-3103. <https://doi.org/10.1099/mic.0.051151-0>
- Knutton, S., McConnell, M. M., Rowe, B., & McNeish, A. S. (1989). Adhesion and ultrastructural properties of human enterotoxigenic Escherichia coli producing colonization factor antigens III and IV. *Infect Immun*, 57(11), 3364-3371. <https://doi.org/10.1128/iai.57.11.3364-3371.1989>
- Kodner, C. M., & Thomas Gupton, E. K. (2010). Recurrent urinary tract infections in women: diagnosis and management. *Am Fam Physician*, 82(6), 638-643. <https://www.ncbi.nlm.nih.gov/pubmed/20842992>
- Koirala, S., Mears, P., Sim, M., Golding, I., Chemla, Y. R., Aldridge, P. D., & Rao, C. V. (2014). A nutrient-tunable bistable switch controls motility in Salmonella enterica serovar Typhimurium. *mBio*, 5(5), e01611-01614. <https://doi.org/10.1128/mBio.01611-14>
- Koosakulnirand, S., Phokrai, P., Jenjaroen, K., Roberts, R. A., Utaisincharoen, P., Dunachie, S. J., Brett, P. J., Burtnick, M. N., & Chantratita, N. (2018). Immune response to recombinant Burkholderia pseudomallei FliC. *PLoS One*, 13(6), e0198906. <https://doi.org/10.1371/journal.pone.0198906>
- Kubori, T., Matsushima, Y., Nakamura, D., Uralil, J., Lara-Tejero, M., Sukhan, A., Galan, J. E., & Aizawa, S. I. (1998). Supramolecular structure of the Salmonella typhimurium type III protein secretion system. *Science*, 280(5363), 602-605. <https://doi.org/10.1126/science.280.5363.602>
- Kutsukake, K., Ikebe, T., & Yamamoto, S. (1999). Two novel regulatory genes, fliT and fliZ, in the flagellar regulon of Salmonella. *Genes Genet Syst*, 74(6), 287-292. <https://doi.org/10.1266/ggs.74.287>
- Laestadius, A., Richter-Dahlfors, A., & Aperia, A. (2002). Dual effects of Escherichia coli alpha-hemolysin on rat renal proximal tubule cells. *Kidney Int*, 62(6), 2035-2042. <https://doi.org/10.1046/j.1523-1755.2002.00661.x>
- Lane, M. C., Alteri, C. J., Smith, S. N., & Mobley, H. L. (2007). Expression of flagella is coincident with uropathogenic Escherichia coli ascension to the upper urinary tract. *Proc Natl Acad Sci U S A*, 104(42), 16669-16674. <https://doi.org/10.1073/pnas.0607898104>
- Lane, M. C., & Mobley, H. L. (2007). Role of P-fimbrial-mediated adherence in pyelonephritis and persistence of uropathogenic Escherichia coli (UPEC) in the mammalian kidney. *Kidney Int*, 72(1), 19-25. <https://doi.org/10.1038/sj.ki.5002230>
- Lapointe, T. K., O'Connor, P. M., & Buret, A. G. (2009). The role of epithelial malfunction in the pathogenesis of enteropathogenic E. coli-induced diarrhea. *Lab Invest*, 89(9), 964-970. <https://doi.org/10.1038/labinvest.2009.69>
- Le Bouguenec, C., & Servin, A. L. (2006). Diffusely adherent Escherichia coli strains expressing Afa/Dr adhesins (Afa/Dr DAEC): hitherto unrecognized pathogens. *FEMS Microbiol Lett*, 256(2), 185-194. <https://doi.org/10.1111/j.1574-6968.2006.00144.x>
- Lecky, D. M., Howdle, J., Butler, C. C., & McNulty, C. A. (2020). Optimising management of UTIs in primary care: a qualitative study of patient and GP perspectives to inform the development of an evidence-based, shared decision-making resource. *Br J Gen Pract*, 70(694), e330-e338. <https://doi.org/10.3399/bjgp20X708173>
- Li, D., & Wu, M. (2021). Pattern recognition receptors in health and diseases. *Signal Transduct Target Ther*, 6(1), 291. <https://doi.org/10.1038/s41392-021-00687-0>
- Li, H., Zhou, X., Huang, Y., Liao, B., Cheng, L., & Ren, B. (2020). Reactive Oxygen Species in Pathogen Clearance: The Killing Mechanisms, the Adaption Response, and the Side Effects. *Front Microbiol*, 11, 622534. <https://doi.org/10.3389/fmicb.2020.622534>

- Liu, X., & Matsumura, P. (1994). The FlhD/FlhC complex, a transcriptional activator of the Escherichia coli flagellar class II operons. *J Bacteriol*, *176*(23), 7345-7351. <https://doi.org/10.1128/jb.176.23.7345-7351.1994>
- Liu, X., & Matsumura, P. (1995). An alternative sigma factor controls transcription of flagellar class-III operons in Escherichia coli: gene sequence, overproduction, purification and characterization. *Gene*, *164*(1), 81-84. [https://doi.org/10.1016/0378-1119\(95\)00480-t](https://doi.org/10.1016/0378-1119(95)00480-t)
- Liu, Y., Zhang, D. F., Zhou, X., Xu, L., Zhang, L., & Shi, X. (2017). Comprehensive Analysis Reveals Two Distinct Evolution Patterns of Salmonella Flagellin Gene Clusters. *Front Microbiol*, *8*, 2604. <https://doi.org/10.3389/fmicb.2017.02604>
- Lloyd, S. A., Tang, H., Wang, X., Billings, S., & Blair, D. F. (1996). Torque generation in the flagellar motor of Escherichia coli: evidence of a direct role for FliG but not for FliM or FliN. *J Bacteriol*, *178*(1), 223-231. <https://doi.org/10.1128/jb.178.1.223-231.1996>
- Lopes, J. G., & Sourjik, V. (2018). Chemotaxis of Escherichia coli to major hormones and polyamines present in human gut. *ISME J*, *12*(11), 2736-2747. <https://doi.org/10.1038/s41396-018-0227-5>
- Lukjancenko, O., Wassenaar, T. M., & Ussery, D. W. (2010). Comparison of 61 sequenced Escherichia coli genomes. *Microb Ecol*, *60*(4), 708-720. <https://doi.org/10.1007/s00248-010-9717-3>
- M. L. Lanz, P. A., C. Birchall, A. Ali, C. Townes, K. Walton, L. Y. Lim, R. S. Pickard, J. Hall. (2013). Comparison of the motility and NF-Kappab activating properties of clinical isolates associated with urinary tract infections. Annual Meeting of the Society of Academic and Research Surgery,
- Macnab, R. M. (1999). The bacterial flagellum: reversible rotary propellor and type III export apparatus. *J Bacteriol*, *181*(23), 7149-7153. <https://doi.org/10.1128/JB.181.23.7149-7153.1999>
- Macnab, R. M. (2003). How bacteria assemble flagella. *Annu Rev Microbiol*, *57*, 77-100. <https://doi.org/10.1146/annurev.micro.57.030502.090832>
- Magill, S. S., Edwards, J. R., Bamberg, W., Beldavs, Z. G., Dumyati, G., Kainer, M. A., Lynfield, R., Maloney, M., McAllister-Hollod, L., Nadle, J., Ray, S. M., Thompson, D. L., Wilson, L. E., Fridkin, S. K., Emerging Infections Program Healthcare-Associated, I., & Antimicrobial Use Prevalence Survey, T. (2014). Multistate point-prevalence survey of health care-associated infections. *N Engl J Med*, *370*(13), 1198-1208. <https://doi.org/10.1056/NEJMoa1306801>
- Mahlich, Y., Zhu, C., Chung, H., Velaga, P. K., De Paolis Kaluza, M. C., Radivojac, P., Friedberg, I., & Bromberg, Y. (2023). Learning from the unknown: exploring the range of bacterial functionality. *Nucleic Acids Res*, *51*(19), 10162-10175. <https://doi.org/10.1093/nar/gkad757>
- Maki-Yonekura, S., Yonekura, K., & Namba, K. (2010). Conformational change of flagellin for polymorphic supercoiling of the flagellar filament. *Nat Struct Mol Biol*, *17*(4), 417-422. <https://doi.org/10.1038/nsmb.1774>
- Mann, R., Mediati, D. G., Duggin, I. G., Harry, E. J., & Bottomley, A. L. (2017). Metabolic Adaptations of Uropathogenic E. coli in the Urinary Tract. *Front Cell Infect Microbiol*, *7*, 241. <https://doi.org/10.3389/fcimb.2017.00241>
- Martinvalet, D., & Walch, M. (2021). Editorial: The Role of Reactive Oxygen Species in Protective Immunity. *Front Immunol*, *12*, 832946. <https://doi.org/10.3389/fimmu.2021.832946>
- Masters, J. R., Hepburn, P. J., Walker, L., Highman, W. J., Trejdosiewicz, L. K., Povey, S., Parkar, M., Hill, B. T., Riddle, P. R., & Franks, L. M. (1986). Tissue culture model of transitional cell carcinoma: characterization of twenty-two human urothelial cell lines. *Cancer Res*, *46*(7), 3630-3636. <https://www.ncbi.nlm.nih.gov/pubmed/3708594>
- McSorley, S. J., Cookson, B. T., & Jenkins, M. K. (2000). Characterization of CD4+ T cell responses during natural infection with Salmonella typhimurium. *J Immunol*, *164*(2), 986-993. <https://doi.org/10.4049/jimmunol.164.2.986>

- McSorley, S. J., & Jenkins, M. K. (2000). Antibody is required for protection against virulent but not attenuated *Salmonella enterica* serovar typhimurium. *Infect Immun*, *68*(6), 3344-3348. <https://doi.org/10.1128/IAI.68.6.3344-3348.2000>
- Mediati, D. G., Blair, T. A., Costas, A., Monahan, L. G., Soderstrom, B., Charles, I. G., & Duggin, I. G. (2024). Genetic requirements for uropathogenic *E. coli* proliferation in the bladder cell infection cycle. *mSystems*, e0038724. <https://doi.org/10.1128/msystems.00387-24>
- Meza-Segura, M., Zaidi, M. B., Vera-Ponce de Leon, A., Moran-Garcia, N., Martinez-Romero, E., Nataro, J. P., & Estrada-Garcia, T. (2020). New Insights Into DAEC and EAEC Pathogenesis and Phylogeny. *Front Cell Infect Microbiol*, *10*, 572951. <https://doi.org/10.3389/fcimb.2020.572951>
- Micali, S., Isgro, G., Bianchi, G., Miceli, N., Calapai, G., & Navarra, M. (2014). Cranberry and recurrent cystitis: more than marketing? *Crit Rev Food Sci Nutr*, *54*(8), 1063-1075. <https://doi.org/10.1080/10408398.2011.625574>
- Minamino, T., & Namba, K. (2008). Distinct roles of the FliI ATPase and proton motive force in bacterial flagellar protein export. *Nature*, *451*(7177), 485-488. <https://doi.org/10.1038/nature06449>
- Morris, G., Gevezova, M., Sarafian, V., & Maes, M. (2022). Redox regulation of the immune response. *Cell Mol Immunol*, *19*(10), 1079-1101. <https://doi.org/10.1038/s41423-022-00902-0>
- Mowbray, C., Tan, A., Vallee, M., Fisher, H., Chadwick, T., Brennand, C., Walton, K. E., Pickard, R. S., Harding, C., Aldridge, P. D., & Hall, J. (2022). Multidrug-resistant Uro-associated *Escherichia coli* Populations and Recurrent Urinary Tract Infections in Patients Performing Clean Intermittent Self-catheterisation. *Eur Urol Open Sci*, *37*, 90-98. <https://doi.org/10.1016/j.euro.2021.12.015>
- Mowbray, C. A., Shams, S., Chung, G., Stanton, A., Aldridge, P., Suchenko, A., Pickard, R. S., Ali, A. S., & Hall, J. (2018). High molecular weight hyaluronic acid: a two-pronged protectant against infection of the urogenital tract? *Clin Transl Immunology*, *7*(6), e1021. <https://doi.org/10.1002/cti2.1021>
- Mueller, M., & Tainter, C. R. (2023). *Escherichia coli* Infection. In *StatPearls*. <https://www.ncbi.nlm.nih.gov/pubmed/33231968>
- Mulvey, M. A., Lopez-Boado, Y. S., Wilson, C. L., Roth, R., Parks, W. C., Heuser, J., & Hultgren, S. J. (1998). Induction and evasion of host defenses by type 1-piliated uropathogenic *Escherichia coli*. *Science*, *282*(5393), 1494-1497. <https://doi.org/10.1126/science.282.5393.1494>
- Murray, B. O., Flores, C., Williams, C., Flusberg, D. A., Marr, E. E., Kwiatkowska, K. M., Charest, J. L., Isenberg, B. C., & Rohn, J. L. (2021). Recurrent Urinary Tract Infection: A Mystery in Search of Better Model Systems. *Front Cell Infect Microbiol*, *11*, 691210. <https://doi.org/10.3389/fcimb.2021.691210>
- Mylotte, J. M. (2005). Nursing home-acquired bloodstream infection. *Infect Control Hosp Epidemiol*, *26*(10), 833-837. <https://doi.org/10.1086/502502>
- Nambu, T., Minamino, T., Macnab, R. M., & Kutsukake, K. (1999). Peptidoglycan-hydrolyzing activity of the FlgJ protein, essential for flagellar rod formation in *Salmonella typhimurium*. *J Bacteriol*, *181*(5), 1555-1561. <https://doi.org/10.1128/JB.181.5.1555-1561.1999>
- Nataro, J. P., & Kaper, J. B. (1998). Diarrheagenic *Escherichia coli*. *Clin Microbiol Rev*, *11*(1), 142-201. <https://doi.org/10.1128/CMR.11.1.142>
- Navarro-Garcia, F., & Elias, W. P. (2011). Autotransporters and virulence of enteroaggregative *E. coli*. *Gut Microbes*, *2*(1), 13-24. <https://doi.org/10.4161/gmic.2.1.14933>
- Nedeljkovic, M., Sastre, D. E., & Sundberg, E. J. (2021). Bacterial Flagellar Filament: A Supramolecular Multifunctional Nanostructure. *Int J Mol Sci*, *22*(14). <https://doi.org/10.3390/ijms22147521>
- NICE, N. I. f. H. a. C. E. (2018). *Urinary tract infection (lower): antimicrobial prescribing*. <https://www.nice.org.uk/guidance/ng109>
- NICE, N. I. f. H. a. C. E. (2021). *British National Formulary*. B. G. a. P. Press.

- Nickel, J. C., & Doiron, R. C. (2023). An Effective Sublingual Vaccine, MV140, Safely Reduces Risk of Recurrent Urinary Tract Infection in Women. *Pathogens*, *12*(3).
<https://doi.org/10.3390/pathogens12030359>
- Nicolle, L. E. (2014). Catheter associated urinary tract infections. *Antimicrob Resist Infect Control*, *3*, 23. <https://doi.org/10.1186/2047-2994-3-23>
- Nowicki, B., Selvarangan, R., & Nowicki, S. (2001). Family of Escherichia coli Dr adhesins: decay-accelerating factor receptor recognition and invasiveness. *J Infect Dis*, *183 Suppl 1*, S24-27.
<https://doi.org/10.1086/318846>
- O'Brien, V. P., Hannan, T. J., Yu, L., Livny, J., Roberson, E. D., Schwartz, D. J., Souza, S., Mendelsohn, C. L., Colonna, M., Lewis, A. L., & Hultgren, S. J. (2016). A mucosal imprint left by prior Escherichia coli bladder infection sensitizes to recurrent disease. *Nat Microbiol*, *2*, 16196.
<https://doi.org/10.1038/nmicrobiol.2016.196>
- O'Neill, L. A., & Bowie, A. G. (2007). The family of five: TIR-domain-containing adaptors in Toll-like receptor signalling. *Nat Rev Immunol*, *7*(5), 353-364. <https://doi.org/10.1038/nri2079>
- O'Neill, L. A., Golenbock, D., & Bowie, A. G. (2013). The history of Toll-like receptors - redefining innate immunity. *Nat Rev Immunol*, *13*(6), 453-460. <https://doi.org/10.1038/nri3446>
- Ohnishi, K., Kutsukake, K., Suzuki, H., & Iino, T. (1990). Gene fliA encodes an alternative sigma factor specific for flagellar operons in Salmonella typhimurium. *Mol Gen Genet*, *221*(2), 139-147.
<https://doi.org/10.1007/BF00261713>
- Ohnishi, K., Ohto, Y., Aizawa, S., Macnab, R. M., & Iino, T. (1994). FlgD is a scaffolding protein needed for flagellar hook assembly in Salmonella typhimurium. *J Bacteriol*, *176*(8), 2272-2281.
<https://doi.org/10.1128/jb.176.8.2272-2281.1994>
- Ortega Martell, J. A. (2020). Immunology of urinary tract infections. *GMS Infect Dis*, *8*, Doc21.
<https://doi.org/10.3205/id000065>
- Ou, Q., Fang, J. Q., Zhang, Z. S., Chi, Z., Fang, J., Xu, D. Y., Lu, K. Z., Qian, M. Q., Zhang, D. Y., Guo, J. P., Gao, W., Zhang, N. R., & Pan, J. P. (2021). TcpC inhibits neutrophil extracellular trap formation by enhancing ubiquitination mediated degradation of peptidylarginine deiminase 4. *Nat Commun*, *12*(1), 3481. <https://doi.org/10.1038/s41467-021-23881-8>
- Owusu-Boaitey, N., Bauckman, K. A., Zhang, T., & Mysorekar, I. U. (2016). Macrophagic control of the response to uropathogenic E. coli infection by regulation of iron retention in an IL-6-dependent manner. *Immun Inflamm Dis*, *4*(4), 413-426. <https://doi.org/10.1002/iid3.123>
- Pfaffl, M. W. (2001). A new mathematical model for relative quantification in real-time RT-PCR. *Nucleic Acids Res*, *29*(9), e45. <https://doi.org/10.1093/nar/29.9.e45>
- Poh, X. E., Wu, K. H., Chen, C. C., Huang, J. B., Cheng, F. J., & Chiu, I. M. (2021). Outcomes for Patients with Urinary Tract Infection After an Initial Intravenous Antibiotics Dose Before Emergency Department Discharge. *Infect Dis Ther*, *10*(3), 1479-1489. <https://doi.org/10.1007/s40121-021-00469-9>
- Popoff, M. Y., Bockemuhl, J., & Brenner, F. W. (2000). Supplement 1998 (no. 42) to the Kauffmann-White scheme. *Res Microbiol*, *151*(1), 63-65. [https://doi.org/10.1016/s0923-2508\(00\)00126-1](https://doi.org/10.1016/s0923-2508(00)00126-1)
- Pruss, B. M., & Matsumura, P. (1996). A regulator of the flagellar regulon of Escherichia coli, flhD, also affects cell division. *J Bacteriol*, *178*(3), 668-674. <https://doi.org/10.1128/jb.178.3.668-674.1996>
- Psotta, C., Nilsson, E. J., Sjoberg, T., & Falk, M. (2023). Bacteria-Infected Artificial Urine Characterization Based on a Combined Approach Using an Electronic Tongue Complemented with (1)H-NMR and Flow Cytometry. *Biosensors (Basel)*, *13*(10).
<https://doi.org/10.3390/bios13100916>
- Qadri, F., Svennerholm, A. M., Faruque, A. S., & Sack, R. B. (2005). Enterotoxigenic Escherichia coli in developing countries: epidemiology, microbiology, clinical features, treatment, and prevention. *Clin Microbiol Rev*, *18*(3), 465-483. <https://doi.org/10.1128/CMR.18.3.465-483.2005>

- Ragnarsdottir, B., Jonsson, K., Urbano, A., Gronberg-Hernandez, J., Lutay, N., Tammi, M., Gustafsson, M., Lundstedt, A. C., Leijonhufvud, I., Karpman, D., Wullt, B., Truedsson, L., Jodal, U., Andersson, B., & Svanborg, C. (2010). Toll-like receptor 4 promoter polymorphisms: common TLR4 variants may protect against severe urinary tract infection. *PLoS One*, *5*(5), e10734. <https://doi.org/10.1371/journal.pone.0010734>
- Ragnarsdottir, B., & Svanborg, C. (2012). Susceptibility to acute pyelonephritis or asymptomatic bacteriuria: host-pathogen interaction in urinary tract infections. *Pediatr Nephrol*, *27*(11), 2017-2029. <https://doi.org/10.1007/s00467-011-2089-1>
- Rao, W. H., Murdoch, C., Johnson, J. R., Evans, G. S., & Finn, A. (2001). Uropathogenic *Escherichia coli*-induced neutrophil adhesion to urinary epithelium is strain-specific and mediated by CD11b/CD18. *Urol Res*, *29*(2), 102-107. <https://doi.org/10.1007/s002400100171>
- Robinson, A. E., Heffernan, J. R., & Henderson, J. P. (2018). The iron hand of uropathogenic *Escherichia coli*: the role of transition metal control in virulence. *Future Microbiol*, *13*(7), 745-756. <https://doi.org/10.2217/fmb-2017-0295>
- Roesch, P. L., Redford, P., Batchelet, S., Moritz, R. L., Pellett, S., Haugen, B. J., Blattner, F. R., & Welch, R. A. (2003). Uropathogenic *Escherichia coli* use d-serine deaminase to modulate infection of the murine urinary tract. *Mol Microbiol*, *49*(1), 55-67. <https://doi.org/10.1046/j.1365-2958.2003.03543.x>
- Rohrwild, M., Coux, O., Huang, H. C., Moerschell, R. P., Yoo, S. J., Seol, J. H., Chung, C. H., & Goldberg, A. L. (1996). HslV-HslU: A novel ATP-dependent protease complex in *Escherichia coli* related to the eukaryotic proteasome. *Proc Natl Acad Sci U S A*, *93*(12), 5808-5813. <https://doi.org/10.1073/pnas.93.12.5808>
- Rosen, D. A., Hooton, T. M., Stamm, W. E., Humphrey, P. A., & Hultgren, S. J. (2007). Detection of intracellular bacterial communities in human urinary tract infection. *PLoS Med*, *4*(12), e329. <https://doi.org/10.1371/journal.pmed.0040329>
- Rosser, C. J., Bare, R. L., & Meredith, J. W. (1999). Urinary tract infections in the critically ill patient with a urinary catheter. *Am J Surg*, *177*(4), 287-290. [https://doi.org/10.1016/s0002-9610\(99\)00048-3](https://doi.org/10.1016/s0002-9610(99)00048-3)
- Russell, S. K., Harrison, J. K., Olson, B. S., Lee, H. J., O'Brien, V. P., Xing, X., Livny, J., Yu, L., Roberson, E. D. O., Bomjan, R., Fan, C., Sha, M., Estfanous, S., Amer, A. O., Colonna, M., Stappenbeck, T. S., Wang, T., Hannan, T. J., & Hultgren, S. J. (2023). Uropathogenic *Escherichia coli* infection-induced epithelial trained immunity impacts urinary tract disease outcome. *Nat Microbiol*, *8*(5), 875-888. <https://doi.org/10.1038/s41564-023-01346-6>
- Russo, T. A., & Johnson, J. R. (2000). Proposal for a new inclusive designation for extraintestinal pathogenic isolates of *Escherichia coli*: ExPEC. *J Infect Dis*, *181*(5), 1753-1754. <https://doi.org/10.1086/315418>
- Sabih, A., & Leslie, S. W. (2021). Complicated Urinary Tract Infections. In *StatPearls*. <https://www.ncbi.nlm.nih.gov/pubmed/28613784>
- Sabih, A., & Leslie, S. W. (2023). Complicated Urinary Tract Infections. In *StatPearls*. <https://www.ncbi.nlm.nih.gov/pubmed/28613784>
- Saini, S., Floess, E., Aldridge, C., Brown, J., Aldridge, P. D., & Rao, C. V. (2011). Continuous control of flagellar gene expression by the sigma28-FlgM regulatory circuit in *Salmonella enterica*. *Mol Microbiol*, *79*(1), 264-278. <https://doi.org/10.1111/j.1365-2958.2010.07444.x>
- Salazar-Gonzalez, R. M., Srinivasan, A., Griffin, A., Muralimohan, G., Ertelt, J. M., Ravindran, R., Vella, A. T., & McSorley, S. J. (2007). *Salmonella* flagellin induces bystander activation of splenic dendritic cells and hinders bacterial replication in vivo. *J Immunol*, *179*(9), 6169-6175. <https://doi.org/10.4049/jimmunol.179.9.6169>
- Sarigul, N., Korkmaz, F., & Kurultak, I. (2019). A New Artificial Urine Protocol to Better Imitate Human Urine. *Sci Rep*, *9*(1), 20159. <https://doi.org/10.1038/s41598-019-56693-4>

- Sato, Y., Takaya, A., Mouslim, C., Hughes, K. T., & Yamamoto, T. (2014). FliT selectively enhances proteolysis of FlhC subunit in FlhD4C2 complex by an ATP-dependent protease, ClpXP. *J Biol Chem*, 289(47), 33001-33011. <https://doi.org/10.1074/jbc.M114.593749>
- Satoh, T., & Akira, S. (2016). Toll-Like Receptor Signaling and Its Inducible Proteins. *Microbiol Spectr*, 4(6). <https://doi.org/10.1128/microbiolspec.MCHD-0040-2016>
- Schilling, J. D., Mulvey, M. A., & Hultgren, S. J. (2001). Structure and function of Escherichia coli type 1 pili: new insight into the pathogenesis of urinary tract infections. *J Infect Dis*, 183 Suppl 1, S36-40. <https://doi.org/10.1086/318855>
- Schreiber, H. L. t., Conover, M. S., Chou, W. C., Hibbing, M. E., Manson, A. L., Dodson, K. W., Hannan, T. J., Roberts, P. L., Stapleton, A. E., Hooton, T. M., Livny, J., Earl, A. M., & Hultgren, S. J. (2017). Bacterial virulence phenotypes of Escherichia coli and host susceptibility determine risk for urinary tract infections. *Sci Transl Med*, 9(382). <https://doi.org/10.1126/scitranslmed.aaf1283>
- Schroeder, G. N., & Hilbi, H. (2008). Molecular pathogenesis of Shigella spp.: controlling host cell signaling, invasion, and death by type III secretion. *Clin Microbiol Rev*, 21(1), 134-156. <https://doi.org/10.1128/CMR.00032-07>
- Selvarangan, R., Goluszko, P., Singhal, J., Carnoy, C., Moseley, S., Hudson, B., Nowicki, S., & Nowicki, B. (2004). Interaction of Dr adhesin with collagen type IV is a critical step in Escherichia coli renal persistence. *Infect Immun*, 72(8), 4827-4835. <https://doi.org/10.1128/IAI.72.8.4827-4835.2004>
- Serrettiello, E., Folliero, V., Santella, B., Giordano, G., Santoro, E., De Caro, F., Pagliano, P., Ferro, M., Aliberti, S. M., Capunzo, M., Galdiero, M., Franci, G., & Boccia, G. (2021). Trend of Bacterial Uropathogens and Their Susceptibility Pattern: Study of Single Academic High-Volume Center in Italy (2015-2019). *Int J Microbiol*, 2021, 5541706. <https://doi.org/10.1155/2021/5541706>
- Servin, A. L. (2005). Pathogenesis of Afa/Dr diffusely adhering Escherichia coli. *Clin Microbiol Rev*, 18(2), 264-292. <https://doi.org/10.1128/CMR.18.2.264-292.2005>
- Shi, W., Kidd, R., Giorgianni, F., Schindler, J. F., Viola, R. E., & Farber, G. K. (1993). Crystallization and preliminary X-ray studies of L-aspartase from Escherichia coli. *J Mol Biol*, 234(4), 1248-1249. <https://doi.org/10.1006/jmbi.1993.1674>
- Sihra, N., Goodman, A., Zakri, R., Sahai, A., & Malde, S. (2018). Nonantibiotic prevention and management of recurrent urinary tract infection. *Nat Rev Urol*, 15(12), 750-776. <https://doi.org/10.1038/s41585-018-0106-x>
- Sim, M., Koirala, S., Picton, D., Strahl, H., Hoskisson, P. A., Rao, C. V., Gillespie, C. S., & Aldridge, P. D. (2017). Growth rate control of flagellar assembly in Escherichia coli strain RP437. *Sci Rep*, 7, 41189. <https://doi.org/10.1038/srep41189>
- Simerville, J. A., Maxted, W. C., & Pahlira, J. J. (2005). Urinalysis: a comprehensive review. *Am Fam Physician*, 71(6), 1153-1162. <https://www.ncbi.nlm.nih.gov/pubmed/15791892>
- Simms, A. N., & Mobley, H. L. (2008). Multiple genes repress motility in uropathogenic Escherichia coli constitutively expressing type 1 fimbriae. *J Bacteriol*, 190(10), 3747-3756. <https://doi.org/10.1128/JB.01870-07>
- Singer, H. M., Erhardt, M., & Hughes, K. T. (2013). RflM functions as a transcriptional repressor in the autogenous control of the Salmonella Flagellar master operon flhDC. *J Bacteriol*, 195(18), 4274-4282. <https://doi.org/10.1128/JB.00728-13>
- Sintsova, A., Frick-Cheng, A. E., Smith, S., Pirani, A., Subashchandrabose, S., Snitkin, E. S., & Mobley, H. (2019). Genetically diverse uropathogenic Escherichia coli adopt a common transcriptional program in patients with UTIs. *Elife*, 8. <https://doi.org/10.7554/eLife.49748>
- Smith, K. D., Andersen-Nissen, E., Hayashi, F., Strobe, K., Bergman, M. A., Barrett, S. L., Cookson, B. T., & Aderem, A. (2003). Toll-like receptor 5 recognizes a conserved site on flagellin required for protofilament formation and bacterial motility. *Nat Immunol*, 4(12), 1247-1253. <https://doi.org/10.1038/ni1011>

- Smith, N. J., Varley, C. L., Eardley, I., Feather, S., Trejdosiewicz, L. K., & Southgate, J. (2011). Toll-like receptor responses of normal human urothelial cells to bacterial flagellin and lipopolysaccharide. *J Urol*, *186*(3), 1084-1092. <https://doi.org/10.1016/j.juro.2011.04.112>
- Song, J., & Abraham, S. N. (2008). TLR-mediated immune responses in the urinary tract. *Curr Opin Microbiol*, *11*(1), 66-73. <https://doi.org/10.1016/j.mib.2007.12.001>
- Soutourina, O. A., Krin, E., Laurent-Winter, C., Hommais, F., Danchin, A., & Bertin, P. N. (2002). Regulation of bacterial motility in response to low pH in *Escherichia coli*: the role of H-NS protein. *Microbiology (Reading)*, *148*(Pt 5), 1543-1551. <https://doi.org/10.1099/00221287-148-5-1543>
- Spencer, J. D., Schwaderer, A. L., Becknell, B., Watson, J., & Hains, D. S. (2014). The innate immune response during urinary tract infection and pyelonephritis. *Pediatr Nephrol*, *29*(7), 1139-1149. <https://doi.org/10.1007/s00467-013-2513-9>
- Stamm, W. E., & Hooton, T. M. (1993). Management of urinary tract infections in adults. *N Engl J Med*, *329*(18), 1328-1334. <https://doi.org/10.1056/NEJM199310283291808>
- Stauffer, C. M., van der Weg, B., Donadini, R., Ramelli, G. P., Marchand, S., & Bianchetti, M. G. (2004). Family history and behavioral abnormalities in girls with recurrent urinary tract infections: a controlled study. *J Urol*, *171*(4), 1663-1665. <https://doi.org/10.1097/01.ju.0000117701.81118.f0>
- Tabel, Y., Berdeli, A., & Mir, S. (2007). Association of TLR2 gene Arg753Gln polymorphism with urinary tract infection in children. *Int J Immunogenet*, *34*(6), 399-405. <https://doi.org/10.1111/j.1744-313X.2007.00709.x>
- Takaya, A., Erhardt, M., Karata, K., Winterberg, K., Yamamoto, T., & Hughes, K. T. (2012). YdiV: a dual function protein that targets FlhDC for ClpXP-dependent degradation by promoting release of DNA-bound FlhDC complex. *Mol Microbiol*, *83*(6), 1268-1284. <https://doi.org/10.1111/j.1365-2958.2012.08007.x>
- Takeuchi, O., & Akira, S. (2010). Pattern recognition receptors and inflammation. *Cell*, *140*(6), 805-820. <https://doi.org/10.1016/j.cell.2010.01.022>
- Tan, A., Alsenani, Q., Lanz, M., Birchall, C., Drage, L. K. L., Picton, D., Mowbray, C., Ali, A., Harding, C., Pickard, R. S., Hall, J., & Aldridge, P. D. (2023). Evasion of toll-like receptor recognition by *Escherichia coli* is mediated via population level regulation of flagellin production. *Front Microbiol*, *14*, 1093922. <https://doi.org/10.3389/fmicb.2023.1093922>
- Tavassolifar, M. J., Vodjgani, M., Salehi, Z., & Izad, M. (2020). The Influence of Reactive Oxygen Species in the Immune System and Pathogenesis of Multiple Sclerosis. *Autoimmune Dis*, *2020*, 5793817. <https://doi.org/10.1155/2020/5793817>
- Tenaillon, O., Skurnik, D., Picard, B., & Denamur, E. (2010). The population genetics of commensal *Escherichia coli*. *Nat Rev Microbiol*, *8*(3), 207-217. <https://doi.org/10.1038/nrmicro2298>
- Thumbikat, P., Berry, R. E., Zhou, G., Billips, B. K., Yaggie, R. E., Zaichuk, T., Sun, T. T., Schaeffer, A. J., & Klumpp, D. J. (2009). Bacteria-induced uroplakin signaling mediates bladder response to infection. *PLoS Pathog*, *5*(5), e1000415. <https://doi.org/10.1371/journal.ppat.1000415>
- Tiba, M. R., Yano, T., & Leite Dda, S. (2008). Genotypic characterization of virulence factors in *Escherichia coli* strains from patients with cystitis. *Rev Inst Med Trop Sao Paulo*, *50*(5), 255-260. <https://doi.org/10.1590/s0036-46652008000500001>
- Tomoyasu, T., Ohkishi, T., Ukyo, Y., Tokumitsu, A., Takaya, A., Suzuki, M., Sekiya, K., Matsui, H., Kutsukake, K., & Yamamoto, T. (2002). The ClpXP ATP-dependent protease regulates flagellum synthesis in *Salmonella enterica* serovar typhimurium. *J Bacteriol*, *184*(3), 645-653. <https://doi.org/10.1128/JB.184.3.645-653.2002>
- Tsujimoto, H., Uchida, T., Efron, P. A., Scumpia, P. O., Verma, A., Matsumoto, T., Tschoeke, S. K., Ungaro, R. F., Ono, S., Seki, S., Clare-Salzler, M. J., Baker, H. V., Mochizuki, H., Ramphal, R., & Moldawer, L. L. (2005). Flagellin enhances NK cell proliferation and activation directly and through dendritic cell-NK cell interactions. *J Leukoc Biol*, *78*(4), 888-897. <https://doi.org/10.1189/jlb.0105051>

- Turner, S. M., Scott-Tucker, A., Cooper, L. M., & Henderson, I. R. (2006). Weapons of mass destruction: virulence factors of the global killer enterotoxigenic *Escherichia coli*. *FEMS Microbiol Lett*, *263*(1), 10-20. <https://doi.org/10.1111/j.1574-6968.2006.00401.x>
- Uehara, A., & Takada, H. (2007). Functional TLRs and NODs in human gingival fibroblasts. *J Dent Res*, *86*(3), 249-254. <https://doi.org/10.1177/154405910708600310>
- Uematsu, S., & Akira, S. (2006). Toll-like receptors and innate immunity. *J Mol Med (Berl)*, *84*(9), 712-725. <https://doi.org/10.1007/s00109-006-0084-y>
- Vallee, M., Harding, C., Hall, J., Aldridge, P. D., & Tan, A. (2023). Exploring the in situ evolution of nitrofurantoin resistance in clinically derived uropathogenic *Escherichia coli* isolates. *J Antimicrob Chemother*, *78*(2), 373-379. <https://doi.org/10.1093/jac/dkac398>
- Vallo, S., Michaelis, M., Rothweiler, F., Bartsch, G., Gust, K. M., Limbart, D. M., Rodel, F., Wezel, F., Haferkamp, A., & Cinatl, J., Jr. (2015). Drug-Resistant Urothelial Cancer Cell Lines Display Diverse Sensitivity Profiles to Potential Second-Line Therapeutics. *Transl Oncol*, *8*(3), 210-216. <https://doi.org/10.1016/j.tranon.2015.04.002>
- Verstak, B., Nagpal, K., Bottomley, S. P., Golenbock, D. T., Hertzog, P. J., & Mansell, A. (2009). MyD88 adapter-like (Mal)/TIRAP interaction with TRAF6 is critical for TLR2- and TLR4-mediated NF-kappaB proinflammatory responses. *J Biol Chem*, *284*(36), 24192-24203. <https://doi.org/10.1074/jbc.M109.023044>
- Vicente-Suarez, I., Brayer, J., Villagra, A., Cheng, F., & Sotomayor, E. M. (2009). TLR5 ligation by flagellin converts tolerogenic dendritic cells into activating antigen-presenting cells that preferentially induce T-helper 1 responses. *Immunol Lett*, *125*(2), 114-118. <https://doi.org/10.1016/j.imlet.2009.06.007>
- von Bernuth, H., Picard, C., Jin, Z., Pankla, R., Xiao, H., Ku, C. L., Chrabieh, M., Mustapha, I. B., Ghandil, P., Camcioglu, Y., Vasconcelos, J., Sirvent, N., Guedes, M., Vitor, A. B., Herrero-Mata, M. J., Arostegui, J. I., Rodrigo, C., Alsina, L., Ruiz-Ortiz, E., Juan, M., Fortuny, C., Yague, J., Anton, J., Pascal, M., Chang, H. H., Janniere, L., Rose, Y., Garty, B. Z., Chapel, H., Issekutz, A., Marodi, L., Rodriguez-Gallego, C., Banchereau, J., Abel, L., Li, X., Chaussabel, D., Puel, A., & Casanova, J. L. (2008). Pyogenic bacterial infections in humans with MyD88 deficiency. *Science*, *321*(5889), 691-696. <https://doi.org/10.1126/science.1158298>
- Wada, T., Hatamoto, Y., & Kutsukake, K. (2012). Functional and expressional analyses of the anti-FlhD4C2 factor gene *ydiV* in *Escherichia coli*. *Microbiology (Reading)*, *158*(Pt 6), 1533-1542. <https://doi.org/10.1099/mic.0.056036-0>
- Wada, T., Morizane, T., Abo, T., Tominaga, A., Inoue-Tanaka, K., & Kutsukake, K. (2011). EAL domain protein *YdiV* acts as an anti-FlhD4C2 factor responsible for nutritional control of the flagellar regulon in *Salmonella enterica* Serovar Typhimurium. *J Bacteriol*, *193*(7), 1600-1611. <https://doi.org/10.1128/JB.01494-10>
- Wada, T., Tanabe, Y., & Kutsukake, K. (2011). *FliZ* acts as a repressor of the *ydiV* gene, which encodes an anti-FlhD4C2 factor of the flagellar regulon in *Salmonella enterica* serovar typhimurium. *J Bacteriol*, *193*(19), 5191-5198. <https://doi.org/10.1128/JB.05441-11>
- Wagenlehner, F. M. E., Bjerklund Johansen, T. E., Cai, T., Koves, B., Kranz, J., Pilatz, A., & Tandogdu, Z. (2020). Epidemiology, definition and treatment of complicated urinary tract infections. *Nat Rev Urol*, *17*(10), 586-600. <https://doi.org/10.1038/s41585-020-0362-4>
- Wang, C., Li, Q., Lv, J., Sun, X., Cao, Y., Yu, K., Miao, C., Zhang, Z. S., Yao, Z., & Wang, Q. (2020). Alpha-hemolysin of uropathogenic *Escherichia coli* induces GM-CSF-mediated acute kidney injury. *Mucosal Immunol*, *13*(1), 22-33. <https://doi.org/10.1038/s41385-019-0225-6>
- Wang, L., Kuang, Z., Zhang, D., Gao, Y., Ying, M., & Wang, T. (2021). Reactive oxygen species in immune cells: A new antitumor target. *Biomed Pharmacother*, *133*, 110978. <https://doi.org/10.1016/j.biopha.2020.110978>
- Wang, L., Rothemund, D., Curd, H., & Reeves, P. R. (2003). Species-wide variation in the *Escherichia coli* flagellin (H-antigen) gene. *J Bacteriol*, *185*(9), 2936-2943. <https://doi.org/10.1128/JB.185.9.2936-2943.2003>

- Wang, S., Fleming, R. T., Westbrook, E. M., Matsumura, P., & McKay, D. B. (2006). Structure of the Escherichia coli FlhDC complex, a prokaryotic heteromeric regulator of transcription. *J Mol Biol*, 355(4), 798-808. <https://doi.org/10.1016/j.jmb.2005.11.020>
- Weichhart, T., Haidinger, M., Horl, W. H., & Saemann, M. D. (2008). Current concepts of molecular defence mechanisms operative during urinary tract infection. *Eur J Clin Invest*, 38 Suppl 2, 29-38. <https://doi.org/10.1111/j.1365-2362.2008.02006.x>
- Welch, A. A., Mulligan, A., Bingham, S. A., & Khaw, K. T. (2008). Urine pH is an indicator of dietary acid-base load, fruit and vegetables and meat intakes: results from the European Prospective Investigation into Cancer and Nutrition (EPIC)-Norfolk population study. *Br J Nutr*, 99(6), 1335-1343. <https://doi.org/10.1017/S0007114507862350>
- Welch, R. A., Burland, V., Plunkett, G., 3rd, Redford, P., Roesch, P., Rasko, D., Buckles, E. L., Liou, S. R., Boutin, A., Hackett, J., Stroud, D., Mayhew, G. F., Rose, D. J., Zhou, S., Schwartz, D. C., Perna, N. T., Mobley, H. L., Donnenberg, M. S., & Blattner, F. R. (2002). Extensive mosaic structure revealed by the complete genome sequence of uropathogenic Escherichia coli. *Proc Natl Acad Sci U S A*, 99(26), 17020-17024. <https://doi.org/10.1073/pnas.252529799>
- Whelan, S., Lucey, B., & Finn, K. (2023). Uropathogenic Escherichia coli (UPEC)-Associated Urinary Tract Infections: The Molecular Basis for Challenges to Effective Treatment. *Microorganisms*, 11(9). <https://doi.org/10.3390/microorganisms11092169>
- Wiles, T. J., Kulesus, R. R., & Mulvey, M. A. (2008). Origins and virulence mechanisms of uropathogenic Escherichia coli. *Exp Mol Pathol*, 85(1), 11-19. <https://doi.org/10.1016/j.yexmp.2008.03.007>
- Woo, K. M., Kim, K. I., Goldberg, A. L., Ha, D. B., & Chung, C. H. (1992). The heat-shock protein ClpB in Escherichia coli is a protein-activated ATPase. *J Biol Chem*, 267(28), 20429-20434. <https://www.ncbi.nlm.nih.gov/pubmed/1400361>
- Wu, X. R., Kong, X. P., Pellicer, A., Kreibich, G., & Sun, T. T. (2009). Uroplakins in urothelial biology, function, and disease. *Kidney Int*, 75(11), 1153-1165. <https://doi.org/10.1038/ki.2009.73>
- Wullt, B., Bergsten, G., Connell, H., Rollano, P., Gebretsadik, N., Hull, R., & Svanborg, C. (2000). P fimbriae enhance the early establishment of Escherichia coli in the human urinary tract. *Mol Microbiol*, 38(3), 456-464. <https://doi.org/10.1046/j.1365-2958.2000.02165.x>
- Yadav, M., Zhang, J., Fischer, H., Huang, W., Lutay, N., Cirl, C., Lum, J., Miethke, T., & Svanborg, C. (2010). Inhibition of TIR domain signaling by TcpC: MyD88-dependent and independent effects on Escherichia coli virulence. *PLoS Pathog*, 6(9), e1001120. <https://doi.org/10.1371/journal.ppat.1001120>
- Yamaguchi, T., Toma, S., Terahara, N., Miyata, T., Ashihara, M., Minamino, T., Namba, K., & Kato, T. (2020). Structural and Functional Comparison of Salmonella Flagellar Filaments Composed of FljB and FliC. *Biomolecules*, 10(2). <https://doi.org/10.3390/biom10020246>
- Yamamoto, S., & Kutsukake, K. (2006). FlIT acts as an anti-FlhD2C2 factor in the transcriptional control of the flagellar regulon in Salmonella enterica serovar typhimurium. *J Bacteriol*, 188(18), 6703-6708. <https://doi.org/10.1128/JB.00799-06>
- Yang, X., Chen, H., Zheng, Y., Qu, S., Wang, H., & Yi, F. (2022). Disease burden and long-term trends of urinary tract infections: A worldwide report. *Front Public Health*, 10, 888205. <https://doi.org/10.3389/fpubh.2022.888205>
- Yonekura, K., Maki, S., Morgan, D. G., DeRosier, D. J., Vonderviszt, F., Imada, K., & Namba, K. (2000). The bacterial flagellar cap as the rotary promoter of flagellin self-assembly. *Science*, 290(5499), 2148-2152. <https://doi.org/10.1126/science.290.5499.2148>
- Zacche, M. M., & Giarenis, I. (2016). Therapies in early development for the treatment of urinary tract inflammation. *Expert Opin Investig Drugs*, 25(5), 531-540. <https://doi.org/10.1517/13543784.2016.1161024>
- Zandbergen, L. E., Halverson, T., Brons, J. K., Wolfe, A. J., & de Vos, M. G. J. (2021). The Good and the Bad: Ecological Interaction Measurements Between the Urinary Microbiota and Uropathogens. *Front Microbiol*, 12, 659450. <https://doi.org/10.3389/fmicb.2021.659450>

- Zasloff, M. (2007). Antimicrobial peptides, innate immunity, and the normally sterile urinary tract. *J Am Soc Nephrol*, 18(11), 2810-2816. <https://doi.org/10.1681/ASN.2007050611>
- Zhang, B., Ramesh, G., Uematsu, S., Akira, S., & Reeves, W. B. (2008). TLR4 signaling mediates inflammation and tissue injury in nephrotoxicity. *J Am Soc Nephrol*, 19(5), 923-932. <https://doi.org/10.1681/ASN.2007090982>
- Zhang, D., Zhang, G., Hayden, M. S., Greenblatt, M. B., Bussey, C., Flavell, R. A., & Ghosh, S. (2004). A toll-like receptor that prevents infection by uropathogenic bacteria. *Science*, 303(5663), 1522-1526. <https://doi.org/10.1126/science.1094351>
- Zhang, J., Li, C., Rahaman, M. M., Yao, Y., Ma, P., Zhang, J., Zhao, X., Jiang, T., & Grzegorzec, M. (2022). A comprehensive review of image analysis methods for microorganism counting: from classical image processing to deep learning approaches. *Artif Intell Rev*, 55(4), 2875-2944. <https://doi.org/10.1007/s10462-021-10082-4>
- Zhao, X., & Drlica, K. (2014). Reactive oxygen species and the bacterial response to lethal stress. *Curr Opin Microbiol*, 21, 1-6. <https://doi.org/10.1016/j.mib.2014.06.008>